Response of Bone to Mechanical Load and Alterations in Circulating Hormones.

Richard A. Hillam

A thesis submitted to the University of Bristol in accordance with the requirements for the degree of Ph.D. in the Faculty of Medicine, Department of Anatomy.

October 1996

Abstract

The architecture and material properties of bone have evolved to enable each bone to fulfill its physiological role in the most efficient way. Bone is a dynamic tissue in which resorption and formation occur during the modelling and remodelling processes. It is the balance between the milieu of osteotropic influences which determines whether the net effect of these processes results in bone formation or bone resorption.

For load-bearing bones there is a close relationship between the bone's architecture and its mechanical strain environment. For other bones, in which load-bearing is not important, strain may not represent an important influence on the structural form of these bones. It is likely that there are differences in the hierarchy of osteotropic control of bone mass in different bones of the skeleton. The relative importance of strain, hormones and other osteotropic influences will depend on the function of each bone. In certain instances, bone form may be determined phylogenetically and osteotropic influences may not affect greatly, the final form of the bone. As such, the bone would be less sensitive to these external influences or would respond to them slowly.

The experiments in this thesis investigate several aspects of the response of bone to external stimuli. The specific studies determine the cellular response of mechanical loading on a resorbing surface of the modelling ulna of a growing rat, the role of parathyroid hormone (PTH) on ovariectomy (OVX) induced osteopenia in the adult rat by investigating the mechanical and structural properties of various long bones, vertebrae and the parietal bone of the skull. The final study investigates regional differences in human bone strain *in vivo* by bonding rosette strain gauges to the tibia and parietal bone.

The results of mechanically loading the ulna demonstrated a highly significant increase in fluorochrome label incorporation on the medial periosteal surface compared with controls ($P< 0.005$). An enzymatic marker of osteoclast activity (tartrate resistant acid phosphatase) was reduced significantly in loaded bones compared with controls ($P< 0.005$), while the histological appearance of the bone surface in controls was altered from one with characteristic features of resorption to those of new mineralised bone formation.

The study investigating the possible role of PTH on OVX induced osteopenia demonstrated a significant interaction between the effects of thyroparathyroidectomy and OVX on the development of trabecular osteopenia in the proximal tibia ($P< 0.05$). However, there were no significant differences between the experimental groups and the controls in terms of parietal thickness or porosity.

The study investigating human tibial and parietal strain *in vivo* demonstrated strain rates and magnitudes that were up to ten times greater in the tibia compared with the calvaria.

From the results, it can be concluded that:
1. There are regional differences in the mechanical strain environment to which different bones of the skeleton are exposed.
2. There are regional differences in the response of different bones to hormonal influences.

Acknowledgements

Many people gave me practical assistance, advice and helpful suggestions during the experiments and preparation of this thesis. Without them, none of this work would have been possible. To list everyone who helped me would be impossible but I should mention the following:

Dr. Jon Beresford at the Bath Institute for Rheumatic Diseases allowed me to use the microdensitometer for measurements of enzyme activity in chapter 2.

Mr Jeremy Burn exhibited great patience and spared a lot of time trying to educate me in electronics and the principles of data capture. No laboratory with a computer or any other piece of electronic equipment should be without him!

Mrs Amanda Dennis from the Bristol University Computer Centre advised on the use of appropriate and meaningful statistical tests and showed me how to analyse the data in chapter 4.

Dr. Harold Frost took the time to give me the benefit of his experience and came to Bristol to give us his enthusiastic sermon on bone remodelling.

Mrs Karen Garwood helped with all the laboratory animal procedures, occasionally getting bitten in the line of duty but she did so with an impressive sense of humour. Great clogs!

Mrs Chris Goodall cut the sections for the work in chapter 4, showed me how to perform the TRAP reactions described in chapter 3 and maintained her great sense of humour while I was messing up her immaculate histology laboratory.

Professor Allen Goodship allowed me to use the facilities in the Department of Anatomy and showed me how to make no money go a long way!

Mr Gareth Gough and Mrs Maureen Redko looked after the laboratory animals and assisted with rat anaesthesia during loading.

Mr Mark Jackson, friend and orthopaedic surgeon at the Bristol Royal Infirmary who implanted the three strain gauges onto my bones, in the experiment described in chapter 5. Next time Mark, please leave enough time for the local anaesthetic to take full effect!

Dr. John Mosley of the RVC advised with recreating an ulnar loading device. John also helped in measuring *in vivo* strain in the experiment described in chapter 2.

Miss Julie Milkins was always willing and helpful in setting up the strain gauge amplifiers and also prepared most of the strain gauges.

Mr Andrew Millest at Zeneca Pharmaceuticals, Macclesfield invited me to the research labs to use the pQCT machine. Mr Sean Breen at the Imaging Department performed the pQCT scanning of the rat tibiae described in chapter 4.

Mrs Helen O' Callaghan performed the ulnar fluorochrome label measurements described in chapter 3.

Professor Clint Rubin hosted me during a stimulating and enjoyable visit to The Department of Orthopaedics, Stony Brook, New York and Professor Susannah Fritton calculated the principal strain magnitudes and angles from the raw human strain data.

Mr Hans Schiessl (Uncle Bone): friend, classic car collector and owner of Stratec GmbH was extremely generous during my visits to the factory in Germany. His overwhelming enthusiasm for bone often kept me awake into the small hours of the morning!

Mr Glenn Wakley advised on the use of the histomorphometry equipment. Glenn and Lyane Hayward were kind enough to collect numerous samples of rat bone during the time when I was incapacitated while measuring bone strains from my skull and tibia.

Mr Pete Walker and Nicky Latham assisted with calibration of strain gauge equipment and load cells. Pete tried hard to make sure that I worked safely and on occasions was the inspiration for memorable moments in the coffee room!

Mr John White made the loading devices (Marks I II and III) and many of the cryomicrotome chucks. Also, thanks for sharpening my diving knife!

Mrs Sandy Wotton at Langford showed me how to use the confocal microscope.

I would especially like to thank Professor Tim Skerry, friend and advisor for all his support, encouragement and suggestions throughout the duration of my Ph.D. He cut the sections and made the microdensitometry measurements in chapter 2. Also, I must thank him for being such a wonderful recipient for the practical jokes which have provided so much amusement for so many people. In addition, I appreciate very much all the plumbing he did for me at home!

Finally, none of this work would have been possible without funding. In the early part of my studies, I was supported by a University of Bristol Post-Graduate Studentship. In particular, I would like to extend my thanks to the Biotechnology and Biological Sciences Research Council for the support of a B.B.S.R.C. Veterinary Research Fellowship which funded the majority of my research training.

Dedication

This thesis is dedicated to my parents and those unfortunate people who are disabled by osteoporosis; a disease which is painful, disfiguring and which has been described as causing bones to crumble like chalk (Jones and Fardell 1996).

Memorandum

This thesis represents the unaided work of the author, except where otherwise acknowledged

Richard A. Hillam

October 1996

Contents

Abstract
Acknowledgements
Dedication
Memorandum
Contents
List of figures and tables

Chapter 1 General Introduction 1

1.1 The form and function of bone 1
1.1.1 Introduction 1
1.1.2 History 4
1.1.3 The adaptation of bone to its function 6

1.2 The effect of mechanical load on bone 9
1.2.1 The nature of the mechanical stimulus 9
1.2.2 Strain gauge studies 12
1.2.3 The effect of exercise and disuse on the skeleton 15
1.2.4 Quantifying the adaptive response of bone to mechanical strain 17

1.3 Transduction of the mechanical stimulus into an adaptive cellular response 22
1.3.1 Introduction 22
1.3.2 Deformation 24
1.3.3 Microdamage 25
1.3.4 Piezoelectricity and streaming potentials 27
1.3.5 Nervous control 28

1.4 The effect of hormones on bone 29
1.4.1 Introduction 29
1.4.2 Oestrogen 29
1.4.3 Parathyroid hormone 32
1.4.4 Calcitonin 35
1.4.5 Thyroid hormones 36

1.5 Cytokines and local factors 38

1.6 Use of the rat as an animal model for bone studies 40

1.7 Summary and objectives 46

Chapter 2 **A model for investigating the cellular events of mechanically loaded resorbing bone** 48

2.1 **Summary** 48

2.2 **Introduction** 50

2.3 **Aims** 53

2.4 **Materials and Methods** 53

2.5 **Results** 68

2.6 **Discussion** 82

2.7 **Conclusion** 89

Chapter 3 **Investigating a technique for supplementing thyroparathyroidectomised rats to physiological levels of thyroxine** 90

3.1 **Summary** 90

3.2 **Introduction** 91

3.3 **Aims** 94

3.4 **Materials and methods** 94

3.5 **Results** 97

3.6 **Discussion** 101

3.7 **Conclusion** 104

Chapter 4 **The role of parathyroid hormone in ovariectomy induced osteopenia in the adult rat** 105

4.1 **Summary** 105

4.2 **Introduction** 106

4.3 **Aims** 108

4.4 **Materials and methods** 108

4.5 Results 124

4.6 Discussion 151

4.7 Conclusion 159

Chapter 5 Investigation of the regional differences in mechanical strain in different bones of the human skeleton 160

5.1 Summary 150

5.2 Introduction 162

5.3 Aims 165

5.4 Materials and methods 165

5.5 Results 179

5.6 Discussion 200

5.7 Conclusion 206

Chapter 6 General discussion and conclusions 207

Proposals for further work 212

Appendices 213

Appendix 1 Appendix to chapter 2 213
A.1.1 *In vivo* ulnar strain gauging 213
A.1.2 *In vitro* load strain calibration of the ulnae 215
A.1.3 Description of the ulnar mechanical loading apparatus 221
A.1.4 Preparation of the methylmethacrylate resin 224
A.1.5 Infiltrating and embedding the ulnae in methylmethacrylate resin 224
A.1.6 Chilling 225
A.1.7 Mounting the antebrachii in preparation for cryosectioning 225
A.1.8 Technique for demonstrating TRAP activity 230
A.1.9 Microdensitometry 230

Appendix 2 Appendix to chapter 4 232
A.2.1 Fluorochrome labels 232
A.2.2 Surgical techniques 233

A.2.3 Mechanical tests of bones 237
A.2.4 Principles of quantitative computed tomography 242
A.2.5 Histomorphometry of the calvarial bones 245

Appendix 3 Appendix to chapter 5 251
A.3.1 Ethical committee approval 251
A.3.2 Choice of strain gauges 251
A.3.3 Preparation of the strain gauges 254
A.3.4 Choice of adhesive 258
A.3.5 Data capture 259
A.3.6 Setting up the strain gauge amplifiers 259
A.3.7 Calibration of the strain gauges 259
A.3.8 Bite force measurements 261
A.3.9 Suggestions for improving the strain measuring technique 262

References 264

List of figures

1.1	schematic diagram to illustrate the temporal sequence of cellular events involved with the bone remodelling cycle	2
1.2	schematic to illustrate the osteotropic influences on bone	3
1.3	graph to illustrate the relationship between stress and strain for a material	10
1.4	schematic to illustrate the principle of axial strain calculation	11
1.5	schematic to illustrate the principle of shear strain calculation	12
1.6	microradiograph showing trabecular osteopenia in the proximal tibia of a seven month old rat, three months after ovariectomy, compared with a control	42
2.1	schematic to illustrate the normal pattern of modelling in the rat ulna	52
2.2	photograph of a single element strain gauge	55
2.3	photograph of an exposed rat ulna prepared for bonding a strain gauge to the medial bone surface	56
2.4	photograph of a single element strain gauge bonded to the medial periosteal surface of the ulna	56
2.5	microradiograph of a rat ulna with a single-element strain gauge bonded to the medial periosteal surface	57
2.6	photograph of a rat during strain recording	58
2.7	photograph of a left & right pair of rat ulnae showing the degree of curvature	59
2.8	photograph of an anaesthetised rat with its left ulna placed between the cups of the loading device	62
2.9	diagram illustrating how the medial periosteal fluorochrome label was measured in study 2	63
2.10	schematic illustrating how the ulnar sections were obtained using the cryostat	65
2.11	diagram illustrating how the medial periosteal fluorochrome labels were measured in study 3	67
2.12	series of photographs taken along the length of a control ulna	70
2.13	strain trace recorded from a rat ulna during landing from 30 cm	72
2.14	strain trace recorded from a rat ulna during walking	73
2.15	bar chart showing a comparison between the left and right label lengths on the medial periosteal surfaces	75
2.16	photographs showing the woven bone response to mechanical loading on the medial periosteal surface of the mid-diaphysis of the ulna	77
2.17a	photographs showing the histological features of the medial periosteal surface of a right control ulna	80

2.17b photographs showing the histological changes on the medial periosteal surface of the ulna in response to loading 81

3.1 schematic showing the anatomy of the thyroid and parathyroid glands 92
3.2 graph illustrating the long-term release characteristics of 15 mg pellets 99
3.3 photograph of a thyroxine implantable pellet after removal post-mortem 100

4.1 schematic to show tibia prepared for pQCT scanning 113
4.2 diagram illustrating the technique used for vertebral compression testing 115
4.3 photograph of a vertebral body mounted in the .45 brass cartridge cases 116
4.4 photograph showing the 3-point loading apparatus 118
4.5 diagram illustrating how the ulnae were mounted for 3-point bending 119
4.6 schematic showing the parameters measured in histomorphometry of the parietal bones 121
4.7 bar chart of the PTH assay results 140
4.8 bar chart of the thyroxine assay results 141
4.9 bar chart of the radial 3-point bending test results 142
4.10 bar chart of the ulnar 3-point bending test results 143
4.11 graph showing a typical load to failure curve for the vertebral bodies 144
4.12 bar chart of the L5 compression test results 145
4.13 bar chart of the L6 compression test results 146
4.14 bar chart of the tibial trabecular BMD measurements 147
4.15 bar chart of the tibial cortical BMD measurements 148
4.16 bar chart of the tibial total BMD measurements 149
4.17 bar chart of the parietal thickness measurements 150

5.1 photograph of the parietal bone surface prepared for gauge bonding 167
5.2 photograph of a planar strain gauge used in the experiment 168
5.3 photograph of a strain gauge bonded to the parietal bone 169
5.4 photographs illustrating gauge positioning on a cadaver skull 170
5.5 a C.T. scan showing a cross-section of the tibia at the mid-diaphysis 171
5.6 photograph of the tibial bone surface prepared for gauge bonding 172
5.7 photograph of the tibial gauge bonded to the tibia 173
5.8 photographs illustrating gauge positioning on a cadaver tibia 174
5.9 photograph of the radiograph showing tibial gauge positioning 175
5.10 diagram of a strain gauge and the formulae used for strain analysis 178
5.11-13 graphs showing bite force and parietal principal strains recorded simultaneously whilst biting between the right molars 180-182

5.14-16 graphs showing bite force and parietal principal strains recorded simultaneously whilst biting between the left molars 183-185
5.17-19 graphs showing bite force and parietal principal strains recorded simultaneously whilst biting between the incisors 186-188
5.20 graph showing parietal principal strains whilst eating a banana 189
5.21 graph showing parietal principal strains whilst grimacing 190
5.22 graph showing parietal and tibial principal strains whilst walking 191
5.23 graph showing parietal and tibial principal strains whilst squatting with a 56 lb. weight 192
5.24 graph showing parietal and tibial principal strains whilst heading a 4.5 kg medicine ball 193
5.25 graph showing parietal and tibial principal strains whilst landing from a height of 45 cm 194
5.26 graph showing tibial principal strains whilst landing from a height of 1.3 m 195
5.27 graph showing the tibial principal strain magnitudes and corresponding principal strain angles during two strides of walking 196
5.28a figure illustrating the angles of the principal strains in the tibia during the mid-stance phase of walking in bare feet 197
5.28b figure illustrating the angles of the principal strains in the tibia during impact loading 197

A.1.1 static load / strain calibration curve 216
A.1.2 dynamic load / strain calibration curve at 1 Hz 217
A.1.3 dynamic load / strain calibration curve at 10 Hz 219
A.1.4 strain rate curve for 20 cycles for a 10 Hz sinusoidal waveform 220
A.1.5a photograph of the loading device and control panel 222
A.1.5b photograph of the loading device during a period of loading 223
A.1.6 schematic diagram of a chilling bath used to snap freeze the bones 227
A.1.7 schematic of the aluminium mounting block 228
A.1.8 schematic of an antebrachium mounted on a brass microtome chuck 229

A.2.1 diagrams to illustrate the surgical approach for thyroparathyroidectomy 234
A.2.2 schematic to illustrate the anatomy of the thyroid and parathyroid glands 235
A.2.3 photograph of an H&E stained section of thyroid and parathyroid gland 236
A.2.4 schematic to illustrate the four basic configurations for mechanical tests 238
A.2.5 schematic to illustrate how the calvariae were embedded in resin 247
A.2.6 microradiograph of an adult rat calvaria 248

A.2.7 illustration showing the site from which parietal sections were cut 249
A.2.8 photograph illustrating how the porosity of the bone varied with the distance from the sagittal suture 250

A.3.1 photograph of a stacked rosette strain gauge 252
A.3.2 photograph of a planar rosette strain gauge 252
A.3.3 schematic showing how the strain gauges were constructed 255
A.3.4 photograph of a strain gauge wired to a D-connector 256
A.3.5 wiring circuits for strain gauges 257
A.3.6 schematic to show how the strain gauges were calibrated 260
A.3.7 schematic to show the bite force transducer 261

List of tables

1.1	summary of the action of various cytokines and local factors on bone	39
2.1	results of the histomorphometry measurements	74
2.2	summary of the histomorphometry results	75
2.3	results of the measurements made of the fluorochrome label lengths on the medial periosteal surface	78
2.4	summary of the label measurements	78
2.5	results of the microdensitometry readings	79
2.6	summary of the microdensitometry readings	79
3.1	results of body weights and blood thyroxine levels from study 1	97
3.2	results of blood thyroxine levels following thyroparathyroidectomy from study 2	98
3.3	results of blood thyroxine levels following pellet implantation from study 2	98
4.1	summary of the basal, three and 12 week PTH assays	127
4.2	results of the PTH assays in three rats excluded from the study	127
4.3	summary of the basal and 12 week thyroxine assays	128
4.4	summary of the basal and 12 week body weights	130
4.5	summary of the 12 week uterine weights	131
4.6	summary of the radial and ulnar three-point bending tests	131
4.7	summary of the lumbar vertebral compression tests	132
4.8	summary of the tibial trabecular, cortical and total BMD measurements	134
4.9	parietal histomorphometry results	137
4.10	summary of the 2-way ANOVA interpretations for all of the results	139
5.1	maximum strain magnitudes recorded from the tibia and skull	198
5.2	maximum strain rates recorded from the tibia and skull	198
5.3	summary of strain magnitude results	199
5.4	summary of strain rate results	199
A.2.1	details of fluorochrome preparation and doses	232

Chapter 1

General Introduction

1.1 The form and function of bone

1.1.1 Introduction

The shape, internal architecture and material properties of bones have evolved to fulfill the individual role of each bone. Modelling and remodelling activities adjust bone mass and geometry to facilitate adaptation to constantly changing mechanical and physiological demands, as it is the combination of bone mass and its architecture which determines a bone's mechanical competence.

Remodelling may be defined as the specific temporal sequence of cellular events (figure 1.1) which occur at a given location of bone. In adult bone remodelling is the most important process responsible for the change in shape and mass of a bone. Modelling can be defined as the process whereby bone resorption and formation take place concurrently but at different sites on the bone surface. This is the process responsible for changes in shape and size during bone growth.

In healthy adult bone cellular activity constantly remodels the matrix. The cellular processes responsible for remodelling are affected by various osteotropic influences (figure 1.2). The effects of mechanical usage, systemic hormones and other local factors all have the potential to modulate the cellular events of the remodelling cycle (figure 1.1). Alterations in the fine balance between resorption and formation occurring in this cycle determine the net effect on bone mass. Under normal circumstances bone may be resorbed from one region and be deposited in another region depending on the balance between the various positive and negative osteotropic influences. In other regions there may be no net change in bone mass.

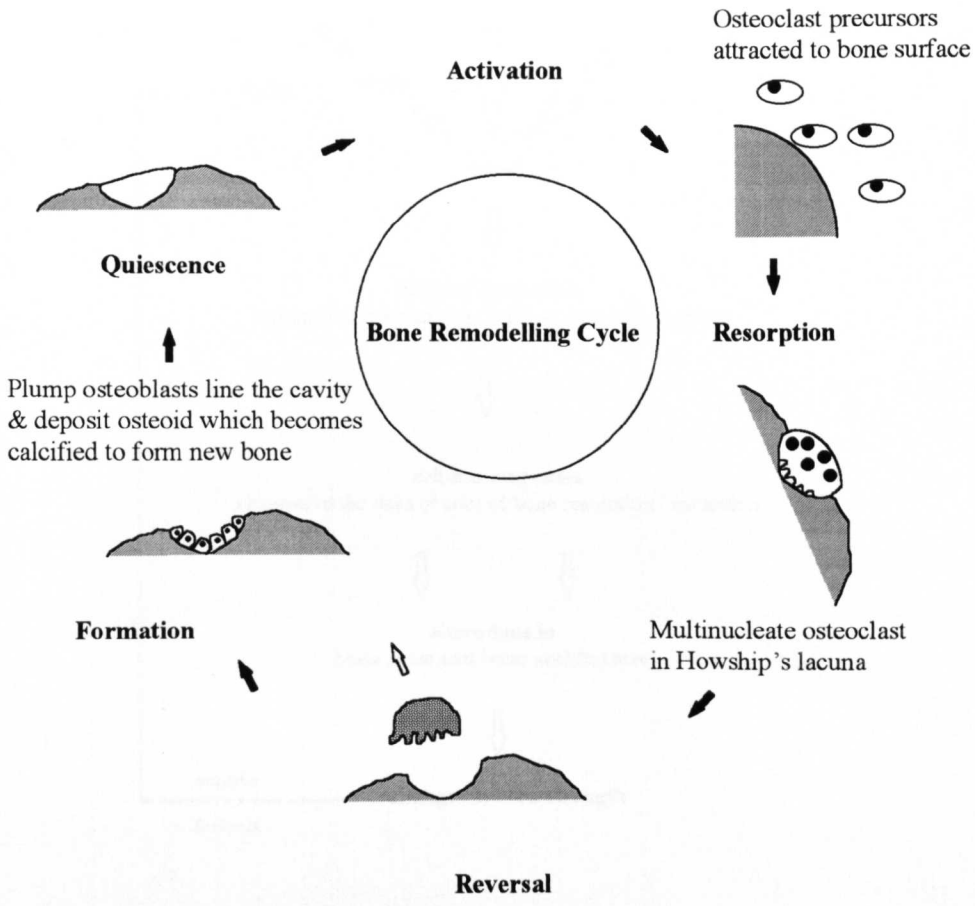

Figure 1.1
Sequence of Cellular Events Responsible for Bone Remodelling

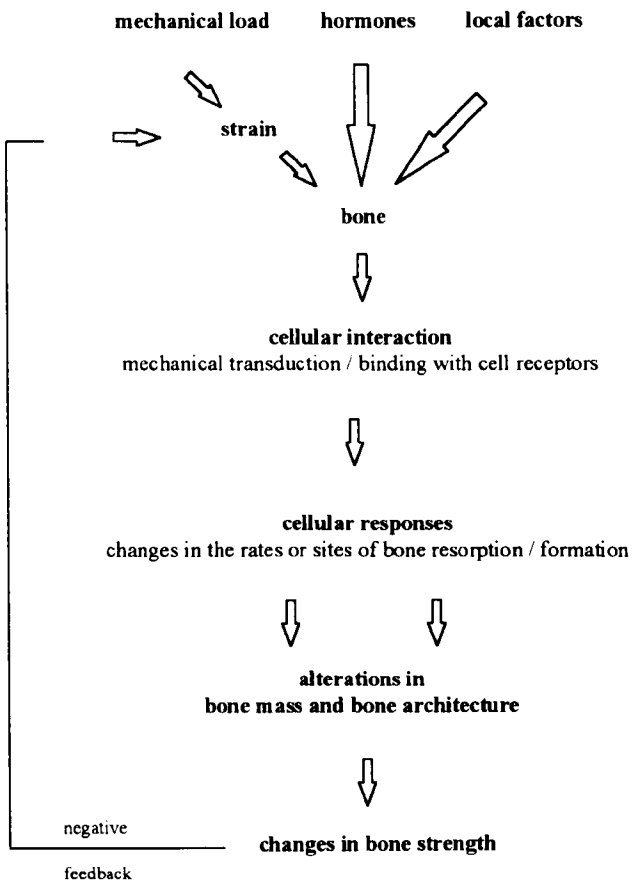

Figure 1.2
Schematic showing the osteotropic influences and their effects on bone

1.1.2 History

It was in 1638 when Galileo suggested an association between a bone's form and its mechanical properties. However, it was not until the 1830's that the architecture of trabeculae and its relation with bone's mechanical function was studied seriously (Wolff 1892). In 1838 an Englishman called Ward studied the proximal femur and made an association between its external form and the arrangement of the trabeculae in the femoral head (Wolff 1892). He suggested that the role of the trabeculae was to support the over-hanging femoral head. He suggested that some of the trabeculae were loaded in compression whilst others were loaded in tension. In 1858 Humphry, an English anatomist, added to this by making a further observation. This was that all the trabeculae arising from the femoral head were perpendicular to the articular surface (Koch 1917). Koch (1917) also described a second observation made by Humphry, that the two principal groups of trabeculae intersect each other at right angles. In contrast, Wolff explained that Humphry had failed to observe the latter point (Wolff 1892).

At a meeting of naturalists in 1867, Hermann von Meyer from Zürich demonstrated some illustrations of human bones and discussed the importance of the arrangement of the trabeculae within bones. A mathematician from Zürich, Professor Culmann was present and became interested (Koch 1917). He studied the anatomy of the trabeculae and following calculations of the lines of stress within a Fairbairn crane, a model for the femur, concluded that the trabeculae within the proximal femur lay along the paths of maximum stress. This enabled the femur to carry the maximum load with the minimum of mass. This has become known as the 'Trajectorial Hypothesis' (Koch 1917).

In 1876 Rauber and later in 1880 Messerer conducted the first series of mechanical tests on bones (Koch 1917). Shortly after, in 1881 Roux proposed a theory on the "functional form of bone". In this he stated that "the bone achieves the external and internal shape best adapted to its function" (Wolff 1892). In this respect, Roux could be considered to have been the first person

to conceive the notion of functional adaptation of bone to a functional stimulus, as a self-regulating process. In 1884 Wolff published "The law of remodelling of the internal architecture of bone after pathological alteration of its external shape" in which he describes the alteration of trabecular architecture arising from changes in bone curvature and stresses (Wolff 1892). However, it is Wolff who in 1892 gained the credit for his theory on the functional form of bone (Koch 1917). This has been summarised as the Law of Bone Remodelling: "The law of bone remodelling is the law according to which alterations of the internal architecture clearly observed and following mathematical rules, as well as secondary alterations of the external form of the bones following the same mathematical rules, occur as a consequence of primary changes in the shape and stressing of the bones." (Wolff 1892). Rewritten in way that is easier to understand the law of remodelling states: "Every change in the form and function of a bone or of their function alone is followed by certain definite changes in their internal architecture and equally definite secondary alterations in their external conformation, in accordance with mathematical laws." (Skerry 1989). This is known commonly now as Wolff's Law.

In 1917 Koch published a long and detailed paper called 'The Laws of Bone Architecture' in which he examined the anatomy and mechanical properties of the human femur. He concluded that:

1. The external form and internal architecture was the result of adaptation to the functional demands placed on the bone.
2. There is a relationship between the structure and stresses experienced at every point.
3. Spongy bone is homogeneous with compact bone and that its strength is similar to compact bone for a given mass.
4. The weakest part of the femur is the femoral neck.
5. The internal structure of the femur is such that it produces great strength with the minimum of material.

6. The law of bone transformation (Wolff's Law) is true for the femur and therefore holds true for all other normal human bones.

1.1.3 The adaptation of bone to its function

The basic length and shape of long bones in the absence of functional load-bearing are predetermined genetically (Fell 1956; Lanyon 1980). However, development of the normal adult form requires physiological activity (Lanyon 1980). This suggests that the precise size and shape of a bone is the result of the combination of the genetic basic form and the processes associated with structural adaptation to the functional demands placed upon it.

The skeleton has several roles. These include: providing protection to vital soft tissue structures such as the brain and spinal cord, facilitating breathing, acting as stiff lever arms and providing sites for muscle, tendon and ligament attachment to enable movement and locomotion.

Currey (1979a) investigated the mechanical properties of three types of bone. Antlers from the male red deer (Cervus elaphus), the tympanic bulla of the fin whale (Balaenoptera physalus) and the femur of an ox (Bos taurus). All of these bones have functions which vary widely. The femur must support the weight of the ox and resist excessive bending and buckling during locomotion. Antlers are used in display for which there are no special mechanical requirements but they must be tough enough to withstand the repeated impact loads encountered in the rutting season. In contrast, the tympanic bulla does not load-bear but is responsible for transmitting sound waves with minimal energy absorption and sound distortion. His findings showed that the antlers had a low degree of mineralisation, were quite elastic and had a high energy to failure (i.e. they were 'tough'). The tympanic bulla of the fin whale was highly mineralised and stiff with low energy to failure. Its properties were very different from those of the antlers; the fact that the tympanic bulla could not withstand high mechanical load is not important because mechanically it is

fairly isolated from the rest of the skull. Its highly mineralised composition, however, enables it to fulfill its role of efficient sound transmission. The mechanical properties of the femoral bone were intermediate between those of the other two bones; with a higher degree of mineralisation than the antlers but lower than the tympanic bullae. With these findings in mind we could consider another region of the skeleton whose role is vital; the cranium. It encloses and protects the brain so despite being relatively unloaded, it must maintain its mass and strength to withstand occasional impacts (Currey 1984). Failure to fulfill this requirement could prove fatal to an individual, even following the most trivial of misadventures.

If all animals of a species had similar bones which possessed similar physical properties without the ability to adapt then the majority of individuals would probably survive with few problems during normal habitual activity. However, it would limit the adaptability of the animal; there would be no scope for improving the chances of survival if the demands placed on the skeleton changed as it could result in a higher incidence of catastrophic fractures while escaping from predators or during hunting.

An individual is born with bones which become increasingly mineralised during growth (Currey 1979b; Currey 1984). The higher the mineral content of a bone, the stiffer it becomes for a given weight. However, as a bone becomes increasingly mineralised, its impact strength decreases, although its bending strength does increase slightly (Currey 1984). The consequential changes in mechanical properties associated with alteration in composition may be purely incidental. However, it is likely that evolutionary pressure resulted in the selection of such properties. Young animals are playful and inquisitive. During play and while exploring their surroundings, they have a tendency to fall and bang into objects. Bones with high impact strength are obviously an advantage to protect against fractures. As an animal grows, it uses its limbs for hunting, escaping from predators and migrating long distances. The requirements from the bones change; they need to be stiff and strong but light

enough so that the animal doesn't have to expend excessive amounts of energy to move the limbs.

The ideal geometry of a bone can be described in terms of the least mass solution for that bone (Currey 1984). This means simply that a bone should possess a combination of adequate stiffness in bending and torsion, without buckling and sufficient strength to enable it to withstand the physical demands placed upon it but with the minimum of mass so that minimal energy is expended in movement. For a long bone the ideal shape would, therefore, be a hollow tube. It is interesting that these considerations apply to terrestrial animals but in aquatic animals other factors affect bone development. Manatee (Trichechus species) which are aquatic mammals have few predators and are also herbivorous. They have no requirement to escape from predators or to chase prey. Their bones are thick and dense i.e. they are pachyostotic and this is thought to assist in reducing their buoyancy to keep them under water (Ridgway and Harrison 1985; Nowak 1991). It is reported that their long bones do not possess substantial medullary cavities (Fawcett 1942; Currey and Alexander 1985)with haemopoietic tissue only present in the vertebrae but not the ribs or bones of the front limb (Dr. D.K. Odell, Sea World, Florida personal communication). The possession of such heavy bones has been highly detrimental to the Trichechus species but only because they have been hunted extensively for their ribs which, because they are solid, have been used as an alternative for ivory and utilised in the manufacture of pistol handles (Nowak 1991)!

In summary, each bone has adapted to produce material properties and a form which are best suited for its specific role.

1.2 The effect of mechanical load on bone

1.2.1 Nature of the mechanical stimulus

The primary mechanical influence exerted on bones originates from body weight and forces generated by muscles acting through articular cartilage, tendons and ligaments.

When stress is applied to any structure, including a bone, it undergoes deformation. The extent of this deformation depends on the magnitude of the stress, the material properties and geometry of the structure. Figure 1.3 shows a typical stress-strain curve for a material. Stress is defined as the load per unit area (Nm^{-2}). Axial deformation is called normal strain and can be defined as the change in length per unit length for any given axis of the structure (figure 1.4). By convention positive strain denotes tension while negative strain denotes compression. A tensile strain of one or 100% indicates a doubling in length and is equivalent to 1,000,000 μstrain. Deformation arising from shear forces is called shear strain and is defined as the shear displacement divided by the width of a shear structure (figure 1.5). Strain is a ratio and therefore, is dimensionless.

It is possible that bone adapts either directly to the applied stress or indirectly to the degree of strain. In 1741 it was André who first suggested that deformation could govern bone shape which was followed 176 years later by Thompson in 1917 (cited by Martin and Burr 1989) and it was Frost who stated that 'Cells probably must "infer" stress levels from strain or strain-related phenomena.' (Frost 1973).

It would be impossible to measure stresses in bone directly. However, since the 1970's strain gauges, used commonly in engineering, have been employed extensively in studies to investigate the relationship between bone surface strain and bone's adaptive response to mechanical load.

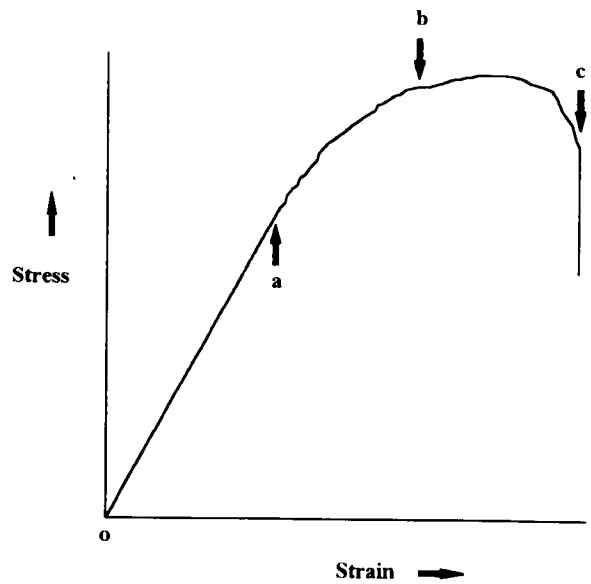

Where: a = the proportional elastic limit
b = the absolute elastic limit (yield point)
c = the failure point

Figure 1.3
Typical stress / strain curve for a material

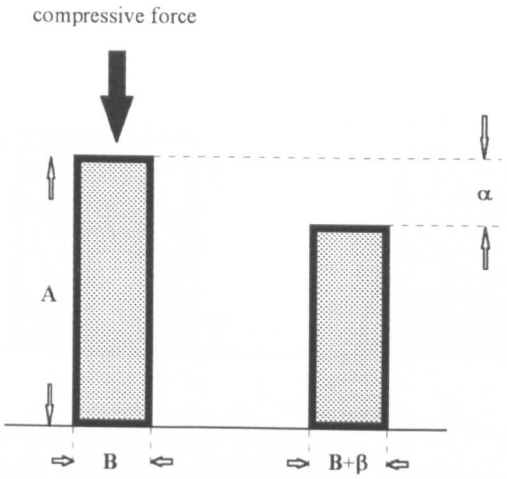

Where: A = original length
B = original width
α = decrease in length
β = increase in width

Axial engineering strain (με) = (α / A) x 1,000,000
Lateral engineering strain (με) = (β / B) x 1,000,000

Poisson's ratio = - lateral strain / axial strain

Figure 1.4
Principle of axial strain calculation

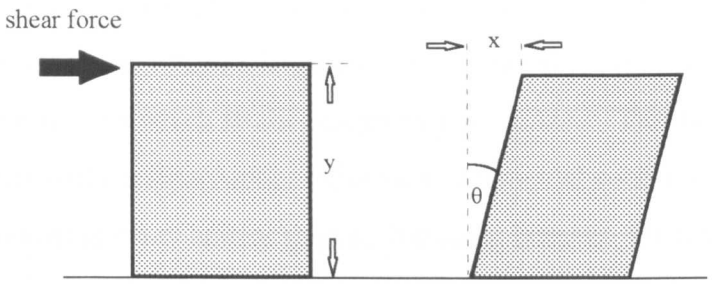

Where: y = width of the shear specimen
x = shear displacement

Shear strain ($\mu\varepsilon$) = (x / y) x 1,000,000

Shear displacements are often described as shear angles (θ).
For small displacements:

θ = x / y (in radians)

Figure 1.5
Principle of shear strain calculation

1.2.2 Strain gauge studies

Strain gauges are small, high precision electrical resistors. They are used in structural engineering to measure surface strain at vital locations that may be prone to fatigue failure. Each gauge is bonded firmly to the structure's surface and changes in electrical resistance are calibrated to specific changes in surface

strain. The changes in resistance are measured using a Wheatstone bridge circuit.

There is no practical way of measuring intracortical stress but because bone is firm and many bones present a large and smooth surface, they represent suitable structures to which strain gauges may be bonded. This has enabled the study of bone surface strain under different experimental conditions both *in vitro* and *in vivo* in many animal species, including humans, for over 50 years.

Gurdjian and Lissner (1944) were the first to document the use of strain gauges *in vivo*. They applied strain gauges to the parietal bones of anaesthetised dogs in a study designed to investigate the effects of head trauma on intracranial pressure. Evans (1953) suggested their use *in vivo* and described an experiment in which the tibia of a live dog had strain gauges applied although specific details were vague. In 1964 Lissner and later in 1966 Lissner and Roberts used strain gauges which were bonded to the spine of living dogs and human cadavers during ejector seat tests (cited by Lanyon 1969).

In 1969, with the advent of modern cyanoacrylate adhesives, came the first detailed accounts of the use of strain gauges to measure physiological bone strain. Lanyon and Smith (1969) described an experiment in which the tibiae of sheep were strain gauged *in vivo* in an attempt to investigate physiological strain patterns. This experiment was conducted as a feasibility study before progressing to *in vivo* strain measurement of the ovine vertebral column (Lanyon 1969). Subsequently, numerous *in vivo* studies have been conducted in animals in an attempt to correlate adaptive bone responses or pathology to mechanical strain (Lanyon and Smith 1970; Lanyon 1972, 1974, 1976; Hylander 1977; Baggott and Lanyon 1977; Goodship *et al* 1979; O'Connor *et al* 1982; Keller and Spengler 1982; Rubin and Lanyon 1981, 1984; Hylander 1984; Bouvier and Hylander 1984; Nunamaker *et al* 1990; Szivek *et al* 1992).

The first *in vivo* human bone strain study was conducted by Lanyon *et al* (1975) when a gauge was bonded to the tibial midshaft of a volunteer, Mr W Hampson, an English orthopaedic surgeon. This was followed recently by a study in which the tibiae of two volunteers were strain gauged (Burr *et al* 1996).

The findings of the animal studies demonstrated remarkable consistency in that the peak magnitude of physiological surface strains, the majority of which were measured in long bones, ranged between 2100 - 3200 μstrain (Rubin and Lanyon 1984). Interestingly, Nunamaker *et al* (1990) measured peak compressive strain magnitudes of 5700 μstrain on the dorsal aspect of the third metacarpal bone in young horses. In contrast, the results of the two human studies showed much lower magnitude peak strains. The peak magnitudes of the principal strains measured by Lanyon *et al* (1975) were 850 μstrain in tension while those measured by Burr *et al* (1996) were 1200 μstrain in compression. The hypothesis of Burr *et al* (1996) was that peak strain magnitudes on the human tibial midshaft would exceed 3000 μstrain during vigorous activity. Although the principal strain magnitudes did not approach 3000 μstrain it is possible that the strains may have been higher at other sites on the tibia or on other bones.

Physiological bone strain has been measured on bones other than long bones. It has been measured from gauges bonded to the mandibles of primates (Hylander 1977, 1984), the parietal bone of primates (Behrents *et al* 1978; Iwasaki 1989), the supra-orbital region of primates (Hylander *et al* 1991), the parietal bone of turkeys and rats (Hillam *et al* 1994; Rawlinson *et al* 1995) and the occipital bone of pigs (Lieberman 1996). Recordings from the primates, turkey and rats demonstrated that the peak strain magnitudes on the surface of the parietal bones were not greater than 100 μstrain while Lieberman showed in the pigs that occipital principal strains did not exceed 100 μstrain and shear strain magnitudes were less than 200 μstrain. These calvarial strains were an order of magnitude lower than those measured previously from long bones of

many animal species. To date there has been no documented evidence of calvarial bone strain recordings made *in vivo* from the human skull.

1.2.3 The effect of exercise and disuse on the skeleton

The skeleton responds to changes in mechanical load by adjusting its mass and geometry to remain mechanically competent with the most efficient use of its mass but in such a way that it maintains an acceptable "safety factor" (Rubin and Lanyon 1984). Indeed, if the skeleton did not possess this ability but simply relied on bones that were over-engineered for habitual activity then for many individuals it would involve inefficient expenditure of energy required for movement and locomotion. There are numerous human and animal studies which have documented adaptive changes in bone mass and architecture in response to altered conditions of mechanical loading.

In 1977 Jones *et al* studied a group of professional tennis players. They compared radiographs taken of both humeri and found that there was a highly significant hypertrophy in the cortices of the playing arms of both men and women. This demonstrated that periods of intermittent exercise could increase bone mass.

A year later Uhthoff and Jaworski (1978) observed osteopenia in the forelimbs of young dogs which were immobilised with the use of plaster casts. Subsequently, they demonstrated disuse osteopenia in a group of older dogs which was reversed following return to normal activity (Jaworski and Uhthoff 1980). These two studies showed that local disuse was responsible for a fall in bone mass but subsequent return to normal use could stimulate restoration of bone mass. This illustrated the dynamic flux in bone mass of long bones, the balance of which was altered in response to the prevailing mechanical environment.

A decade later two human studies revealed interesting results. In 1990 Leblanc *et al* investigated the effects of prolonged immobilisation in a group of volunteers who had undertaken bed rest for 17 weeks. They demonstrated significant bone loss in the entire skeleton except for the skull which gained in bone mass. Subsequently Garland *et al* (1992) showed bone loss in patients with spinal cord injury. This bone loss occurred in all regions of the skeleton except the skull which remained unchanged. Generalised osteopenia in the majority of the skeleton following whole-body immobilisation is not surprising, however, it is interesting that the skull maintained or even gained its bone mass following apparent disuse. It is possible that under these circumstances the skull experienced no change in its mechanical environment or could even have experienced an increased loading stimulus through talking and eating. Alternatively, certain bones of the skull could respond to mechanical load in a way that is different from long bones and vertebrae. Indeed, O'Connor *et al* (1982) mentioned the concept of regional differences in skeletal response to the bone's mechanical environment.

There have been numerous other cross-sectional and longitudinal studies of the effects of exercise on bone mineral density in humans (Karlsson *et al* 1993; Bassey and Ramsdale 1994; Fehling *et al* 1995; Casez *et al* 1995). Cross-sectional studies often demonstrated greater increases in bone mass as a result of exercise-induced loading, than longitudinal studies. Chilibeck *et al* (1995) suggested that cross-sectional studies may be biased in that athletes had genetically more muscle and higher bone mass before commencing exercise programs. Hence, longitudinal studies may be more appropriate. However, the difficulty with such human studies is that most people have different lifestyles and compliance can often pose a problem.

Further studies of tennis players (Calder *et al* 1992) demonstrated that differences between playing and non-playing arms were greater than the differences between dominant and non-dominant arms in those who did not

play tennis (Chilibeck *et al* 1995) which implied a local effect of mechanical usage on skeletal adaptation.

A recent study found similar differences in the physical properties of the humeri of tennis players and attempted to investigate the geometrical properties of the bones (Haapasalo *et al* 1996). Interestingly, they found the greatest differences in players who had started playing at a young age. A possible explanation for this observation is that young players have bones and muscles that are growing. Therefore, it is possible that adaptive responses are more rapid because the bone and muscle tissue are metabolically very active. In addition, during modelling alterations in bone shape and mass may occur more quickly than in remodelling adult bones, which are no longer developing. The decreased response to mechanical loading with increased age could be due to a remodelling process which is slower than modelling, possibly together with reduced metabolic activity of the bone cells responsible for the transduction mechanism whereby load produces a cellular response. In addition, it may be due to alterations in the nature of the bone matrix with possible disruption of the cell-matrix connections (Rubin *et al* 1992). Age-related changes have also been observed in animal studies where adaptive responses to mechanical strain have been quantified in terms of strain magnitudes (section 1.2.4).

1.2.4 Quantifying the adaptive response of bone to mechanical strain

In 1964 Frost proposed the Flexural-Drift Laws of lamellar bone architecture (Frost 1973). He proposed that dynamic strain was responsible for the remodelling of lamellar bone in a defined way. He proposed a "minimum effective strain" (MES) required to initiate this adaptive lamellar bone response. In a review of this theory Frost (1973) described how bone that was subjected to flexural deformities underwent remodelling "drifts", in response to time-averaged flexural strains, to produce uniaxial loading when "flexural strain becomes satisfactorily minimised." The flexural drift rule stated that: All

bone surfaces tend to drift towards the concavity that arises during repeated dynamic flexure. He stated that the natural curvature of long bones existed to counteract the eccentric pull of muscles so that flexural moments were neutralised. Frost's views appeared logical, however, at the time he first published his theory there was no published work on *in* vivo physiological bone strain measurements. Frost's hypotheses required testing experimentally. This task, he was to leave to others.

Experiments conducted by Hert *et al* (1969;1971a) and Liskova and Hert (1971) showed that intermittent but not static mechanical loading of the rabbit tibia produced an increase in endosteal and periosteal cortical bone. This confirmed the need for dynamic forces to stimulate remodelling/modelling changes. Unfortunately, the response to mechanical loading was not quantified in terms of mechanical strain. Eight years later Churches *et al* (1979) showed that they could induce new bone formation in ovine metacarpals by loading transcortical steinmann pins. Although they did not measure load-induced bone strain, they were able to demonstrate a load-related response in the amount of new bone formed.

Goodship *et al* (1979) bonded strain gauges to the radial shafts of a group of pigs. Some of these had undergone ulnar osteotomy while the others were controls. They observed that overloading of the radius resulted in increased compressive principal strains on the craniomedial radial surface but that as the radius underwent hypertrophy and its cross-sectional area increased, the strain magnitude returned to normal. In the osteotomy animals this was associated with a radial cross-sectional area similar to the combined area of the radius and ulnae in the controls. It was suggested that the strain limits were universal for all bones. This study was important in that it correlated strain magnitude with an adaptive response to increased loading. However, it was not possible to control the conditions of loading.

Shortly after, Rubin and Lanyon (1981) developed an *in vivo* model in which the ulna of a rooster was functionally isolated by sectioning the ulna proximally

and distally. The cut ends were capped with stainless steel cups through which steinmann pins were placed. These emerged through the skin which allowed controlled external loading or clamping. They showed that intermittent dynamic loading at 0.5 Hz at compressive strains of 2100 μstrain at a strain rate of 10,000 μstrain per second produced an increase in bone mineral content (BMC). They had measured previously *in vivo* strain and found it to be approximately 2100 μstrain during vigorous wing flapping. It was an important finding that 36 cycles per day (cpd) produced a greater response than 5 cpd but similar increases in BMC to 1800 cpd. With this model they had demonstrated that a low number of cycles of dynamic loading which produced strains that were physiological in magnitude but abnormal in distribution were capable of increasing bone mass in a dose responsive way.

Shortly after, O'Connor *et al* (1982) made a very important observation. They showed in sheep antebrachii which were loaded externally that the magnitude of the loading response was affected by rate of strain change. The greatest response was associated with the highest loading strain rate ratios compared with normal walking.

In a later review by Frost (Frost 1983), he suggested that the MES range was between 800-2000 μstrain. This of course assumed that all bones would respond in a similar way to their mechanical environment and failed to consider the possibility of regional differences in the role and physiology of different bones. In addition, it was likely that in a given bone, the strain threshold for remodelling would be dependent on the specific pattern of strain i.e. distribution (Lanyon *et al* 1982) and the strain rate (O'Connor *et al* 1982).

Subsequent studies using the isolated avian ulna demonstrated that static loads did not produce the increase in bone observed after dynamically loading (Lanyon and Rubin 1984). This finding supported the previous findings of Hert *et al* (1969; 1971a) and Liskova and Hert (1971). In further experiments using the isolated ulna model in turkeys Rubin and Lanyon (1985) established a

relationship between the change in the loaded ulnar cross-sectional area and the loading strain magnitude and observed a threshold of 1000 μstrain before any response was apparent. Subsequently, Pead and Lanyon (1990) demonstrated that loading conditions which produced similar peak principal shear strain magnitudes in torsion and longitudinal compression were most osteogenic in longitudinal compression. This emphasized the importance of considering strain distribution in evaluating the osteogenic potential of mechanical loads.

Rubin *et al* (1992) described a greatly diminished osteogenic response to loading of the isolated turkey ulna in three year old birds compared with those aged one year. In this experiment the bones were loaded for 300 cpd at 3000 μstrain. Similarly, using the four point tibial bending model in the rat, thresholds of 1050 μstrain for lamellar and woven bone formation on the endosteal surface were described in retired breeder rats (Turner *et al* 1994). Subsequently, Turner *et al* (1995) demonstrated an increase in endosteal strain threshold (1700 μstrain) in older rats. However, strain was not measured directly in these experiments; it was calculated theoretically.

In 1993, a rat *in vivo* loading model was described in which the seventh and ninth caudal vertebrae were pinned. External loads applied to the pins produced compression loading of the eighth caudal vertebra (Chambers *et al* 1993; Chow *et al* 1993). This model demonstrated new trabecular and periosteal bone formation in response to the applied loads. However, there was no evidence that recordings were taken of *in vivo* physiological strains from the eighth caudal vertebrae before deciding on the loading regime of 150 N. This load has been shown to produce around 700 μstrain in compression (Fox *et al* 1995) which, despite being physiological for many bones such as the tibia, may not be physiological for all bones including caudal vertebrae. Indeed preliminary data (Hillam unpublished data) showed that normal strain recorded from a rat *in vivo*, from a single-element strain gauge bonded to the lateral aspect of the seventh caudal vertebra, parallel to its long axis, did not exceed

200 μstrain even during the most vigorous of activities. In addition, a load of 150 N which is applied indirectly in Chambers' model via a pulley system, has been shown subsequently to generate considerably higher strains than 700 μ strain (Dr. L. Miller, Glaxo Pharmaceuticals, USA personal communication). These findings suggest that the load of 150 N may be deforming the eighth caudal vertebrae to strain magnitudes which are at least four times greater than those experienced *in vivo*. Although the model has the potential advantage that both trabecular and cortical bone can be studied, it suffers from the potential disadvantages associated with surgical trauma and the presence of implants. Although the eighth caudal vertebra is loaded indirectly, the pins are located in very close proximity and it is, therefore, possible that inflammatory mediators could affect the bone by the regional acceleratory phenomenon (Frost 1983). The authors described a substantial degree of new woven periosteal bone as a result of loading. In a rat model of femur fracture healing it has been shown that loose fixator pins can stimulate profound formation of new woven bone along the entire length of the femur (Harrison and Goodship unpublished data). This raises the question whether the observations made in the caudal vertebral loading model may have been due, at least in part, to indirect functions other than direct strain-related mechanisms influencing the eighth vertebra.

A model by which the rat ulna is loaded non-invasively *in vivo* was developed by Torrance in 1993. Medial periosteal formation at the mid-diaphysis was shown to occur in a strain magnitude dependent manner. It has the advantage over the four point tibial loading system in that there is no trauma near the sampling point because the points of load application are the carpus and olecranon, whereas the bone is sampled at the mid-diaphysis (Torrance *et al*, 1994). The strain magnitudes used are supraphysiological (3500-4500 μstrain) and daily loading takes only four minutes without signs of lameness upon recovery from anaesthetic.

Rubin and McLeod (1994) described the non-uniform strain properties of strain magnitude and strain energy density across a bone's cortex. They proposed an alternative to the strain magnitude paradigm for the maintenance of bone morphology. They suggested that strain frequency may play an important part of the osteogenic stimulus. They hypothesised that low magnitude strains in the 15-50 Hz range may be as osteogenic as the lower frequency, high magnitude strains (McLeod and Rubin unpublished) after demonstrating that frequency dependent, low strain magnitude loads induced bony ingrowth into orthopaedic implants (Rubin and McLeod 1994).

1.3 Transduction of the mechanical stimulus into an adaptive cellular response

1.3.1 Introduction

There is considerable evidence to suggest that mechanical strain provides a major stimulus which affects bone modelling and remodelling (section 1.2.4). In order to produce an adaptive response, this stimulus must be detected and translated into appropriate cellular activity.

In the 1930's John W.S. Pringle of the University of Oxford was the first person to investigate the function of cuticle sensors in the exoskeleton of arthropods (cited by Zill and Seyfarth 1996). It was noted that these sensors were concentrated at certain locations such as sites of muscle attachment and were orientated in a precise and consistent way. Subsequently, these sensors have been identified as exoskeletal strain gauges. Their orientation has been identified as being either perpendicular or parallel to the long axis of the leg. In this respect they function as 90° rosette strain gauges (Zill and Seyfarth 1996). Their function is believed to be related to coordination of locomotion and orientation memory (Zill and Seyfarth 1996). Although no such discreet sensors have been identified in bone, it is likely that certain bone cells possess a similar function, indeed, it is accepted generally that some function of strain i.e.

magnitude, rate, distribution, gradient, energy or frequency is perceived by bone cells, however, it has also been suggested that the matrix itself may be responsible for responding to the imposed loads (Justus and Luft 1970; Treharne 1981; Skerry *et al* 1988, 1990).

Lanyon (1984) proposed that strain information distributed throughout the bone may be 'integrated' and assessed by the resident osteocytes. They may communicate the strain information by the extensive network of interconnecting canaliculae. That the osteocytes respond to the effects of strain was shown by Skerry (1989) who described an increase in G6PD activity in the osteocytes of the avian ulna only six minutes after mechanical loading *in vivo*. The activity of individual osteocytes was not affected significantly but the number of osteocytes demonstrating G6PD activity was increased. The number of osteocytes affected was observed to be proportional to the strain magnitude at that site within the bone. Although this showed a strain magnitude-dependent response within osteocytes, it did not confirm that osteocytes were responsible for actually perceiving the strain stimulus in a physiological capacity. Indeed, even if the osteocytes had reacted directly to strain this response may have represented a functional mechanism originally possessed by osteoblasts but retained as a vestigial process by the osteocytes, following entrapment within the lacunae. Alternatively, the osteocytes' activity may have been a secondary effect following a primary response to mechanical deformation elsewhere.

A recent *in vitro* study also supported the hypothesis that osteocytes may be responsible for the mechanosensory mechanism in bone. In 1995 Klein-Nulend *et al* showed in cultures of chicken calvarial cells that osteocytes were sensitive to pulsating fluid flow which stimulated a release of prostaglandin E, whereas, osteoblasts and periosteal fibroblasts released no prostaglandin E. The authors concluded that osteocytes were the most sensitive bone cells involved with mechanotransduction, however, they only looked at prostaglandin release in what is likely to be a very complex mechanism. In contrast, Rawlinson *et al*

(1995) looked at prostanoid release into the culture media of organ cultures of rat calvariae subjected to two regimes of mechanical strain. They found no significant differences in the concentration of prostaglandin E_2 and 6-keto-prostaglandin $F_{1\alpha}$ compared with un-loaded controls.

A number of mechanisms by which strain is transduced into a primary cellular response have been proposed and are discussed in the following sections.

1.3.2 Deformation

Justus and Luft (1970) suggested that tension within the matrix may result in a rise in the concentration of extra-cellular calcium. This rise, which they proposed to be independent of cellular activity, would stimulate osteoclast activity. This theory has not been adopted widely, because it is generally considered more likely that the mechanical transduction mechanism is mediated by cells such as the osteocytes, osteoblasts and lining cells.

Deformation could bring about a cellular response through changes in hydrostatic pressure, shear forces generated by fluid flow or direct deformation of the matrix and bone cells.

Fluctuation in hydrostatic pressures have also been suggested to affect osteocytes (Jendrucko *et al* 1976). They calculated that in the human tibia intralacunar pressures of 50 MPa could be produced, theoretically, as a result of weight bearing. It is uncertain how pressure changes might affect cells because they are liquid-filled bodies which in a hydraulic system would probably not deform much with changes in pressure as their contents are unlikely to be very compressible. Weinbaum *et al* (1994) hypothesize that fluid shear stresses are responsible for osteocytic mechanotransduction. The study of Klein-Nulend *et al* (1995) provided evidence to support this hypothesis in that cultures of osteocytes responded to pulsating fluid flow but not to intermittent changes in hydrostatic pressure.

In vivo, Skerry (1989) calculated that physiological strain would produce a maximum change in dimension of an osteocyte of less than 30 nm. This theoretical calculation was made assuming uniform deformation of the cells and also assumed that the cells deformed in proportion to the bone as a whole. It is possible that such a small change in size may not trigger a significant response without some means of 'signal amplification'. This could feasibly be mediated by effects on the cytoskeleton or the attachment of the cells' cytoplasmic processes to the surrounding matrix. Skerry *et al* (1988; 1990) have shown rapid bone matrix proteoglycan reorientation following brief periods of mechanical loading *in vivo* and *in vitro*. They proposed that this reorientation, which lasts for over 24 hours after loading may be a mechanism facilitating "strain memory" within the bone and suggested that changes in the physical properties in the matrix may affect the cellular response through the interaction between the matrix proteoglycans, cell membrane and cytoskeleton of bone cells. Indeed there is evidence from *in vitro* studies, using tensegrity (tensional integrity) cell models, that cell surface receptor molecules, called integrins (Hynes 1987), are involved in mechanotransduction by transmitting strains present in the extra-cellular matrix to stretch-activated ion channels in the cell membrane (Rodan 1991) or through the cell membrane to the microtubule network of the cells' cytoskeleton (Wang *et al* 1993; Wang *et al* 1994).

1.3.3 Microdamage

Microdamage can be defined as the formation of multiple, small, discontinuous cracks which occur in regions of high stress within the bone matrix (Currey 1984). This process is regarded commonly as being responsible for 'fatigue' or 'stress' fractures following repetitive loading cycles in humans and animals.

Grieg (1931) was first to suggest that microdamage could stimulate remodelling in bone and this was supported by Carter (1984). In 1981 Rubin and Lanyon showed that as few as 36 loading cycles at 2100 μstrain were all

that were necessary to stimulate an adaptive response. Theoretically, repetitive loading at these strain magnitudes would only produce fatigue failure after approximately one million cycles (Carter 1984). Therefore, it is likely that the osteogenic stimulus in Rubin and Lanyon's model may not involve microdamage.

Microdamage has been reported to be important in the etiology of the metacarpal stress fractures ("bucked shins") in race horses (Nunamaker *et al* 1990) and of fatigue fractures of metatarsals and tibiae of army recruits (Burr *et al* 1996). Strain gauge studies in human volunteers have shown that the maximum principal strains that occur at the tibial midshaft; the site of these fatigue fractures are around -1200 μstrain during vigorous activity (Burr *et al* 1996) while Nunamaker *et al* (1990) reported mean maximum principal strain magnitudes of -4841 μstrain on the dorsal surface of the metacarpal mid-shaft (i.e. the site of stress fractures) in two year-old Thoroughbreds during maximum exertion. These animals were trained at 10,000 to 12,000 cycles per month and had experienced clinical signs of stress injury at between 35,000 - 53,000 cycles. However, microdamage leading to these gross injuries would have occurred after a lower number of cycles.

There is evidence that the amount of microdamage within cortical bone accumulates with age (Burr 1993; Biewener 1993; Schaffler *et al* 1995). Microcallus formation has also been demonstrated in the trabeculae of the human spine (Hahn *et al* 1995) indicating that microdamage occurs in trabecular bone also. It is logical to suggest that microdamage would influence remodelling activities, in an attempt to restore the material properties of bone. However, the mechanism by which microdamage arising from normal physiological activity affects the cellular processes of bone remodelling is not clear. In addition, it is possible that microdamage-related cell activity may represent primarily a repair process rather than a physiologically important mechanotransduction mechanism.

Bentolila *et al* (in press) have demonstrated microdamage with evidence of intracortical remodelling in loaded ulnae of rats so this may prove a useful model with which to investigate the cellular mechanisms involved in microdamage-related cellular remodelling.

1.3.4 Piezoelectricity and streaming potentials

Electrical effects on the regeneration of tissue have been described in amphibians by Smith (1967) and mammals by Becker and Spadaro (1972). Subsequent work has investigated the existence of bioelectricity and the effects of applied electrical fields on bone cells *in vitro* and osteogenesis, disuse osteopenia and fracture healing *in vivo*.

Piezoelectricity can be described as "pressure electricity" brought about by applying stress to a crystalline structure. Piezoelectricity has been described in dry bone by Fukada and Yasuda (1957) and Bassett and Becker (1962). It has also been reported to exist in dry tendon (Fukada and Yusada 1964). In dry bone its effect is considered to be the main mechanism for the generation of strain-related electrical potentials (SRPs) (Eriksson 1976) which arise from deformation of the collagen component of the bone matrix (Becker 1978). However, in wet bone Cochran *et al* (1989) and Otter *et al* (1990) reported that the predominant mechanism responsible for SRPs is thought to be from a different mechanism. This electrokinetic effect is known as a streaming potential. It is considered to arise from the flow of ions within fluid that is forced through the small pores within the bone matrix as a result of stress-generated pressure gradients (Dillaman *et al* 1991).

Lanyon and Hartman (1977) described SRPs in sheep both *in vivo* and *in vitro*. They observed that the magnitude and form of these potentials were related to the bone strain magnitude and strain rate. Similarly, Otter *et al* (1992) described streaming potentials in canine bone, *in vivo* and *in vitro* using the same bones, in an attempt to compare *in vivo* and *in vitro* data. Apart from SRPs, Otter *et al* (1990) described transcortical streaming potentials *in vivo*

from the canine tibia which were considered to arise from pulse-related, transcortical pressure gradients. By injecting protamine sulphate into the femoral artery Otter *et al* (1993) were able to reduce the magnitudes of the strain related potentials and even reverse the voltage signs. Unfortunately, the procedure proved fatal and therefore, investigation of the long term effects of modulating streaming potentials on bone remodelling were not possible.

Exogenous electric fields have also been used to enhance bone healing (Bassett *et al* 1977; Otter *et al* 1996) and reduce the rate of disuse osteopenia in the functionally isolated canine fibula (Skerry 1989) and in the functionally isolated avian ulna (McLeod and Rubin 1992).

Because cells are known to possess transmembrane electrical potentials and because of the profound effect of neuronal action potentials on the effector organs, it is likely that streaming potentials represent an important mechanical transduction mechanism.

1.3.5 Nervous control

It was Gros, who in 1846 first described the presence of nerves within bone. He described how nerves entered along side the nutrient artery and remained associated with the blood vessels. The presence of both myelinated and unmyelinated nerve fibres was observed later by Variot and Remy (1880). Nerves supplying bone are responsible for pain sensation and also affect blood flow (Duncan and Shim 1977). How nerve supply might affect bone modelling and remodelling is not known. It is possible that the sympathetic innervation could influence indirectly these cellular activities by its effect on blood supply and consequent effect on streaming potentials. However, Hert *et al* (1971b) demonstrated that neurectomy did not affect the osteogenic effect of mechanical loading of the rabbit tibia. Despite the rich periosteal and endosteal innervation of bone it would appear that central innervation does not influence directly the functional adaptation of bone to intermittent loading.

There are numerous gap junctions which allow osteocytes to communicate with one another and with osteoblasts on the bone surface (Doty 1981; Aarden *et al* 1994). The cellular processes and these gap junctions which facilitate this inter-cellular communication could be considered a form of primitive nervous system within bone.

1.4 The effect of hormones on bone

1.4.1 Introduction

Agents which exert an effect on bone cells are described as being osteotropic in action. There are several hormones which have direct and indirect effects on bone cells. Osteotropic hormones include: Thyroid hormone, parathyroid hormone, parathyroid hormone-related peptide, calcitonin, androgens, oestrogens, glucocorticoids and growth hormone. Vitamin D may also be considered an osteotropic hormone. These hormones can affect a range of different cell types: periosteal or endosteal osteoblasts, other lining cells, bone marrow cells, osteoclasts, muscle, kidney, intestine.

1.4.2 Oestrogens

There are three naturally occurring oestrogens in the human: oestrone, oestradiol and oestriol. In premenopausal women, oestradiol is the most abundant and the most potent of the three oestrogens. Oestriol is a metabolic product of the other two oestrogens and it only has weak oestrogenic actions. Oestradiol is produced mainly (about 90%) in the ovaries by direct secretion. The remaining 10% is produced peripherally by conversion of oestrone, androstenedione and testosterone in adipose tissue. In the premenopausal female, half of the androgen synthesis (testosterone and androstenedione) occurs in the ovaries. The other half is produced in the adrenal glands. After menopause, oestradiol levels fall by more than 90% and oestrone becomes the

most abundant. It is produced peripherally by conversion of androstenedione in adipose tissue.

For nearly sixty years, it has been recognized that bone loss associated with osteoporosis is most common in postmenopausal women (Albright *et al* 1940). It has been demonstrated that decreased ovarian function is associated with bone loss by calcium balance studies (Heaney *et al* 1977, 1978a, 1978b) and by looking at cortical bone thickness of the metacarpal bone (Lindsay *et al* 1980). This postmenopausal bone loss is now widely accepted and modern imaging techniques such as dual energy Xray absorptiometry (DEXA) and quantitative computed tomography (QCT) measure quantitatively this loss in the whole body or specific parts, for example, in the spine, wrist or hip.

Bone loss associated with loss of ovarian hormones has also been demonstrated in animals. The adult rat model of ovariectomy-induced osteopenia has been characterised thoroughly and is used extensively in research into oestrogen-mediated effects on bone remodelling (section 1.6).

It is well established that prophylactic treatment with oestrogens in the form of hormone replacement therapy (HRT) around the time of menopause can protect against osteopenia and if given later, after the onset of menopause will retard the rate of bone loss (Christiansen and Riis 1990). This has also been demonstrated in animal models (Kalu 1991).

Clearly, oestrogens have a profound effect on bone cells, particularly in respect to bone resorption. However, their mechanism of action remains unclear (Mundy 1993; Braidman *et al* 1995). Oestrogen receptors have been demonstrated in cells of the osteoblast lineage (Komm *et al* 1988; Eriksen *et al* 1988; Ikegami *et al* 1994) and there are reports of their presence in osteoclasts (Oursler *et al* 1990; Pensler *et al* 1990) and osteocytes in the human, pig and guinea pig and also chondrocytes in the pig (Braidman *et al* 1995).

It is possible that the effects of oestrogens on osteoclasts are mediated indirectly through the osteoblast (Mundy 1993). TGFβ is known to inhibit osteoclastic bone resorption in some *in vitro* systems (Chenu *et al* 1988; Pfeilschifter *et al* 1988) and it is possible that oestrogen-mediated release of TGFβ is responsible, at least in part for a decrease in bone resorption. It is likely that another possible mechanisms of action of oestrogens includes the inhibition of prostaglandin release and effects on cells of the immune system (Mundy 1993). Despite uncertainty regarding oestrogen's specific mechanisms of action, its bone sparing effect is thought to act by blocking: osteoclastogenesis, activation of mature osteoclasts and apoptotic osteoclast death (Pacifici 1996).

In 1987 Frost proposed that the endocrine and other changes associated with the menopause resulted in an alteration of the "setpoint" of the "mechanostat". Indeed it has been documented that exercise and weight-bearing did not stimulate the same degree of bone formation in ovariectomized rats compared with ovary-intact rats (Hume *et al* 1989) and amenorrhoeic women compared with eumenorrhoeic women (Rodan 1991). There is evidence now from subsequent clinical studies that there may be a synergistic effect between mechanical loading and oestrogens on bone formation in certain regions of the skeleton (Notelovitz 1991; Kohrt *et al* 1995). This synergism has also been demonstrated *in vitro* using organ cultures of rat ulnae (Cheng *et al* 1996). They observed additive effects of mechanical loading and oestrogen in the ulnae from male rats. However, the effects were synergistic in the bones from female rats.

Further investigations are required into the cellular mechanism of action of oestrogen and its interaction with mechanical loading and other osteotropic hormones such as parathyroid hormone, before the mechanism of postmenopausal bone loss can be understood better. This may prove necessary for the development of successful strategies aimed at the prevention and therapy of postmenopausal osteoporosis.

1.4.3 Parathyroid hormone and its paradoxical effect on bone

Parathyroid hormone (PTH) is an 84 amino acid straight-chain polypeptide. It is produced and stored by the chief cells of the parathyroid glands. The glands derive their embryological origin from the third and fourth pharyngeal pouches during development. The major regulator of PTH secretion from these glands is the concentration of ionised blood calcium, with low levels of calcium triggering PTH release and high levels inhibiting it. Chronic stimulation of the chief cells results in their replication. Other factors also influence PTH release: magnesium has a similar effect to calcium although quantitatively modest in comparison and there is recent evidence from *in vitro* studies that phosphorus can stimulate PTH release (Almaden *et al* 1996). Catecholamines stimulate release although little is known about its physiological importance. In addition, metabolites of vitamin D are known to inhibit PTH synthesis. However, it is not known whether the mechanism is direct or indirect. It is likely that the effects are indirect; mediated by increases in blood calcium (Kronenberg *et al* 1993). There are two receptors for PTH, the PTH-1 receptor and the recently discovered PTH-2 receptor (Usdin *et al* 1995).

Humoral hypercalcaemia of malignancy (HHM), which is the humoral hypercalcaemia observed in some cases of human neoplasia was first described as long ago as 1941 (Stewart 1993). It has been shown subsequently that typical patients have little or no skeletal involvement with the neoplasia and that the hypercalcaemic condition reverses upon successful treatment of the tumour (Stewart 1993). However, it wasn't until 1987 that a peptide called parathyroid hormone-related peptide (PTHrP) was discovered and found to be responsible for HHM (Suva *et al* 1987; Burtis *et al* 1987; Stewart *et al* 1987; Moseley *et al* 1987). PTHrP is a larger polypeptide than PTH and is only similar in its amino acid sequence in the binding region of the molecule. This enables both PTH and PTHrP to bind competitively to the same receptor (PTH-1) (Abou-Samra *et al* 1989) and with similar affinities (Orloff *et al* 1989).

Little is known about the true physiological role of PTHrP (Walsh *et al* 1995). However, it is known to affect osteoblasts (Suva *et al* 1987), stimulate bone resorption both *in vivo* (Horiuchi *et al* 1987) and *in vitro* (Evely *et al* 1990), enhance renal calcium absorption (Martin 1990) and modulate growth of rabbit kidney proximal cell tubule cells *in vitro* (García-Ocaña 1995).

Parathyroid hormone exerts its principal effects on kidney and bone although there are receptors for PTH / PTHrP in many other tissues (Orloff *et al* 1989). Its effects on the kidney serve to stimulate reabsorption of calcium but inhibit reabsorption of phosphate from the glomerular filtrate. In addition it stimulates synthesis of 1,25 dihydroxyvitamin D_3 in the kidney which in turn stimulates absorption of calcium and phosphate from the intestine. Sytemically, the overall effect of PTH is to raise blood calcium and lower phosphate levels. The physiological effects of PTH on bone are complex and remain unclear. It has been shown to be responsible for stimulating osteoclastic resorption (Nijweide *et al* 1986; Mundy & Roodman 1987). However, in a study using injections of radiolabelled PTH it has also been shown to be associated with forming but not resorbing cortical bone surfaces in young growing rats (Fermor and Skerry 1995).

For some time PTH-induced osteoclastic resorption has been thought to be the result of an indirect mechanism by which PTH acts primarily on PTH receptors on the osteoblasts (Rodan & Martin 1981; McSheehy & Chambers 1986). However, there is recent evidence that osteoclasts may respond directly to PTH as well. In a study by Tong *et al* (1995) osteoclasts from mouse long bone that were treated with PTH and plated out onto dentine slices produced more resorption pits than untreated osteoclasts. In addition they also demonstrated osteoclastic receptors for PTH. In separate experiments, it has been shown that osteoclasts plated onto devitalised bovine cortical bone produced higher levels of superoxide anion (an indicator of osteoclastic activity) when they were exposed to PTH, compared with controls (Datta *et al* 1995).

Heaney (1965) and Jasani (1965) proposed that there may be an increased sensitivity of bone to the resorptive effects of PTH following menopause. Several studies have been conducted in animals, humans and *in vitro* to test this hypothesis. Orimo *et al* (1972) looked at the femora and tibiae of intact and ovariectomized rats following treatment with PTH and concluded that bone was more sensitive to the resorptive effects of PTH in the absence of endogenous oestrogens. Recently a human study was conducted by Fujiyama *et al* (1995) investigating bone mineral density and metabolic markers of bone turnover in a group of post menopausal patients. Half were euparathyroid, the remainder being hypoparathyroid. They found that the hypoparathyroid condition protected against age-related bone loss, particularly early after menopause. In addition *in vitro* studies have also demonstrated that oestrogen could protect against PTH stimulated bone resorption (Pilbeam and Raisz 1988; Most *et al* 1995). The findings of these studies lend support to Heaney and Jasani's hypotheses.

As well as stimulating bone resorption PTH has also been shown paradoxically to stimulate bone formation when it is infused intermittently into humans (Reeve *et al* 1980; Slovik *et al* 1986; Lindsay *et al* 1993). There are also numerous examples of the anabolic effect of PTH when administered intermittently: to intact rats (Gunness-Hey & Hock 1984; Oxlund *et al* 1993; Jerome 1994) to rats after ovariectomy (Liu *et al* 1991) and to rats following hindlimb immobilisation (Ma *et al* 1995). In addition, it has also been demonstrated that PTH protects against ovariectomy-induced bone loss in rats when administered at the time of ovariectomy (Liu & Kalu 1990).

Currently, research is directed predominantly at investigation of the anabolic effect of PTH (Reeve 1996). However, the findings of Fujiyama *et al* (1995) are worthy of further investigation in an attempt to gain further insight into the possible interaction between PTH and oestrogen. A study conducted by Sims *et al* (1994) failed to demonstrate a protective effect of parathyroidectomy on ovariectomy-induced osteopenia in rats, however, the study was flawed

because young, growing animals were used. Continual formation of trabecular bone may have complicated interpretation of the results. Unfortunately they did not have a group of basal controls, killed at the start of the experiment, to compare with the end controls. Therefore, it is possible that if older rats had been used the results may have been different.

1.4.4 Calcitonin

Calcitonin was discovered 30 years ago (Mundy 1993). It is a 32 amino-acid polypeptide produced by the thyroid gland parafollicular cells (C-cells) which are derived embryologically from the neural crest. The pituitary gland and other neuroendocrine cells can also act as sources of calcitonin (Becker *et al* 1980; Fischer and Born 1987; Deftos 1987). However, non-thyroidal sources of calcitonin are unlikely to contribute to its concentration in the blood (Deftos 1993).

Calcitonin receptors are most concentrated in the bone, kidney and hypothalamus (Goltzman and Mitchell 1985) and are similar structurally to the PTH/PTHrP receptor (Deftos 1993). Two isoforms of the calcitonin receptor, C1a and C1b have been identified in rats (Sexton *et al* 1993) and mice (Ikegame *et al* 1995), the specific roles of which remain unclear.

As long ago as 1968 Friedman *et al* demonstrated in fetal rat long bones that calcitonin inhibited osteoclastic resorption. *In vivo* (Au 1975; Binstock & Mundy 1980) and *in vitro* (Wener *et al* 1972) it has been shown that the effects of calcitonin are transient. It inhibits the formation of osteoclasts from precursors and results in the transformation of mature osteoclasts into mononuclear cells (Baron and Vignery 1976). Within minutes of administration calcitonin results in shrinkage of the osteoclasts, consequently inhibiting bone resorption (Deftos and Glowacki 1984; Moonga *et al* 1992) which results in a reduction of the blood calcium ion concentration. Its effect overall is to conserve bone mass. It is interesting that not all osteoclasts

possess calcitonin receptors. Indeed, Nicholson *et al* (1987) failed to demonstrate any binding of radio-labelled salmon calcitonin to cultures of embryonic chick osteoclasts which suggested that avian osteoclasts did not respond to calcitonin directly. In addition, Ikegame *et al* (1996) reported the appearance of calcitonin receptor-deficient osteoclast-like cells in cultures of mouse cells exposed continuously to calcitonin, which may help to explain the transient effect of calcitonin ("escape phenomenon"). There are reports that calcitonin also acts to inhibit osteocytes and stimulate osteoblasts, although these are controversial (Deftos and Glowacki 1984).

The physiological importance of calcitonin in calcium homeostasis and control of bone remodelling remains unclear. It is possible that its role may be to inhibit bone resorption transiently when there is no need for bone turnover to maintain extracellular calcium levels, for example, after a meal when calcium is absorbed from the intestine (Mundy 1993). Hillsley and Frangos (1996) have suggested that together with PTH, calcitonin may play a role in altering fluid flow through the bone by altering osteoblast hydraulic conductivity at the endosteum. Whether the transient effects of calcitonin are likely to have significant implications on bone mechanotransduction in terms of fluid flow remain to be seen. *In vivo* experiments investigating the effects of PTH and calcitonin on the generation of strain-induced streaming potentials may be useful to test this hypothesis.

Therapeutically calcitonin is used for the treatment of osteoporosis, Paget's disease and HHM, with non-mammalian calcitonin possessing greater potency than mammalian calcitonin in its anti-resorptive effects.

1.4.5 Thyroid hormones

Thyroxine (T_4) is produced by the thyroid gland. It is stored within the colloid of the thyroid follicles. Its release is stimulated by the thyrotropic hormone, thyroid stimulating hormone (TSH) Once released into the circulation T_4 may

undergo deiodination at several sites, including the liver and kidney. The product of this deiodination is tri-iodothyronine (T_3).

The production and release of thyroid hormones relies on negative feedback of T_3 and T_4 on the pituitary gland which in turn affects the release of TSH, with no evidence to suggest that thyroxine secretion is regulated by effects on bone remodelling or calcium homeostasis.

In the circulation in man about 99% of thyroxine is bound with high affinity to a globulin protein. However, in rats only about 75% of the thyroxine is bound with low affinity to albumin. These differences in protein-binding reflect the differences in thyroxine half-life between humans and rats. In humans, the half-life is seven days whereas in rats it is about 12 hours (Davies 1993). It is only the free-T_3 and the free-T_4 that are biologically active. Davies (1993) reports that free-T_3 is about four times more potent than free-T_4. However, this is likely to depend on the target tissue and there are probably species differences, as Alini *et al* (1996) describe T_3 as being at least 50 times more potent than T_4 at stimulating bovine growth plate chondrocyte hypertrophy.

The thyroid hormones possess a role in skeletal physiology. They are required together with growth hormone in the young growing animal for normal endochondral ossification to occur (Vaughan 1981). Recently Alini *et al* (1996) have described the requirement for T_3 or T_4 for normal chondrocyte differentiation and collagen type X synthesis leading to chondrocyte hypertrophy and subsequent matrix calcification *in vitro*. Most of the literature refers to abnormalities in thyroid hormone metabolism and their consequent pathological effects on bone. Direct stimulation of bone resorption by thyroid hormones has been demonstrated *in vitro* (Mundy *et al* 1976) and in clinical cases of hyperthyroidism, it has been associated with osteopenia in humans (Seeman *et al* 1982) and in rats (Rosen *et al* 1993) whereas, in cases of hypothyroidism it has been shown in humans that the rates of bone turnover were reduced (Mosekilde and Melsen 1978).

1.5 Cytokines and local factors

The influence of mechanical load and systemic hormones can alter the quality and architecture of bone by the concerted activity of haemopoietic and bone cells, the spatial and temporal coordination of which are mediated through a diverse range of local chemical factors. Although the work in this thesis examines the effects and possible interactions of a variety of mechanical and hormonal influences, it does not investigate the complex role of such paracrine factors, a thorough review of which is beyond the scope of this introduction.

A cytokine may be defined as a soluble (glyco)protein, non-immunological in nature, released by living cells of the host, which acts non-enzymatically in picomolar to nanomolar concentrations to regulate host cell function to control the modelling and remodelling of tissues. They can be described as symbols in an intercellular language who's actions are on tissues rather than individual cells (Nathan and Sporn 1991).

The area of cytokine research related to bone has expanded massively in the last decade, making it difficult to interpret with clarity, the physiological relevance of much of this *in vitro* work due to results which often appear contradictory. Future *in vitro* experiments should take into account the complex extracellular milieu to enable the design of studies to establish the physiologic and pathophysiologic relevance of the action of cytokines on a tissue *in vivo* (Nathan and Sporn 1991).

Osteotropic cytokines and local factors include: interleukins (IL-1 and IL-6), tumour necrosis factor (TNF), lymphotoxin, insulin-like growth factors (IGF-I and IGF-II), transforming growth factor (TGF_{β}), prostaglandins (PG's), leukaemia inhibitory factor (LIF), macrophage and granulocyte/macrophage colony stimulating factors (CSF-M & CSF-GM) and nitric oxide.

Table 1.1

Summary of actions of cytokines and local factors

Cytokine/local factor	Bone resorption	Bone formation
IL-1	YES - *in vitro* + *in vivo*	YES - *in vivo*
IL-6	YES - *in vitro*	~
TNF	YES - *in vitro*	~
TGF_{β}	YES - *in vitro*	YES - *in vitro* + *in vivo*
LIF	YES - *in vitro*	~
IGF's	~	YES - *in vitro*
PG	YES - *in vitro*	YES - *in vivo*

Three recent studies in this field have demonstrated some interesting findings which are pertinent to this thesis:

a) In 1994 Kawaguchi *et al* investigated the effects of 3,5,3'-triiodothyroacetic acid (triac) and triiodothyronine (T_3) on resorption of fetal rat long bones and neonatal mouse calvariae *in vitro*. The findings showed that bone resorption was dependent on prostaglandins in the mouse calvariae but prostaglandin-independent in the rat long bones. Despite bones from different species and at different stages of development being used, these results suggested a possible difference between the parietal bone and the long bones in the mechanisms leading bone resorption.

b) Shortly after the findings of Kawaguchi *et al* were published, Finkelman *et al* (1994) demonstrated elevated levels of IGF-II and TGF-ß in human calvaria compared with iliac crest and vertebral bodies from the 10 aged male donors. This provided further evidence to suggest that there are regional differences between calvarial bone and bone from other sites in terms of their physiology.

c) In 1995 Rawlinson *et al* conducted studies into the effects of mechanical loading on organ cultures of rat ulnae and also rat parietal bones from the same

animals. The parietal bones were loaded at two load magnitudes. One was 100 μstrain, which had been shown to be physiological for these bones and the other magnitude was 1000 μstrain which was the same magnitude used to load the ulnae. This also had been shown previously to be physiological for rat ulnae. The results showed that there were no differences in the amount of PGE_2 and 6-keto-$PGF_{1\alpha}$ released into the culture medium compared with control calvariae. In contrast, differences had been observed in the loaded ulnae which released significantly higher amounts of these compounds into the culture medium compared with controls. Additionally, the loaded ulnae also demonstrated higher G6PD activity whereas the loaded calvariae did not, compared with controls. These data showed clear differences between calvarial bones and the long bones from the same animals, in their response to physiological mechanical loading. This experiment used whole bones in organ culture, so it cannot be assumed that identical processes would occur *in vivo*, however, within the limits of *in vitro* investigations it represents one of the clearest demonstrations of regional differences in bone physiology to date.

These three studies have demonstrated a requirement to investigate further regional differences in bone physiology with a need to extend the investigations to the living animal.

1.6 Choice of an animal model for research into normal human bone biology and human bone diseases

There is only one perfect *in vivo* model for human bone research; the human. Obviously, this is neither practical or ethical. Careful consideration has to be given to the choice of an *in vivo* model.

In a review article on the ovariectomised rat model of post menopausal bone loss (Kalu 1991), three characteristics for an animal model of disease cited

from Wessler (1976) are that the model should be convenient, relevant and appropriate. Convenience refers to the ease with which the model can be used. The rat is small, amenable to handle and easy to house. It therefore fulfills this criterion. Relevance refers to the comparability of a phenomenon under investigation in the model with that in the human. Rats have been shown to be good models for post menopausal cancellous bone loss (Kalu 1991; Wronski & Yen 1991). In ovariectomized rats, there is early rapid cancellous bone loss associated with an increased bone turnover. Later bone turnover slows down and the rate of bone loss declines. These effects are reproducible and mimic the human response to ovariectomy or the post-menopausal condition (figure 1.6). Appropriate refers to the complex of other factors which influence the choice of that animal as a suitable model. The rat is cheap, widely available and details of its physiology are well understood because of its very widespread use in many other fields of biological research and toxicology. In addition, the disadvantages are outweighed by the advantages when considering the criterion of relevance so that it also fulfills the final criterion of appropriateness.

There are at least four reasons why rats have not been universally adopted for research into postmenopausal bone loss (Kalu 1991):

1. Because osteoporosis in humans is a common disease many studies have used bone biopsies from affected patients. In this respect, there has always been a constant source of human bone for research. This meant that for a long time there was little pressure to find and characterise a suitable animal model.
2. Compared with humans, rats' bone mass remains stable for a long time relative to their life span.
3. The rat skeleton is commonly perceived to grow continuously throughout life. For this reason the rat has often been considered unsuitable as a model for a disease that occurs in the mature human skeleton after cessation of growth.
4. The pattern of bone remodelling in the rat has been considered too different from that in humans to make the former a good model for human bone research (Frost 1973).

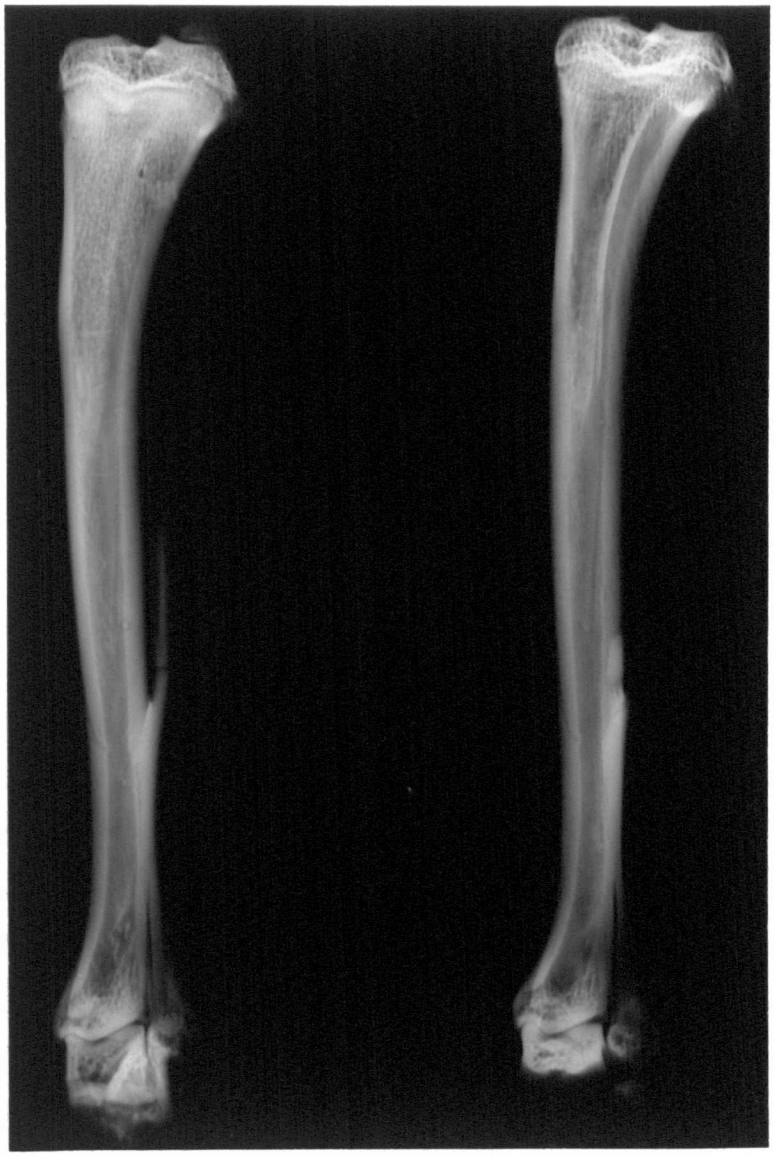

Figure 1.6
Microradiograph of two rat tibiae.
The bone on the left is from an intact rat while the one on the right is from an OVX rat and demonstrates clearly the extent of trabecular osteopenia in the proximal diaphysis.

All of these points can be addressed in way that supports the use of the rat as a suitable model for human bone research. Considering each point in turn:

1. Increasing pressure by ethical committees and the fact that bone biopsies have limited use, particularly when trying to assess the efficacy of new therapies means that there has been pressure to develop a convenient animal model.

2. Rats do not have a menopause like humans. In fact, aging female rats experience very irregular oestrus cycles from about 10 months of age. Later, ovulation stops completely, often developing a state of permanent oestrus by the age of 19 months (Lu *et al* 1979). This is associated with continuous production of ovarian sex hormones which act to conserve bone mass. However, ovariectomy overcomes this problem (Saville 1969) and mimics the fall in sex hormones seen after the human menopause.

3. Although rats, particularly ovariectomised ones, tend to increase body weight with increasing age, this should not be equated with an increase in skeletal size. The growth of the rat tibia is linear until about 170 days (Berg & Harmison 1957). Between 6 and 18 months the proximal tibial growth plate thins, starts ossifying and endochondral ossification stops. By 18 months the growth plate closes (Kimmel 1991). The proximal femur also closes but doesn't do so until about 24 months (Hagaman *et al* 1991). In addition, the rate of longitudinal growth of the vertebrae is so low by 7 to 8 months that it is barely detectable (Mori *et al* 1990). Many studies have used the male rat and it is a fact that many of the growth plates do not close until about 30 months of age (Kimmel 1991). However, rat studies into post-menopausal osteopenia usually involve ovariectomised females. These facts disprove the widely held concept that rat bone grows continually throughout life. This was due to the fact that young rats (3-6 months old) that were still growing rapidly were chosen commonly for experiments. The complications associated with growth can be minimised by using rats 9-12 months old (Wronski & Yen 1991).

4. The notion that rat cortical bone lacks Haversian systems and doesn't remodel is incorrect. Young rats under about 8 months old do not have Haversian systems but they do appear in small numbers when the rats are

older (Ruth 1953). Various studies have demonstrated cortical remodelling in rat bone:

i) In the femur in response to dietary calcium deficiency during lactation (Ruth 1953).

ii) In the tibia following fracture healing (Lowe *et al* 1983).

iii) In the tibia as a result of PGE_2 administration (Jee *et al* 1990).

iv) Preliminary findings also suggest that intracortical remodelling occurs in response to high mechanical loads in the rat ulna (Bentolila *et al* in press).

Summary

Advantages of using the ovariectomised rat in bone research

1. Development of osteopenia with a rapid phase of cancellous bone loss in the early phase of oestrogen deficiency.

2. The rate of bone loss is associated with the rate of bone turnover.

3. The rate of bone turnover and development of osteopenia is suppressed in the ovariectomised rat with oestrogen treatment.

4. Treatment of rats with bisphosphonates soon after ovariectomy reduces the rate of bone turnover and protects against osteopenia.

Disadvantages of using the ovariectomised rat in bone research

1. Expense: The rats should ideally be between 9-12 months of age. This means that they are expensive because they have to kept housed for a long time before they reach the required age.

2. Temporary stimulation of the growth plate: There is a transient (1-2 months) slight increase in longitudinal bone growth following ovariectomy (Wronski *et al* 1989) which theoretically will result in an increase in trabecular bone mass. In reality, it would appear that the effect on trabecular bone mass is minimal (Wronski & Yen 1991).

3. Slow changes in the vertebral bodies: Changes in vertebral trabecular bone can take up to 9 months before they become apparent (Wronski *et al* 1989).

4. Renal dysfunction in older animals: The use of senescent rats greater than about 15 months may be complicated by renal impairment with consequent effects on bone metabolism.

5. Debate over osteoblast function: Unlike humans (Parfitt *et al* 1981; 1983) which experience impaired osteoblast function in the late stages after menopause, this is not seen in rats (Wronski & Yen 1991).

1.7 Summary and objectives

The preceding chapters describe how the basic size and shape of a bone are determined genetically. Superimposed on this are systemic factors and the local effects of the bone's mechanical environment, particularly in bones that have a primary load-bearing function, i.e. the long bones and vertebral bodies. Constant adaptation of bones in response to fluctuating mechanical environments optimise their mechanical properties, with the most efficient use being made of the minimum mass of bone, to enable them to withstand the greatest physical demands they are likely to encounter.

Functional adaptation is influenced largely by load-induced strain. Various functions of strain, in particular strain magnitude, strain rate and strain distribution are known to influence this adaptive process. In addition, strain gradients, strain energy density and strain frequency may also be important. The physiological processes by which the mechanical stimulus is transduced into a cellular response are not clear but possible mechanisms include combinations of: physical cell-matrix interactions, fluid flow and streaming potentials, acting directly or indirectly via local biological factors such as cytokines, growth factors, prostaglandins, nitric oxide and possibly neurotransmitters. Superimposed on local strain-related factors are the modulating effects of hormones such as: sex hormones, growth hormone, vitamin D, parathyroid hormone, calcitonin and thyroid hormones. The interaction of all these factors is complex and often the results of *in vitro* experiments designed to investigate the effects of individual components of it in isolation, have produced contradictory results.

There is evidence to suggest that there are regional differences in the response of bone cells to systemic and local influences in different bones and possibly in different parts of the same bone, which may reflect a genetically programmed difference in the hierarchy of functional control between bones of different regions of the skeleton.

The processes by which coupled bone formation occurs and the mechanism of interaction between oestrogen, parathyroid hormone and mechanical loading are not understood well. In addition, there may be significant regional differences in the skeletal response to the inordinate combinations of osteotropic stimuli that occur *in vivo*, which would complicate further the enormously difficult task of unravelling bone's complex physiology.

The broad objectives of this thesis are to investigate the mechanical and hormonal factors which influence bone structure with an attempt to consider possible regional differences.

The thesis is divided into three main parts:

1. A study of the cellular events associated with mechanically loading a resorbing, modelling bone surface, using the *in vivo* rat ulna loading model. The work in this chapter was the basis of a paper published in the Journal of Bone and Mineral Research, a copy of which has been included at the back of the thesis.

2. A study to investigate the possible interaction between oestrogen and parathyroid hormone in various bones of the skeleton using adult ovariectomised rats, under similar conditions of physiological activity.

3. A study to investigate possible regional differences in physiological bone strain *in vivo* in a human volunteer (me!).

Chapter 2

A model for investigating the cellular events of mechanically loaded resorbing bone

2.1 Summary

A model was required for investigating the cellular processes involved with mechanical loading of resorbing bone. A modification of the rat ulna loading model was adopted to investigate the cellular response to the mechanical loading. The rat ulna undergoes resorption at the medial periosteal surface as a result of modelling drift, which occurs during growth. In addition, the rat is now a widely accepted model for the study of human bone biology. It was, therefore, a convenient model to choose.

The antebrachii of 11 female Wistar rats weighing 85-95g were loaded under general anaesthesia for six consecutive days. The limbs were loaded by axial compression with a peak force of 7 N, using a sinusoidal wave-form at a frequency of 10 Hz, for four minutes a day. One rat sustained a fractured ulna and was killed. Two fluorochrome labels were administered, one 24 hours before loading commenced and another at the end of the experiment. 24 hours after the last period of loading, the rats were killed. The antebrachii were dissected free of muscle, dehydrated in ethanol and embedded in methylmethacrylate resin. 100 micron thick sections were obtained from the ulnar mid-diaphysis and dynamic histomorphometry was performed blind to assess the percentage of the medial periosteal surface that had incorporated label, in order to characterise the response to this regimen of mechanical loading in 90 g female Wistar rats.

The results showed that loading was responsible for a highly significant increase in medial periosteal label incorporation in the left loaded ulnae compared with the right controls. Eight of the 10 showed an increase in label incorporation. Two of these demonstrated signs of woven bone formation on

the medial periosteal surface which was not apparent on the contralateral ulnae.

A second group of rats were loaded in a second study. A group of six female Wistar rats weighing 85-95 g were anaesthetised and loaded for six consecutive days in an identical way to the previous group of 11. Two fluorochrome labels were administered. One immediately after the first period of loading and the second immediately after the fifth day of loading. The rats were killed six hours after the final period of loading. After removal of the skin, the antebrachii were removed and snap frozen after dipping them in PVA. Cryostat sections were taken from the undecalcified antebrachii of six of the rats, by counting down 4 mm from the proximal head of the radius. Seven micron thick sections were obtained from equivalent sites in the loaded and control ulnae, 4-5 mm distal from the proximal radial head. These sections were examined for fluorochrome label incorporation, histology and TRAP reaction at the medial periosteal surface.

The results showed that the effects of mechanical loading on the medial periosteal surface were to: abolish the TRAP reaction observed in control bones, produce calcein incorporation where there had previously been none and change the periosteal lining cell profile in that flattened lining cells were replaced by deeply-staining, cuboidal osteoblasts. This is the first demonstration *in vivo* of direct inhibition of bone resorption by mechanical loading.

In summary, one of 17 rats sustained a fractured ulna. 75 % of the surviving 16 rats demonstrated adaptive bone formation on the medial periosteal surface in response to loading without any signs of woven bone formation.

2.2 Introduction

The strength of a bone is determined by the amount of bone material, its material properties and the bone's geometry. There is compensation for a decrease in bone mass by alterations in the spatial distribution of bone (Cheng *et al* 1995). However, if functionally inappropriate bone loss occurs in which bone mass falls below a critical level then the ability to compensate by architectural reorganisation is ineffective and the bone becomes weaker and susceptible to failure, even as a result of normal physiological activity, with consequent fracture, disability and pain. This is a problem in diseases such as postmenopausal osteoporosis and rheumatoid arthritis. It is the net effect of all the positive and the negative osteotropic influences that result in alterations in bone mass. Mechanical loading has been shown in numerous experiments to have a positive effect on bone mass (Hert *et al* 1971; Rubin and Lanyon 1981; Rubin and Lanyon 1984; Goodship *et al* 1979; Torrance *et al* 1994). However, the mechanism by which mechanical loading is transduced into an adaptive response is not understood well. Reorientation of proteoglycan within the matrix has been reported *in vivo* and *in vitro* following short periods of mechanical loading in both cortical and trabecular bone of various species (Skerry *et al* 1988; Skerry *et al* 1990). Cellular responses have also been observed following loading. Pead *et al* (1988) demonstrated 24 hours after a single period of loading in the isolated turkey ulna that [^{3}H]uridine incorporation in osteocytes was six times higher in loaded bone compared with control bone. Using the same model, Skerry *et al* (1989) found that the activity of glucose 6-phosphate dehydrogenase (G6PD) was higher in the periosteal cells of loaded bone and the number of osteocytes displaying this activity was also increased. This all occurred six minutes after a single period of loading. G6PD is the first enzyme and the rate-limiting step in the pentose phosphate pathway and its activity can be considered a measure of cellular biosynthesis.

There have been reports of the use of exercise regimes for the prevention or modulation of bone loss seen in postmenopausal osteoporosis (Bassey *et al* 1994). However, the cellular processes in early response to loading on resorbing bone surfaces are not understood well. Pead *et al* (1988) demonstrated transformation of a quiescent periosteal bone surface into one that showed signs of bone formation using a single period of mechanical loading in the adult, avian isolated ulna model. Despite this, further investigations are necessary to unravel the cellular processes by which loading converts a quiescent or resorbing surface into one which forms new bone.

Studies into bone's adaptive response to mechanical loading should be investigated in bones that experience fluctuations in load and therefore, mechanical strain during normal activity. This is important if the findings are to have physiological relevance. An appropriate model was required for the investigation of the early cellular events that occur in response to loading of a previously resorbing bone surface. The requirements for such a model were that it would necessarily have to be one that was *in vivo*. It would have been impossible to study such a complex process *in vitro*. In addition, the animal model would have to be acceptable as a model for human bone research and the bone under investigation would have to experience mechanical loading during physiological activity. Torrance *et al* (1994) described a model for non-invasive loading of the rat ulna. This model involved mechanically loading the antebrachium of anaesthetised 250 g male rats, where the flexed carpus and olecranon were placed between the padded cups of the hydraulic loading device which axially compressed the radius and ulna. The result of this was to generate supraphysiological mechanical strains along the long axis of the bone at the mid-point of the ulna. This stimulated new bone formation on the medial periosteal surface at the mid point of the ulnar diaphysis which had previously undergone resorption, during the process of modelling, to produce lateral curvature of the ulna (figure 2.1).

A model was required which could provide bone that would lend itself to being sectioned in a cryostat without having to be decalcified. The reason for this is

that the process of decalcification destroys RNA, rendering the tissue useless for molecular biology techniques such as: polymerase chain reactions (PCR) to amplify mRNA message, differential display and *in-situ* hybridisation. Cutting bone from rats greater than 100 g proves difficult because the bone tends to shatter when it is sectioned and as such, is unsuitable for histology. It was decided to use rats of 85 - 95 g for the experiment.

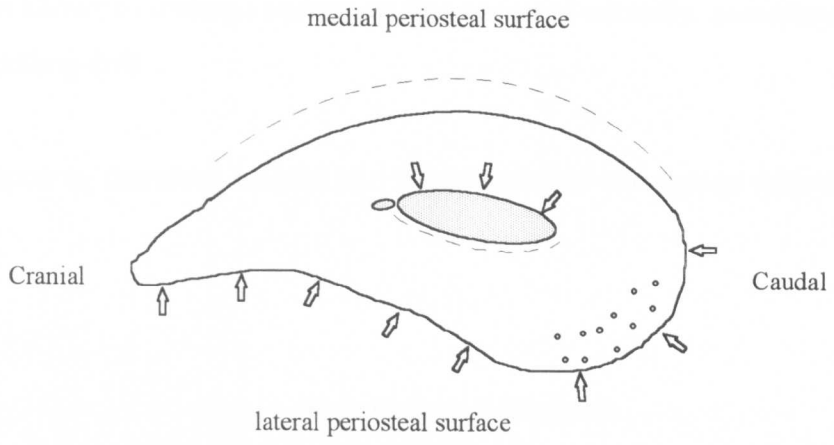

Figure 2.1
Transverse section of the ulna to illustrate the pattern of bone formation & resorption in the normal modelling bone

2.3 Aims

1. First to investigate the normal pattern of modelling down the medial periosteal surface of the ulnae in 85-95 g female Wistar rats, by looking at fluorochrome label incorporation using a confocal microscope.
2. Secondly to load the left antebrachii in a group of rats to quantify any adaptive response along the medial periosteal surface, using dynamic histomorphometry.
3. Finally to investigate any cellular response to a period of loading at a site that was known to undergo resorption that occurred normally, associated with the modelling drift.

The chapter is, therefore, divided into three studies to correspond with these aims.

2.4 Materials and Methods

Study 1

Two 90 g female Wistar rats were injected subcutaneously (s/c) with calcein at a dose of 15 mg/kg (appendix 1) six days apart. 12 hours after the last injection the rats were killed with sodium pentobarbitone (Euthatal, RMB, UK). The antebrachii were dissected free after removing the skin. The majority of the musculature was removed carefully, ensuring the medial periosteal surface was left intact and the bones were placed in 70% ethanol. The bones were dehydrated fully in ascending concentrations of ethanol then infiltrated and embedded in methylmethacrylate monomer (appendix 1). The embedded bones were sectioned along their entire length into 250 micron thick sections using an annular saw (Microslice 2, Metals Research, Cambridge, UK). The fluorochrome labels within the sections, along the entire diaphyseal lengths, were photographed using a confocal microscope (Biorad Model 500, Biorad, UK).

Study 2

In-vivo strain measurement

120 ohm, 1 mm, single element strain gauges (type FLK-1-11, Tokyo Sokki Kenkyojo Co., Tokyo, Japan) (figure 2.2) were bonded to the midpoint of the medial surface of the left ulna of five female Wistar rats (200-250 g) (a detailed description of this technique is given in appendix 1).

The rats were first premedicated with pethidine (Arnolds, Shrewsbury, UK) at 20 mg/kg body weight by subcutaneous injection (s/c). They were then anaesthetised with halothane Ph. Eur. (Fluothane, ICI Pharmaceuticals, Macclesfield, UK) and maintained under anaesthetic using a face mask until the end of surgery.

The left antebrachium was prepared for aseptic surgery. The medial or lateral midshaft of the ulna was exposed by minimal dissection, so as to preserve as much soft tissue as possible. An area of the midshaft approximately 12 mm long was exposed and prepared for bonding by carefully removing the periosteum (figure 2.3). The bone surface was then degreased using a fine cotton bud soaked with a 1:1 (by volume) mixture of diethyl ether and chloroform. The strain gauge was bonded onto the surface of the bone, with its long axis parallel to the long axis of the ulna (figures 2.4 and 2.5), using cyanoacrylate adhesive (Superglue, Loctite, UK). A secure bond between the gauge and the bone was ensured by applying firm digital pressure with a polythene-gloved finger for one minute. The lead wires were passed subcutaneously to emerge between the shoulders and were secured to the skin by means of a suture and a drop of Superglue. These were then connected to a ribbon cable which was fed into a strain gauge amplifier (Bell and Howell, Basingstoke, UK) whose output was fed into an analogue to digital (A/D) 12-bit capture card (RTI-815, Analog Devices, Norwood, MA, USA) fitted to an Opus IBM-compatible PCIII computer. Custom software was used to capture the data ('Super', D. McNally, University of Bristol).

Zero strains were defined when the animals were lifted from the ground and did not struggle. Strains were recorded from the ulnae when the rats walked on a flat surface, climbed a 45 degree inclined plane and when they jumped from a ledge 30 cm above a hard floor (figure 2.6).

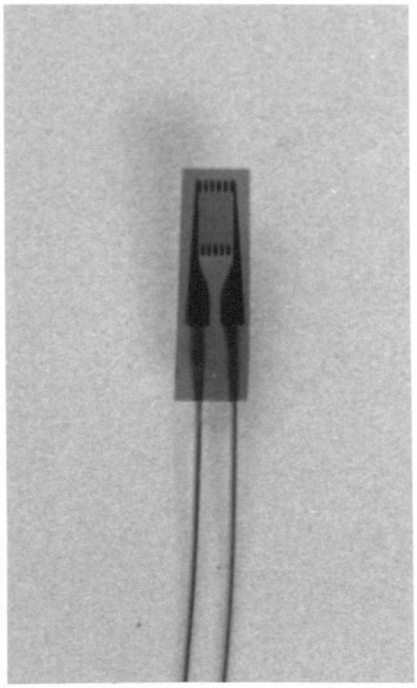

Figure 2.2
Photograph of a single-element strain gauge

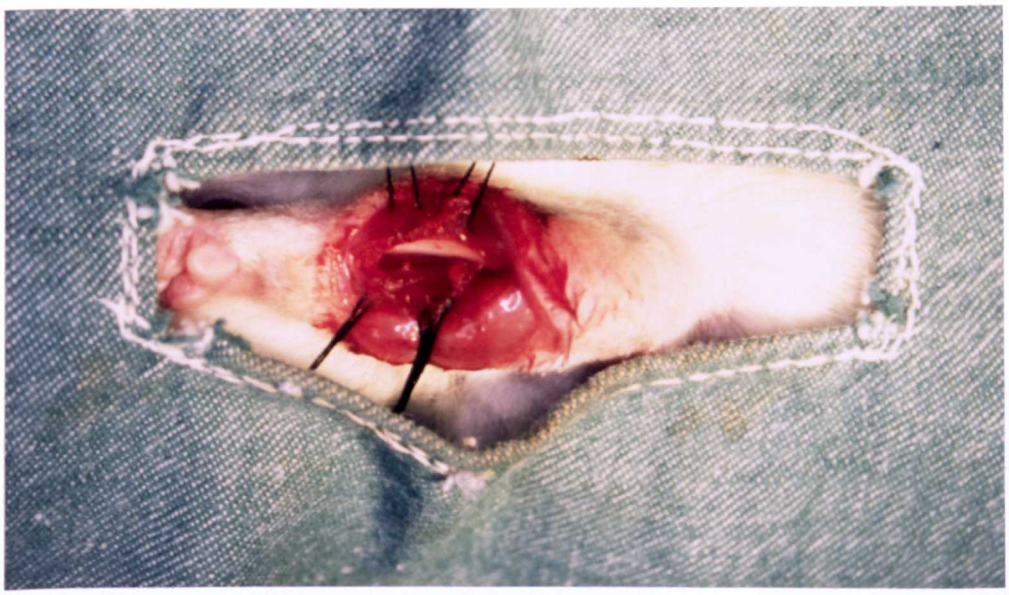

Figure 2.3
Photograph of the medial periosteal surface
of a rat ulna prepared for strain gauge bonding

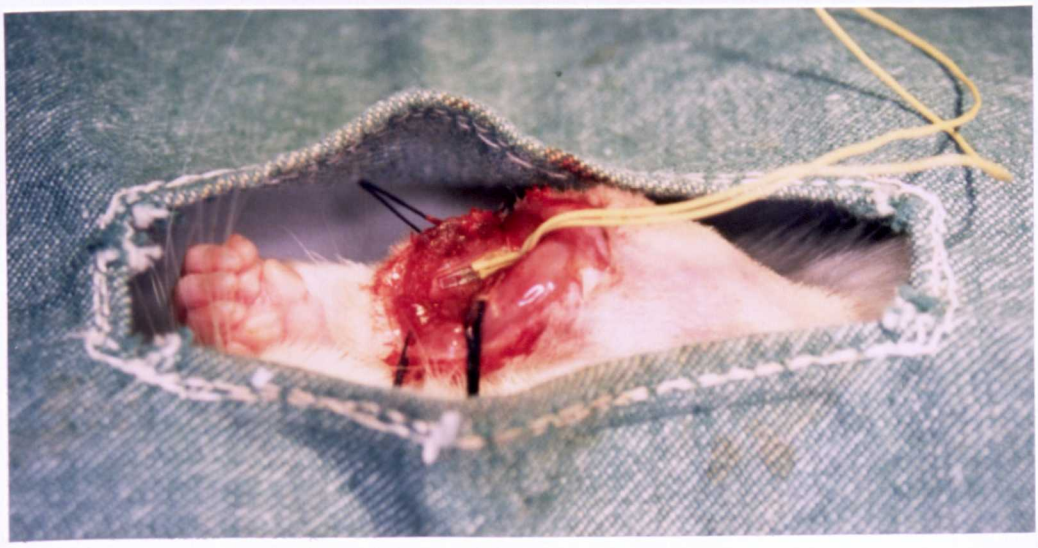

Figure 2.4
Photograph of a single-element strain gauge bonded
to the medial periosteal surface of a rat ulna

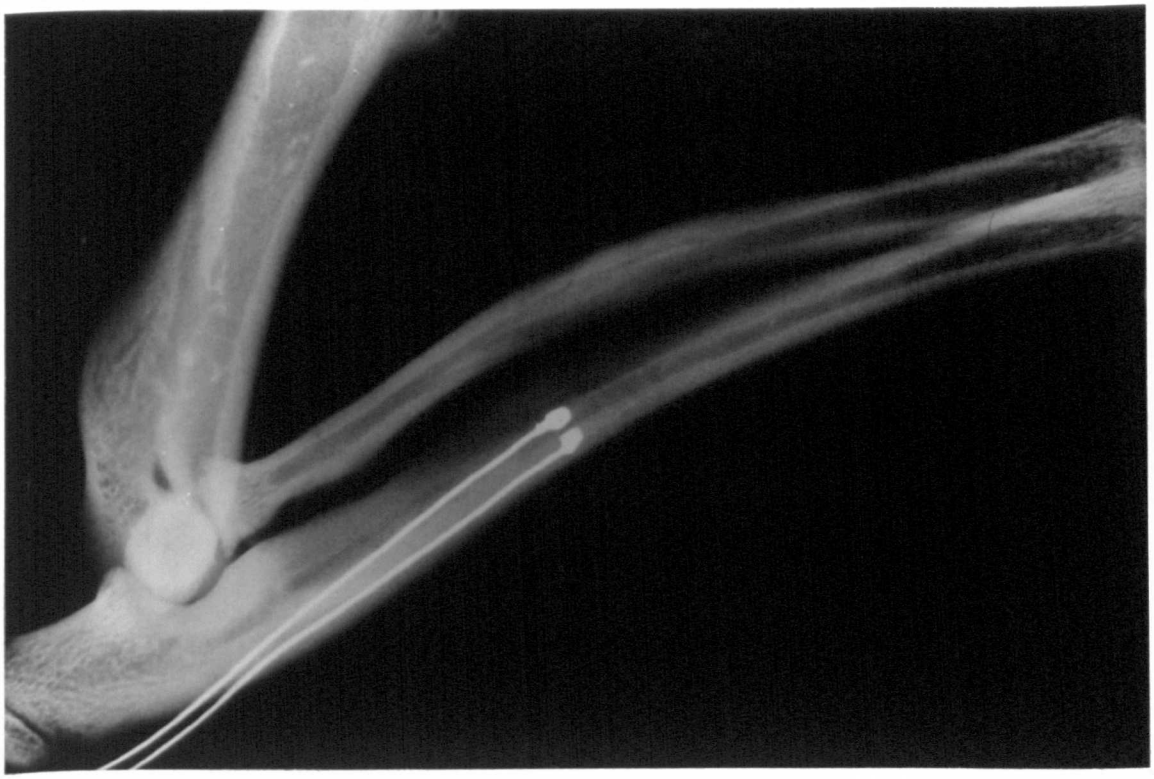

Figure 2.5
Microradiograph of a rat ulna with a single-element strain gauge bonded onto the medial periosteal surface

Figure 2.6
Photograph of a rat during *in vivo* strain recording

In vitro load/strain calibration

The left forelimbs were removed from three Wistar rats (body weight 85-95 g). Using the same surgical approach as that used in the *in vivo* study, the same type of strain gauges were bonded to the medial midshaft of the ulnae in an identical way. The elbow and flexed carpus were placed between the padded cups of a materials test machine (Dartec, Stourbridge, UK) and compressed axially. Due to the natural curvature of the ulna (figure 2.7), it could be assumed that this loading caused the bone to bend in a similar direction to that during physiological loading. The applied force was increased incrementally so that the relationship between applied load and the induced bone strain could be determined. The load required to produce 4000 μstrain was recorded (appendix 1).

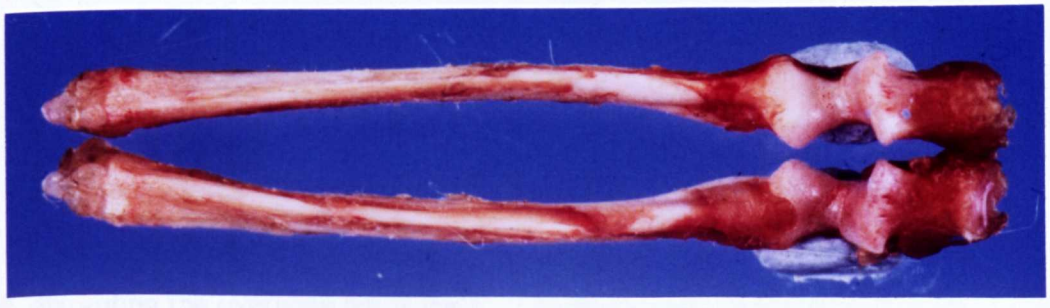

Figure 2.7
Photograph of a pair of rat ulnae showing the extent of the diaphyseal curvature

In vivo loading

11 female Wistar rats weighing 82-100 g (mean 92 g) were injected with calcein s/c at a dose of 15 mg/kg 24 hours before loading commenced. 24 hours after the fluorochrome injection the rats were anaesthetised with a 1:1 mixture (by volume) of xylazine (Rompun, Bayer UK, Bury St. Edmunds, UK) and ketamine (Vetalar, Parke-Davis, Pontypool, UK) at a dose of 1 ml/kg body weight by intra-peritoneal (i/p) injection. This equated to a dose of 10 mg/kg of xylazine and 50 mg/kg of ketamine. The left elbow and flexed carpus were placed between the cups of the loading device (figure 2.8) and compressed cyclically at a frequency of 10 Hz (sine wave-form) between one and seven Newtons (N). The loading was performed for four minutes on six consecutive days.

A second injection of fluorochrome (oxytetracycline, Terramycin Q50, Pfizer, UK) was administered s/c at a dose of 20 mg/kg immediately after loading on the sixth day. The rats were killed by overdose of sodium pentobarbitone (Euthatal, RMB, UK) 24 hours after the second injection of fluorochrome.

Sample collection and preparation

The left and right antebrachii were dissected free, with careful removal of the musculature so that the medial periosteal surface was left intact, without disrupting the overlying periosteum. The bones were then placed in 70% ethanol. After complete dehydration in ascending concentrations of ethanol the antebrachii were measured and the midpoint was marked on each ulna with a graphite pencil. The bones were then infiltrated and embedded in methylmethacrylate (appendix 1). Starting at a point 1 mm distal to the midpoint of each embedded bone, four 100 micron sections were cut in a proximal direction, using an annular saw (Microslice 2, Metals Research, Cambridge, UK). The blade was 250 microns thick which meant that the procedure produced several sections very close to the midpoint Each section was mounted on a microscope slide using Vecta shield fluoromount (Vectalabs, UK). The sections from the right and left antebrachii were then

examined under a light microscope. An equivalent left/right pair of sections were selected by assessing comparable radial and ulnar features such as shape of the medullary cavity and profile of the periosteal perimeter.

Measurement of fluorochrome labels

Using a UV microscope (Leica model DMRB) and a histomorphometry system (Osteomeasure, Osteometrics Inc., USA) medial periosteal bone perimeter and label lengths were measured blind by a histomorphometry technician. To standardise the sampling procedure measurements were made from the most caudal point of the section to the most cranial aspect, along the medial periosteal surface (figure 2.9).

Label perimeters were calculated by dividing the label lengths by the length of the medial periosteal surface and expressing the label lengths as a percentage of the medial periosteal bone surface.

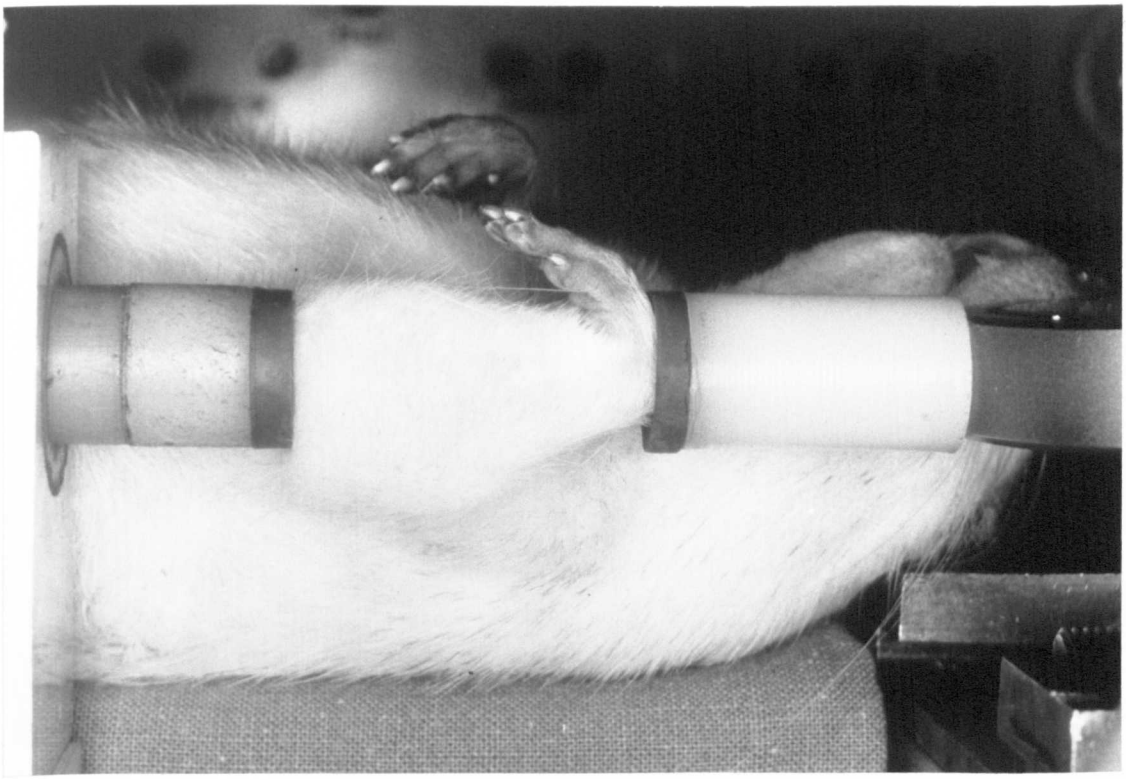

Figure 2.8
Photograph of an anaesthetised rat showing how the forearm is placed in the cups of the loading device

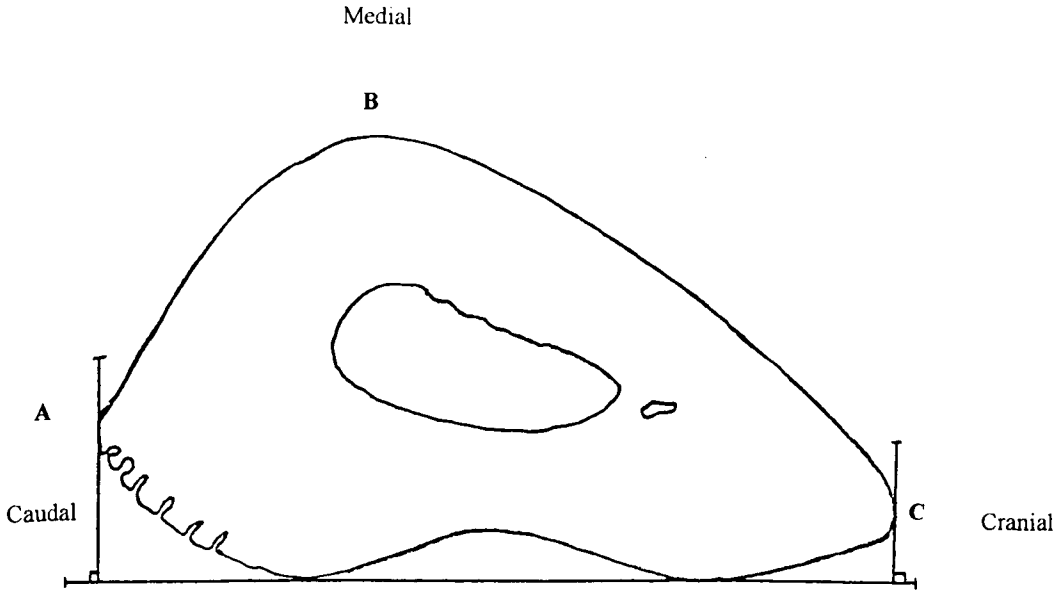

The label length was measured along the medial periosteal surface from the most caudal point (A), via the most medial point (B), to the most cranial point (C)

Figure 2.9
Diagram illustrating how the medial periosteal fluorochrome label was measured in study 2

Study 3

Loading

A group of six female Wistar rats (body weight 85-95 g) were anaesthetized and loaded in exactly the same way as the described in study 2. Immediately after the first period of loading, each rat was injected s/c with an aqueous solution of calcein (Sigma, St. Louis, MO) at a dose of 15 mg/kg. A second injection of calcein was given immediately after the loading period on the fifth day. This was done to mark sites of bone formation at the start and end of the experiment. Six hours after the final period of loading on the sixth day, the rats were killed by cervical dislocation.

Sample collection

Immediately after death, the intact left and right antibrachii were dissected free and the skin was removed. Each antibrachium was then dipped in a 10 % aqueous solution of polyvinyl alcohol (PVA) (Sigma) for 20 seconds. They were then snap-frozen by dropping them into a bath of N-hexane ("Low in aromatic hydrocarbons", BDH Supplies, Poole, UK) chilled to -70° C with dry ice and industrial methylated spirit (appendix 1). The frozen specimens were then placed in cold plastic containers which contained a small piece of clean paper tissue and stored over dry ice in a -80°C freezer until processing. The paper absorbed any surplus N-hexane which could have affected the mounting procedure, described in the next section.

Specimen mounting and cryosectioning

Using PVA, the distal end of each specimen was then mounted vertically onto a solid brass microtome chuck such that the long axis of the specimen was perpendicular to the face of the chuck (appendix 1). The blocks were trimmed using a heavy-duty cryomicrotome (Model OTF, Brights Instrument Co., Huntingdon, UK), fitted with a new, sharpened tungsten carbide blade, until both the radius and the ulna were visible in the section. This point represented a common, consistent and easily visible landmark in all the samples. The

blocks were then trimmed a further four mm distally so that sections could be taken from relatively equivalent sites in all the samples. This was confirmed by assessing the profile of the bone sections under a light microscope at regular intervals (figure 2.10). Seven micrometer sections were collected onto slides coated with Vectabond (Vector Labs, Burlingame, CA). Cutting of the sections for histology was done using the motor of the cryostat to move the block over the knife. This ensured that there were no sudden, jerky movements as the knife cut through the block which would have resulted in shattered and folded sections. Use of the motor also produced sections of consistent thickness. The sections were then stored covered with aluminium foil at -35° C.

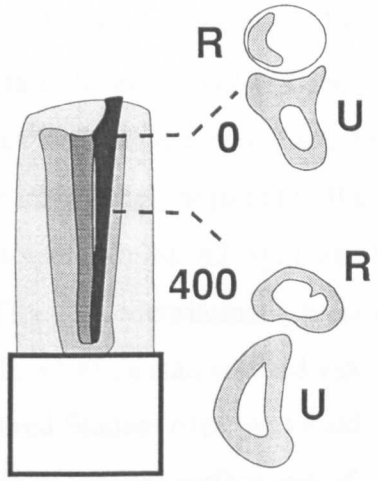

Figure 2.10

The sample site at which sections are taken for analysis is located because of the fixed relationship of the radius and ulna. After chilling, the blocks are mounted perpendicularly on the microtome chuck, with the elbow uppermost then trimmed until the first section is cut in which both the radius and the ulna appear (O). At this level, the ulna (U) is predominantly cortical and trabecular bone but the radial head (R) appears characteristically as a crescent of subchondral bone in an ellipse of hyaline cartilage. The block is then trimmed a further 4 mm (400 x 10 μm sections) to the sample site (400).

Histology and enzyme cytochemistry

Three sections from each block were mounted unstained in glycerol/PBS (Citifluor, Canterbury, UK) for UV microscopy. The length of labelled surface was measured over a 400 micrometer length of the ulnar medial periosteal surface from photographs of sections from control and loaded bones from each animal. The length of labelled surface was measured from the most medial point of the ulna in a cranial direction (figure 2.11).

Serial sections were either stained for conventional histology in aqueous Wright's stain (Diffquick-Baxters, Reading, UK) or were reacted to demonstrate the activity of the enzyme tartrate-resistant acid phosphatase (TRAP) using a modification of the method of Webber *et al* (1988) by incubation first in naphthol AS BI phosphate solution at 37° C, followed by fast garnet GBC/sodium tartrate solution at 4° C (appendix 1). Sections were photographed with a Leica DMRB microscope and TRAP activity was measured in the cell layer immediately adjacent to the bone surface using a Vickers M85 microdensitometer (mask A2, spot size 1, wavelength 650 nm) (appendix 1). Results of the microdensitometry were expressed as mean integrated extinction (MIE x100), a standardised value comparable between different machines. A paired Student *t*-test was used to assess the significance of differences in the length of labelled surface and of the enzyme activity between the loaded and control limbs of each animal.

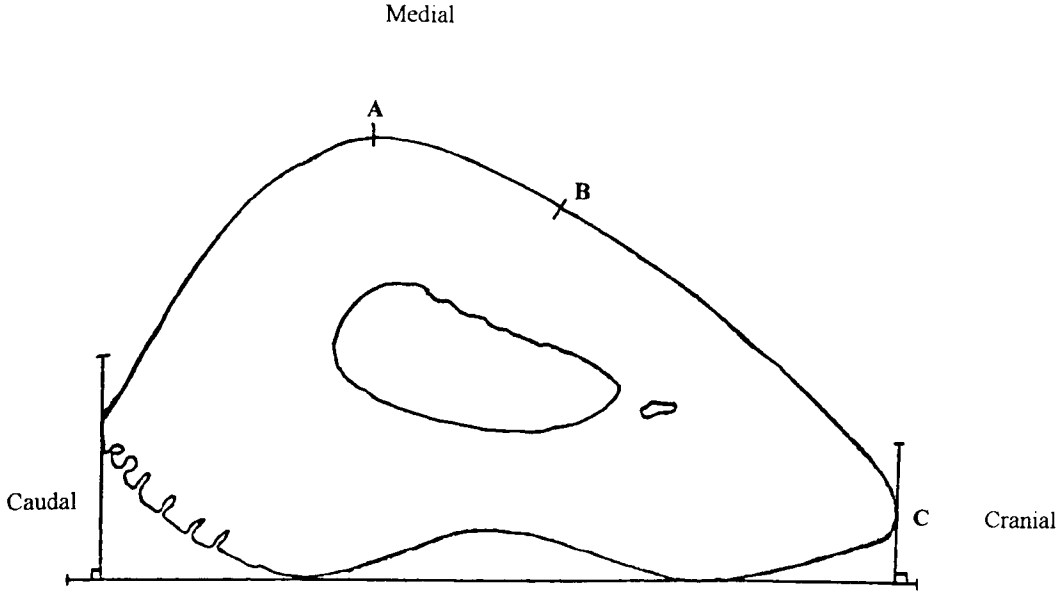

The label length was measured along the medial periosteal surface from the most medial point (A) to point (B), 400 μm in a cranial direction towards point C

Figure 2.11
Diagram illustrating how the medial periosteal fluorochrome label was measured in study 3

2.5 Results

Study 1

Figure 2.12 shows a series of confocal pictures taken of sequential sections along the length of a normal unloaded ulna. The bright lines represent the two fluorochrome labels which have incorporated into forming bone surfaces. The inner label on the medial periosteal surface was the first fluorochrome to be administered.

It could be seen that the pattern of modelling was not constant along the entire length of the diaphysis. Proximal to the mid-point, a double label could be seen which showed that this surface was forming. Distal to the mid-point, no label was seen which indicated that no net apposition of mineralised new bone was occurring.

Figure 2.12
Series of confocal pictures obtained along the diaphysis of a control, unloaded rat ulna.

The top left image is from the most proximal section with each successive image underneath taken from the next section distally. The top right image is from the diaphyseal midpoint. The bottom right image is from the most distal section.

The horizontal scale bar represents 500 μm.

Study 2

***In vivo* strain measurement**

Peak tensile strain magnitudes were recorded from the lateral periosteal surface. Magnitudes of +1540 μstrain were measured. Peak compressive strain magnitudes were recorded from the medial periosteal surface. Magnitudes of -1550 μstrain were measured. These peak strain magnitudes were associated with landing from a height of 30 cm (figure 2.13). Walking produced strain magnitudes of approximately +600 to +800 μstrain on the lateral periosteal surface and -800 to -1000 μstrain on the medial periosteal surface (figure 2.14). Generally, the rats were reluctant to move around very much on the slope and the results were generally very inconsistent.

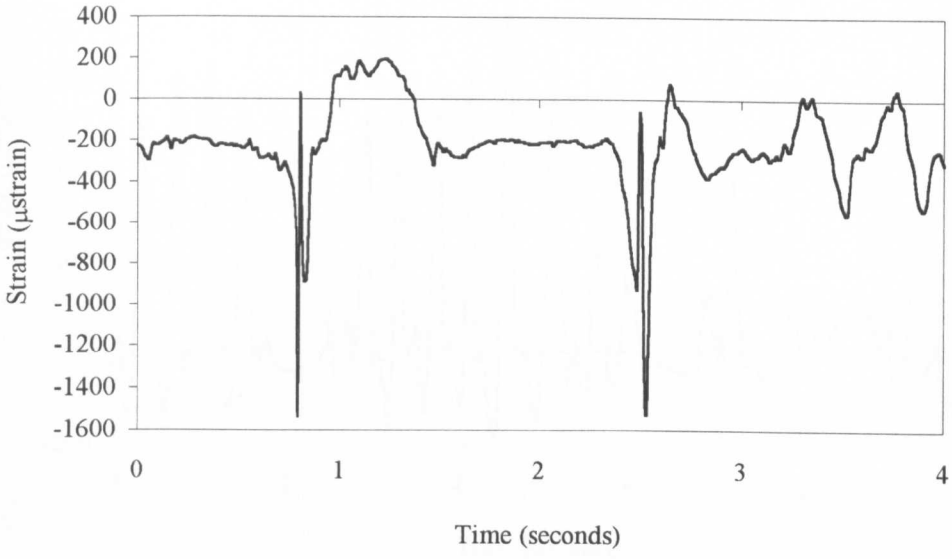

Figure 2.13
Strain trace recorded from the medial ulnar periosteal surface during two landings from a height of 30 cm. The landings are represented by the two spikes.

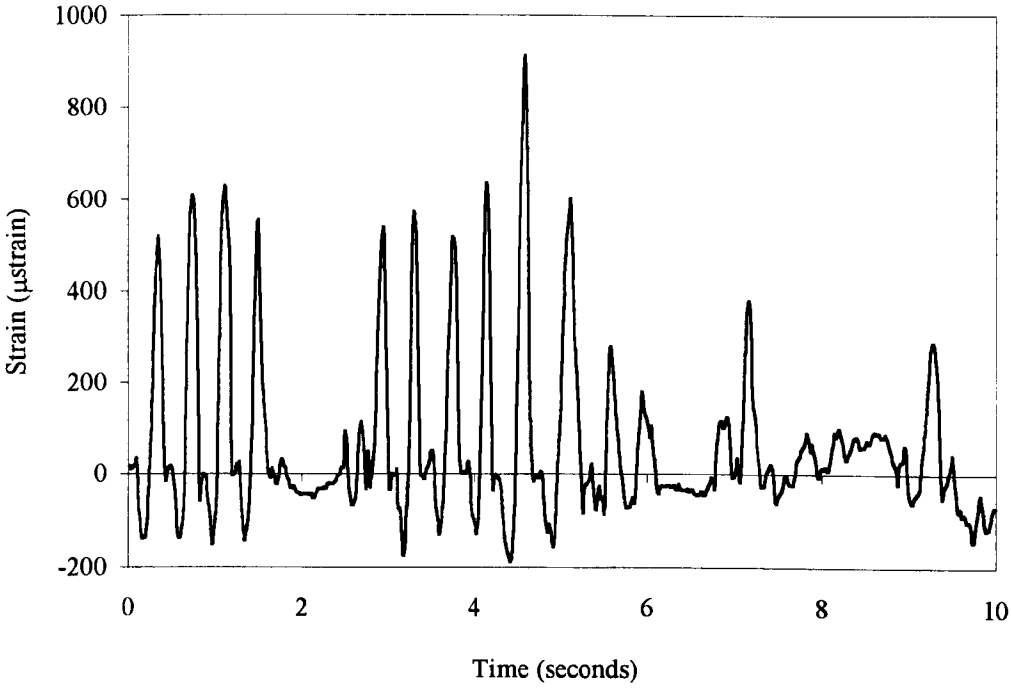

Figure 2.14
Strain trace recorded from the lateral ulnar periosteal surface during walking

In vitro load-strain calibration of the ulnae from 90 g rats

An axial compressive force produced approximately -3500 to -4500 μstrain on the medial periosteal mid-diaphysis. Loading at 10 Hz produced mean (± SEM) peak strain rates for the loading part of each cycle of 116,700 (800) μstrain/second whilst those for the unloading part of the cycle were 129,700 (700) μstrain/second (appendix 1).

In vivo loading

One rat sustained a fractured ulna on the second day of loading and was killed. The remaining rats survived to the end of the experiment without further complications.

Histomorphometry

Table 2.1: results for the histomorphometry of the medial periosteal surface

Rat	LMP mm	LCL mm	LCL %	LOL mm	LOL %	RMP mm	RCL mm	RCL %	ROL mm	ROL %
1	2.562	0.711	28	1.597	62	2.620	0.681	26	1.529	58
2	2.541	0.948	37	2.130	84	2.541	0.898	35	1.120	44
3	2.637	1.020	39	1.739	66	2.604	0.743	29	0.913	35
4	2.704	0.941	35	1.951	72	2.570	0.666	26	1.216	44
5	2.604	0.708	27	2.159	82	2.499	0.697	28	0.983	39
6	2.546	0.835	33	1.609	63	2.493	0.939	38	1.719	69
7	2.626	0.955	36	1.853	71	2.554	0.740	29	1.344	53
8	2.446	0.801	33	2.044	84	2.300	0.624	27	1.033	45
9	2.396	0.882	37	1.939	81	2.456	0.684	28	0.824	34
10	2.332	1.251	54	1.867	80	2.444	1.338	55	1.998	82

Where:

LMP = Left medial periosteal perimeter length
LCL = Left calcein label length
LOL = Left oxytetracycline label length
RMP = Right medial periosteal perimeter length
RCL = Right calcein label length
ROL = Right oxytetracycline label length

Table 2.2: Summary of the histomorphometry results

Fluorochrome label lengths	Left ulnae	Right ulnae
Mean first label (calcein) % (± SEM)	36 (2)	32 (3)
Mean second label (oxytetracycline) % (± SEM)	75 (3)	50 (5)

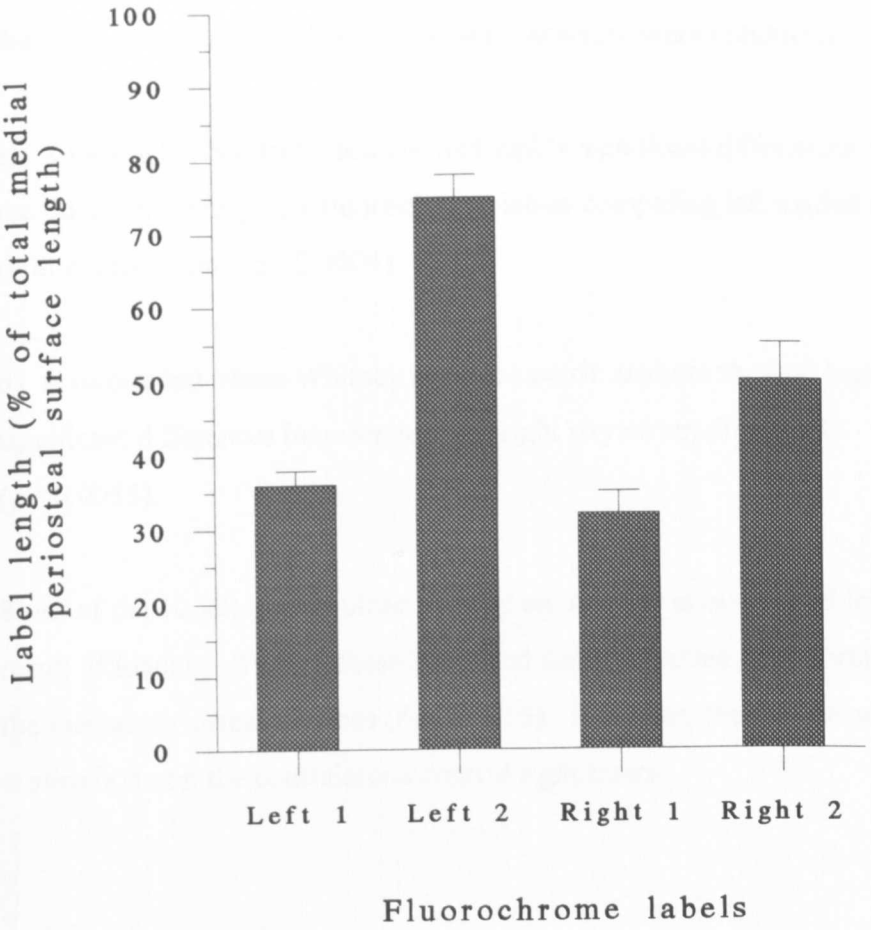

Figure 2.15 Graph showing a comparison of the left and right label lengths on the medial periosteal surfaces

Statistical analysis

1. First fluorochrome label length

A two tailed Student t-test showed no significant differences between the inner calcein fluorochrome labels comparing left loaded ulnae with right control ulnae ($p= 0.3157$).

2. Second fluorochrome label length

Bartlett's test for homogeneity of variance showed that the differences between the standard deviations were not quite significant ($p= 0.0521$), therefore, parametric and non-parametric analyses were conducted.

a) A two-tailed Student t-test showed highly significant differences between the outer oxytetracycline fluorochrome labels comparing left loaded ulnae with right control ulnae ($p= 0.0004$).

b) A two-tailed Mann-Whitney non-parametric analysis showed highly significant differences between left and right oxytetracycline labels ($p= 0.0015$).

8 out of the 10 left loaded ulnae showed an increase in outer label length as a result of loading. Two of these 8 showed signs of woven bone formation on the medial periosteal surfaces (figure 2.16). However, there were no signs of woven bone on the contralateral control right bones.

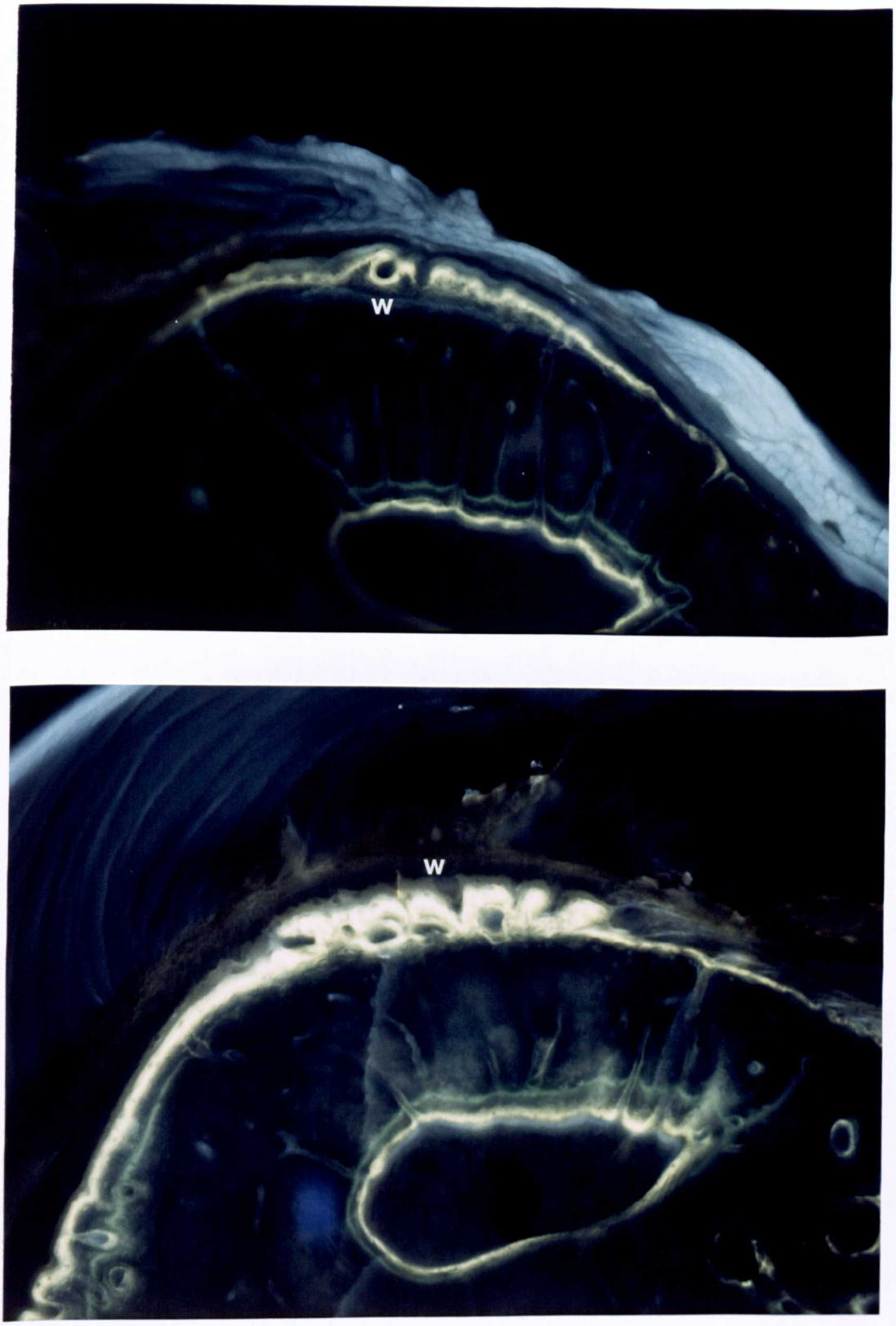

Figure 2.16
Two photographs showing the formation of woven bone (W) on the medial periosteal surface

Study 3

Fluorochrome labelling

Table 2.3: Results of medial periosteal fluorochrome label measurements

Rat	Medial periosteal label length of left loaded ulna (μm)	Medial periosteal label length of right control ulna (μm)
1	400	0
2	230	0
3	240	0
4	340	20
5	340	45
6	370	50

Table 2.4: Summary of label measurements

Mean label length	Left ulnae	Right ulnae
μm (± SEM)	320 (28)	19 (10)

A two-tailed paired Student t-test showed highly significant differences between the label lengths ($p < 0.0001$).

Because of the small numbers, a two-tailed Mann-Whitney non-parametric test was also performed. The differences were still highly significant ($p = 0.0022$).

Histology and enzyme cytochemistry

The medial periosteal surfaces of the control (right) ulnae were scalloped and lined with flattened cells. In addition, no osteoid was evident. This region of periosteal cells demonstrated high TRAP activity (figure 2.17a). In contrast, the equivalent surface of the loaded (left) ulnae was covered by a thin layer of pink osteoid which in turn was lined with deeply-staining, rounded osteoblasts. TRAP activity was barely evident (figure 2.17b).

Microdensitometry

Table 2.5: Results of microdensitometry

MIE x 100	
Left loaded ulnae	Right control ulnae
8	29
4	24
3	18
5	21
5	25
4	17

Table 2.6: Summary of microdensitometry results

Mean TRAP activity	Left ulnae	Right ulnae
MIE x 100 (± SEM)	4.8 (0.7)	22.3 (1.9)

A two-tailed paired Student t-test demonstrated highly significant differences ($p < 0.0001$).

Again, because of the small numbers, a two-tailed Mann-Whitney non-parametric test was also performed. The differences were still highly significant ($p = 0.0022$).

Figure 2.17a

1
Undecalcified section of the mid-diaphysis of an unloaded right ulna photographed under U.V. light to show the fluorochrome labels.

Where:
M = medial, L = lateral, Cr = cranial & Cd = caudal periosteal surfaces.

Fluorochrome label incorporation on the medial periosteal surface is normally minimal with only sparse areas of uptake (arrow).

2
High power undecalcified section showing the irregular medial periosteal surface (P) covered by a layer of tightly adherent, flattened periosteal cells.

3
High power undecalcified section demonstrating the intense TRAP activity (T) on the normal modelling medial periosteal surface.

Figure 2.17b

1
Undecalcified section of the mid-diaphysis of a loaded left ulna photographed under U.V. light to show the fluorochrome labels.

In contrast to the control ulna, there is substantially more fluorochrome label incorporation along the medial periosteal surface (V).

2
High power undecalcified section showing the smooth medial periosteal surface covered by a layer of plump, deeply staining osteoblasts (Ob). In addition, there is a layer of pink staining osteoid (o) which will become mineralised to form bone.

3
High power undecalcified section demonstrating a decrease in the TRAP activity on the normal modelling medial periosteal surface (m) as a result of loading.

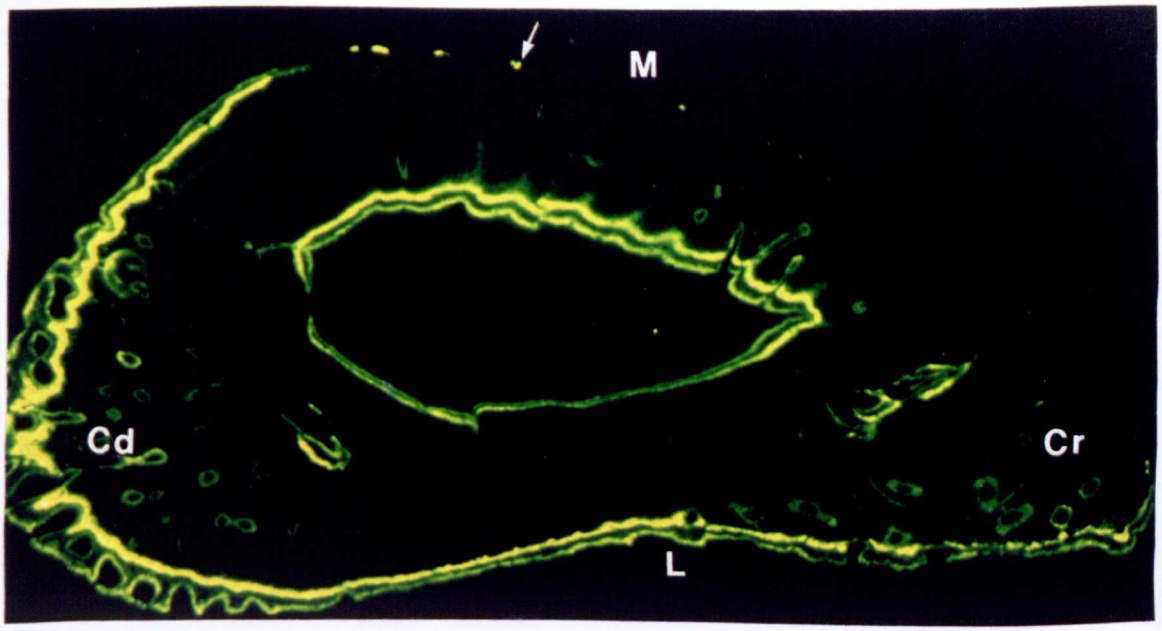

1

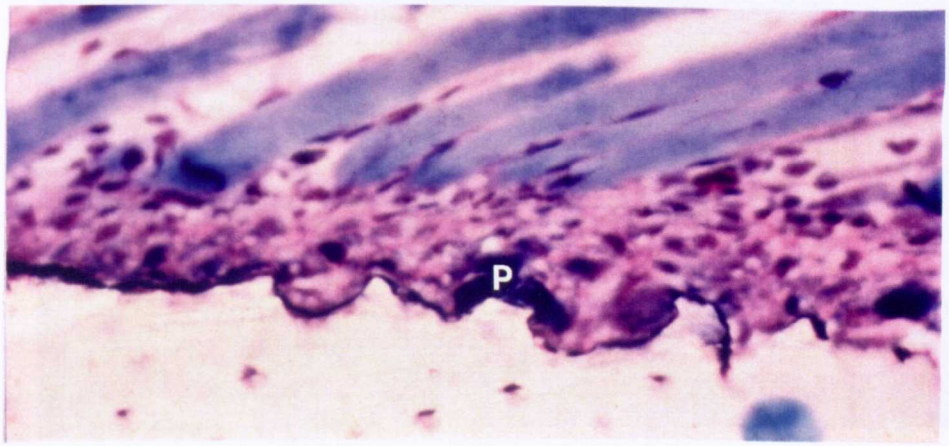

2

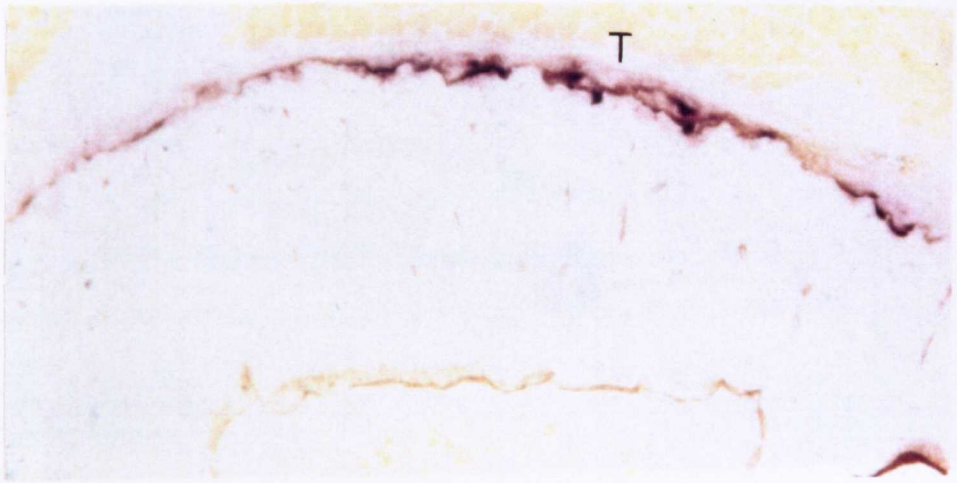

3

Figure 2.17a

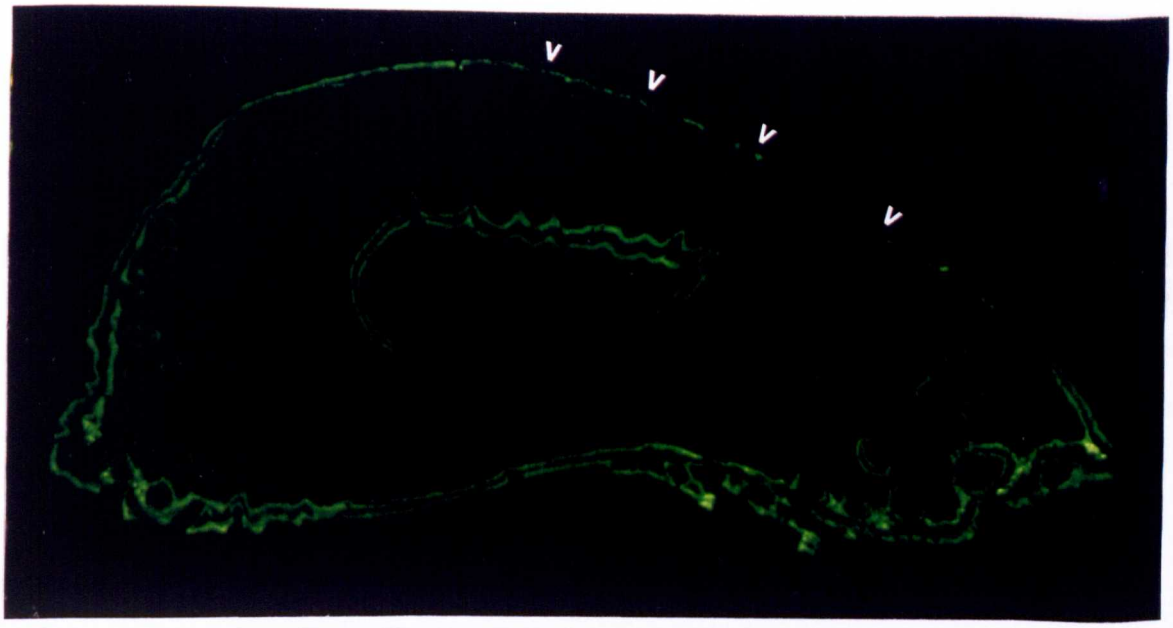

1

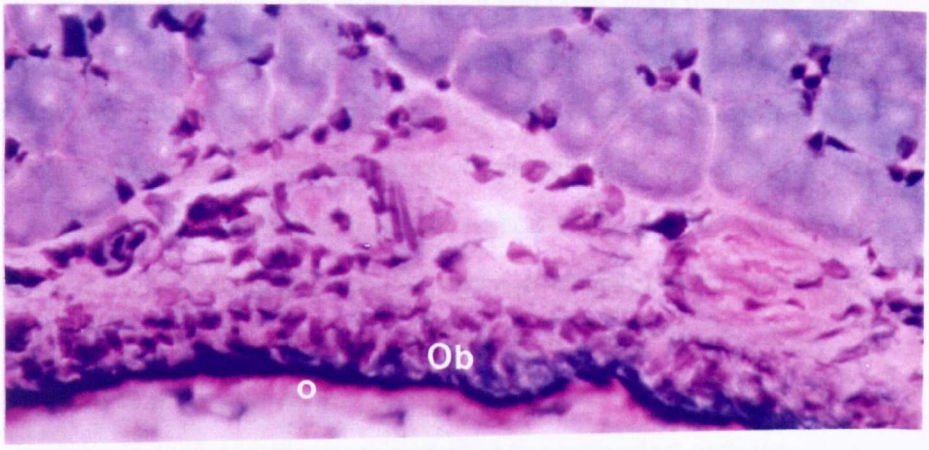

2

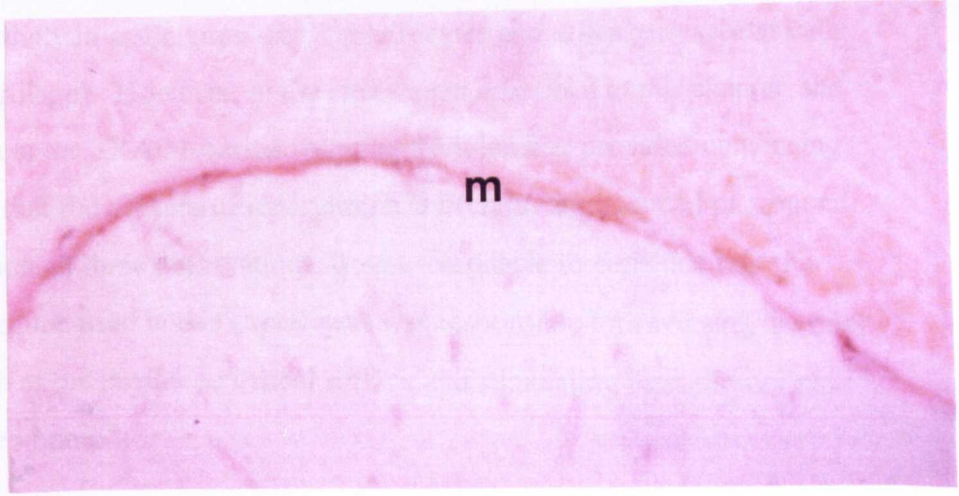

3

Figure 2.17b

2.6 Discussion

The results of these studies show that six days of brief daily loading inhibits periosteal resorption and stimulates new bone formation at the medial periosteal surface of the mid-diaphysis of the ulna in young, growing 90 g female rats.

Six days of loading were associated with three changes: Firstly, fluorochrome label was incorporated into the medial periosteal surface. This indicated that mineralised bone was being formed on a surface which had previously undergone resorption. Secondly, histology demonstrated a change in the periosteal lining cells. In control bones, some of the cells were flattened, and occasional large cells (possibly osteoclasts) were visible. In the loaded bones, the periosteum was lined with densely staining, plump osteoblasts and a layer of pink-staining osteoid was evident between these cells and the mineralised bone surface. Occasional newly incorporated osteocytes were also visible. Finally, there was high TRAP activity at the mid-diaphyseal, medial periosteal surface, which had previously undergone resorption in control bones. This activity diminished dramatically as a consequence of loading. The intensity of the TRAP reaction is used commonly as a marker for osteoclast activity, although it is not totally specific for this (Cole and Wezeman (1987) reported TRAP activity in association with chondrocytes and other perivascular cells within cartilage). However, in the experiment described in this chapter, the reduction in the TRAP reaction resulting from loading provided convincing evidence that the process of resorption had been greatly reduced or stopped. Considering all three observations, it was reasonable to conclude that the loading regime used in this experiment was responsible for reversing the bone resorption at the medial periosteal surface and stimulating formation of new mineralised bone.

The sequential confocal images produced of the unloaded ulnae demonstrated that medial periosteal resorption did not occur down the entire length of the

ulna. For this reason, this model required reliable and reproducible sampling at the diaphyseal mid-point. In study two, this was achieved by sectioning the bone 1 mm distal to a mark made at the mid-diaphysis then taking four sections proximally to sample through the mid-point. When comparing left and right ulnae from the same animals, demonstration of similar medial periosteal perimeter and similar calcein fluorochrome label lengths, helped confirm that comparisons were made between sections taken from equivalent anatomical positions in both bones. Because the results of study 2 demonstrated no significant differences, between the left and right ulnae, in the lengths of the first label administered before loading commenced, it helped confirm that the differences between the left and right medial periosteal label lengths at the end of the study were due to an effect of the loading stimulus. Measurement of label lengths was performed 'blind' by an independent observer to ensure an unbiased measuring technique. Accurate sampling was achieved in study three by cutting down a known distance from the proximal radial head which represented a fixed anatomical landmark. A useful aid was to compare the shape and features of the sections of both the ulna and the radius with those cut from the contalateral limb. If there was great disparity between the appearance of the sections taken from the two limbs then it was assumed that the sampling sites were not equivalent. Using this technique, it was found that medial periosteal resorption occurred 1-1.5 mm proximal and 2-3 mm distal to the sampling site used. Torrance (1993) reported that loading of the ulna caused shortening compared with the control bone. This was also observed in other studies not presented in this thesis. This is not a surprising finding; Hert (1969) and Simon (1978) described how excessive traction and increases in growth plate forces, compared with normal physiological loading, resulted in a decrease in the growth rate of the epiphyseal plate. However, in the small rats used in this experiment, this effect did not appear to complicate accurate sampling.

The use of 85-95 g rats meant that it was possible to obtain undecalcified sections. The advantage of this was that sequential sections could be used for

fluorochrome label examination, histology and histochemical techniques without having to resort to several techniques to process the bones. Examination of sequential sections in this case would have been impossible. In this respect, undecalcified cryosectioning was quick and convenient, however, it is a difficult technique if high quality sections are to be obtained. The weight of the rats at the end of the experiment were 100 - 110 g and this possibly represented the heaviest rat from which good cryostat sections could be obtained. Above this weight, the bones are thicker and the sections appear to shatter more easily during sectioning.

The results of the *in vivo* strain gauging showed that the maximum compressive strain magnitude was -1550 μstrain and recorded from the medial periosteal surface. The maximum tensile strain was +1540 μstrain and recorded from the lateral periosteal surface. Torrance (1993) investigated the relationship of medial periosteal strain to lateral periosteal strain at the mid-diaphysis and showed that the ratio between the two was approximately 1.2. This suggested that the maximum tensile strain of +1540 μstrain on the lateral periosteal surface would have been equivalent to approximately -1900 μstrain at the medial periosteal surface.

The *in vivo* strain measurements were made in rats heavier than those used for the loading due simply to the practical difficulty of placing the strain gauges onto the much smaller bones of younger rats. Also, it is possible that in small rats, the strain gauges could possibly have produced a reinforcement effect on the small ulnae and any strains measured subsequently may have been artificially low (Little *et al* 1990).

Rubin and Lanyon (1984) reported that peak strain magnitude in a variety of animals was between 2000-3000 μstrain. In this experiment, peak strain magnitude measured was -1550 μstrain, however, it is likely that in normal physiological conditions, the rats would have produced higher strain magnitudes during more vigorous activities. The maximum strain measured

relates to the bone surface directly under the gauge used to make the recording. If high strain gradients exist throughout the bone then repositioning the gauge a small distance away could result in very different patterns. Additionally, in this experiment only single element gauges were used instead of multiple-element rosettes. This was because of the small size of the bones in this weight of rat. Unlike rosette gauges, single element gauges cannot be used to calculate principal strains; they only detect strain parallel to the gauge element. Hence, these limitations should be borne in mind when interpreting these strain data. If one assumes that the maximum physiological strain magnitude likely to be experienced in the rat ulna is ±3000 μstrain, then external loading to engender 4000 μstrain could be expected to produce an adaptive response. This was demonstrated in the results described by Torrance *et al* (1994) who reported that no new bone was seen on the medial periosteal surface at strain magnitudes below 3000 μstrain. Because of the natural curvature of the ulna, physiological activity would accentuate this curvature. In this respect, the externally applied load could be considered to produce similar strain distributions to those produced *in vivo*, therefore, loads producing strain magnitudes higher than those experienced *in vivo* were required to produce an adaptive response. However, if loaded to excessively high magnitudes any changes observed could have been a pathological response to microdamage.

The strains measured in this work were dependent on: axial alignment of the strain gauge on the bone, anatomical position of the gauge on the bone and variation in length and natural curvature of the bones. Seven N engendered approximately -4000 to -4500 μstrain on the medial periosteal surface of 90 g female Wistar rats.

Rubin and McLeod (1994) suggested that a loading frequency of 20 Hz was more osteogenic than 1 Hz However, Torrance *et al* (1994) reported that loading of the rat ulna at 20 Hz did not produce more bone than loading at

10 Hz In fact they observed maximum bone formation in response to loading at 3500-4500 μstrain at 10 Hz. It is for this reason that a loading regime of 7 N at a frequency of 10 Hz was chosen for these loading experiments.

Strain rate has also been reported to influence adaptive bone response to mechanical loading (O'Connor *et al* 1982). Strain rates were investigated by Mosley (1996) who described an increase in the length of the diaphysis which demonstrated medial periosteal surface label incorporation when loading at strain rates of 100,000 μstrain/second, compared with strain rates of 30,000 μ strain/second. Loading in this experiment at loads of 1-7 N at 10 Hz produced peak strain rates in excess of 100,000 μstrain/second. It is feasible that by using higher strain rates than this may enable the use of lower strain magnitudes in the loading protocol.

In experiments using this model, a consistent response will depend on consistent reproduction of the loading-related strain conditions. Choosing rats of the same strain, sex and as equal an age and weight as possible should help reduce any potential sources of variation. An assumption that has to be made is that there is little variation in the natural curvature of the ulna between different individuals. It is also absolutely necessary to reproduce to a high degree of accuracy, the external loading conditions This experiment was conducted using the material test machine in position-control. There is a significant disadvantage of this. Unlike load-control where feedback from the load cell controls the loading cycle; in position-control on the Dartec, the operator had to manually adjust the displacement of the ram to maintain the load cycle between 1 and 7 N. Because of creep within the system, presumably in the cartilage and ligaments, constant adjustment was necessary. This was evident, particularly within the first minute of loading. Unfortunately, it was not possible to convert the Dartec to load-control due to cost. This limitation introduced a potential large source of error and for this reason, the same operator loaded the rats each day. Because of the relation between applied strain rates and osteogenic response, this model may benefit

from a ramped-square loading wave form. Unlike the sine wave, the ramped-square wave form would apply a more consistent and longer period of loading at a pre-determined strain rate. It was not possible with the Dartec to produce a consistent ramped wave form and it was for this reason that a sine wave was chosen.

An interesting finding in two bones that was the appearance of woven bone on the medial periosteal surface. This bone was not apparent on the medial periosteal surface of the contralateral bones. Woven bone has been described by Martin and Burr (1989) as a repair response to mechanical over-strain conditions, however, Rubin *et al* (1995) explain its development as a rapid adaptive response to a potent mechanical stimulus. In this model, the strain conditions produced by axial loading were likely to vary because the bending moment generated in a curved bone would have been highly dependent on the degree of curvature and geometry of the bone. Hence slight variation in bone size and shape could have caused variation in the biological response. This variation, together with slight changes in the Dartec ram displacement pattern, could have resulted in over-loading, explaining the woven bone response and fractures that occur occasionally using this model (Hillam unpublished data; J.Mosley, Royal Veterinary College, personal communication). However, in this experiment only one bone fractured. Conversely, there are occasions when the bones fail to respond, reflected by the two which didn't demonstrate any new label incorporation, compared with the unloaded controls. In this case, rat 10 in study 2 showed inner label lengths that were around 55% compared with the remaining nine animals that were around 35%. This suggested that the sampling site for rat 10 may have been different from that in the others. Potential variation in the response to loading could be reduced by the use of more sophisticated digital loading apparatus which would increase the precision of the loading conditions. Indeed, this appears to be the case when using a more up-to-date loading device, in which the loading conditions can be defined accurately by programming the ram displacement parameters to give a 2 Hz ramped-square wave, producing a constant strain rate of 100,000

μstrain sec^{-1} on the loading and unloading phases of each cycle (T.M. Skerry, University of York, personal communication 1996). This system has reduced variation and abolished fractures in experiments with the same model.

Intermittent administration of PTH has been documented as stimulating new bone formation (Tada *et al* 1990; Dempster *et al* 1993; Jerome 1994). It is an interesting observation made by Schultz *et al* (1995) that xylazine and ketamine anaesthesia in rats resulted in dramatic rises in circulating levels of PTH. In this experiment, it is possible that transient rises in systemic PTH could have contributed to the bone formation observed at the medial periosteal surface. Xylazine and ketamine were chosen because the combination was convenient to administer and avoided the health and safety risks associated with halothane. However, it was noted that the extremities appeared less well perfused with blood than conscious animals. Hypovolaemia is a well documented effect of xylazine. It is also possible that this could have effected the response to loading. In addition, the recovery time from xylazine and ketamine was much longer than halothane. This could have effected the overall health of the animals and have potentially diminished the response to the loading stimulus. Further experiments are indicated to investigate possible effects of the type of anaesthetic on the osteogenic response to loading.

An advantage of this method of loading bone *in vivo* compared with other techniques such the avian ulna loading model (Rubin and Lanyon 1981, 1984) and the rat caudal vertebral loading model (Chambers *et al* 1993) is that it does not involve surgery and is therefore non-invasive. Additionally, unlike the rat tibia four-point loading model (Turner *et al* 1991) the point of application of the load is distant from the sampling site. During loading, there were no external signs of trauma to the soft tissues at the points of loading and the rats displayed no signs of lameness on recovery from the anaesthetic, following a period of loading. In addition, the point of application of load was distant from the sampling site and any response was less likely to be complicated by mediators of inflammation which are responsible for the regional acceleratory

phenomenon (Frost 1983). Finally, there was an internal control; the contralateral limb.

The observed pattern of bone formation observed following a period of resorption is similar to the reversal phase described in the bone remodelling cycle. This model could represent a convenient way of investigating the cellular events associated in both the reversal and the activation phases. This could be achieved by loading the ulnae for a period known to be sufficiently long enough to stimulate new bone formation at the medial periosteal surface. If loading was then stopped and the rats killed at various intervals after cessation of loading then the temporal sequence of cellular events involved in osteoclastic activation could be investigated.

2.7 Conclusion

Mechanical loading of the ulnae in 85-95g female Wistar rats produced cellular changes and incorporation of calcein fluorochrome label on the medial periosteal surface at the mid-diaphysis, all of which were consistent with stimulating active bone formation on a bone surface which had been previously resorbing. These observations were associated with a 10 Hz sinusoidal loading regime which produced dynamic axial strains of -4000 to -4500 μstrain at the mid-diaphyseal, medial periosteal surface.

Chapter 3

Investigating a technique for supplementing thyroparathyroidectomised rats with physiological levels of thyroxine

3.1 Summary

Two pilot studies were performed in an attempt to establish the release characteristics of two doses of subcutaneous implantable thyroxine pellets. The purpose of these studies was to supplement rats, which had undergone thyroparathyroidectomy, to achieve consistent blood levels of thyroxine which were within the normal physiological range.

The two doses of pellets chosen were 75 mg and 15 mg. One week after surgery, the 75 mg implants caused profound loss of body condition and blood levels which were four times higher than the mean basal level. The 15 mg pellets did not produce the severe loss of body condition observed with the higher dose pellets but the blood thyroxine levels were always higher than the basal controls over the nine week period. In particular, the pellets tended to produce very high levels in the early period after implantation. After one week, the levels were on average three to four times higher than basal controls. Subsequent measurements fell exponentially. However, the nine week levels were still higher than the basal controls. The measurements taken at one and three weeks following implantation with the 15 mg pellets demonstrated a large range of blood thyroxine.

The pellets proved unreliable and incapable of producing constant levels of hormone within the physiological range and were, therefore, deemed unsuitable for supplementing thyroparathyroidectomised rats with thyroxine.

3.2 Introduction

It has been well documented that thyroid hormones affect greatly the body's basal metabolic rate. In addition, there is evidence that the thyroid hormones also affect the rate of cellular remodelling activity in bone. Mundy *et al* (1976) demonstrated the direct stimulation of bone resorption by thyroid hormones *in vitro*, using organ cultures of fetal rat long bones, while Mosekilde and Melsen (1978) and Eriksen *et al* (1985;1986) documented effects on bone histomorphometric parameters in hyperthyroid and hypothyroid human patients. Excess thyroid hormones stimulated increases in bone formation and bone resorption rates with the net effect being a decrease in trabecular bone mass and an increase in cortical porosity. The bone changes observed in hypothyroid patients were described as being opposite to those seen in the hyperthyroid patients.

Chapter 4 describes an experiment in which the role of parathyroid hormone on the development of ovariectomy-induced osteopenia was investigated in the rat. This study was performed by removing the parathyroid glands in two groups of rats so that they could be deprived of parathyroid hormone. The parathyroid glands in rats are located commonly as two discrete structures at the cranial poles of the thyroid gland (figure 3.1). However, the parathyroid tissue is often not clearly visible at this site because it may be distributed as multiple islets of tissue throughout the substance of the thyroid gland (Casewell and Fennell 1970). For this reason, a thyroparathyroidectomy was considered to have been more successful at removing all of the parathyroid tissue than parathyroidectomy alone. In addition, thyroparathyroidectomised rats would have lost most of their thyroid tissue, with only small remnants of the gland remaining in place, possibly adherent to the trachea and the recurrent laryngeal nerves. The loss of this gland would also have deprived the rats of thyroxine (T_4) and calcitonin. As a result of thyroparathyroidectomy, it was likely that the loss of thyroid hormones would have affected bone cell

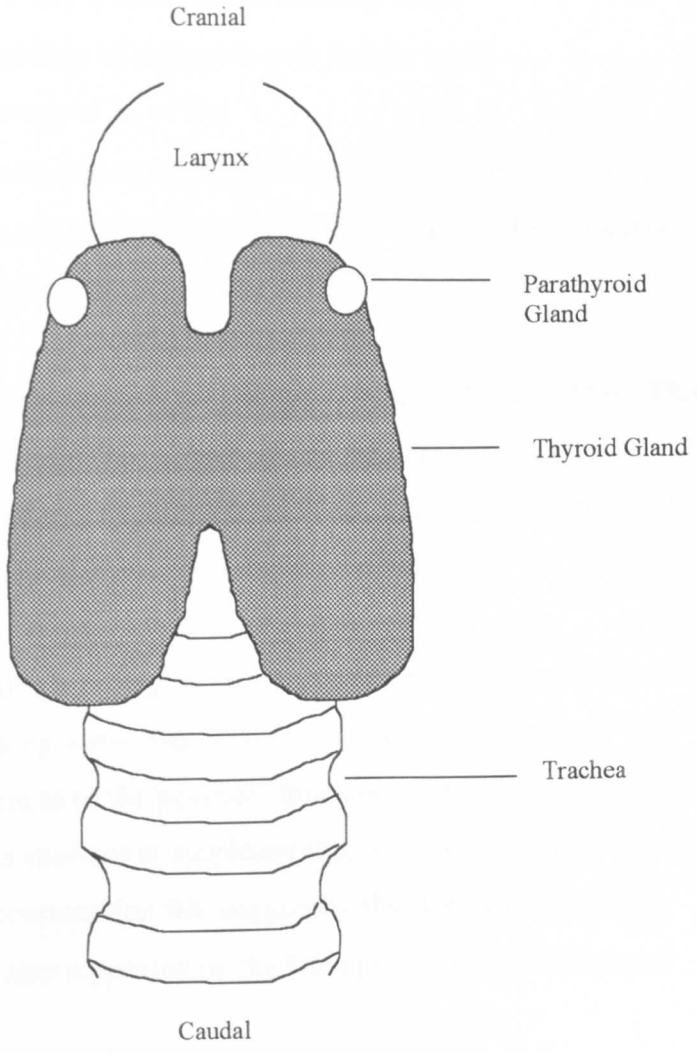

Figure 3.1
The anatomy of the thyroid and parathyroid glands

metabolism. Therefore, it was considered necessary to assess the possibility of supplementing the rats with thyroxine to restore levels to the physiological range. There were several options available for thyroxine supplementation:

1. Administration of thyroxine in the drinking water.
2. Gavaging a solution of thyroxine on a regular basis.
3. Regular injections of T_4 or T_3.
4. Constant administration of thyroxine solution by implanted mini-pump.
5. Use of subcutaneous slow release, bio-degradable pellet implants containing thyroxine.

In rats the half-life of thyroxine is only about 12 hours (Davies 1993). This means that supplementation has to be commenced immediately after performing thyroparathyroidectomy. In addition, it must be administered on a daily basis if physiological levels are to be maintained.

It was decided that despite being the most convenient option, administration of hormone in the drinking water was likely to be an unreliable way of supplementation because of the possible variation in the volume of water consumed. Previous attempts at supplementing with thyroxine in this way showed that water consumption fell, suggesting that the rats disliked the solution.. This was also supported by the findings of Hirsch & Hagaman (1986).

Regular oral dosing by gavage, involving the injection of a small volume of thyroxine solution into the stomach using a syringe and stomach tube, or parenteral administration by injection were methods which may have guaranteed constant levels of thyroxine. However, both procedures, if repeated on a daily basis could have led to excessive stress on the animals. Indeed, stress has been shown to affect significantly the blood levels of the thyroid hormones following surgery and different anaesthetic or bleeding techniques (Davies 1993).

Use of a mini-pump was ruled out because the duration of the experiment was to be three months whereas the mini-pump's maximum release period was only one month. Use of these implants would have required three surgeries and it was considered that this would have caused too much stress on the animals. In addition, the cost of three mini-pumps per rats was considered excessive.

There have been several reports of the successful use of implantable pellets containing thyroxine in the little brown bat (Damassa *et al* 1985) and in cotton rats (Derting 1989). Derting reported that the thyroxine implants proved more reliable than injection. Therefore, it was decided to investigate the implantable pellets as a method of supplementing with thyroxine in rats which had been thyroparathyroidectomised.

3.3 Aims

The aim of this study was to determine the effective dose of an implantable thyroxine slow release pellet which gave consistent physiological levels of thyroxine, for a period of three months, in the thyroparathyroidectomised rat.

The specific objectives were:

1. To assess normal physiological range of total blood thyroxine.
2. To determine the effects of 15 and 75 mg implantable thyroxine pellets on the blood thyroxine levels in thyroparathyroidectomised rats.

3.4 Methods

I Assessing normal levels of thyroxine

47 x 130 g female Wistar rats were anaesthetised with fluothane. 1 ml of blood was taken from each rat by cardiac puncture. The blood was left to clot for 20 minutes at room temperature before it was centrifuged and the serum

was drawn off. Serum was assayed for total blood T_4 using a fluorescence polarization immunoassay (IMx T_4 assay, Abbott Laboratories, Illinois, USA). This was performed by a commercial veterinary biochemistry laboratory (Grange Laboratories, Wetherby, W. Yorkshire, UK).

II Study one

To determine the release characteristics of 75 mg pellets

Six male Wistar rats (385-460 g) were divided randomly into two groups; group A and group B. The rats were anaesthetised with xylazine (Rompun, Bayer, Suffolk, UK) and ketamine (Vetalar, Gwent, UK) at a dose of 12 mg/kg and 50 mg/kg respectively. Group A were thyroparathyroidectomised (appendix 2) and the rats of group B were also thyroparathyroidectomised but in addition had a 75 mg T_4 pellet (Innovative Research Of America, Ohio, USA) implanted subcutaneously approximately three to four cm away from the incision via a tunnel formed through the subcutaneous fascia using closed artery forceps.

Each pellet was checked visually for external damage prior to implantation. Care was taken to prevent damage to the pellets' surface during handling so that its release characteristics wouldn't be affected.

Blood samples were taken by cardiac puncture pre-operatively and one week post-operatively, again under xylazine and ketamine anaesthesia. Individual body weights were recorded at the same time. Whole blood was left to clot for half an hour at room temperature before it was centrifuged. Serum was then stored at -20° C until analysis for total T_4. At the end of the experiment the rats were killed by i/p injection of sodium pentobarbitone (Euthatal, RMB, UK) and all of the pellets were collected and examined.

III Study two

To determine the release characteristics of 15 mg pellets

Ten Wistar ex-breeder males (450-500 g) were anaesthetised (xylazine and ketamine at the same doses described previously). Pre-operative basal blood samples taken by cardiac puncture then the rats underwent thyroparathyroidectomy. Blood sampling was repeated at one and five and a half weeks post-operatively. Four of these rats had 15 mg pellets implanted subcutaneously immediately after the bleeding at five and a half weeks. These implanted rats were then re-anaesthetised (xylazine and ketamine) and bled at one, three, six and nine weeks post-implantation. At the end of the experiment the rats were killed by i/p injection of sodium pentobarbitone (Euthatal) and all of the pellets were collected and inspected for fragmentation or damage.

3.5 Results

I Normal levels of thyroxine in 47 130 g female Wistar rats

Expressed as mean total blood thyroxine in nmol/l (± SD):

65.9 (12.3)

The data was distributed normally so the physiological range for the rats could be expressed as: 41.3 - 90.5 nmol/l (mean ± 2SD)

II Study one

One of the implanted rats died 24 hours after the first surgery. By one week post-implantation, the two remaining rats with pellets had developed poor coats and looked very thin. They subsequently died two hours after the second anaesthetic. In contrast, the animals in the other group looked very healthy and recovered well from anaesthesia.

Table 3.1 Body weights (grams) and total T_4 (nmol/l).

	Basal body weight	Body weight after 1 week	Basal blood total T_4	Blood total T_4 after 1 week
Group A				
Rat 1	460	428	74.4	27.7
Rat 2	460	450	72.6	50.2
Rat 3	440	424	64.0	36.0
Group B				
Rat 1	410	-	81.5	-
Rat 2	406	374	60.5	248.7
Rat 3	385	360	62.2	300.9

Mean loss of body weight in rats from group A was 4.3 % of original weight but that for rats in group B was 7.3 %.

Basal total blood thyroxine was 69.2 ± 8.3 nmol/l (mean ± SD). The mean one week post-operative thyroxine level was 38.0 nmol/l for group A but was 274.8 nmol/l for group B, which was four times greater than the basal mean.

II Study two

Table 3.2 Results of total T_4 before pellet implantation (nmol/l) (mean ± SD).

Basal	1 week post-op	5.5 weeks post-op
54.2 +/- 12.1	< 2.0	4.8 (3.9)

These data show that the mean thyroxine level one week after surgery was below the detection resolution of the assay. At five and half weeks post-operatively, the level had risen slightly but they remained very low.

One rat died after blood was taken one week after implantation. The one week post-implantation blood thyroxine level was < 2.0 nmol/l. However, all data from this rat was excluded from the study.

Table 3.3 Total T_4 levels following implantation of the pellets (mean ± SD).

1 week post-op	3 weeks post-op	6 weeks post-op	9 weeks post-op
211.2 (51.8)	99.2 (29.7)	87.7 (6.7)	71.9 (8.0)

These results are summarised in figure 3.2

Post-mortem inspection showed that in all of the implanted rats from both studies, the pellets were contained in a pocket of myxoedematous tissue. Examination of every pellet revealed the presence of a fine transverse fissure (figure 3.3).

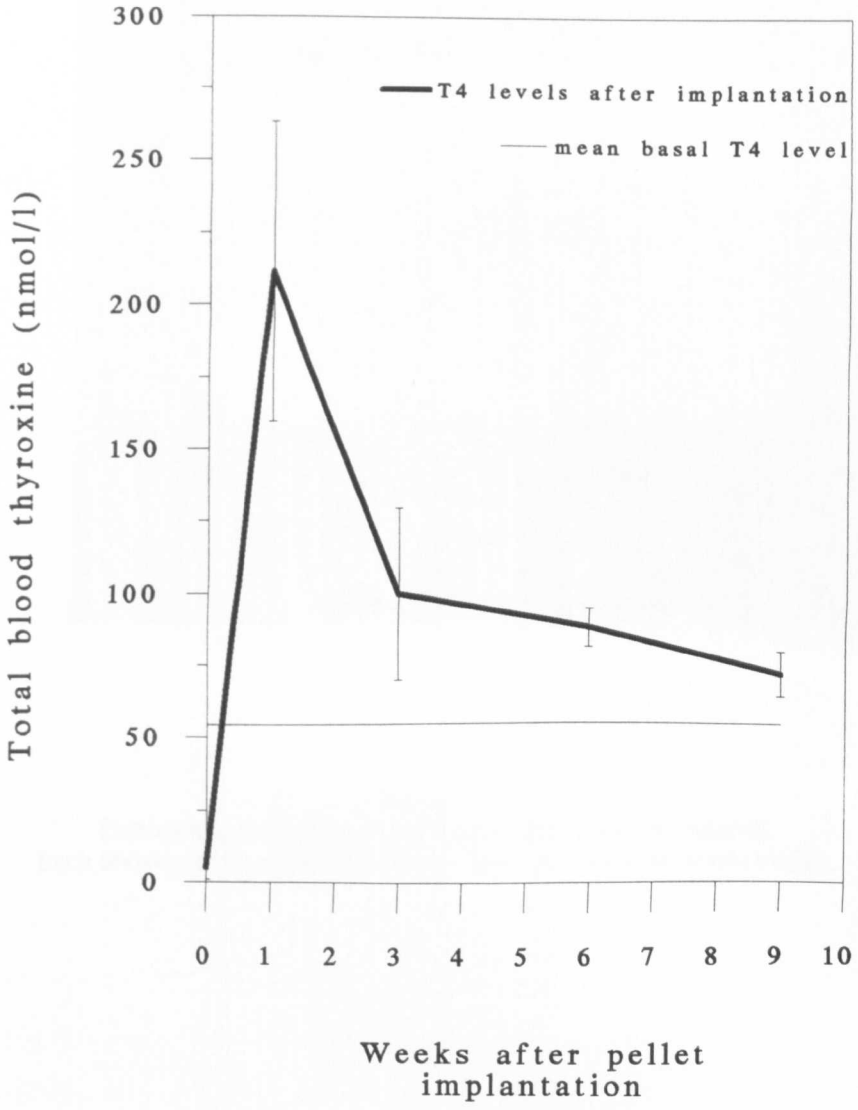

Figure 3.2 Release characteristics of 15 mg thyroxine pellets

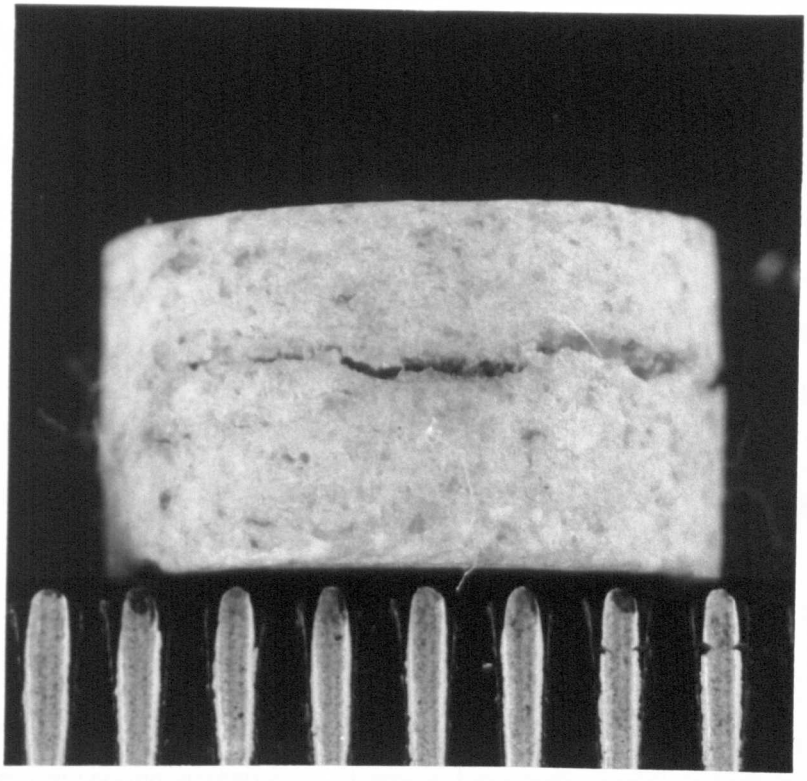

Figure 3.3
Photograph of a thyroxine implantable pellet after its removal.
Each division of the scale represents 1 mm. The fissure is clearly visible.

3.6 Discussion

The physiological range of thyroxine in rats was determined as 41.3 - 90.5 nmol/l. The aim was to supplement thyroparathyroidectomised rats to levels between this range, consistently for three months.

Study one

Following advice from Innovative Research of America, 90 day-release pellets containing 75 mg of thyroxine were selected initially because this dose was apparently the most appropriate for supplementation to physiological blood levels in 400 g rats. However, the one week post-operative blood thyroxine levels combined with the signs of poor body condition indicated that the thyroxine dose of these pellets were pathologically high. Signs of poor health included emaciation, dirty and greasy coats.

Unfortunately, thyroxine levels could only be assessed one week post-operatively because the poor health of the animals resulted in their death shortly after the second anaesthetic. It would have been useful to look at long term hormone release patterns and see if the blood levels remained fairly constant or whether they fell quickly.

Numbers were low in this pilot study but the dramatic increase in blood total thyroxine was sufficiently convincing to justify repeating the study with a lower dose pellet. It should be noted that damage to the pellet may alter hormone release rates (Dr. S. Shaffey, Innovative Research of America, personal communication) but in this experiment, great care had been taken to handle the pellets gently. The finding of transverse fissures may have been a normal feature of the pellets' release mechanism, however, it was possible that these fissures were the cause of the high thyroxine levels, brought about by an increase in the surface area available for resorption. It was also interesting to note that the mean total thyroxine level in group A one week after thyroidectomy were approximately 50% of the basal mean. This was

surprising because if the thyroid gland had been removed fully it might be possible that any remaining islets of thyroid tissue would hypertrophy to replace the function of any lost tissue and gradually, over a long period, restore thyroxine levels to normal. However, these thyroxine levels one week after surgery suggested that appreciable thyroid tissue must have been left *in situ* following the operation. This was an important observation because it suggested the possibility of leaving nests of parathyroid tissue behind within the retained thyroid gland.

The method of anaesthesia and even the technique used for obtaining blood samples has been reported to affect blood thyroxine measurements (Davies 1993). Davies described how stress due to handling, transportation, minor surgery or anaesthesia could all reduce blood levels of thyroid stimulating hormone, total and free thyroxine and tri-iodothyronine in rats. For each rat in this study, the type of anaesthetic and method of blood sampling was identical.

Study 2

One week post-implantation, the mean thyroxine value was nearly four times greater than the mean basal value. This data showed clearly that even by nine weeks post-implantation, the total thyroxine levels were still above the basal levels (figure 3.2).

Even the 15 mg pellets appeared unsatisfactory for providing thyroxine supplementation because of the wide variation in the amount of hormone released. The rat that was excluded from this study failed to release any detectable amounts of thyroxine after a week. In a separate study, not documented in this thesis, two other rats which had undergone pellet implantation following complete thyroidectomy also failed to release any detectable thyroxine, even after three months.

Post-mortem inspection showed that in each rat, the pellet was contained in a pocket of myxoedematous tissue. In every case there was the appearance of the fine transverse fissure as described previously in study 1. Because this was a consistent finding in both experiments, it is likely that the development of a fissure was a normal degradation feature of the implanted pellets. However, it could still have been the cause of the inconsistent release characteristics due to the variation in surface area available for hormone release. This could have explained the differences in blood thyroxine levels.

Although blood levels were only slightly higher than the mean basal level by six to nine weeks post implantation, the extreme hyperthyroid state at one week after implantation was considered unacceptable because of the likely increase in bone resorption.

Compared with study one where the one week post-thyroidectomy thyroxine levels had risen dramatically in rats that had not received pellets, it was interesting to note that in study two, thyroxine levels in the unsupplemented rats remained very low, even at five and a half weeks after surgery. This implied a far more thorough thyroidectomy. The advantage of this was that any parathyroid tissue disseminated throughout the thyroid gland (Casewell and Fennell 1970) was more likely to have been excised. However, the disadvantage was that the need for thyroxine supplementation was more important.

The pellets proved expensive and were very unreliable in their hormone release properties. Generally, hormone levels peaked within three weeks after implantation then fell gradually. One of the thyroparathyroidectomised rats with an implanted 15 mg pellets failed to demonstrate any release of hormone one week after implantation.

3.7 Conclusion

Following thyroparathyroidectomy, thyroxine levels fall to consistently low levels which persist for at least five and a half weeks. The conclusions drawn from this experiment are that implantable pellets are not suitable for physiological thyroxine supplementation. The reasons for this are that the blood levels achieved are highly variable and in addition the mean levels are particularly high in the early period following implantation.

Chapter 4

The role of parathyroid hormone in the development of ovariectomy-induced osteopenia in the adult rat

4.1 Summary

The experiment was designed to test the hypothesis that parathyroidectomy reduces bone loss which occurs after ovariectomy

Removal of the parathyroid glands was achieved by complete thyroparathyroidectomy; an immunoradiometric assay, specific for rat PTH, confirmed successful removal of the parathyroid glands. At the end of the 12 week experiment, the rats were killed and bones were removed for analysis. The proximal tibiae were scanned by quantitative computed tomography to assess bone mineral density. The lumbar vertebrae (L5 and L6) were compressed to failure, whilst the radii and ulnae were tested in three point bending. The calvariae were examined by histomorphometric analysis.

The results demonstrated significantly higher trabecular BMD in the proximal tibiae of the OVX+tPTX group than the OVX group. The strength of the L5 vertebral bodies was not quite significantly different when comparing the OVX+tPTX group with the OVX group but this may have been attributable to the relatively short duration of the experiment and the low numbers in the groups. There was evidence of an interaction between the effects of ovariectomy and thyroparathyroidectomy in the result of the trabecular and cortical BMD. The results of the three point bending tests did not demonstrate any independent effects or an interaction, although an interaction in the radii was not quite significant ($p = 0.052$). No significant differences between any groups were apparent.

4.2 Introduction

The role of parathyroid hormone (PTH) in post menopausal osteopenia remains unclear. It has been proposed that there may be an increased sensitivity of bone to the resorptive effects of PTH following menopause (Heaney 1965 and Jasani 1965). Several workers have performed studies in both animals and humans in an attempt to disprove this hypothesis. The findings have been equivocal. A study looking at the femora and tibiae of intact and ovariectomized rats following treatment with PTH, concluded that bone was more sensitive to the resorptive effects of PTH in the absence of endogenous oestrogens (Orimo *et al* 1972). There has also been a recent human study looking at bone mineral density and metabolic markers of bone turnover in a group of post menopausal patients. Half were euparathyroid, the remainder being hypoparathyroid. The findings were that the hypoparathyroid condition protected against age-related bone loss, particularly early after menopause (Fujiyama *et al* 1995). Both of these studies support Heaney and Jasani's hypotheses. However, there has been a recent study in which rats were divided into four groups: sham controls, ovariectomy (OVX), parathyroidectomy (PTX) and OVX+PTX. Histomorphometry of the distal femora revealed no significant differences in trabecular bone volume or trabecular spacing between the OVX and the OVX+PTX groups. The conclusion drawn from this study was that PTX did not reduce OVX-induced bone loss (Sims *et al* 1994). Also, in another human study, serum calcium and urinary hydroxyproline (a marker of collagen breakdown) were measured in a group of women. These women were divided into three sub-groups: premenopausal controls, post menopausal controls and a group of post - menopausal osteoporotics. Each person was infused continuously with PTH over three days. The authors concluded that oestrogen deficiency did not increase the sensitivity of bone to PTH (Tsai *et al* 1989). So data from these two latter studies provided evidence to disprove Heaney and Jasani's hypotheses.

Controversy exists over the effects of primary hyperparathyroidism on skeletal bone mass and spinal fractures in post menopausal women. There are reports of both decreased bone density with increased prevalence of vertebral fractures (Kochersberger *et al* 1987) but also reports of increased bone mass and trabecular connectivity in mild hyperparathyroidism in post menopausal women (Parisien *et al* 1995). There are also numerous reports of the therapeutic use of PTH to protect against bone loss following immobilisation or ovariectomy in rats (Liu & Kalu 1990; Tada *et al* 1990; Liu *et al* 1991; Ma *et al* 1995; Okimoto *et al* 1995) and after menopause in humans (Reeve *et al* 1980; Slovik *et al* 1986; Dempster *et al* 1993).

Immobilization osteopenia in dogs has been shown to be dependent on parathyroid and thyroid hormones (Burkhart and Jowsey 1967) In addition, parathyroid activity has also been shown to be responsible for the development of osteopenia in cats which were fed a low-calcium diet (Jowsey and Raisz 1968).

It has already been established (chapter 1, section 1.6) that the ovariectomized aged female rat represents an acceptable and convenient model for the study of post menopausal osteoporosis. In the study of Sims *et al* (1994) younger rats (three months old) were used. These animals would have been still growing so that new trabecular bone would have been produced continually by longitudinal bone growth. It is likely that this may have confused interpretation of the data. To investigate further the role of PTH in the development of post menopausal osteoporosis, an experiment was designed choosing 10 month old virgin female rats as the model for post menopausal osteoporosis, in an attempt to overcome this possible complication caused by the continual formation of growth-related trabecular bone.

4.3 Aims

The hypothesis tested was that parathyroidectomy prevents the osteopenia induced by ovariectomy in adult rats kept under identical conditions.
The specific aims of the study were to assess:
1) Mechanical strength of the lumbar vertebrae by loading to failure in compression and the strength of the radii and ulnae using three-point bending tests.

2) Bone mineral density (BMD) of the proximal tibia using quantitative computed tomography.

3) Thickness and porosity of the parietal bones using histomorphometry.

4.4 Materials and methods

42 ten month old virgin female Wistar rats were divided randomly into five groups and weighed:

Group 1:	Basal controls	n=6
Group 2:	Sham operated controls	n=6
Group 3:	Ovariectomized (OVX)	n=10
Group 4:	Thyroparathyroidectomized (tPTX)	n=9
Group 5:	OVX + tPTX	n=11

Anaesthesia

Two techniques were used:
1. Intraperitoneal (i/p) injection of a 50:50 by volume mixture of xylazine (Rompun, 22.5 mg/ml, Bayer, Bury St. Edmunds, UK) and ketamine (Vetalar, 100 mg/ml, Parke-Davis, Pontypool, UK) at a dose rate of 1.0 ml/kg body weight.

2. *Inhalation of fluothane* (Halothane, Zeneca Pharmaceuticals, Macclesfield, UK) using a Fluovac vaporiser (International Market Supply, Cheshire, UK).

Blood sampling

Blood was sampled at the start of the experiment, after three weeks and at the end of the experiment (12 weeks):

1. Immediately after induction of anaesthetic, all sham, OVX and OVX+tPTX rats had approximately 1.5 mls of blood removed by cardiac puncture using a 2 ml hypodermic syringe and 1 inch 21 gauge needle. The blood was allowed to clot. After centrifugation, the serum was removed and stored at -80°C for future assay of normal control levels of thyroxine (T_4) and parathyroid hormone (PTH).
2. After three weeks the rats were anaesthetised with fluothane. Blood samples were collected and stored as described above.
3. After three months the rats were anaesthetised with fluothane and blood was collected and stored, as described previously, immediately before being killed.

Fluorochrome labels

Details of the fluorochrome preparation are described in appendix 2.

1. At the start of the experiment, on the day of surgery all rats were given a subcutaneous (s/c) injection of calcein. The dose administered was 15 mg/kg body weight.
2. 14 days before the end of the experiment the rats were injected s/c with xylenol orange at a dose of 90 mg/kg.

3. Finally, 24 hours before the end of the experiment a s/c injection of oxytetracycline (Terramycin Q50, Pfizer Ltd., Sandwich, UK) was given at a dose of 20 mg/kg.

Basal group

The basal controls were injected with calcein s/c then killed 24 hours later with an intraperitoneal (i/p) injection of pentobarbitone (Euthatal, Rhone-Merieux Ltd , Essex, UK). The tibiae, lumbar vertebrae, calvariae, radii and ulnae were removed and placed in 70 % ethanol.

Ovariectomy

The rats were blood sampled following anaesthesia with xylazine and ketamine. They were then ovariectomized, details of which are described in appendix 2. Calcein was injected s/c before recovery.

Thyroparathyroidectomy

The rats were anaesthetised with xylazine and ketamine and a blood sample was taken. The rats then underwent thyroparathyroidectomy, details of which are described in appendix 2. Calcein was injected s/c before recovery.

Sham surgery

The sham operated controls were anaesthetized with xylazine and ketamine and blood samples were obtained. Sham surgery involved approaches identical to those used for ovariectomy and thyroparathyroidectomy. However, the ovaries and thyroid/parathyroid glands were left intact and *in situ*. The purpose of this was to provide controls which had undergone procedures that were as similar as possible to the OVX and OVX+tPTX groups. This ensured that any possible differences in the results were directly attributable to the absence of ovaries and thyroid/parathyroid glands.

The rats were then injected with calcein (s/c) before being allowed to recover.

At the end of the experiment the uteri from all OVX, OVX+tPTX rats and the shams were dissected out and weighed. This was conducted to ensure success of the OVX procedure; if all ovarian tissue is removed, the uteri involute and are much smaller compared with shams, particularly if the latter are in a state of oestrus.

Killing

1.5 mls of pentobarbitone (Euthatal, Rhone-Merieux Ltd., Essex, UK) was given by intracardiac injection, except for the basal group which were given i/p injections.

Bone collection

The left radii and ulnae, lumbar vertebrae, right tibiae and the half of each calvaria were retained for mechanical testing, pQCT and histomorphometry. The bones for mechanical testing were left with their associated muscles intact and wrapped tightly in cling film to prevent dehydration. They were then stored at -20° C. Those kept for pQCT and histomorphometry were placed in 70 % ethanol.

Blood Parathyroid Hormone Assay

Serum was assayed using a Nichols Institute rat parathyroid hormone immuno radiometric assay (IRMA) (Immunotopics Inc., San Clemente, USA, distributed by Nichols Institute, Essex, UK). The procedure was performed according to the kit instructions. All samples were assayed in duplicate and in each case, gamma counting was performed over three minutes instead of the recommended one minute. The value was then divided by three to give a mean value per minute. This was done to increase accuracy.

Blood Thyroid Hormone Assay

Serum was assayed for total blood T_4 using a fluorescence polarization immunoassay (IMx T_4 assay, Abbott Laboratories, Illinois, USA).This was performed by a commercial veterinary biochemistry laboratory (Grange Laboratories, Wetherby, W. Yorkshire, UK).

Peripheral quantitative computed tomography (pQCT)

The tibiae were scanned at Zeneca pharmaceuticals, Alderley Park, Macclesfield using a Stratec 960A pQCT machine (Stratec GmbH, Birkenfeld, Pforzheim, Germany). The tibiae were placed in glass tubes filled with 70% ethanol (figure 4.1). These were then held firmly in the machine's positioning device. After an initial scout view, three slices were scanned at seven, eight and nine mm distal to the proximal tibial condyles (tibial plateau). The scans were performed at a resolution of 0.148 mm.

Analysis was performed with: 'Special Analysis Software version 5.1' (Stratec GmbH) using: contmode 2, peelmode 2 (threshold of 0.7) and cortmode 1 (appendix 2). The values of the three scans for trabecular, cortical and total bone were averaged to give a mean value of BMD.

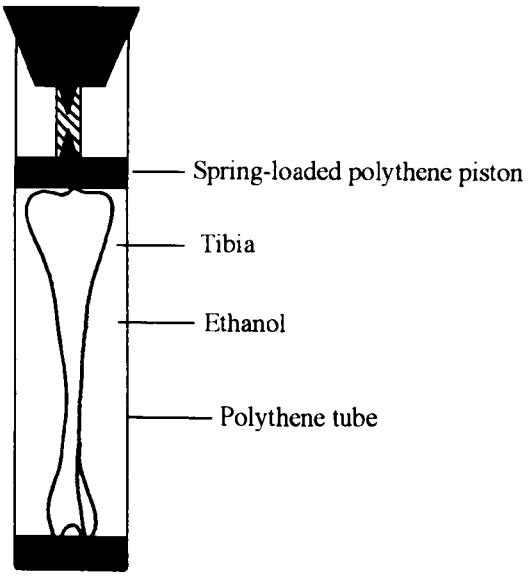

Figure 4.1
Diagram to illustrate preparation of the tibiae for pQCT scanning

Mechanical Testing of the Lumbar Vertebrae

The vertebrae were thawed for two to three hours and allowed to reach room temperature. All soft tissues were dissected off the bone and the remnants of the intervertebral discs were removed from the end plates. The neural arch and transverse processes were removed carefully using a junior hacksaw, ensuring that the cortical shell was not damaged. The cut bone edges were then gently

filed smooth and flush with the vertebral body using a watch-maker's file. At all times the bone was kept moist with Hartmann's lactated Ringer's solution (Aquapharm, UK) as it has been shown that temperature and state of hydration can dramatically alter the physical properties of bone (Dempster and Liddicoat 1952; Evans 1973; Reilly and Burstein 1974; Brinckmann 1988). For compression testing, the vertebral bodies were placed in a system that was repeatable and allowed even loading over the entire endplate (appendix 2). Brass cups were prepared by trimming down Colt .45 ACP centrefire pistol ammunition (CBC, Brazil) cases from 22 mm down to 14 mm and 7 mm in length. The 14 mm case was then filled with liquid dental plaster (Green Grade, Ultrahard Suprastone, Kerr, Peterborough, UK). As the plaster began to set, a vertebral body was pressed 1.5 mm into the plaster such that the bone was just held supported with its long axis in a vertical position (figure 4.2). Once set, the other cup (7 mm) was filled with dental plaster then a plastic support made from a 5 ml hypodermic syringe (Monoject, Sherwood Medical, Sussex, UK) was placed over the top of the cup. The first cup containing the bone was lowered down the centre of the tube until the bone just indented the surface of the liquid plaster in the lower cup. At this point, the plaster was allowed to set. Once set, the cups were then carefully placed between the rams of a materials test machine (Dartec, Stourbridge, UK). The upper ram was gently lowered until it just came into contact with the upper cup. At this point the Dartec was programmed to compress the bone in position control at 3 mm/minute until failure (figures 4.2 and 4.3). The force and displacement data were collected using an analogue to digital (A/D) 12-bit capture card (RTI-815, Analog Devices, USA) fitted to a personal computer (Viglen 486DX, 33 MHz) running custom software ('Super', D.McNally, University of Bristol) and sampling at a frequency of 26 Hz.

The results were discarded if any rotation of the bone occurred during compression due to the unpredictable loading pattern imposed on the bone.

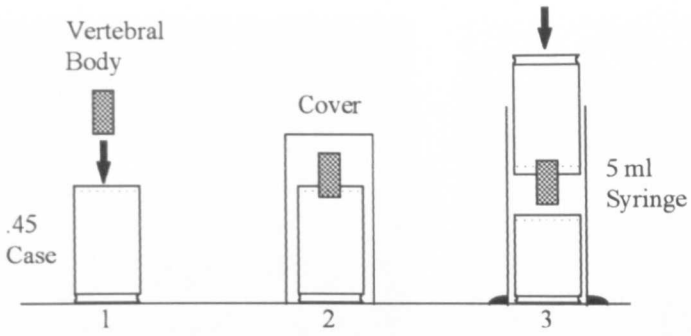

Mounting trimmed L5 & L6 in dental plaster
The bone was kept moist at all times

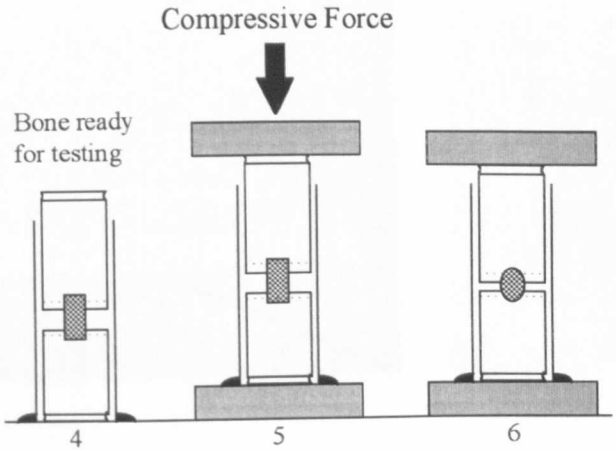

Compression to failure in the Dartec

Figure 4.2
Mechanical Testing of L5 & L6 Vertebral Bodies to Failure in Compression

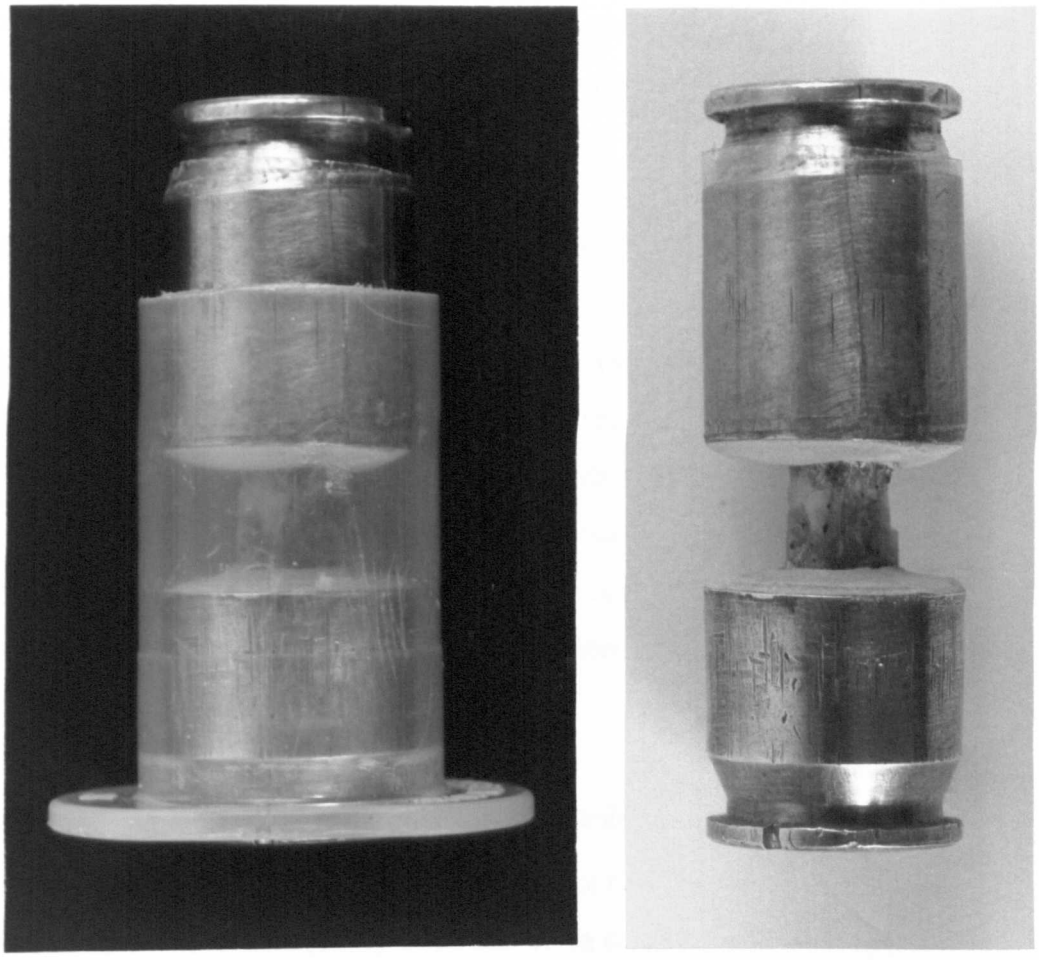

Figure 4.3
Photographs of a lumbar vertebral body mounted in .45 cartridge cases for compression testing. The photograph on the left shows the preparation in a trimmed 5 ml syringe prior to testing whereas the photograph on the right is intended to show more detail of the mounted vertebral body.

Three-point Mechanical Bending Tests of the Radii and Ulnae

The frozen antebrachii were thawed and allowed to come to room temperature. The radii and ulnae were then dissected free of muscle and kept moist by soaking in physiological saline (Hartmann's lactated Ringer's solution, Aquapharm, UK).

The bones to be tested were placed in a custom made aluminium jig such that the mid-point of each bone was mid-way between the two supports, 12 mm apart and held in position with minimal force applied by the indenter (figure 4.4). Care was taken to place every radius and ulna reproducibly in the jig. This was achieved by measuring the length of each bone using vernier calipers then marking the mid-point with a pencil. The bones were then placed in the jig with their medial periosteal surface facing the central indenter, such that the indenter caused failure by increasing the natural longitudinal curvature of the bone (figure 4.5).

Mechanical loads were applied using a mini hydraulic actuator (Dartec, Stourbridge, UK) programmed in position control to move at 0.2 mm $sec.^{-1}$. Data was recorded at a frequency of 64 Hz. using custom software (Super). Load was recorded from a high-accuracy (0.03% full range output, non-linearity) 100 N S-beam strain gauge load cell (model TW750, Transducer World, Aylesbury, UK).

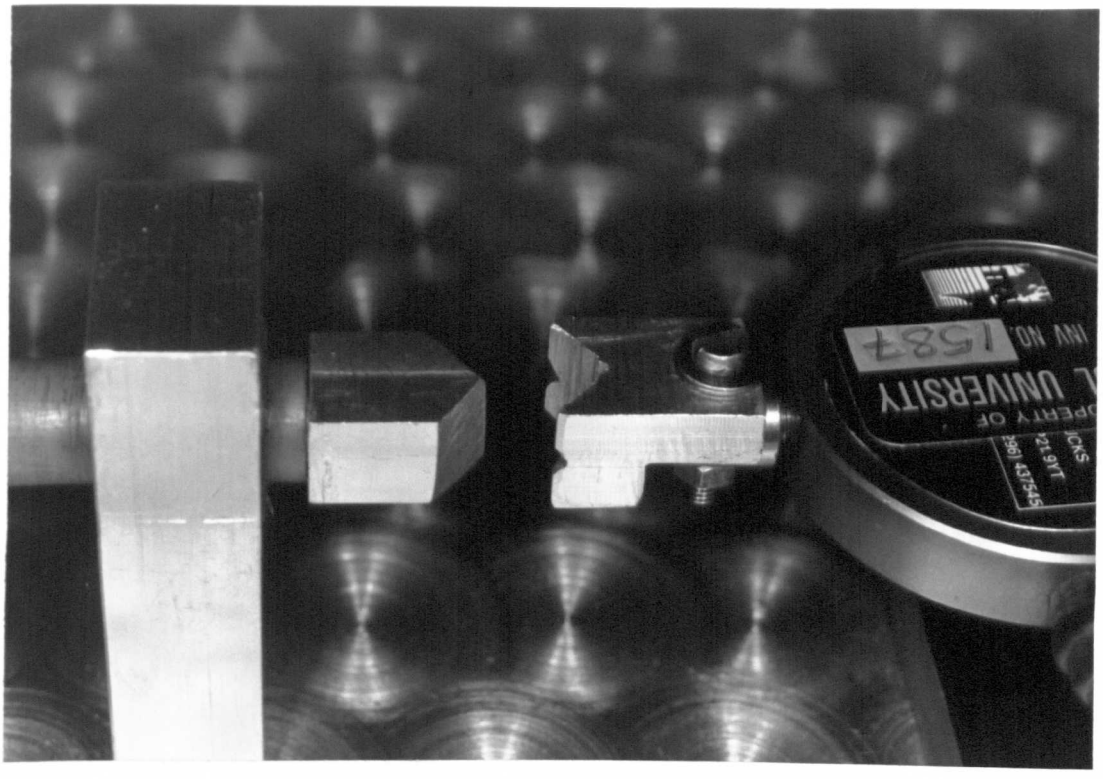

Figure 4.4
Photograph of the 3-point testing apparatus

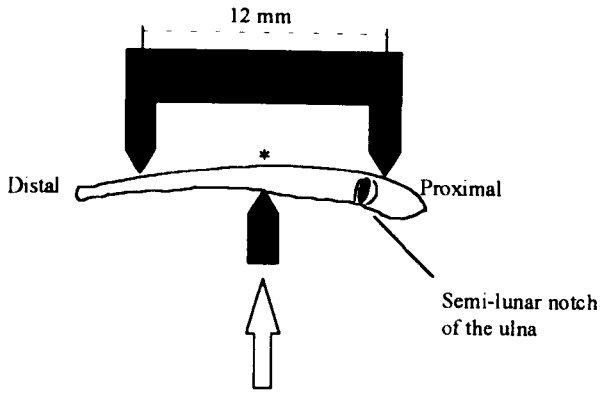

Indenter applying load to the
medial periosteal surface of the ulna

* = point of mechanical failure

Figure 4.5
Diagram to illustrate the apparatus used to test the radii and ulnae in 3-point bending

Measuring the calvarial sections

The parietal bones were dehydrated in increasing concentrations of ethanol until they had been completely dehydrated in 100 % ethanol. They were then infiltrated for six weeks in methylmethacrylate before being polymerised (appendix 1). The embedded bones were then trimmed from the sagittal suture, sectioning parallel to the suture until a point 2 mm from the sagittal suture had been reached (appendix 2). 5 micron thick sections were cut on a microtome (Reichert-Jung, model 2040, Germany), stained with toluidine blue and mounted in DPX (Merck, UK).

The histomorphometry was performed on a Leica microscope (model DMRB), at a magnification of x 5, using a digital bit pad (Calc Comp Drawing Board III, 16 cm x 16 cm, Osteometrics Inc.) and commercial bone histomorphometry software (Osteomeasure™ version 2.31, Osteometrics Inc., Atlanta, USA).

Three parameters were measured (figure 4.6):

1. Parietal thickness
2. Bone area
3. Marrow cavity area

The width of the parietal bone section equated to six fields of view under the microscope. To ensure sampling was well away from the coronal and lamboid sutures, measurements were only made from the two central fields of view (total of 2.4 mm).

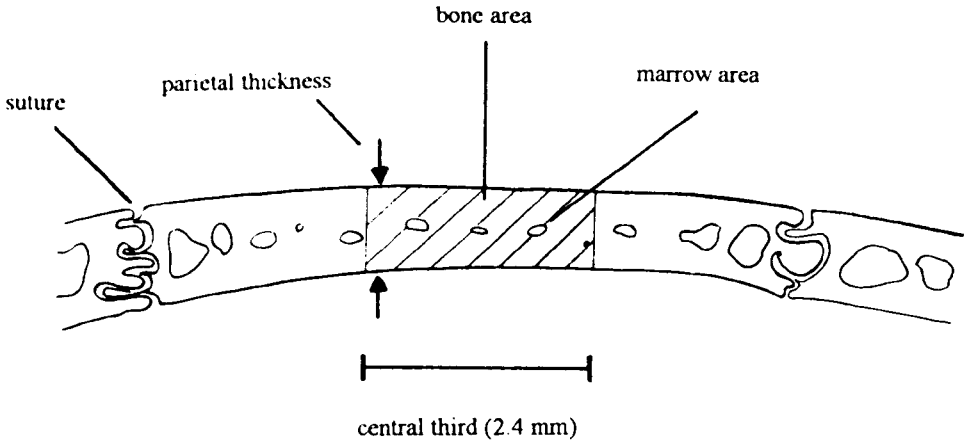

Figure 4.6
Diagram illustrating the parameters measured
in histomorphometry of the parietal bones

Analysis of the results

Data from the mechanical tests and the pQCT were analysed using Instat™ version 2.01 (Graphpad Software, San Diego, CA, USA) and Systat™ version 5.02 for Windows (Systat Inc., IL, USA).

Instat was used for descriptive statistics, Student t-tests, Bartlett's test for homogeneity of variance, 1-way analysis of variance (ANOVA) and multiple comparison post-hoc tests (Tukey-Kramer and Bonferroni). It was also used for non-parametric ANOVA (Kruskal-Wallis) and post-hoc analysis (Dunn) tests.

Systat was used for the Lilliefors test for normality and two-way ANOVA. The two-way ANOVA was used to test for independent effects of ovariectomy and of thyroparathyroidectomy and to look for any interaction between the effects of these two procedures.

The data was first tested for normality using Lilliefors test and for homogeneity of variance using Bartlett's test. If normally distributed with no significant differences between the standard deviations, a parametric analysis was conducted. If the data was not normally distributed and could not be transformed (using natural logarithms) to achieve normality, or the differences between standard deviations were significant, non parametric analysis was performed.

Parametric analysis

For comparisons between only two groups data were analysed using the Student t test. For repeat measurements, a paired Student t test was employed otherwise an unpaired test was used. A Student t test is also subject to the requirements of parametric analysis. All groups subjected to the Student t test were checked first for normality and homogeneity of variance using the tests mentioned earlier.

For comparisons between more than two groups a two-way ANOVA was performed. Following this, a parametric one-way ANOVA was used to examine the groups of data for any significant differences (F test). If the results of the ANOVA F-test indicated a difference, post-hoc, multiple comparison tests were performed. For analysis of data where type I (α) errors had to be avoided, a Bonferroni test was employed because of the conservative nature of the test. However, in cases where more rigorous analysis was required, a Tukey-Kramer test was used because it is less prone to type II (β) errors. (Type I errors occur when significant differences are found incorrectly. Conversely, type II errors occur when real significant differences are missed).

Non parametric analysis

A non-parametric two-way ANOVA and a Kruskal-Wallis non-parametric one-way ANOVA were used. If appropriate this was then followed with Dunn's non-parametric multiple comparison test, to analyse differences between groups. Any data which did not quite satisfy requirements for parametric analysis (normal distributions and equal standard deviations) then both parametric and non parametric analysis was performed. If the results differed then the results of the test which did not disprove the null hypothesis were used in interpretation of the data unless there was a good reason to do otherwise. For example, looking at the raw data would indicate presence of outliers which could be omitted, providing their values were more than two standard deviations from the mean.

In all cases two-tailed tests were employed at an arbitrary confidence interval of 95% ($p= 0.05$).

4.5 Results

Summary

1. **Three-point bending**

This technique did not reveal any significant differences in the mechanical strength of the radii or ulnae between any group.

a) Radii: There were no independent effects of ovariectomy ($p= 0.71$)or thyroparathyroidectomy ($p= 0.30$) and no demonstrable interaction ($p= 0.052$).
b) Ulnae: There were no independent effects of ovariectomy ($p= 0.41$)or thyroparathyroidectomy ($p= 0.06$) and no demonstrable interaction ($p= 0.052$).

2. **Compression testing of the L5 vertebral bodies**

Bones from the OVX group were significantly weaker than bones from the sham group ($p< 0.05$) and the tPTX group ($p< 0.001$).

There were significant independent effects of both ovariectomy ($p= 0.001$) and thyroparathyroidectomy ($p= 0.007$) but no interaction ($p= 0.589$).

3. **Compression testing of the L6 vertebral bodies**

Bones from the OVX group were significantly weaker than those from the tPTX group ($p< 0.01$).

Similar to the L5 results, there were significant independent effects of both ovariectomy ($p= 0.011$) and thyroparathyroidectomy ($p= 0.009$) but no interaction ($p= 0.403$).

4. **Trabecular QCT of the proximal tibial diaphysis**

The BMD was significantly higher in the sham and tPTX groups compared with the OVX and OVX+tPTX groups. In addition, the BMD in the OVX+tPTX group was significantly higher than that of the OVX group

($p < 0.01$). There was no significant difference in the BMD of the basal group compared with the end sham group ($p > 0.05$).

Sham vs. OVX	$p < 0.001$
Sham vs. OVX+tPTX	$p < 0.01$
tPTX vs. OVX	$p < 0.001$
tPTX vs. OVX+tPTX	$p < 0.001$

There were highly significant independent effects of both ovariectomy ($p < 0.001$) and thyroparathyroidectomy ($p = 0.002$) with demonstration of an interaction ($p = 0.031$).

5. **Cortical QCT of the proximal tibial diaphysis**

There were some major differences in the cortical BMD between groups. The sham group had a significantly lower BMD than the OVX+tPTX ($p < 0.05$) and the OVX ($p < 0.001$) groups. There was no significant difference between the basal and sham groups ($p > 0.05$).

There were highly significant independent effects of ovariectomy ($p < 0.001$) but not of thyroparathyroidectomy ($p = 0.475$). However, there was demonstration of a significant interaction ($p = 0.004$).

6. **Total QCT of the proximal tibial diaphysis**

The tPTX group had a significantly higher BMD than the OVX group ($p < 0.01$) with no significant difference between the basal group and the end sham group ($p > 0.05$).

There were highly significant independent effects of both ovariectomy ($p = 0.026$) and thyroparathyroidectomy ($p = 0.021$) but no demonstration of an interaction ($p = 0.107$).

7. **Histomorphometry of the parietal bones**

The thickness of the OVX group was significantly higher than the tPTX group ($p< 0.05$).

There was no significant independent effect of ovariectomy ($p= 0.064$) on parietal thickness but one was demonstrated with thyroparathyroidectomy ($p= 0.044$). There was no evidence of an interaction between these two effects ($p= 0.235$).

There were no significant differences in parietal porosity between any groups.

There were no significant independent effects of ovariectomy ($p= 0.310$) or of thyroparathyroidectomy ($p= 0.243$) and no significant interaction between these two effects on parietal porosity ($p= 0.566$).

Specific results

PTH assay

Table 4.1

Serum PTH levels, expressed as mean (± SEM)

Group	Basal	tPTX 3 weeks	tPTX 12 weeks	OVX+tPTX 3 weeks	OVX+tPTX 12 weeks
Number (n)	10	7	7	7	7
[PTH] pg/ml	25.9 (2.5)	2.27 (0.21)	2.56 (0.35)	2.94 (0.67)	2.71 (0.56)

These data are represented graphically in figure 4.7

Three rats were excluded from the study in the light of these results. One animal from the tPTX group and two from the tPTX+OVX group had a PTH level appreciably higher than any of the other rats (tPTX ± OVX) at either the three week or the 12 week time-point.

Table 4.2 PTH results of three rats excluded from the study

Results are expressed as mean blood concentration ([PTH]) in pg/ml

	tPTX	tPTX+OVX # 1	tPTX+OVX # 2
3 week [PTH]	11.48	25.1	4.7
12 week [PTH]	3.3	4.9	34.3

Lilliefors test for normality

The data was distributed normally.

Homogeneity of variances

Bartlett's test demonstrated extremely significant differences between the standard deviations ($p < 0.0001$) and still showed significant differences after logarithmic transformation ($p < 0.01$).

Parametric analysis

A Bonferroni test of the transformed data showed highly significant differences between the basal group and all the other two groups.

In each case $p < 0.001$.

Non parametric analysis

Because of the differences between standard deviations, non-parametric analysis was also employed. A Kruskal-Wallis and post-hoc Dunn test showed significant differences between:

Basal vs. tptx (3)	$p < 0.001$
Basal vs. ovx+tptx (3)	$p < 0.05$
Basal vs. tptx (12)	$p < 0.01$
Basal vs. ovx+tptx (12)	$p < 0.01$

Blood thyroxine assay

Table 4.3 Mean total blood thyroxine, nmol/l (± SEM):

Group	Time = 0 (basal)	12 weeks
Basal/Sham	49.9 (2.2) (n=13)	31.3 (1.8) (n=6)
tPTX	-	17.8 (3.1) (n=7)
OVX + PTX	-	17.2 (3.1) (n=7)
OVX	-	50.7 (2.5) (n=6)

These data are represented graphically in figure 4.8

Comparison of the basal and 12 week sham group

An unpaired two-tail Student t test showed highly significant difference between the basal T_4 levels and the 12 week sham T_4 levels ($p < 0.0001$). However, there was no difference between the basal group and the 12 week OVX group ($p = 0.837$).

Analysis of the 12 week data

Lilliefors test for normality

The data was logarithmically transformed to produce a normal distribution.

Test for homogeneity of variances

Bartlett's test of the transformed data showed significant differences between group standard deviations ($p = 0.0275$), therefore, the untransformed data was analysed.

Parametric analysis

A one-way ANOVA followed by a Tukey-Kramer test showed significant differences between the following groups:

Sham vs. tPTX	$p < 0.05$
Sham vs. OVX+tPTX	$p < 0.01$
Sham vs. OVX	$p < 0.001$
OVX vs. tPTX	$p < 0.001$
OVX vs. OVX+tPTX	$p < 0.001$

Non parametric analysis

A non-parametric ANOVA (Kruskal-Wallis test) followed by a non-parametric multiple-comparison (Dunn) test demonstrated significant differences between:

OVX (t=12) vs. tPTX (t=12)	$p < 0.01$
OVX (t=12) vs. OVX+tPTX (t=12)	$p < 0.001$

Body weight

Table 4.4 Mean body weight in g (± SEM)

	Time = 0 (basal)	12 weeks
Sham (n=6)	364 (14)	399 (19)
tPTX (n=7)	357 (15)	369 (8)

Lilliefors test for normality

The data was normally distributed.

Homogeneity of variances

Bartlett's test showed no significant differences between the variances - ($p = 0.451$).

Paired comparisons of the basal and 12 week groups

A paired, two-tailed Student t test showed no significant difference between the sham rats at time = 0 and time = 12 weeks ($p = 0.205$). Similarly there was no difference for the tPTX rats at these two time points ($p = 0.122$).

Despite lack of significant differences between the two groups for the two time points, the means for both groups tended to increase slightly in weight over the 12 week duration of the experiment.

Parametric multiple comparison analysis

A one-way ANOVA showed no significant differences between the four sets of data ($p = 0.209$).

Uterine weights

Table 4.5 Mean uterine weight in grams (± SEM):

	Sham	OVX + tPTX	OVX
Number	6	7	10
Weight	0.88 (0.08)	0.26 (0.02)	0.33 (0.03)

Lilliefors test for normality

The data was not normally distributed.

Non parametric analysis

ANOVA followed by Dunn's test showed that there were significant differences between the following groups:

Sham vs. OVX	$p < 0.05$
Sham vs. OVX+tPTX	$p < 0.001$

Three-point bending tests of the radii and ulnae

Table 4.6 Load to failure is presented as mean force in N (± SEM)

	Sham	tPTX	OVX + tPTX	OVX
Radii	43.8 (4.3) (n=6)	38.2 (4.9) (n=7)	42.5 (4.7) (n=7)	39.9 (4.2) (n=9)
Ulnae	38.2 (4.9) (n=6)	26.6 (2.9) (n=7)	25.7 (1.9) (n=7)	28.1 (3.3) (n=9)

These data are represented graphically in figure 4.9 and 4.10

Radii and ulnae

Lilliefors test for normality

Data for both the radii and the ulnae were not normally distributed, even after logarithmic transformation.

Non parametric analysis

A non-parametric two-way ANOVA demonstrated no independent effects of ovariectomy (radii - p= 0.71, ulnae - p= 0.41) or of thyroparathyroidectomy (radii - p= 0.30, ulnae - p= 0.06).

There was no significant interaction in the ulnae (p= 0.48) but in the radii the interaction wasn't quite significant (p= 0.052).

For both the radii and ulnae, analysis of the data using a non-parametric ANOVA (Kruskal-Wallis) demonstrated no significant differences between any group:

Radii	p= 0.192
Ulnae	p= 0.180

Compression-to-failure tests of the lumbar vertebrae

Figure 4.11 illustrates a typical load to failure trace.

Table 4.7 Force (N) to failure presented as mean (± SEM)

	Sham	tPTX	OVX + tPTX	OVX
L5 vertebrae	413 (24) (n=5)	472 (19) (n=6)	380 (34) (n=6)	294 (18) (n=10)
L6 vertebrae	397 (24) (n=5)	476 (20) (n=4)	399 (19) (n=6)	356 (18) (n=9)

These data are represented graphically in figure 4.12 and 4.13

1. L5 vertebrae

Lilliefors test for normality

The data were normally distributed

Homogeneity of variances

The variances were not significantly different (p= 0.577).

Parametric analysis

A two-way ANOVA demonstrated significant independent effects of ovariectomy ($p< 0.001$) and of thyroparathyroidectomy ($p= 0.007$) but no significant interaction ($p= 0.589$).

A 1-way ANOVA and a Bonferroni test, showed significant differences between:

Sham vs. OVX	$p< 0.05$
tPTX vs. OVX	$p< 0.001$

There was no significant difference between:

OVX+tPTX vs. OVX	$p= 0.076$

2. L6 vertebrae

Lilliefors test for normality

The data were normally distributed

Homogeneity of variances

The variances were not significantly different ($p= 0.929$).

Parametric analysis

A two-way ANOVA demonstrated again highly significant independent effects of ovariectomy ($p= 0.011$) and of thyroparathyroidectomy ($p= 0.009$). Similar to the L5 results, there was no significant interaction ($p= 0.403$).

A one-way ANOVA and a Bonferroni test showed a significant difference between:

tPTX vs. OVX	$p< 0.01$

Table 4.8

Bone mineral density (BMD) expressed as mean mg/cm^3 (± SEM):

	Basal (n=5)	Sham (n=6)	tPTX (n=7)	OVX + tPTX (n=7)	OVX (n=10)
Trabecular BMD	328 (16)	304 (8)	318 (10)	239 (19)	173 (7)
Cortical BMD	1029 (12)	1028 (16)	1065 (7)	1073 (9)	1096 (6)
Total BMD	861 (17)	821 (19)	888 (17)	822 (13)	809 (15)

These data are represented graphically in figure 4.14, 4.15 and 4.16

Trabecular BMD

Comparison between left and right basal BMD

Left BMD = 326 ± 17 Right BMD = 328 ± 16

An unpaired Student t-test showed no significant difference (p= 0.94).

Comparison of basal and 12 week BMD

An unpaired, two-tail Student t test showed no difference (p= 0.12) between the basal group and the sham group.

Analysis of 12 week data

Lilliefors test for normality

The data was normally distributed

Test for homogeneity of variances

Bartlett's test showed no significant differences in standard deviations (p= 0.077).

Parametric analysis

A two-way ANOVA demonstrated highly significant independent effects of ovariectomy ($p < 0.001$) and thyroparathyroidectomy ($p = 0.002$). There was also a significant interaction ($p = 0.031$).

A one-way ANOVA followed by a Bonferroni test showed that there were significant differences between the following groups:

Sham vs. OVX	$p < 0.001$
Sham vs. OVX+tPTX	$p < 0.01$
tPTX vs. OVX	$p < 0.001$
tPTX vs. OVX+tPTX	$p < 0.001$
OVX vs. OVX+tPTX	$p < 0.01$

2. Cortical BMD

Comparison between left and right basal BMD

Left BMD = 1034 ± 12 Right BMD = 1029 ± 12

An unpaired Student t-test showed no significant difference ($p = 0.81$).

Comparison of basal and 12 week BMD

An unpaired, two-tail Student t-test showed no difference ($p = 0.25$) between the basal group and the sham group

Analysis of 12 week data

Lilliefors test for normality

The data was normally distributed.

Test for homogeneity of variances

A Bartlett's test showed no significant differences in standard deviations ($p = 0.167$).

Parametric analysis

A two-way ANOVA demonstrated highly significant independent effects of ovariectomy ($p < 0.001$) but no effect of thyroparathyroidectomy ($p = 0.475$). However, there was a significant interaction ($p = 0.004$).

A one-way ANOVA followed by a Bonferroni test showed that there were significant differences between the following groups:

Sham vs. OVX	$p < 0.001$
Sham vs. OVX+tPTX	$p < 0.05$

3. Total BMD

Comparison between left and right basal BMD

Left BMD = 864 ± 20 Right BMD = 861 ± 17

An unpaired Student t-test showed no significant difference ($p = 0.92$).

Comparison of basal and 12 week BMD

An unpaired, two-tail Student t-test showed no difference ($p = 0.16$) between the basal group and the sham group

Analysis of 12 week data

Lilliefors test for normality

The data was normally distributed.

Test for homogeneity of variances

Bartlett's test showed no significant differences between standard deviations ($p = 0.881$).

Parametric analysis

A two-way ANOVA demonstrated highly significant independent effects of ovariectomy ($p = 0.026$) and thyroparathyroidectomy ($p = 0.021$). There was no significant interaction ($p = 0.107$).

A one-way ANOVA followed by a Bonferroni test showed that there were significant differences between the following groups:

tPTX vs. OVX $p < 0.01$

Parietal histomorphometry

Table 4.9 Summary data from the histomorphometry (mean ± SEM)

	Sham (n=5)	tPTX (n=7)	OVX + tPTX (n=7)	OVX (n=10)
Thickness (μm)	568 (29)	551 (13)	630 (18)	679 (56)
M.Ar./T.Ar. (%)	1.74 (0.3)	1.68 (0.4)	1.14 (0.3)	1.93 (0.5)

1. Parietal thickness

Comparison between the left and right basal thickness

Left thickness (μm) = 583 ± 39 Right thickness (μm) = 574 ± 41

A paired Student t-test showed no significant differences ($p = 0.6372$).

Analysis of the 12 week data

Lilliefors test for normality

The data was distributed normally.

Test for homogeneity of variances

The sample size was too small to perform a Bartlett's test but because the data was distributed normally, parametric analysis was performed.

Parametric analysis

A two-way ANOVA demonstrated no significant independent effects of ovariectomy ($p = 0.064$) but significant independent effects of thyroparathyroidectomy ($p = 0.044$).

There was no significant interaction ($p = 0.235$).

A one-way ANOVA followed by a Tukey test showed significant differences between the following groups:

OVX vs. tPTX $p < 0.05$

These data are represented graphically in figure 4.17

2. Parietal porosity

This was defined as (M.Ar./T.Ar.) x 100 and expressed as a percentage where:

M.Ar. = marrow area.

T.Ar. (tissue area) = marrow area + bone area.

Comparison between left and right basal porosity

Left parietal porosity = 3.35 ± 1.3 Right parietal porosity = 4.10 ± 1.3

A paired Student t-test showed no significant differences (p= 0.6014).

Analysis of the 12 week data

Lilliefors test for normality

The data required transformation using natural logarithms to achieve a normal distribution.

Test for homogeneity of variances

The sample size was too small to perform a Bartlett's test but because the data was distributed normally, parametric analysis was performed.

Parametric analysis

A two-way ANOVA demonstrated no significant independent effects of ovariectomy (p= 0.310) or of thyroparathyroidectomy (p= 0.243).

There was no significant interaction (p= 0.566).

A one-way ANOVA showed no significant differences between groups (p= 0.4438).

Dynamic histomorphometry could not be performed because unmeasurably small areas of the calvarial bone had incorporated fluorochrome labels.

Table 4.10 Summary table of two way ANOVA results

	Independent effect of OVX	Independent effect of tPTX	Interaction between OVX & tPTX
Radial 3 pt	No (0.71)	No (0.30)	No (0.052)
Ulnar 3 pt	No (0.41)	No (0.06)	No (0.48)
L5 strength	Yes (0.001)	Yes (0.007)	No (0.589)
L6 strength	Yes (0.011)	Yes (0.009)	No (0.403)
Trabecular BMD	Yes (<0.001)	Yes (0.002)	Yes (0.031)
Cortical BMD	Yes (<0.001)	No (0.475)	Yes (0.004)
Total BMD	Yes (0.026)	Yes (0.021)	No (0.107)
Parietal thickness	No (0.064)	Yes (0.044)	No (0.235)
Parietal porosity	No (0.310)	No (0.243)	No (0.566)

(P values are in brackets)

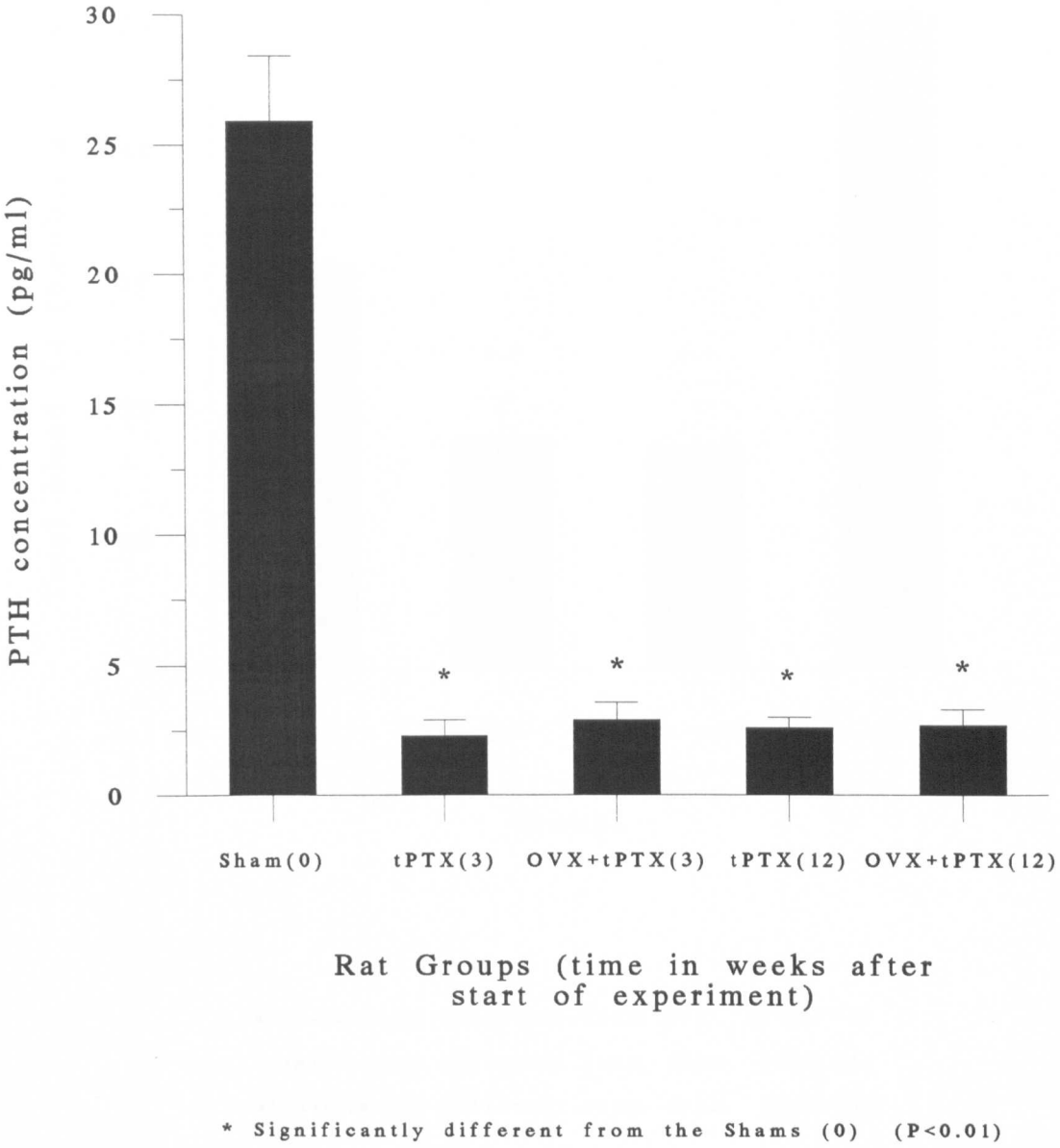

Figure 4.7 Blood PTH IRMA Assay

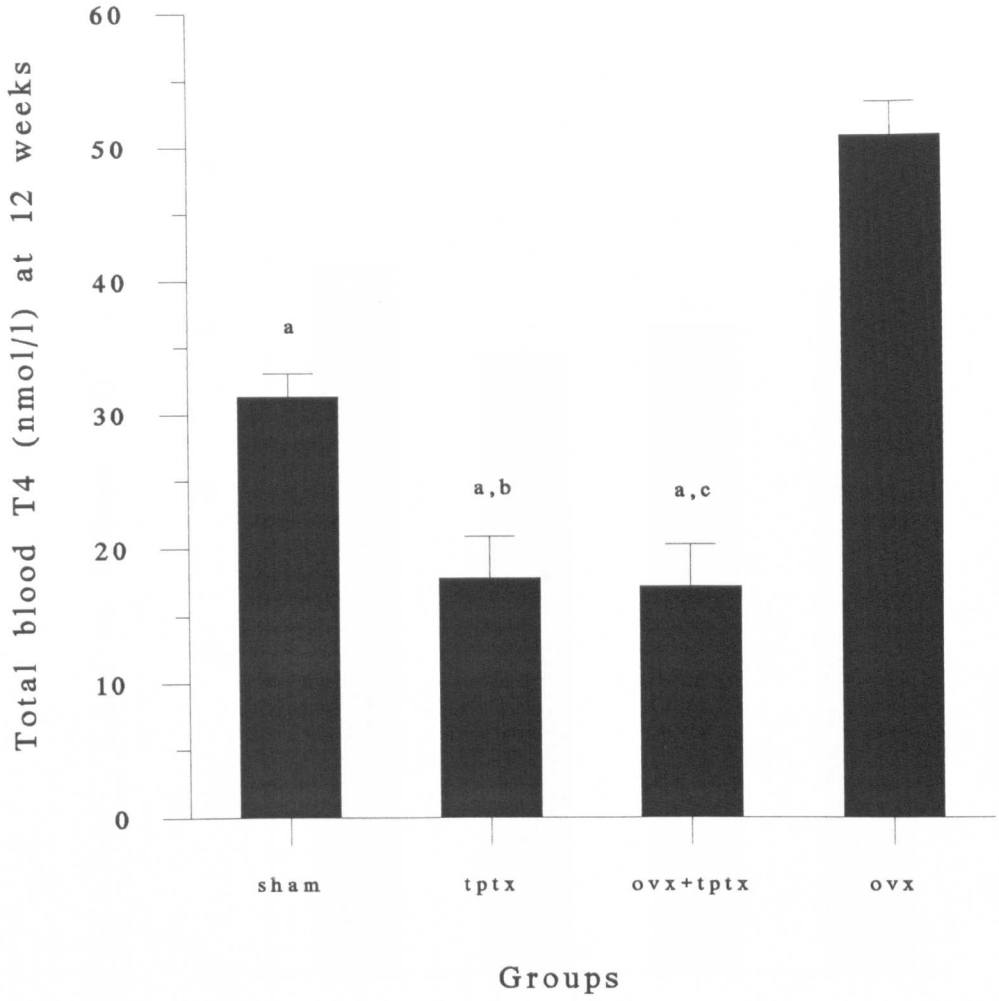

a - Significantly different from ovx (P<0.001)

b - Significantly different from sham (P<0.05)

c - Significantly different from sham (P<0.01)

Figure 4.8 Blood Thyroxine Assay

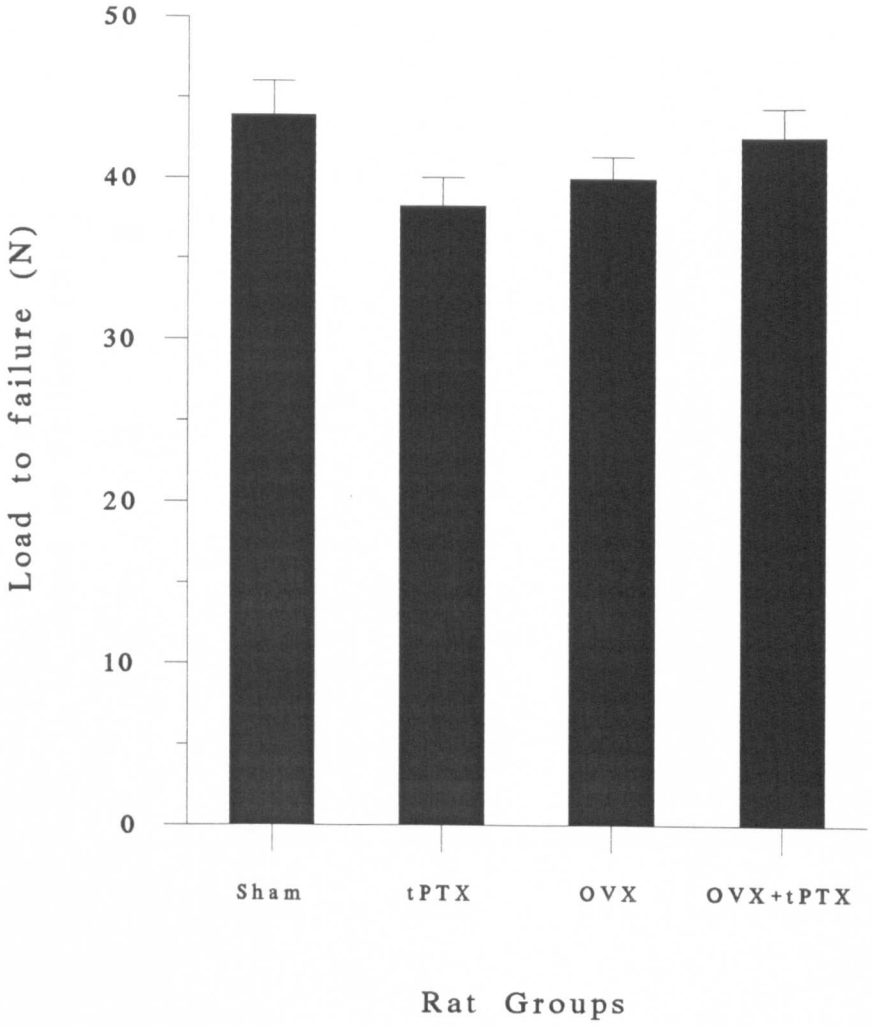

Figure 4.9 Radial Three Point Tests

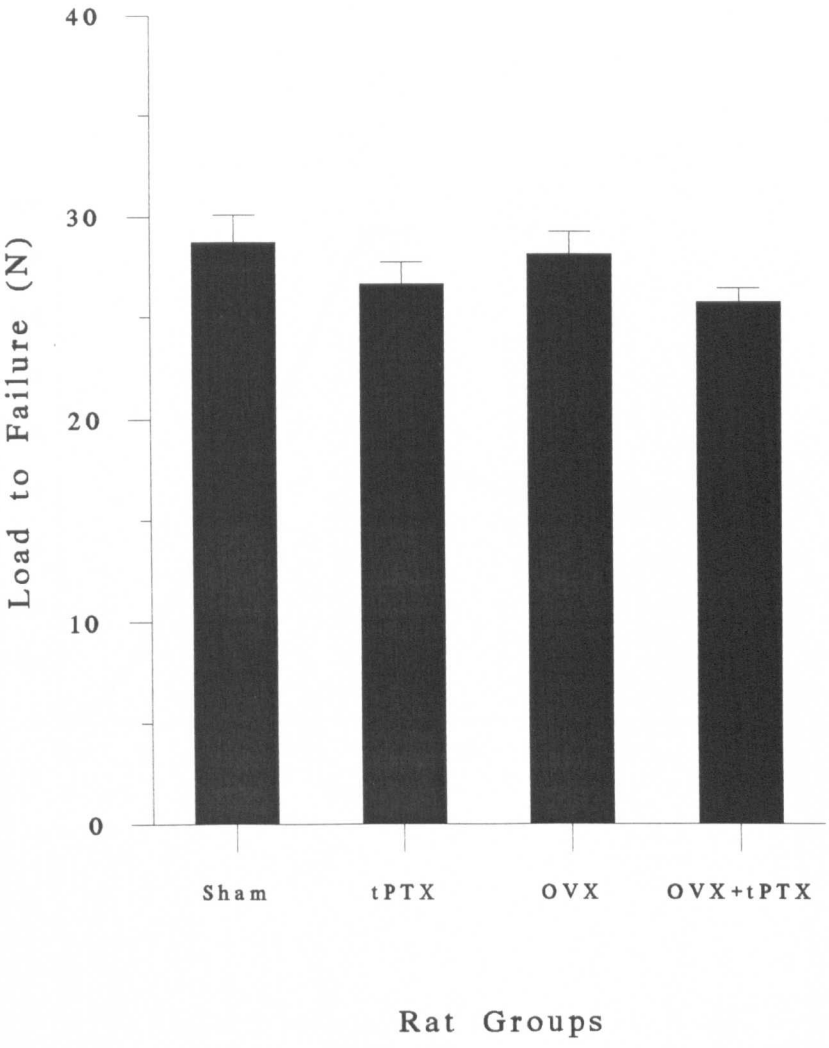

Figure 4.10 Ulnar Three Point Tests

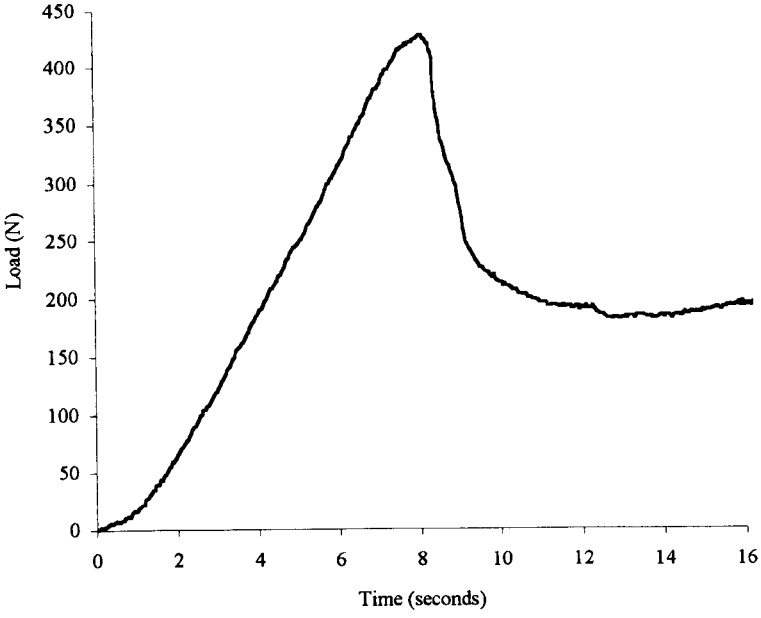

Figure 4.11
Typical load to failure curve for a vertebral body

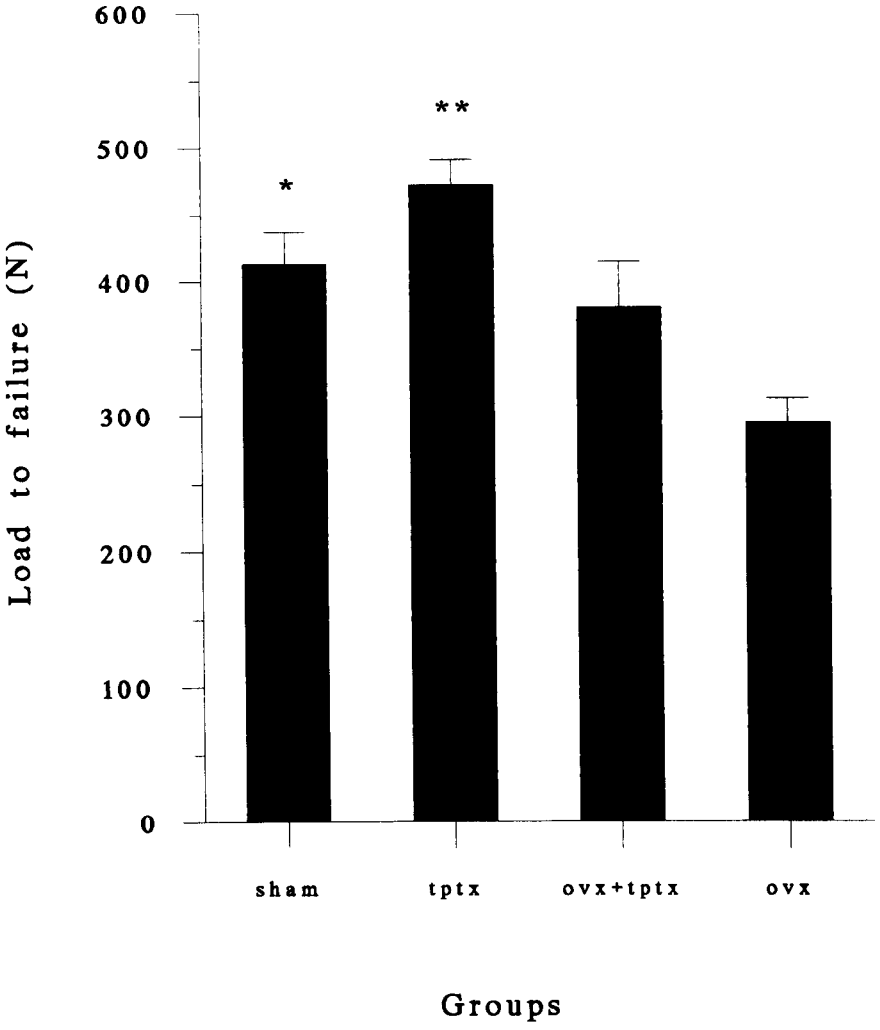

* Significantly different from OVX (P<0.05)

** Significantly different from OVX (P<0.001)

Figure 4.12 Compression Tests of L5 Vertebrae

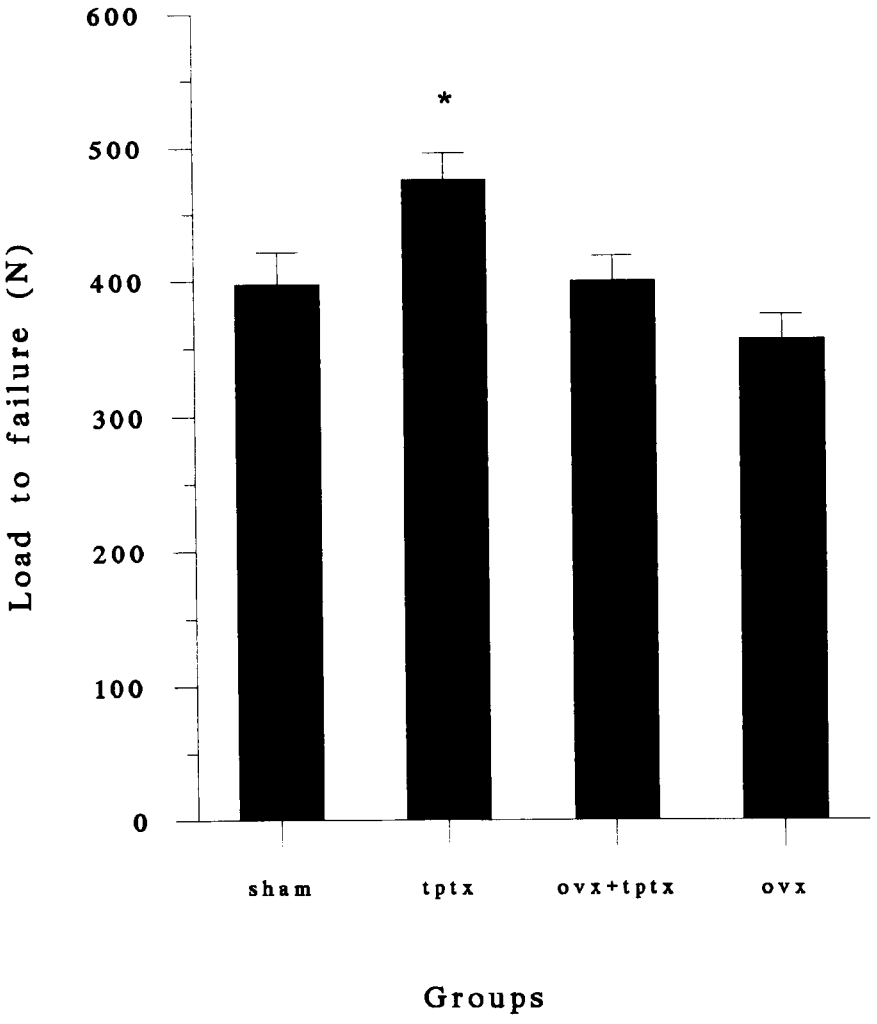

* Significantly different from OVX (P<0.01)

Figure 4.13 Compression Tests of L6 Vertebrae

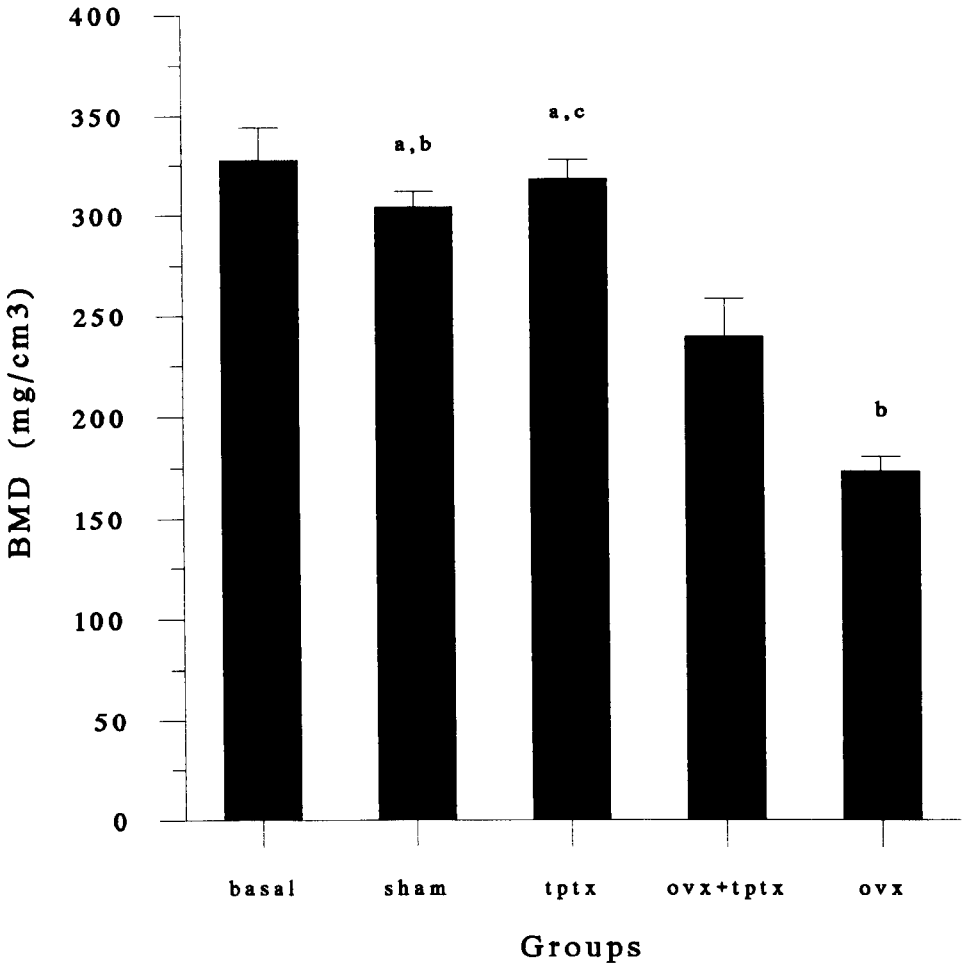

a - Significantly different from OVX (P<0.001)
b - Significantly different from OVX+tPTX (P<0.01)
c - Significantly different from OVX+tPTX (P<0.001)

(Basal results are shown for comparison)

Figure 4.14 Trabecular BMD

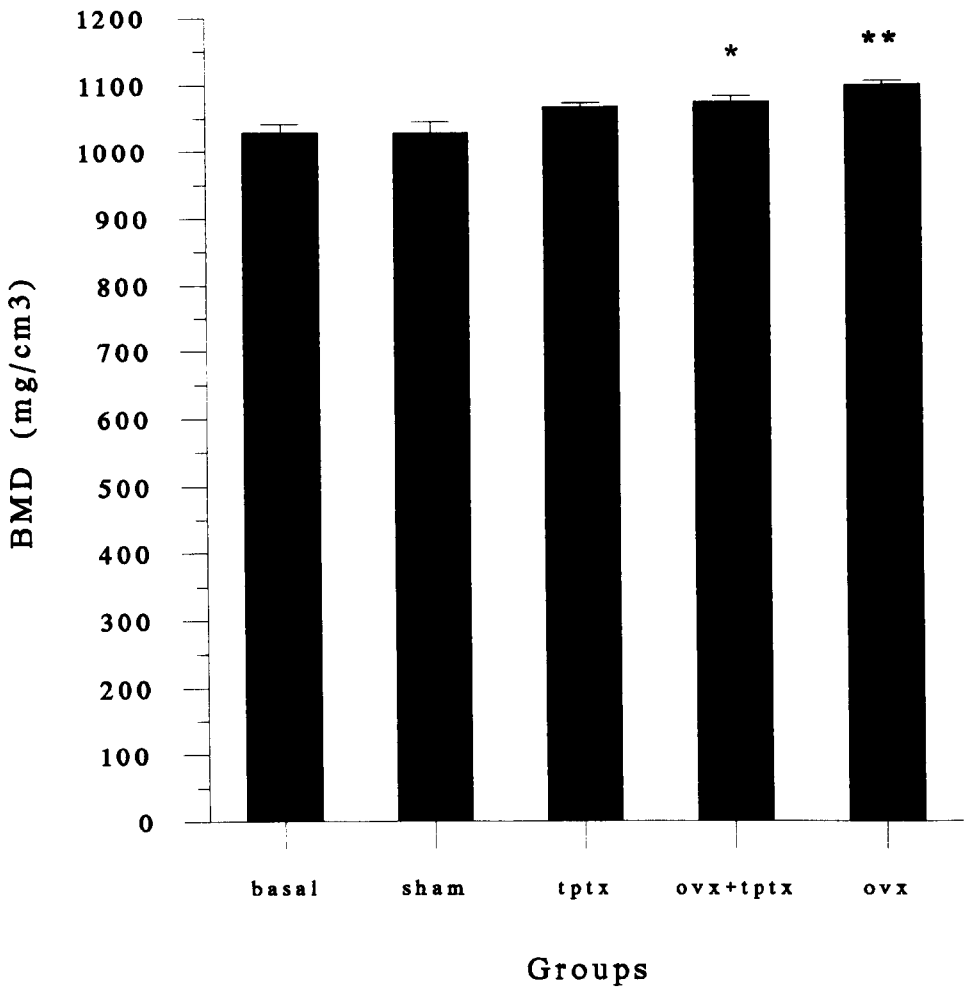

* Significantly different from sham (P<0.05)
** Significantly different from sham (P<0.001)

(Basal results are shown for comparison)

Figure 4.15 Cortical BMD

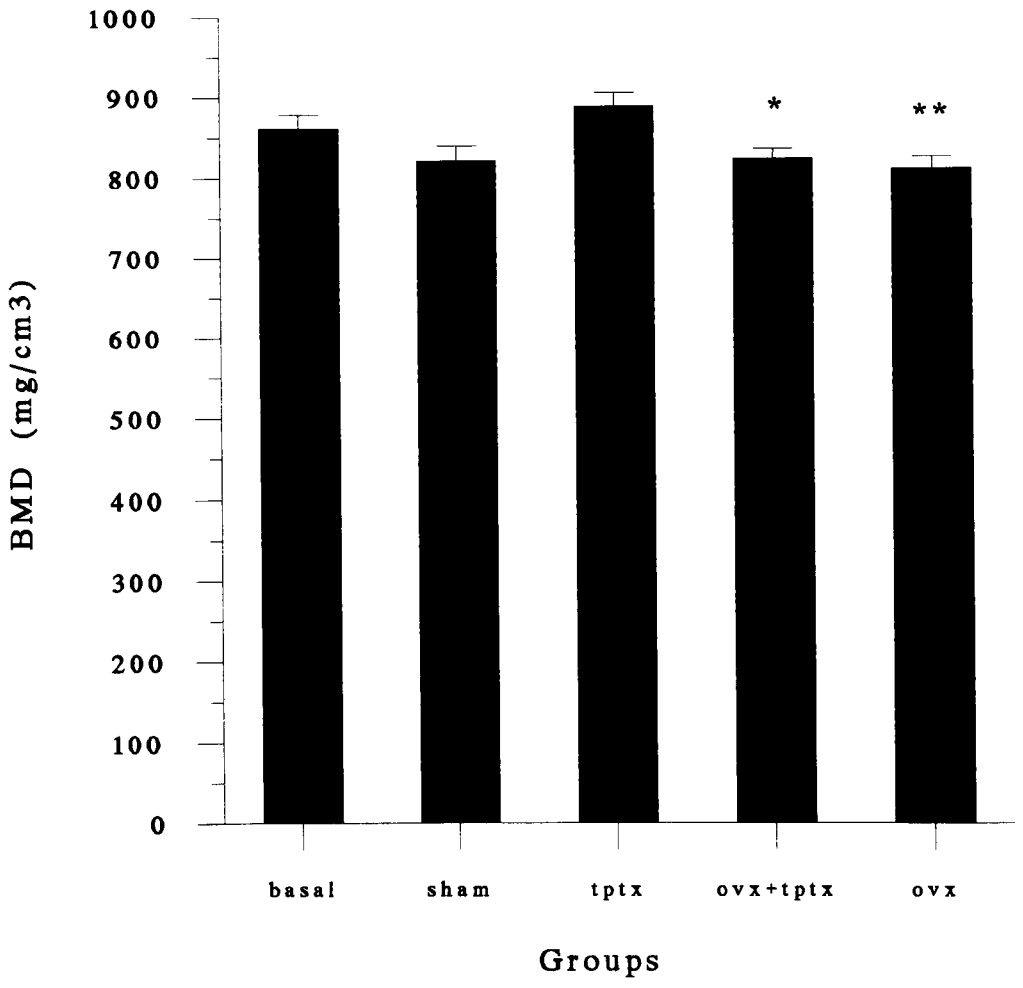

* Significantly different from tptx (P<0.05)

** Significantly different from tptx (P<0.01)

(Basal results are shown for comparison)

Figure 4.16 Total BMD

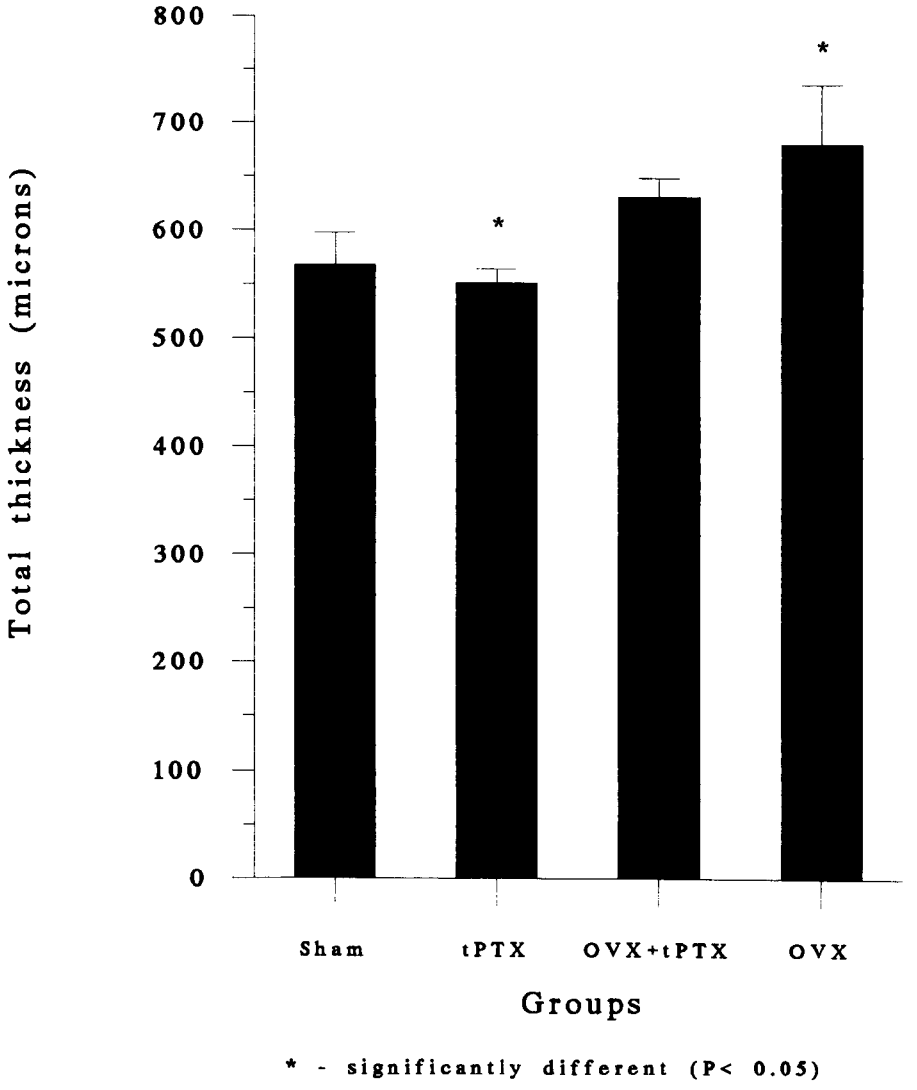

Figure 4.17 Parietal thickness measurements

4.6 Discussion

This experiment has shown that parathyroidectomy reduces ovariectomy-induced trabecular osteopenia in the proximal tibiae of adult rats. The trabecular bone mass of the OVX + tPTX group was mid-way between the control and OVX groups. Differences between these groups were significant. Throughout the duration of the experiment there were no significant changes in either trabecular, cortical or total BMD when comparing basal with 12 week sham measurements. This suggested skeletal maturity of the rats at the start of the experiment. However, comparing the mean values for all bone parameters, there was a trend for BMD to decrease over the 12 weeks. This may have reflected age-related bone loss.

It was an interesting finding that ovariectomy caused a significant increase in cortical BMD comparing control shams with the basal group. It is well documented that postmenopausal osteoporotics undergo increased endosteal remodelling resulting in a thinning of the cortex and a compensatory increase in cortical diameter (Sedlin 1964). Similar changes have also been described in ovariectomized rats (Hietala 1993; Danielsen *et al* 1993). However, the finding that cortical BMD in the OVX group was 7 % higher than the shams and basal groups is surprising because in postmenopausal osteoporosis cortical porosity is not affected (Broulik *et al* 1982). Any loss of cortical bone tends to occur at the endosteal surface. In these results, it would appear that the cortical bone has become denser. Cortical osteonal remodelling is not common in rats, so it is not possible to explain these results in terms of changes of bone mass within intracortical remodelling spaces. If porous endocortical bone is excluded then the apparent density of the remaining cortical bone will increase. This may affect to a greater extent the cortical bone of the OVX rats because a higher rate of endocortical remodelling could feasibly result in more porous or trabeculated endocortical bone. However, it is most likely that the results are due to a partial volume effect, the thresholding algorithm used by the pQCT software to define the cortical envelope or a combination of both of these effects (appendix 2). Histomorphometry could be used to confirm this.

Indeed, Jerome (personal communication 1996) has also observed similar effects for the BMD values obtained for cortical bone. He has attempted to overcome this problem by using a different protocol for defining cortical bone BMD. He samples the bone at a known anatomical landmark rather than sampling at a known distance from the articular margin. In addition, he does not use the pixel thresholding algorithm for calculating cortical bone volume but makes the assumption that the volume remains constant and thereby analyses a constant volume of the cortical envelope. On the other hand Gasser (personal communication 1996) has suggested using a different thresholding algorithm (peel mode of 0.93) to define most accurately the cortical bone area. The pQCT protocol used for this experiment was optimised by Zeneca Pharmaceuticals (Macclesfield, UK) for investigating trabecular bone in the proximal tibia and for this reason may not have been suitable for looking at the effects on the cortical envelope. It would appear that substantial characterisation of the specific anatomical region of interest needs to be performed in addition to correlation with histomorphometry in order to optimise the algorithms used in the pQCT analysis. Indeed, pQCT is not a substitute for conventional static and dynamic histomorphometry but should be regarded as a complimentary analysis tool (Gasser 1995).

It can take up to 9 months before changes are noticeable in rat lumbar vertebrae due to the slow response to a treatment (Wronski *et al* 1989). However, the results of the L5 vertebral compression test suggested a higher compressive strength of the vertebrae from the OVX + tPTX group compared with the OVX group. Although the difference between the two groups had a p value of 0.076, it has to borne in mind that apart from the slow response observed commonly in vertebrae, the group sizes were small and the Bonferroni test used to analyse the data is conservative, i.e. it tends to under estimate differences. It is possible that if the group sizes were bigger and the duration of the experiment were extended, greater differences between groups would have become apparent.

Failure to demonstrate clear differences in the other mechanical tests could be attributed to low sensitivity of the tests and low numbers in the groups. For this reason, statistical power analysis would be indicated to estimate the numbers of rats chosen for a repetition of this experiment. The radii and ulnae are composed entirely of cortical bone and this may have accounted for the lack of differences seen in these tests. It is known that trabecular bone has a higher metabolic rate than cortical bone because of the larger surface area:volume ratio and the greater number of cells per unit volume. It is therefore likely that the changes occurring in these bones was extremely small.

The results of the calvarial histomorphometry demonstrated incorporation of unmeasurably small amounts of label. This implied that no net formation of newly mineralised bone had occurred. The results of the thickness measurements demonstrated a significant difference between the tPTX and OVX groups, however, neither of them were significantly different from the shams. In addition, there were no significant differences between any group in parietal porosity. These latter two findings suggested that no significant net bone resorption had occurred over the three month period. It was interesting that Davies (1995) described very similar porosity in the parietal bone of shams (2.1 % ± 0.4) compared with those (1.74 % ± 0.30) in this study. In contrast, Davies (1995) described significantly higher porosity in the OVX group (12.2 % ± 3.1) compared with the shams. The study described by Davies (1995) was different in two ways. Firstly, the rats were ovariectomised around the age of puberty, whereas, in this study they were 10 months old. In addition, the rats were killed 20 months after ovariectomy but in this study they were killed after three months. It is possible that the increase in parietal porosity observed by Davies may have been a result of ovariectomy at a younger age but it is also possible that changes may take considerably longer to develop in calvarial bone compared with trabecular bone in the proximal tibia or even the lumbar vertebrae. This may be due to a metabolic rate which is lower in the bone cells of parietal bone or, simply reflect regional differences in their sensitivity and response to osteotropic influences.

A two way ANOVA demonstrated significant interactions between the effects of OVX and tPTX in several instances. This finding supports the hypothesis that there is an interaction between the effects of oestrogens and PTH on bone. In other instances, the effects of OVX or tPTX alone had significant independent effects but without demonstration of an interaction. In the ulnar three point bending tests an independent effect of tPTX alone didn't quite achieve significance ($p = 0.06$). In the case of the radial three point bending tests, no independent effect of OVX or tPTX was observed but the interaction only just failed to achieve significance ($p = 0.052$).

It is possible that tests more sensitive than compression to failure or three point bending may have shown more evidence of interaction, for example, dynamic histomorphometry. However, histomorphometry of vertebral bodies is complicated by problems of trying to standardise sampling sites and in the case of cortical bone, often the changes are minimal. Davies (1995) found no differences in tibial cortical bone parameters when comparing long-term adult OVX with sham rats.

Circulating PTH was measured at three and 12 weeks after the start of the experiment. This technique was a direct way of assaying circulating PTH, unlike serum ionised calcium. However, it must be borne in mind that the type and dose of anaesthetic used on the rats can affect dramatically PTH levels (Schultz *et al* 1995). They found that ketamine and xylazine but not ketamine alone, elevated serum PTH dramatically when compared with controls. The effects of halothane were not investigated. Significant differences in blood PTH concentration in basal measurements compared with those made from the OVX and OVX+tPTX groups at three and 12 weeks confirm successful parathyroidectomy. Three rats were excluded from the experiment as a result of this analysis. It is difficult to understand why in two rats, PTH levels fell over the period from three to 12 weeks. In the other rat, the PTH level gradually increased over the 9 week period. It is likely that any parathyroid tissue left after surgery, either ectopically or within remnants of retained

thyroid tissue, underwent hyperplasia and increased secretion of PTH in a compensatory response.

Success of the ovariectomy surgery was demonstrated by observing significant differences in uterine weight in ovary-intact compared with ovariectomized rats. There was a dramatic loss of uterine weight in ovariectomized rats compared with controls. In addition, failure to demonstrate ovaries by visual inspection post-mortem, was used as an additional criterion to confirm successful surgery.

Criticism could be levelled at this experiment for the fact that the thyroparathyroidectomized rats did not receive supplementary thyroxine. This was due to the difficulty and cost of supplementing reliably to physiological levels (chapter 3). Parathyroidectomy alone would have removed the need to supplement with thyroxine but this procedure in adult rats is difficult practically for several reasons:

1. The parathyroid glands are small in adult rats and often buried in the thyroid tissue. They are consequently difficult to visualise.
2. Casewell & Fennell (1970) reported that it is a common finding in rats that the parathyroids exist as multiple foci of glandular tissue rather than discrete, identifiable structures at the cranial poles of the thyroid gland. This was supported by my own subjective observations following numerous dissections. These foci may be disseminated not only through the thyroid tissue but also ectopically, lying along the trachea, mediastinum, thymus and brain. These ectopic sites reflect the same embryological origin of the parathyroid and thymus and the subsequent tissue migration.

There is nothing that can be done to solve the problem of ectopic parathyroid tissue but by removing the entire thyroid gland, any risk of leaving parathyroid tissue behind in this gland is eliminated. Complete thyroparathyroidectomy, therefore, should have reduced the number of non-responders. This was an

important consideration in this experiment because of the cost of housing rats to 10 months of age.

It has been documented that hypothyroidism does influence bone metabolism in adult humans (Mosekilde & Melsen 1978, Eriksen *et al* 1986). It reduces the rate of bone turnover and may therefore slow any response to a treatment. In this experiment, the rats were not athyroid; but had low thyroxine levels with a mean that was approximately one third of that in the 12 week OVX groups and one half of that in the 12 week shams. The likely reason for the discrepancy in the T_4 levels between the OVX and the sham groups, is that the sham blood samples had been allowed to warm up over two days following a freezer failure. In the light of these results, remaining serum from the OVX rats were assayed. Assuming that ovariectomy does not affect T_4 levels, the results from the 12 week sham group should be ignored. In addition, it has also been reported that anaesthetic type and bleeding technique can also affect levels of circulating thyroxine (Davies 1993). Davies compares carbon dioxide and halothane anaesthesia with cervical dislocation. However, he did not investigate the effect of xylazine and ketamine anaesthesia. It is not clear from his results what effect individual anaesthetics had because he used various combinations of different anaesthetics with different bleeding techniques. However, orbital sinus puncture tended to produce lower thyroxine levels than cardiac puncture and bleeding from the vena cava or from the tail. Any form of stress, be it transportation, minor surgery or previous anaesthesia tended to lower thyroxine levels. In this experiment, xylazine and ketamine were used for sampling to determine the basal levels of PTH and thyroxine. However, halothane was used for subsequent sampling. It is unlikely that this would have produced any variation because the bleeding technique was identical in all cases and there were three and nine weeks between bleeding times. This should have allowed sufficient time for recovery from stress.

There are reports by Hirsch & Hagaman (1986) and R.C. Mühlbauer (personal communication, 1996) to suggest that the effects of under-supplementation of

thyroxine on rat bone is minimal. Hirsch & Hagaman report identical bone changes in three groups of thyroidectomized rats given different doses of T_4 supplementation. Two groups received T_4 by injection. One group received a high dose while the other group received a low dose. The third group received T_4 in the drinking water. They report that these findings were in agreement with data from other studies (unpublished). Interestingly, they also reported that the T_4 levels in the group supplemented in the water were highly variable. In addition, there were no significant differences in body weight between sham rats and tPTX rats at the start and at the end of the experiment. Body weight has been a criterion used to determine adequacy of thyroxine supplementation (Goulding and Gold 1989). Therefore, in this experiment, it is possible that lack of thyroxine supplementation may have had minimal effects on the results because no significant difference in the 12 week body weight could be demonstrated between the sham and tPTX groups.

The tPTX rats would also have had their source of calcitonin removed. Chronic calcitonin deprivation in the rats may have acted to counter the effect of parathyroidectomy. It has been shown that femora from rats that were calcitonin deficient for two months were shorter and lighter than controls (Hirsch & Hagaman 1986). However, it has been suggested that this effect is only short-lived (Hirsch & Hagaman 1986) because in a longer study (14 months) it was found that bones from calcitonin-deficient female rats were not different from controls in terms of length, density or calcium content. Nonetheless the consideration of calcitonin-deficiency has to be borne in mind when interpreting the results.

In future experiments, it would be necessary to resolve the issue of appropriate supplementation of thyroxine. After the discovery that the thyroxine pellets used in an attempt to restore thyroxine, were extremely unreliable in their release characteristics, producing very inconsistent results, the two most practicable ways to do this might be by:

1. Performing pure parathyroidectomy. This would require a high degree of skill and require group sizes two to three times the final number required, in order to be guaranteed an adequate number of responders in each group.

2. Performing a cranial thyroparathyroidectomy in which the cranial half of the thyroid gland was removed, together with the parathyroid glands. This would still require large groups but might prove easier practically. Hyperplasia of remaining thyroid tissue would be likely to restore fully thyroxine levels to physiological levels.

Both of these techniques have the advantage that the calcitonin production would be conserved physiologically. As mentioned earlier, there is nothing that can be done to overcome the potential complication from ectopic parathyroid production.

The results of this experiment suggest that ovariectomy-induced osteopenia may be reduced by parathyroidectomy. In this respect the conclusion drawn differs from an earlier rat experiment by Sims *et al* (1994). However, in that experiment younger rats were used, which may have been growing still. Further, the femur was investigated and not the proximal tibia. It is possible that the distal femur may have responded in a way that was different from the tibia.

Further experiments are indicated to investigate further the role of PTH and its possible interaction with oestrogens in the development of postmenopausal osteoporosis.

4.7 Conclusion

Ovariectomy produced a profound reduction in trabecular bone mineral density of the proximal tibiae. Thyroparathyroidectomy reduced the amount of this bone loss significantly.

Chapter 5

Investigation of the regional variation in mechanical strain in different bones of the human skeleton

5.1 Summary

An experiment is described in which rosette strain gauges were attached to the parietal bones of the skull and the anterio-medial surface of the mid shaft of the tibia in a human. *In vivo* strain recordings were taken during a range of activities in an attempt to compare strain magnitudes and strain rates between the two sites. This is the first experiment described in which *in vivo* recordings have been made from the human skull.

The scope of the experiment was limited by ethical committee restrictions. The duration of the experiment was limited to one day and implantation of the gauges had to be conducted under local anaesthesia. This meant that multiple positioning of gauges around the tibia was not possible. Unfortunately, it was not possible to get any additional volunteers, although this was probably not that surprising!

One parietal gauge failed to function properly from the outset and unfortunately, the remaining gauge fell off later in the experiment due to direct impact from heading a 4.5 kg medicine ball!

From the raw strain data collected from the two functioning gauges, principal and shear strain magnitudes and rates were calculated.

Except for heading the medicine ball, all other activities in which recordings were made for both tibial and skull strain data showed strain magnitudes and rates which were higher in the tibia than in the skull. These differences range from a factor of four to ten.

During strenuous activity, the highest principal strains in the tibia were tensile and directed along the long axis of the bone. The greatest principal strain magnitude recorded in the tibia was +2060 μstrain while the greatest shear strain magnitude was 2900 μstrain.

Absolute strain magnitudes were low in the skull and similar to those recorded previously in animals. The greatest strain magnitudes were associated with direct blows to the forehead with a ball, however, these were little more than the magnitudes produced by facial expressions and chewing toffee.

The results of this experiment confirm that there are regional differences in the strain environment experienced by tibial midshaft and the parietal bone of the calvaria. It is highly likely that that there are fundamental differences between the two sites in the biological mechanisms responsible for the maintenance of bone mass.

In addition, the results of this experiment provide further evidence that calvarial bone and calvarial-derived bone cells may not be appropriate for the study of post-menopausal osteoporosis and the response to mechanical loading because results from such experiments may not be representative of results obtained from similar experiments using vertebral and long bone cell and organ cultures.

5.2 Introduction

The principal function of the long bones is to enable locomotion and load-bearing. As such they are likely to experience a wide range of different loads, depending on the level of physiological activity. Standing, for example, would impose low magnitude static loads whilst running and turning quickly during a game of hockey would subject the bones to high magnitude dynamic forces which would impose a range of different bending moments on the tibia and other limb bones. Consequently, due to the wide variety of daily activities, they experience wide ranges of mechanical deformation (strain). In contrast, in calvarial bones such as the parietal bone where the primary function is to protect the brain, it is likely that they only experience low loads and consequently low strain magnitudes because they do not support the body weight, are not involved with locomotion and don't have such extensive muscle attachments.

Bone loss, in long bones and vertebrae, occurs in disuse and in postmenopausal osteoporotics with the decline in oestrogen levels. However, this does not appear to be the case in skull bones. Gallagher *et al* (1987) found that the head is more resistant to postmenopausal bone loss than other regions of the body. It has also been shown that prolonged bed rest (Leblanc *et al* 1990) and spinal cord injury (Garland *et al* 1992) result in bone loss from the appendicular and axial skeleton but not from the skull. In addition, Kleerekoper & Avioli (1993) report that osteoporotic fractures do not occur in the skull.

Parietal bone grafts are used commonly for reconstructive craniofacial (Tessier 1982) and spinal surgery (Casey *et al* 1995). One of the major advantages of using cranial bone in grafts is the enhanced survival of the grafts relative to endochondral bone (Koenig *et al* 1995). There are reports from animal experiments to suggest that calvarial bone undergoes less resorption following transplantation, compared with endochondral bone grafts. This has been

shown in rabbits and monkeys (Zins and Whitaker 1983) and also in sheep (Phillips and Rahn 1988).

It would be potentially fatal for an animal to sustain a fracture either of a limb bone or of the skull. Loss of the use of a limb would prevent an animal from hunting, roaming to find new grazing or escaping from predators. However, growing massive bones that were 'over-engineered' to withstand stresses that were greatly in excess of those encountered habitually would be costly in terms energy expenditure involved during locomotion. It might also restrict the range of limb movement. More efficient use could be made of an animal's energy and nutrient resources if the limb bones were capable of withstanding the most commonly encountered habitual forces, with an inbuilt safety factor but at the same time were equipped with a mechanism to facilitate functional adaptation to changes in the mechanical environment. Failure of the calvarial bones could be fatal because of potential damage to the brain. Calvarial bone is designed with spongy bone called diploë sandwiched between two layers of cortical bone. This enables the skull to absorb the energy of penetrating blows to the skull, with a reduced risk of full thickness penetration and consequent injury to the brain, without having to be unduly thick and heavy. The degree of variation in the calvaria's mechanical environment is not likely to be as great as that in the limb bones. Indeed, if this were the case the need to adapt to changes in this mechanical environment would not be very important; providing the calvaria always maintained an adequate safety factor to withstand occasional direct blows.

It is the ability of the cells within long bones to detect damage or a function or combination of functions of strain i.e. magnitude, rate or frequency that enables them to remodel adaptively to variations in their mechanical environment (Rubin and McLeod 1994). Rubin (1984) proposed that bone cells have an "optimum strain environment". Any deviation from this ideal environment results in an adaptive response which will re-establish the bone's optimum state. Hillam *et al* (1994) demonstrated in several different species

that regional differences exist in physiological strain magnitude when measured simultaneously in the calvaria and long bones of the same animal.

It is possible that there may be different mechanisms by which bone cells of the calvaria maintain bone mass compared with bone cells in other parts of the skeleton. Either calvarial bone perceives higher strain magnitudes during physiological activity compared with long bones. Alternatively, calvarial bone may respond differently from long bone to low strains.

In the design of future *in* vitro experiments, intended to elucidate the pathophysiology of disuse osteopenia and postmenopausal osteoporosis, it is important that the most appropriate cell or organ culture model is used. It was Lanyon *et al* (1977) who stated that "the physiological relevance of experiments is important if the findings and conclusion drawn are to have clinical relevance". Rawlinson *et al* (1995) demonstrated clear differences in the response of rat calvarial and ulnar cells, maintained in both organ and cell cultures, in terms of their early response to dynamic mechanical strain. Despite these possible differences in the response to mechanical strain of cells from the calvaria and long bones, calvarial-derived bone cells are used commonly for *in vitro* experiments to determine the effects of mechanical loading. Further, the magnitudes to which these cells are loaded often exceeds those experienced in long bones *in vivo,* by several orders of magnitude. For example Yeh and Rodan (1984) subjected osteoblast cells cultured on collagen ribbons to strains of 100,000 μstrain.

The hypothesis tested in this experiment is that there is no difference in physiological strain magnitude experienced in the human calvaria compared with the tibia, during physiological activity.

5.3 Aims

The purpose of this experiment was to determine whether physiological strain magnitudes and rates encountered in the human parietal bone, at a site used for bone graft donation, were comparable with those in the human tibia during a range of equivalent activities. This was performed to test the hypothesis that all bones are subjected to similar peak strain magnitudes (greater than 800 μstrain) during habitual activity.

Strain analysis would be achieved by bonding rosette strain gauges to the anteriomedial surface of the tibial mid-diaphysis and the parietal bones of the calvaria.

5.4 Methods

Strain gauges

The rosette strain gauges (Type EA-06-060RZ-120, Measurement Group, Basingstoke, UK) were prepared for *in vivo* implantation (appendix 3) and sterilised with ethylene oxide.

Subject

The experimental subject was a normal, healthy, 70 kg, 29 year old male.

Surgical implantation of the strain gauges onto the parietal bones and the tibia

The right tibia and scalp were shaved and prepared for aseptic surgery using chlorhexidine surgical scrub (Hibiscrub, Zeneca Pharmaceuticals, Alderley Park, Macclesfield, UK) and a mixture of ethanol and chlorhexidine (Hibitane, Zeneca). The operation was performed under bupivacaine local anaesthesia (Marcain 0.25% with 1:200,000 adrenaline, Astra Pharmaceuticals Ltd., Hertfordshire, UK). This was injected subcutaneously (s/c) 5-10 minutes before surgery commenced.

1) Parietal bones

A 7 cm incision was made 2-3 cm lateral to the sagittal midline of the skull. The skin was retracted and haemorrhage was controlled using electrocautery (Ellman Surgitron, Ellman International MFG, N.Y., USA). A 1.5 x 1.5 cm area of periosteum was elevated and the underlying bone was gently scraped free of any remaining soft tissue. The bone was then dried and degreased with a 1:1 mixture of diethyl ether and chloroform using sterile cotton buds. After achieving haemostasis, cyanoacrylate tissue adhesive (Histoacryl, B. Braun Melsungen AG, Melsungen, Germany) was applied to the back of the gauge mount. Care was taken to ensure that the entire gauge mount was coated with adhesive. The gauge was placed onto the prepared bone surface (figure 5.1), such that gauge element b (figure 5.2) was parallel to the sagittal plane of the skull (figures 5.3 and 5.4). Firm digital pressure was applied onto the gauge for one minute to ensure firm bonding of the whole gauge mounting onto the prepared bone surface. Polythene gloves (Poly gloves, type 0020, Millpledge, Notts., UK) were worn to prevent sticking of the gauge to the skin. Once in place, the gauge was connected to the strain gauge amplifiers and integrity of the gauge was confirmed by checking that each gauge element balanced. The gauge was then disconnected and the incision was closed so that the lead wires passed out of the posterior edge of the incision. The same procedure was performed on the contralateral parietal bone. Once both sides had been completed, the lead wires were folded in two and coiled up then firmly pressed down against the scalp with a surgical dressing. This prevented snagging of the lead wires which would lead to dislodging of the strain gauges from the bone.

2) Tibia

Local anaesthetic was injected s/c over the mid-shaft of the anterio-medial aspect of the tibia (figure 5.5). A 7 cm incision was made parallel to the long axis of the tibia. The bone surface was prepared in the same way as the calvaria (figure 5.6). Care was taken to bond the gauge with the gauge element b lying parallel to the long axis of the bone (figure 5.7 and 5.8). This was subsequently confirmed by radiography (figure 5.9).

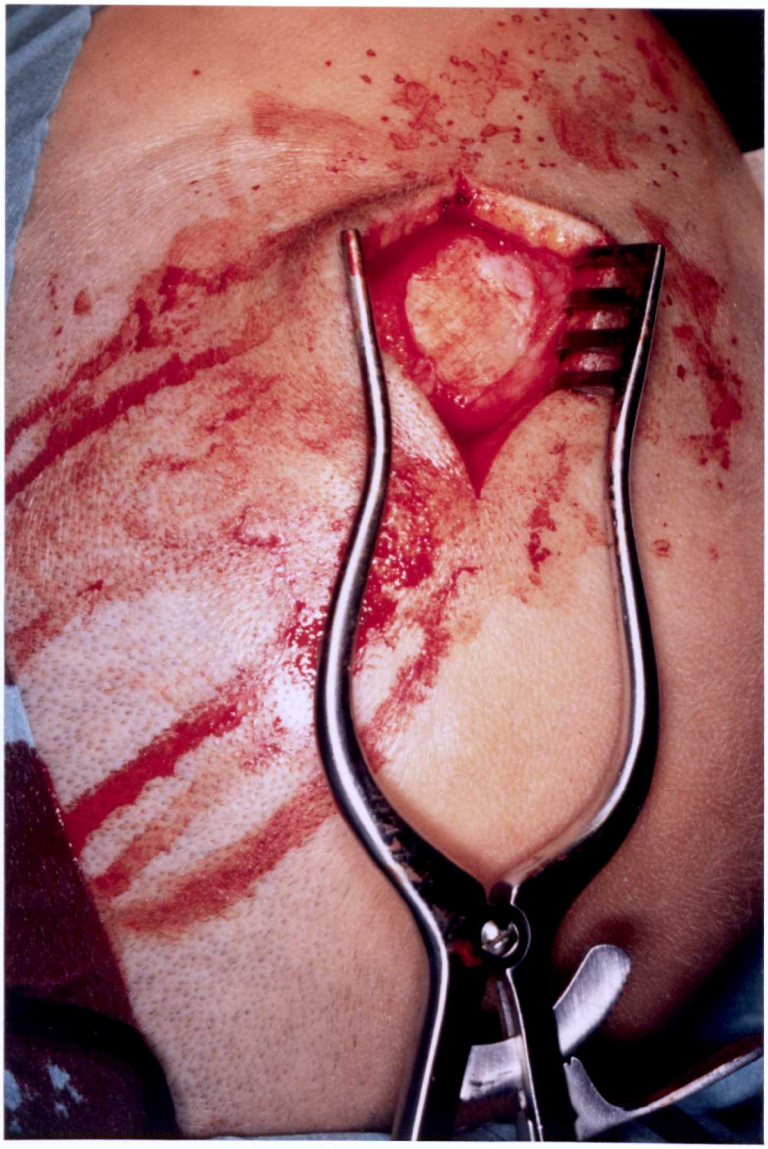

Figure 5.1
Photograph of the parietal bone prepared for gauge bonding

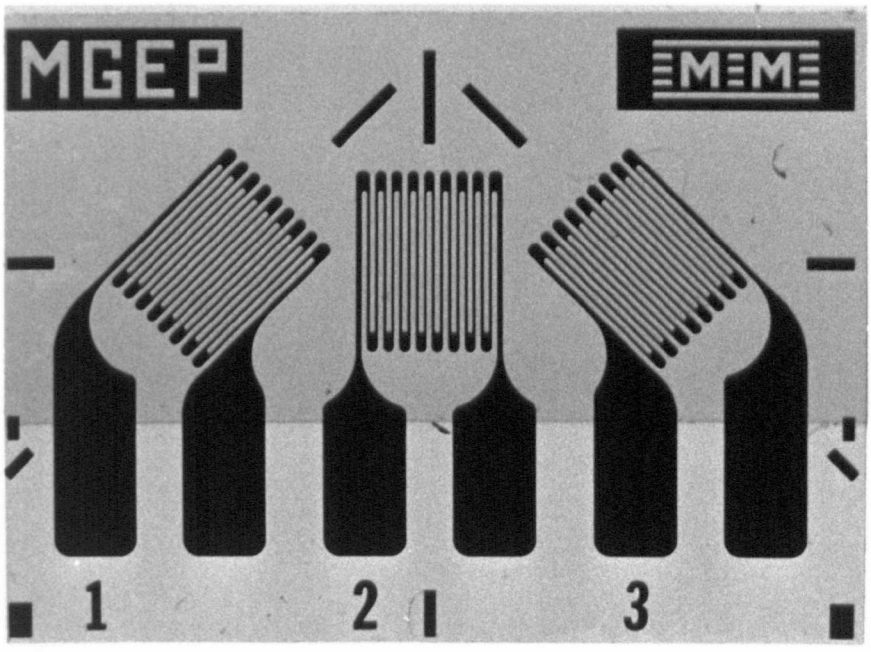

Figure 5.2
Photograph a planar strain gauge used in the experiment

Figure 5.3
Photograph of a strain gauge bonded onto the parietal bone

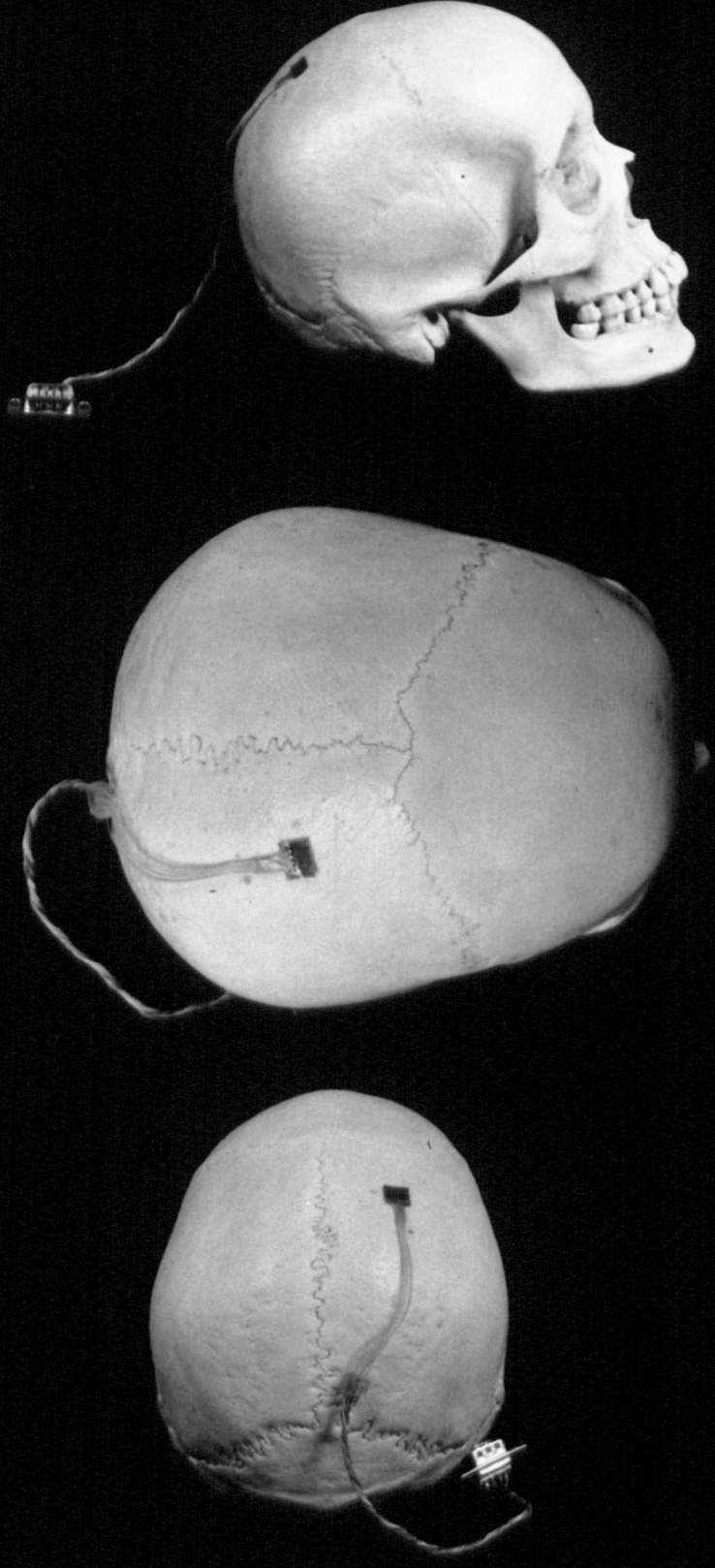

Figure 5.4

photographs illustrating gauge positioning on a cadaver skull

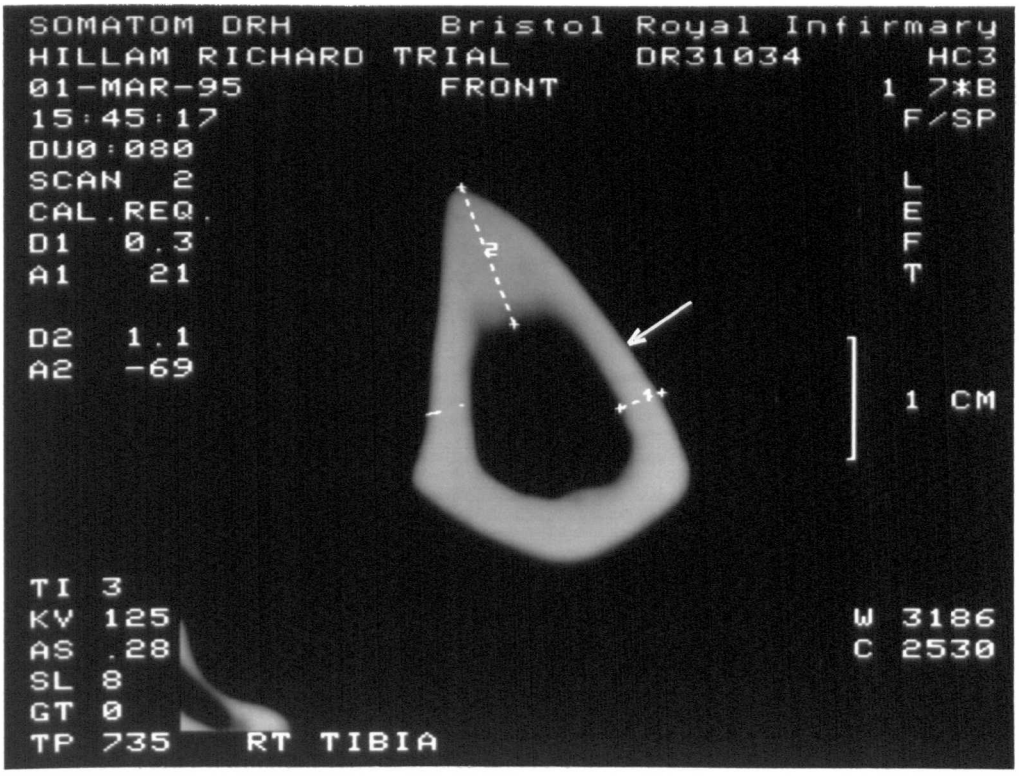

Figure 5.5
C.T. scan of the tibial mid-diaphysis. The arrow indicates the point at which the strain gauge was bonded

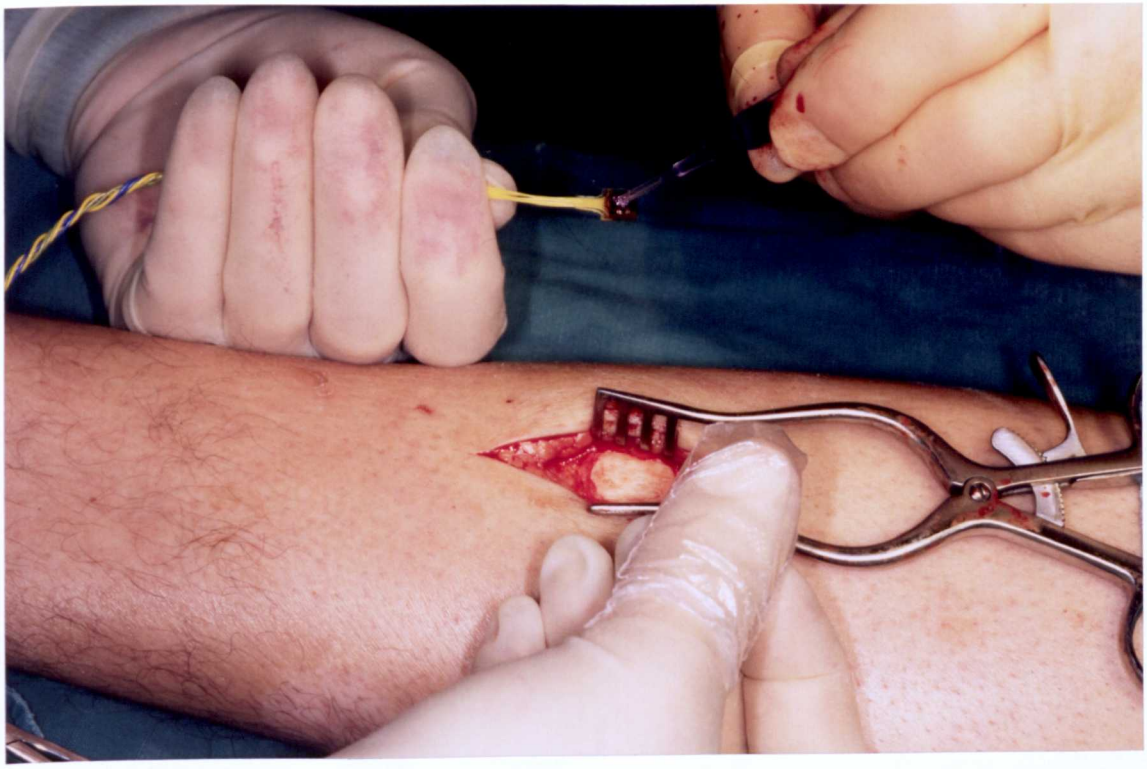

Figure 5.6
Photograph of the tibial bone surface prepared for gauge bonding

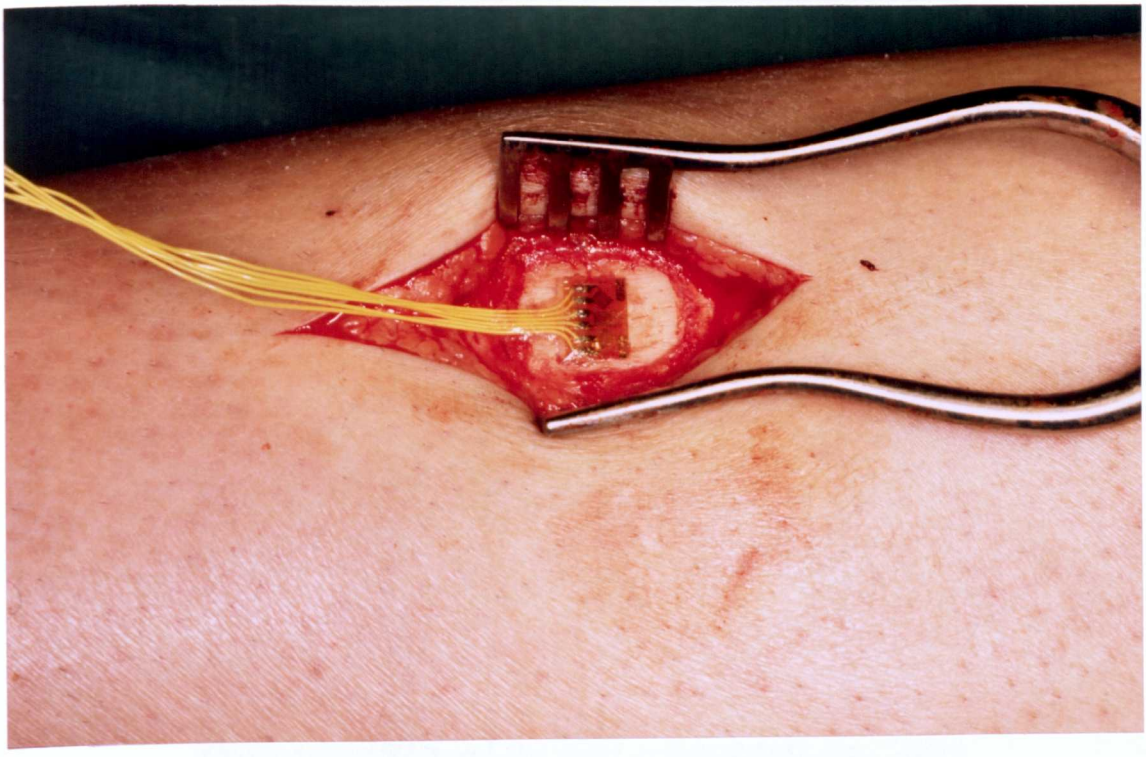

Figure 5.7
Photograph of the rosette strain gauge
bonded to the anterio medial surface of the tibia

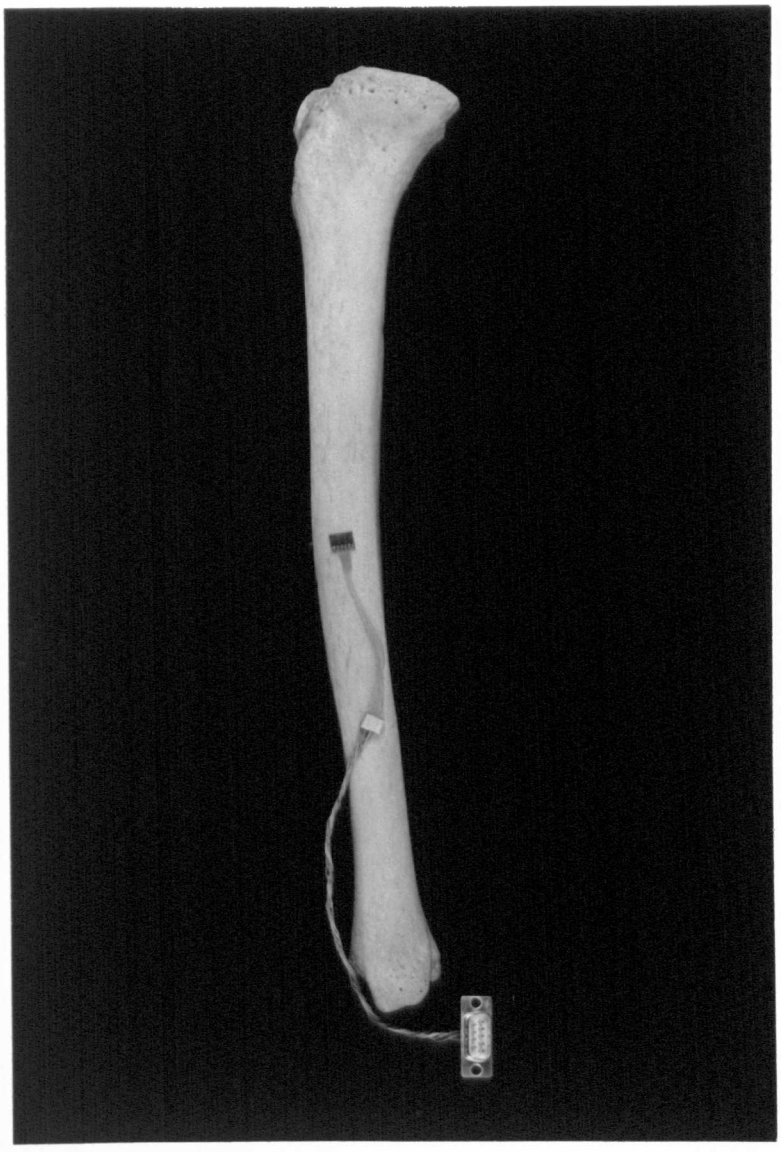

Figure 5.8
Photograph of a planar strain gauge bonded to the anterio-medial surface of the mid-diaphysis of a human tibia

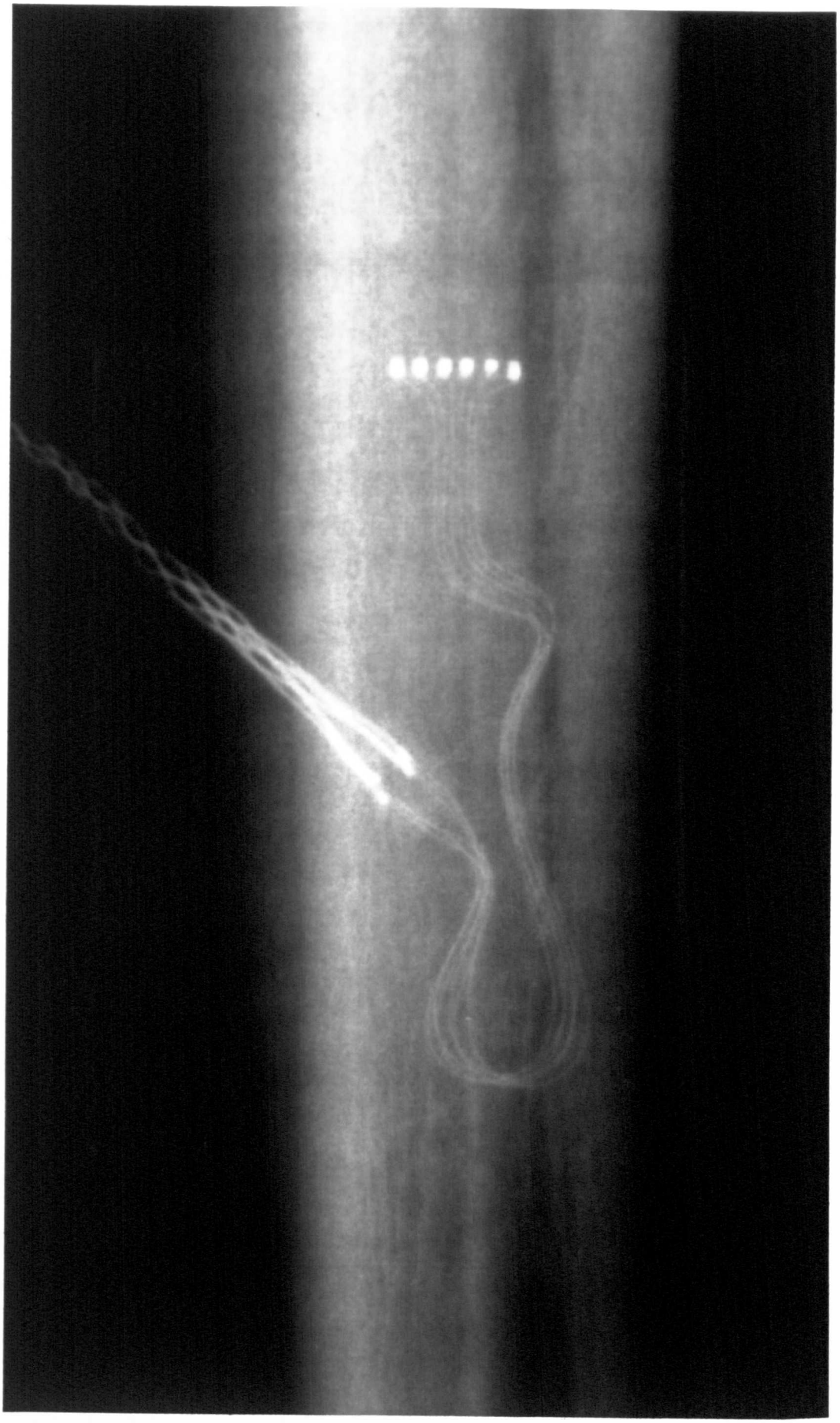

Figure 5.9
Radiograph of the tibial strain gauge *in situ*

Strain recording

The strain amplifiers were switched on and allowed to warm up and stabilise for an hour before the start of the experiment. Before recording any data each gauge element had to be balanced so that there was no potential difference across the Wheatstone bridge (appendix 3). The gauges were balanced in a completely relaxed position (so that the bones were subjected to the minimum of stress) so that a recorded strain of zero, actually represented as near to absolute zero strain as possible. Between every activity, the gauges were re-zeroed. In the case of the skull, gauge balancing was achieved in a relaxed sitting position with no neck muscle or face muscle activity. In the case of the tibia the gauge was balanced with the foot off the ground and the leg in a relaxed position.

Strain was recorded at a frequency of 50 Hz for sedentary activities where no impact transients were expected and at 500 Hz for more strenuous activities where there would be impact loading such as jumping.

Activities

1) Biting onto a dental occlusal force meter (Medical Physics Department, Sunderland District General Hospital, UK).
2) Eating various foods: including a banana and toffee.
3) Smiling, grimacing and pulling various facial expressions.
4) Walking.
5) Performing squats while carrying a 56 lb. weight.
6) Heading a 4.5 kg medicine ball.
7) Climbing onto and jumping off a small stool, 45 cm high and landing on a force plate (model 9287, Kistler, Switzerland).
8) Jumping off a step ladder, 130 cm off the ground and landing on a force plate.

Except for the 130 cm jump, all activities were performed in socked feet. For the 130 cm jump, rubber soled, leather boots (Trader, Debenhams, UK) weighing 0.6 kg were worn.

After a day of recording, the gauges were removed under local anaesthesia. The operation sites were closed and dressings applied.

Strain analysis

Principal strain magnitudes, angles and shear strain were calculated from the individual strain element data (figure 5.10).

Principal strains are defined as the maximum tensile strain and the maximum compressive strain acting at a point where there is zero shear strain. By definition compressive principal strains (denoted by a negative sign) always act at right-angles to tensile principal strains (denoted by a positive sign).

Shear strain is defined as the principal compressive strain subtracted from the principal tensile strain. It is a measure of the shear acting at a point and is a maximum at 45 degrees to the principal strain axes.

The principal strain angle is the angle between the principal tensile strain axis and the axis of gauge element a. A positive sign denotes that the principal tensile strain axis is anti-clockwise relative to the axis of gauge a. A negative sign indicates a clockwise direction.

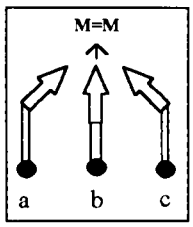

Theoretical point of strain analysis

Planar rosette strain guage
Three gauge elements (⇧):
a, b & c at 45 degrees

Calculation of principle strains:
(where e_1 = tension & e_2 = compression)

$$e_1 = 1/2\,(e_a + e_c) + 1/2\,[(e_a - e_c)^2 + (2\,e_b - e_a - e_c)^2]^{1/2}$$

$$e_2 = 1/2\,(e_a + e_c) - 1/2\,[(e_a - e_c)^2 + (2\,e_b - e_a - e_c)^2]^{1/2}$$

Where: e_a, e_b and e_c represent the normal strains from the individual gauge elements a, b and c respectively

Max. shear strain: $e_1 - e_2$

Principle angle: $$\frac{1}{2}\tan^{-1}\left[\frac{2e_b - e_a - e_c}{e_a - e_c}\right]$$

Where: $e_a > e_c$ then the angle is from the gauge a axis to the axis of e_1
Where: $e_a < e_c$ then the angle is from the gauge a axis to the axis of e_2

A negative angle denotes a clockwise direction relative to the long axis of the bone and proximal to the rosette, whereas a positive angle denotes a counter-clockwise direction

Figure 5.10 Strain Analysis

5.5 Results

It was evident following the start of data acquisition that the left sided parietal gauge had failed. Gauge element b did not produce any values other than 'noise' (approximately 10 μstrain) which was unmeasurably low. The results from this gauge could not be analysed properly, however, the raw strain magnitudes from the two functioning gauge elements were comparable with the right rosette in that they didn't exceed 200 μstrain.

The right parietal gauge worked well up to the latter part of the experiment when it debonded following a direct impact from the medicine ball. The time at which this occurred was obvious because of the immediate formation of a large haematoma and subsequent strain recordings consisted only of low level noise. From this point all data from this gauge were discarded. The tibial gauge remained bonded and functional throughout the experiment.

Figures of the results:

5.11 - 5.19	Skull strain whilst biting onto the occlusal force meter.
5.20	Pattern of parietal strain whilst eating a banana.
5.21	Pattern of strain during facial expression (grimacing).
5.22	Strain pattern whilst walking.
5.23	Pattern of strain whilst performing squats with a 56 lb. weight.
5.24	Pattern of strain during impact of medicine ball on skull.
5.25	Pattern of strain during landing from a height of 45 cm.
5.26	Strain pattern during landing from a height of 1.3 m.
5.27	Tibial principal strain magnitudes and angles whilst walking.
5.28a	Figure of tibial principal strain angles at midstance of the walk.
5.28b	Figure of tibial principal strain angles during impact loading.

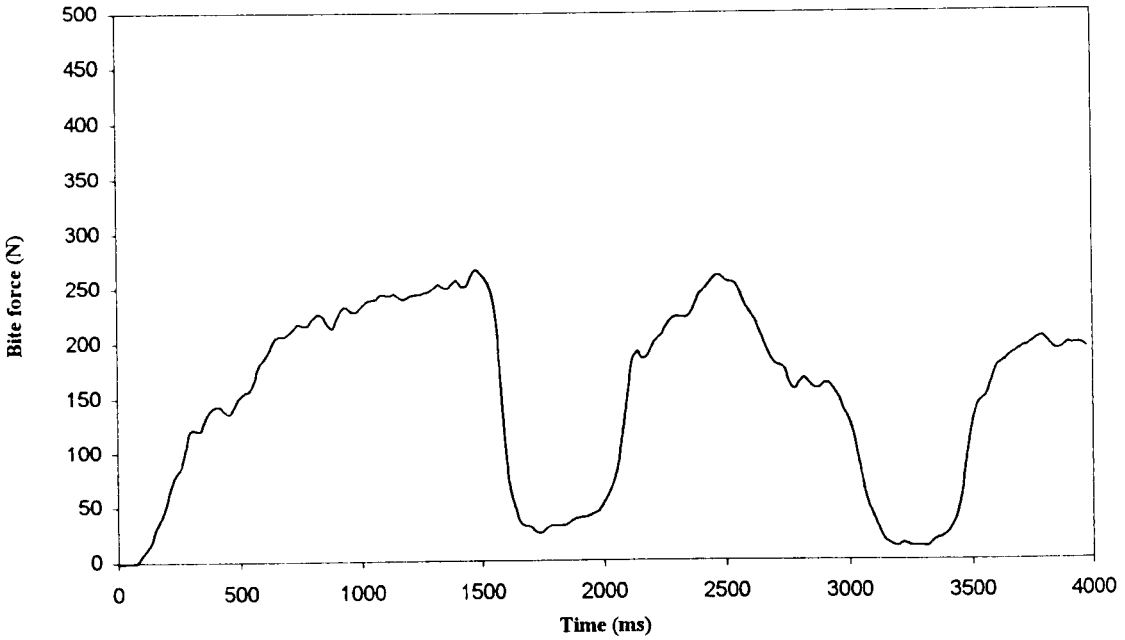

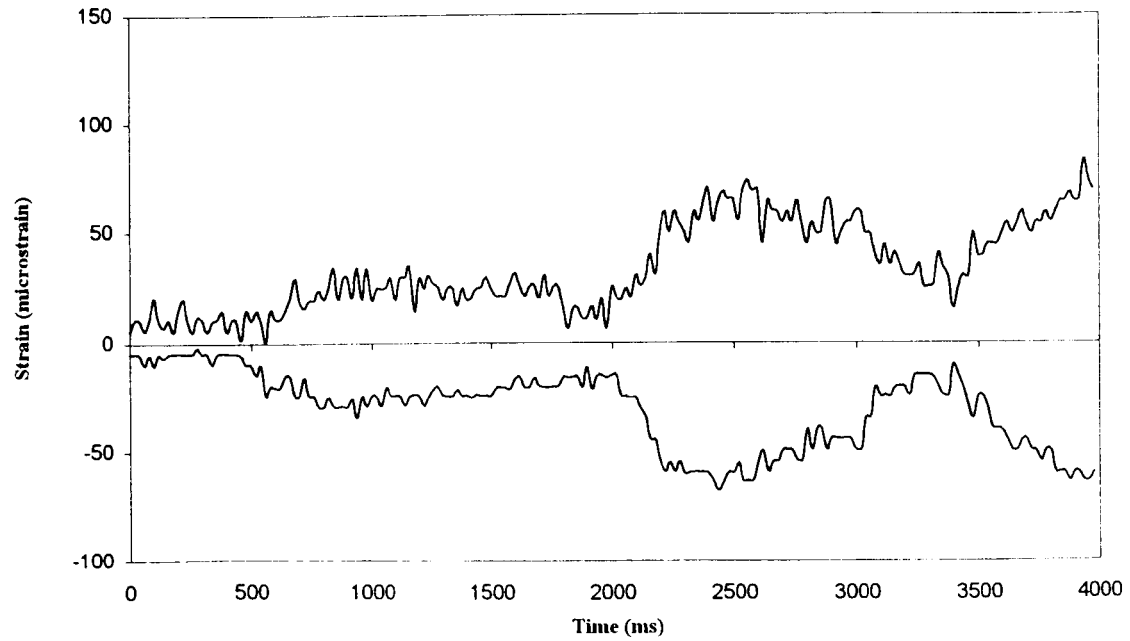

Figure 5.11
Bite force and parietal strain recorded simultaneously whilst biting on the bite force transducer with the right molars - first recording

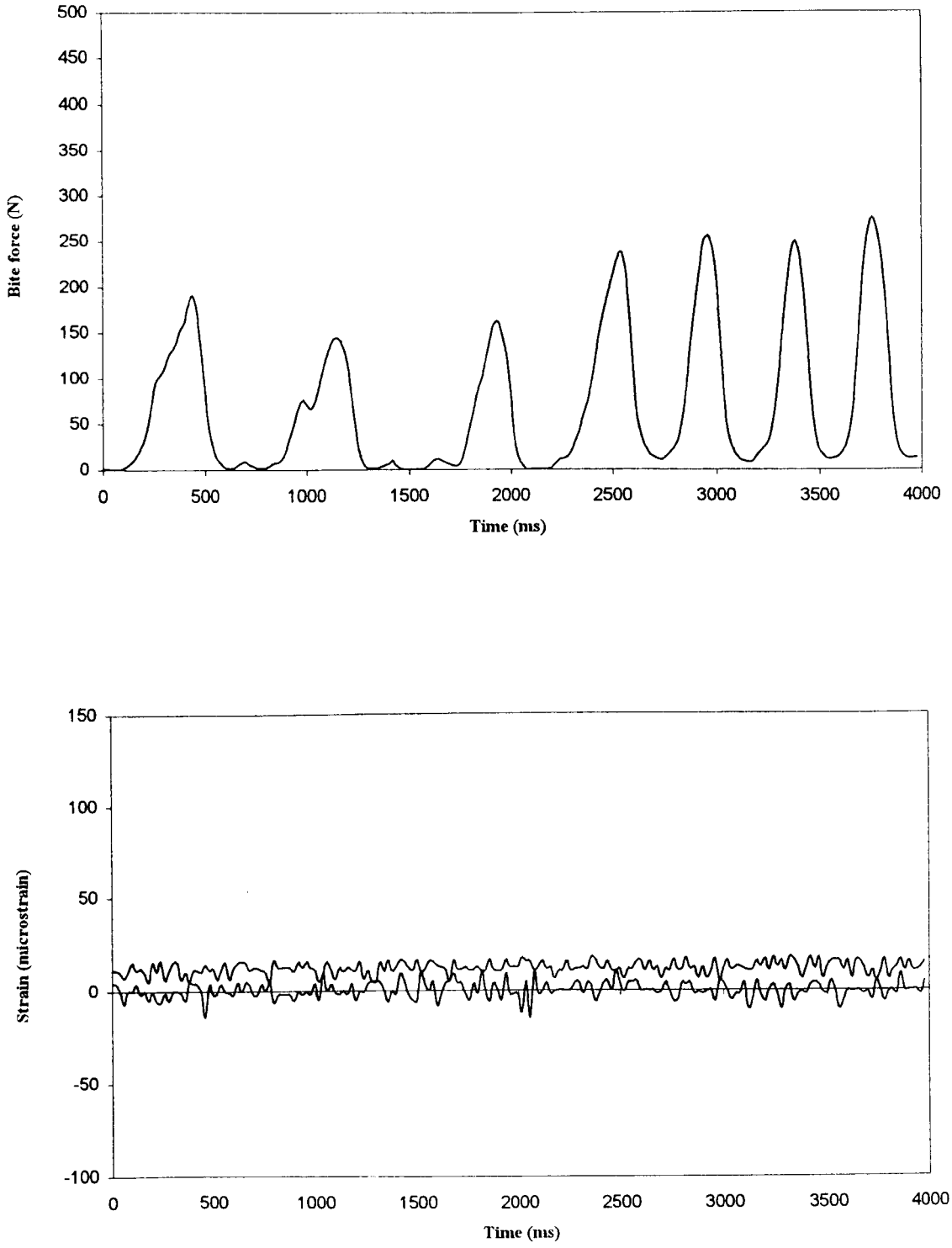

Figure 5.12
Bite force and parietal strain recorded simultaneously whilst biting on the bite force transducer with the right molars - second recording

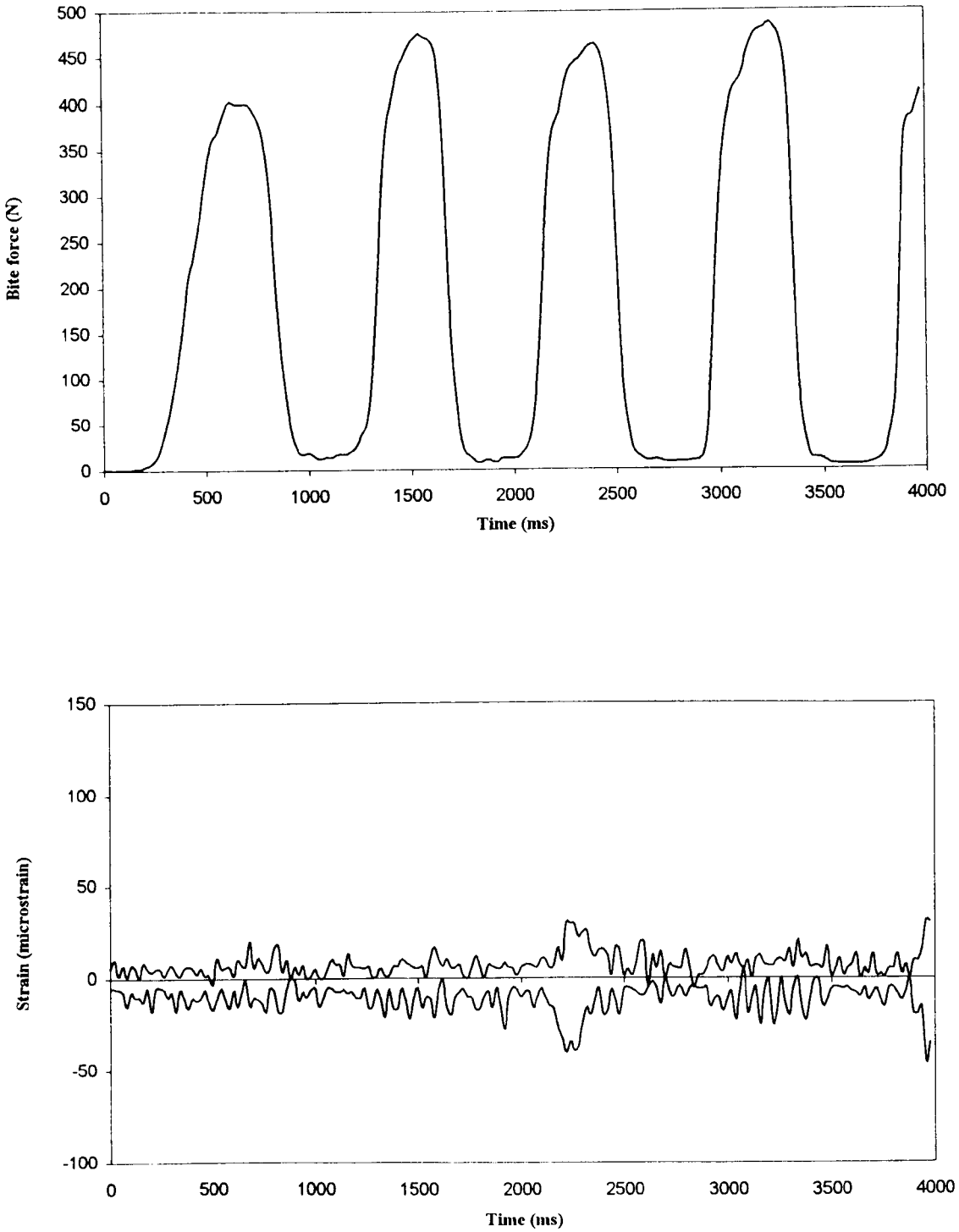

Figure 5.13
Bite force and parietal strain recorded simultaneously whilst biting on the bite force transducer with the right molars - third recording

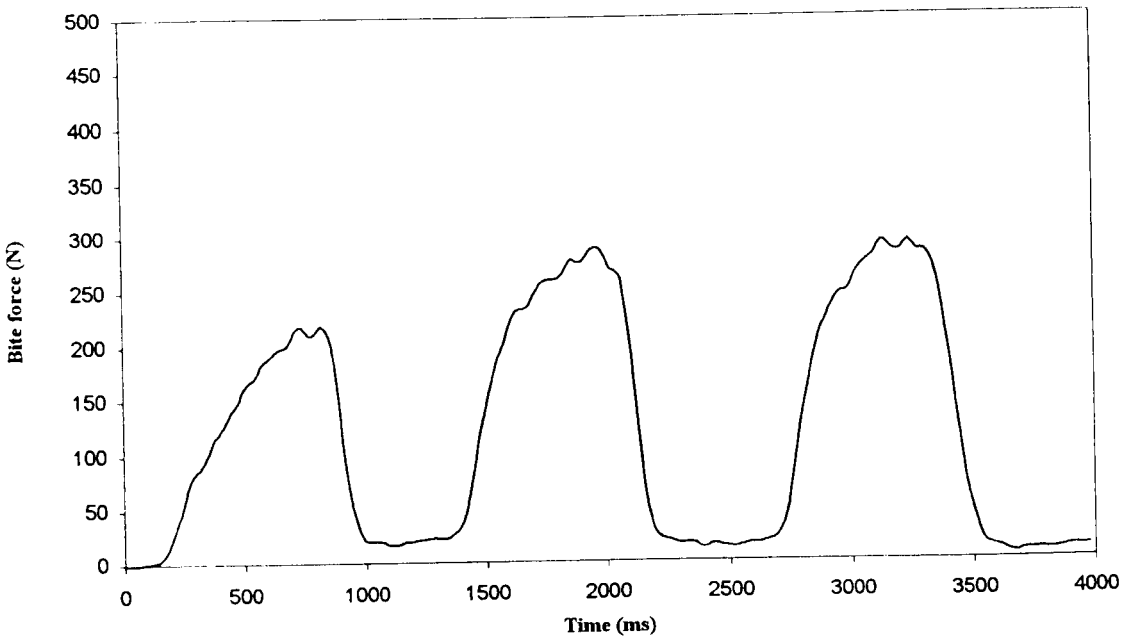

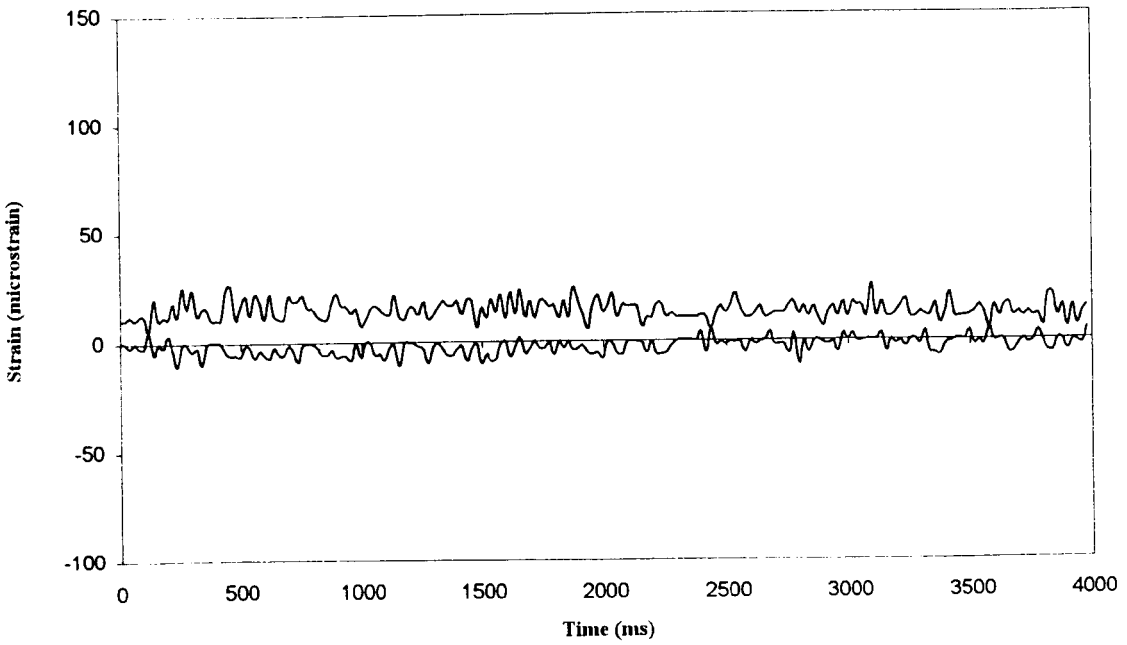

Figure 5.14
Bite force and parietal strain recorded simultaneously whilst biting on the bite force transducer with the left molars - first recording

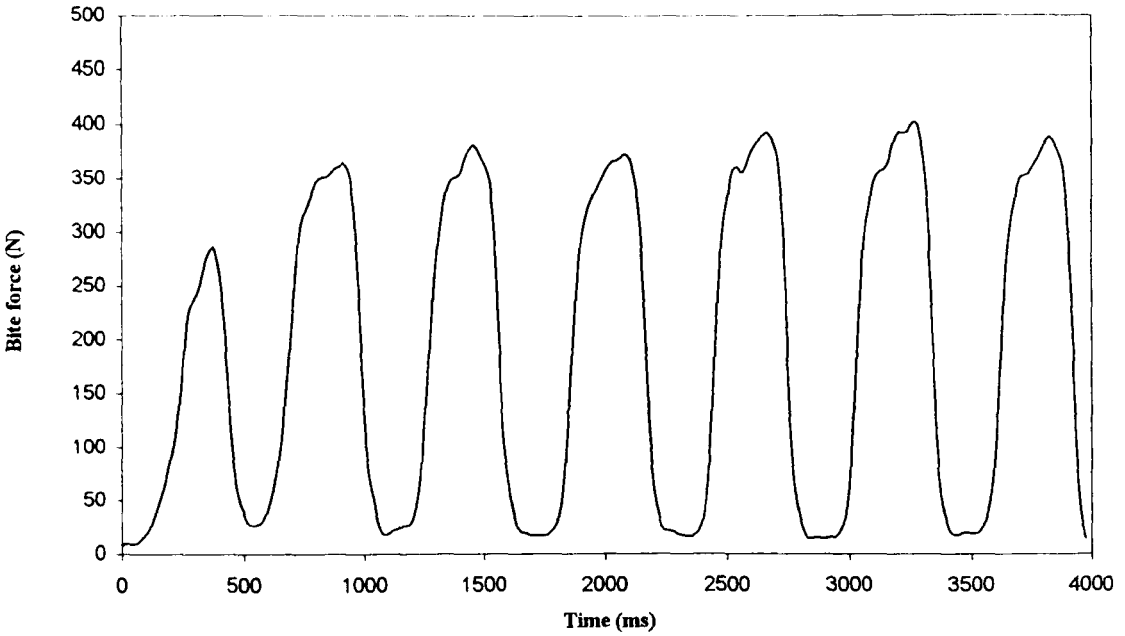

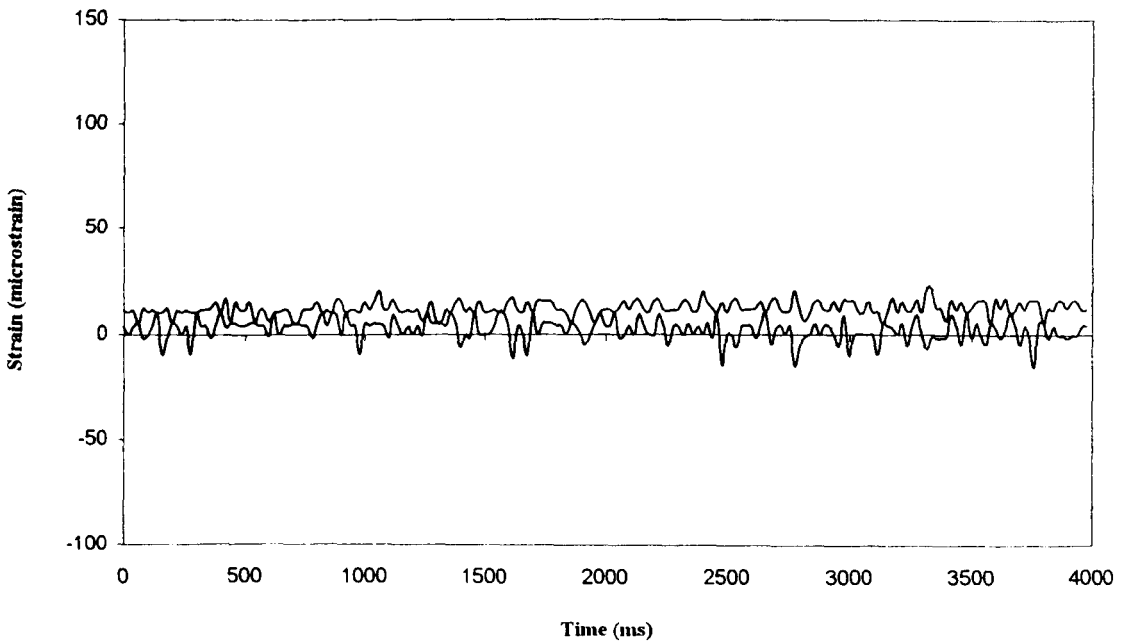

Figure 5.15
Bite force and parietal strain recorded simultaneously whilst biting on the bite force transducer with the left molars - second recording

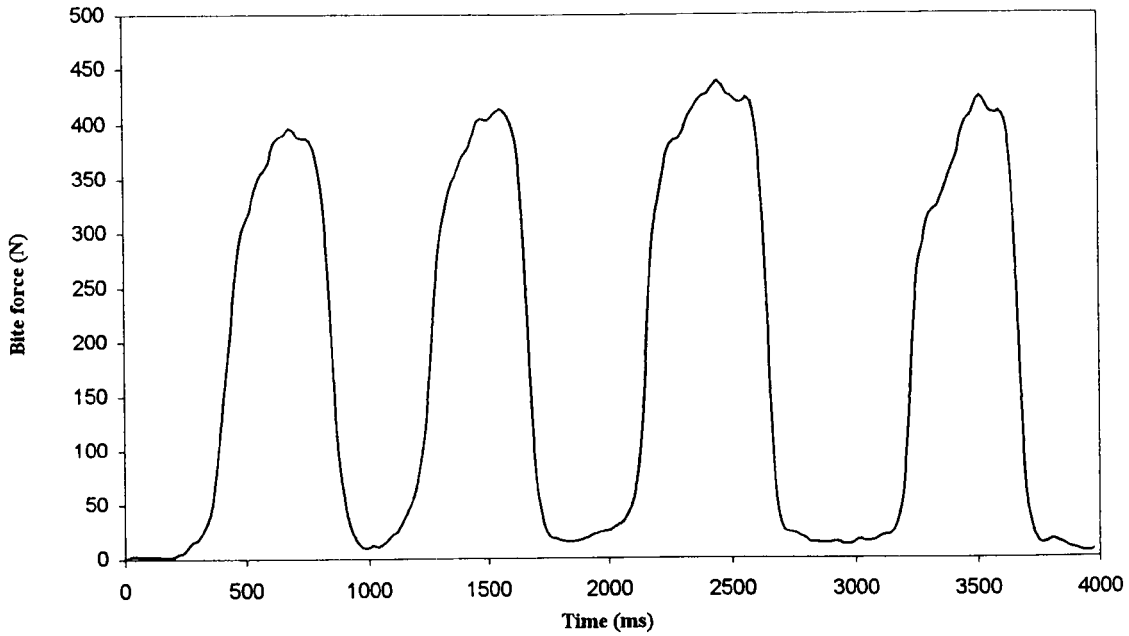

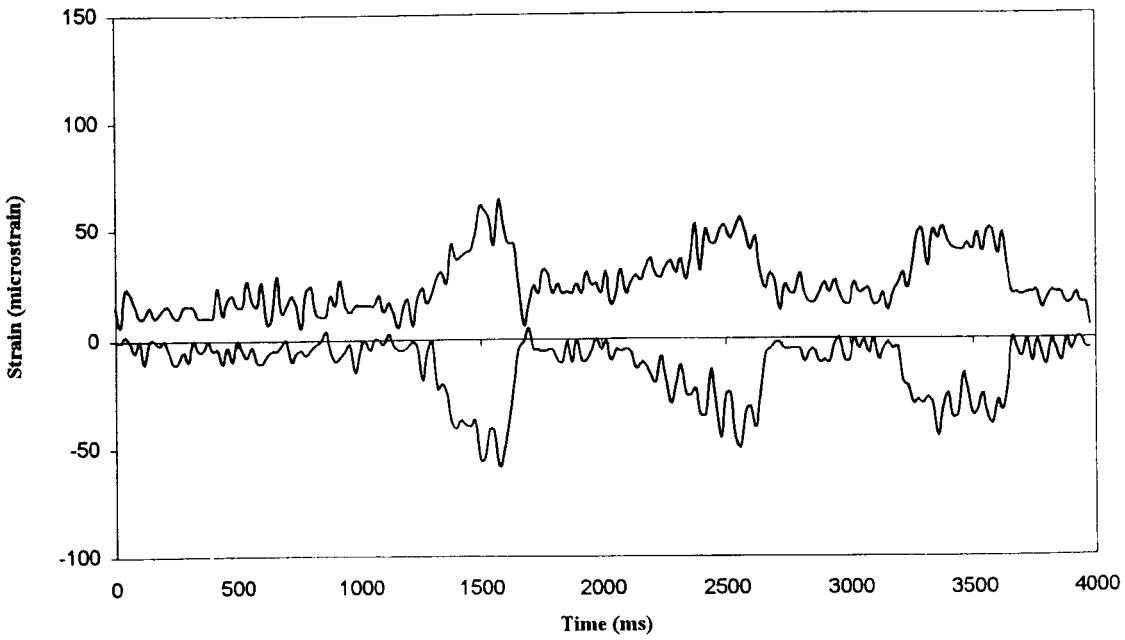

Figure 5.16
Bite force and parietal strain recorded simultaneously whilst biting on the bite force transducer with the left molars - third recording

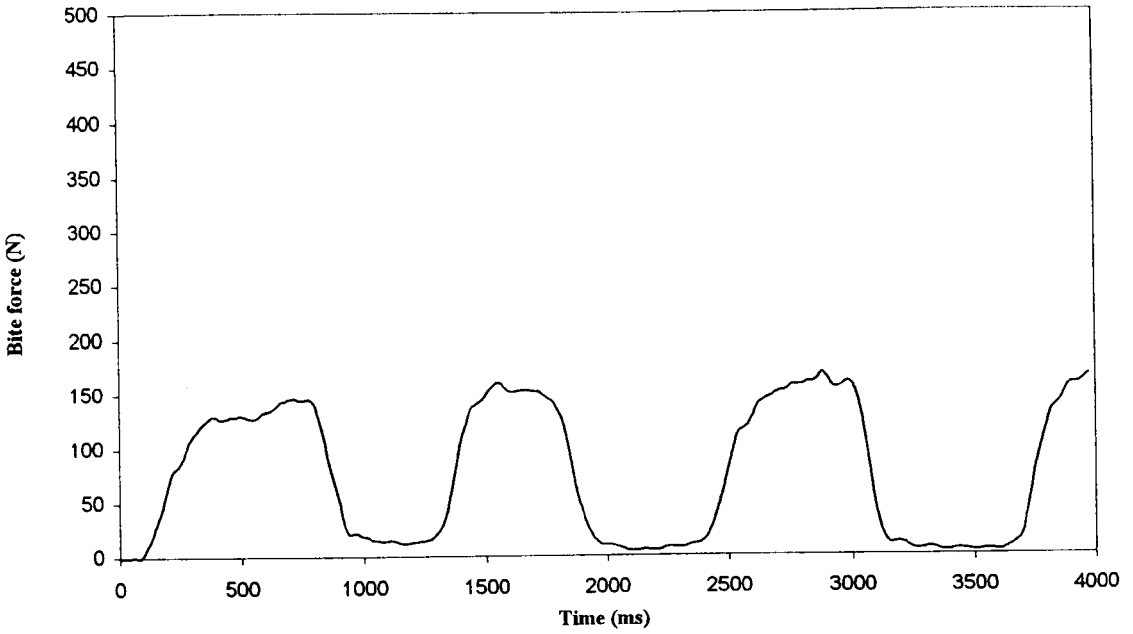

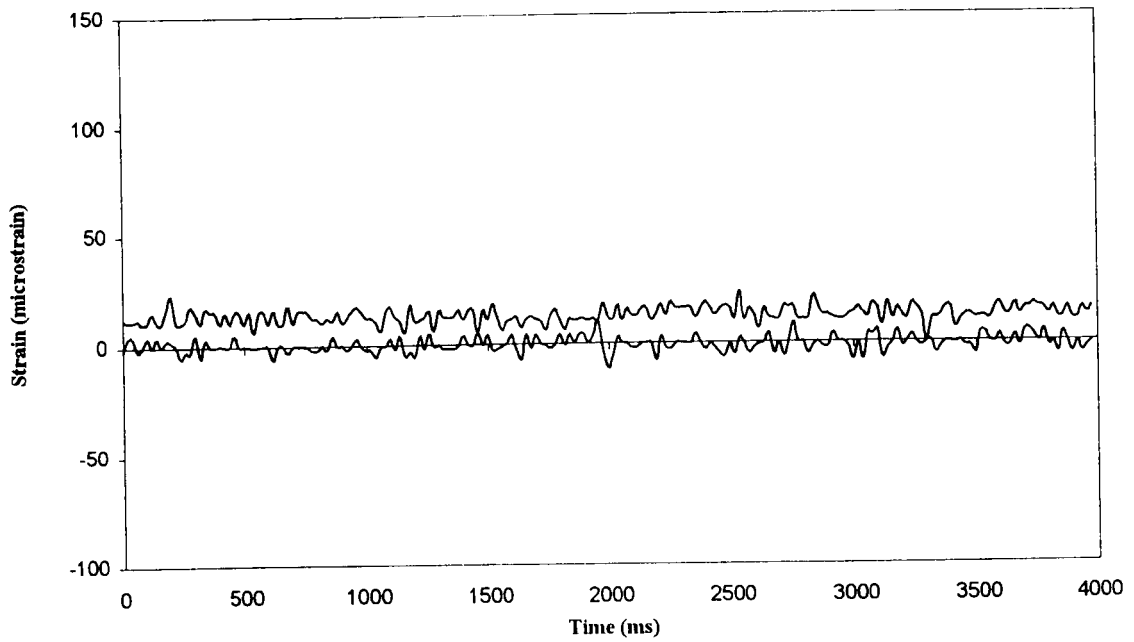

Figure 5.17
Bite force and parietal strain recorded simultaneously whilst biting on the bite force transducer with the incisors - first recording

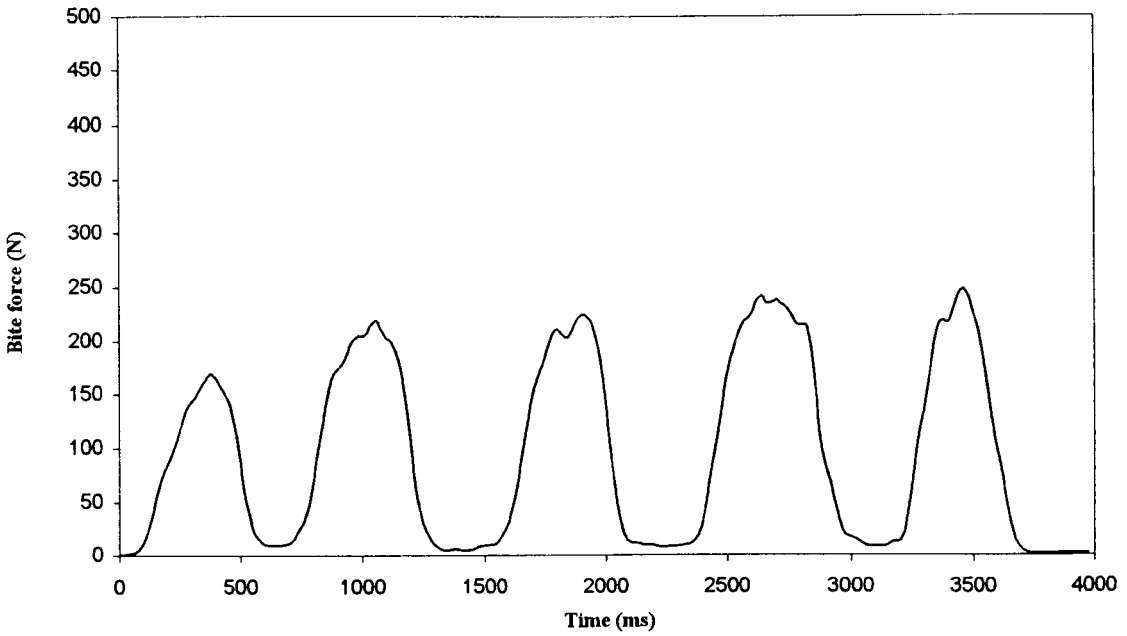

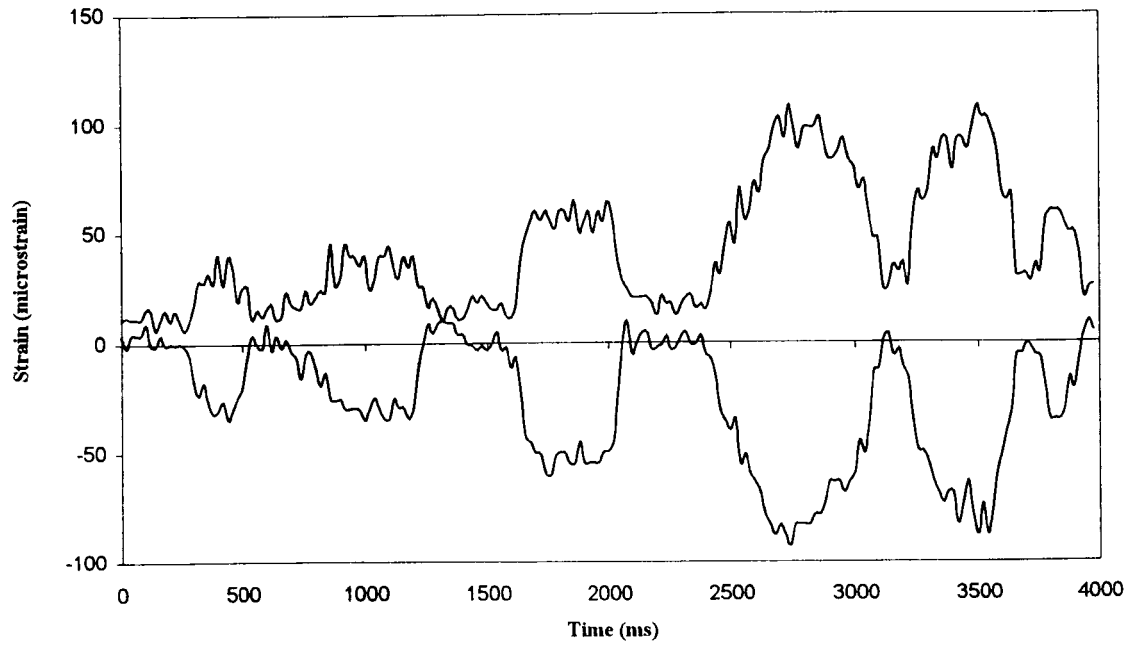

Figure 5.18
Bite force and parietal strain recorded simultaneously whilst biting on the bite force transducer with the incisors - second recording

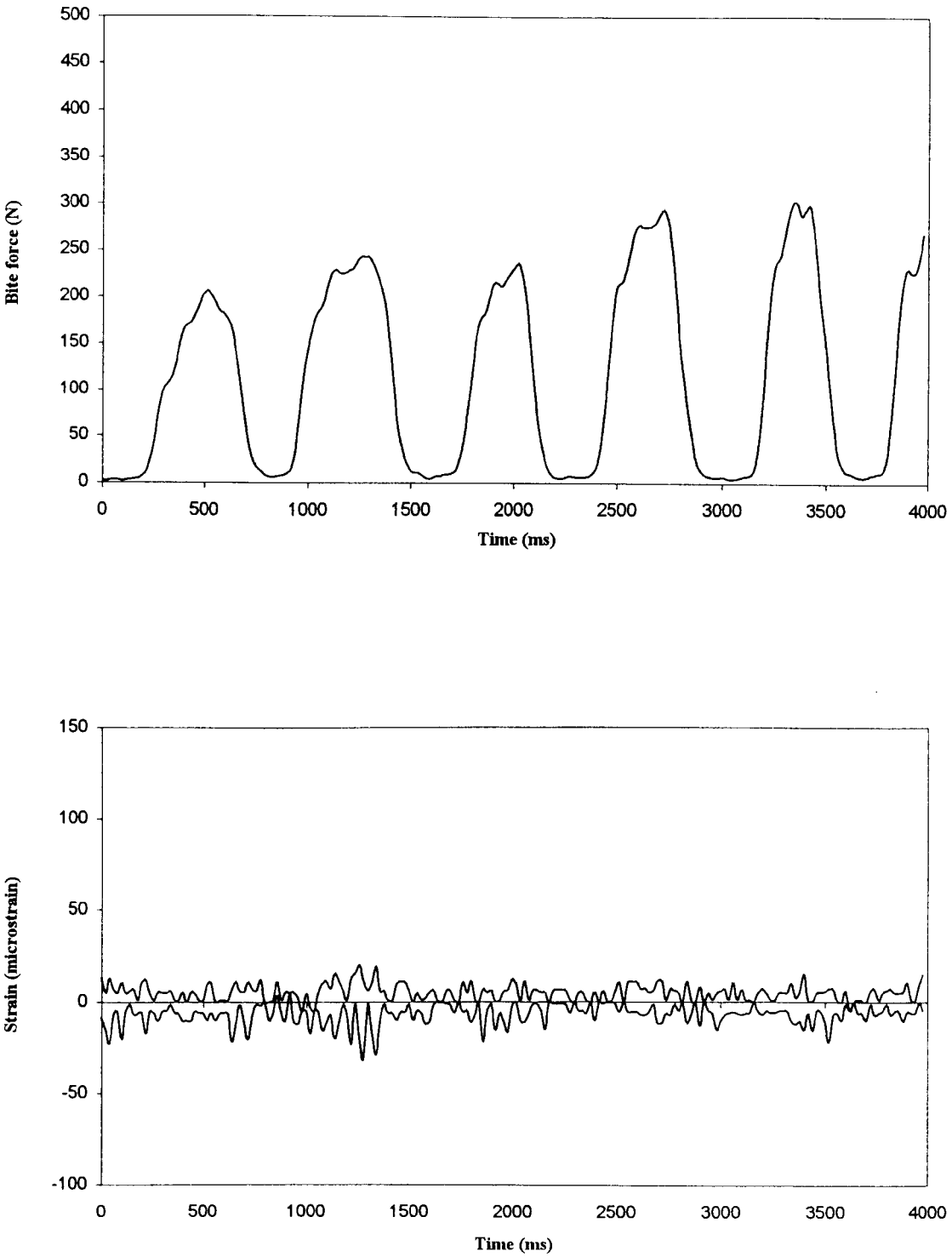

Figure 5.19
Bite force and parietal strain recorded simultaneously whilst biting on the bite force transducer with the incisors - third recording

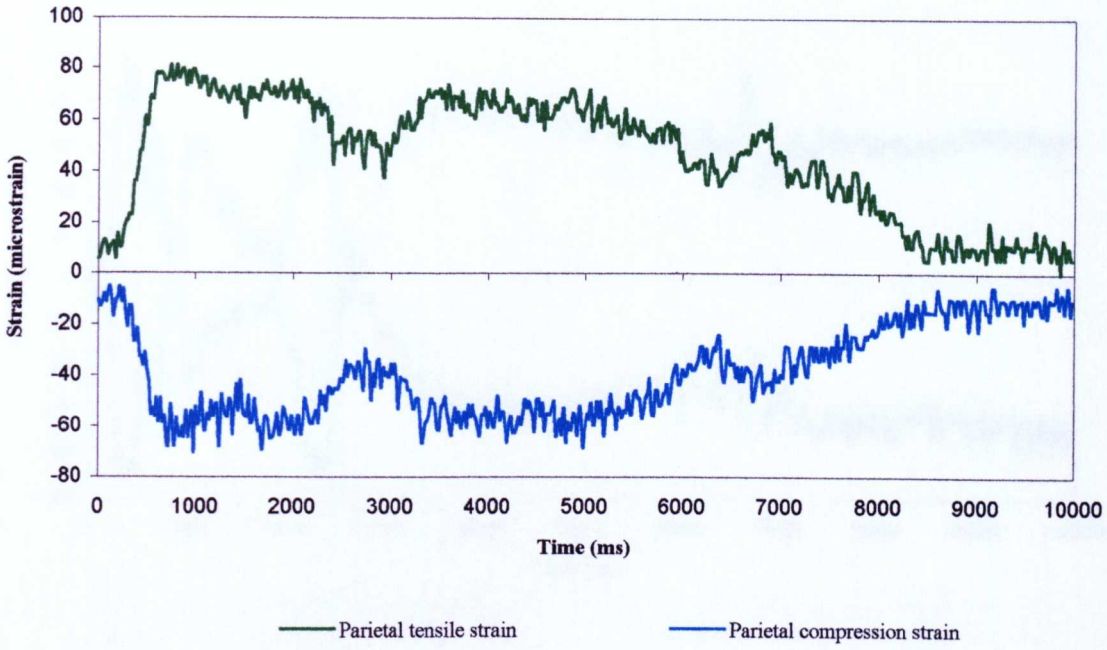

Figure 5.20
Parietal principal strains recorded while eating a banana

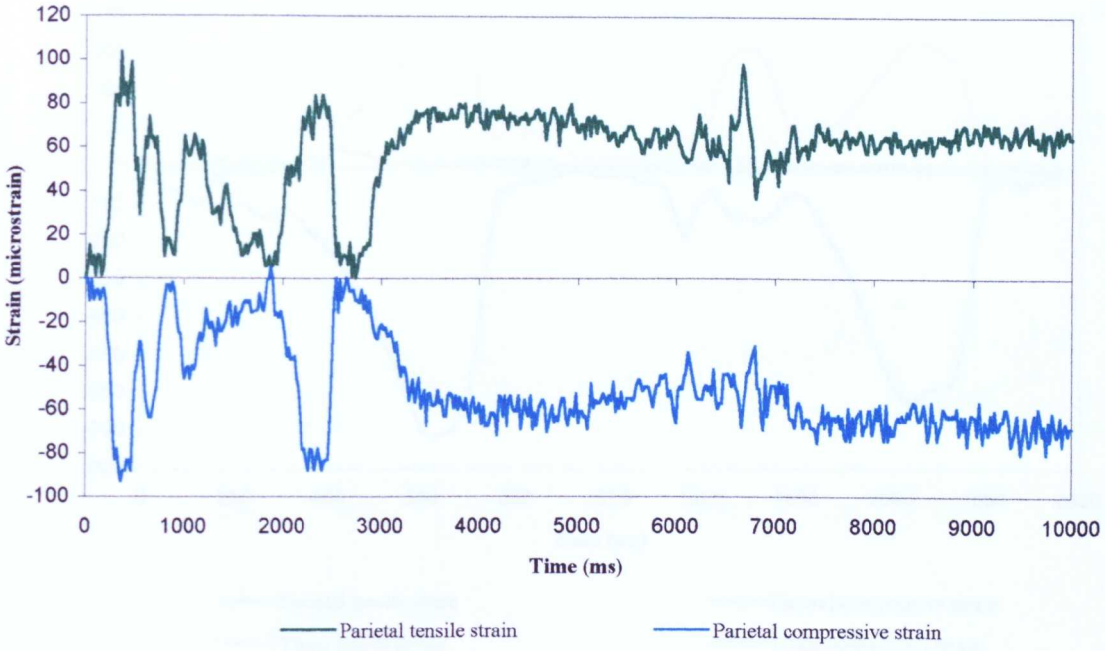

Figure 5.21
Parietal principal strains recorded while grimacing

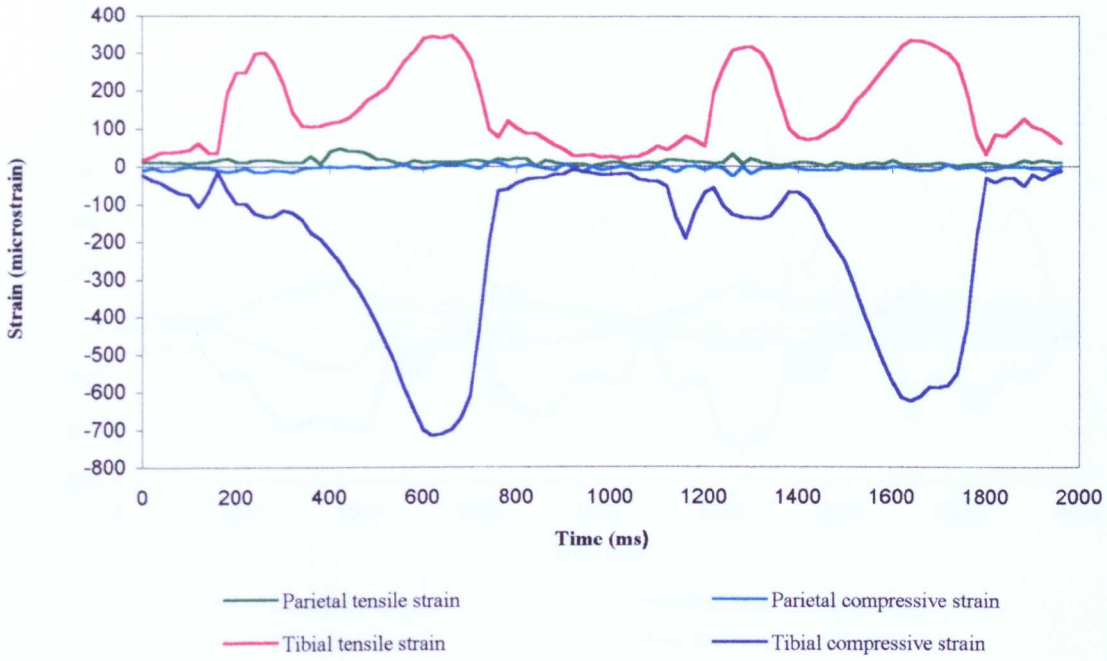

Figure 5.22
Parietal and tibial principal strains
recorded during two strides of walking

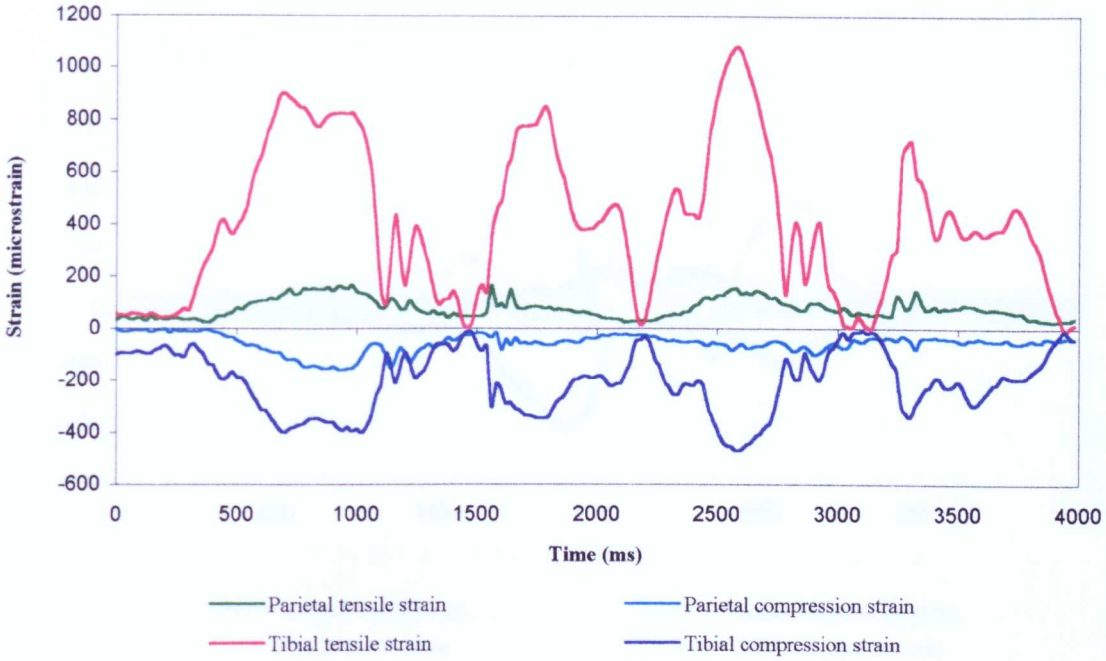

Figure 5.23
Parietal and tibial principal strains
recorded while squat-lifting a 56 lb. weight

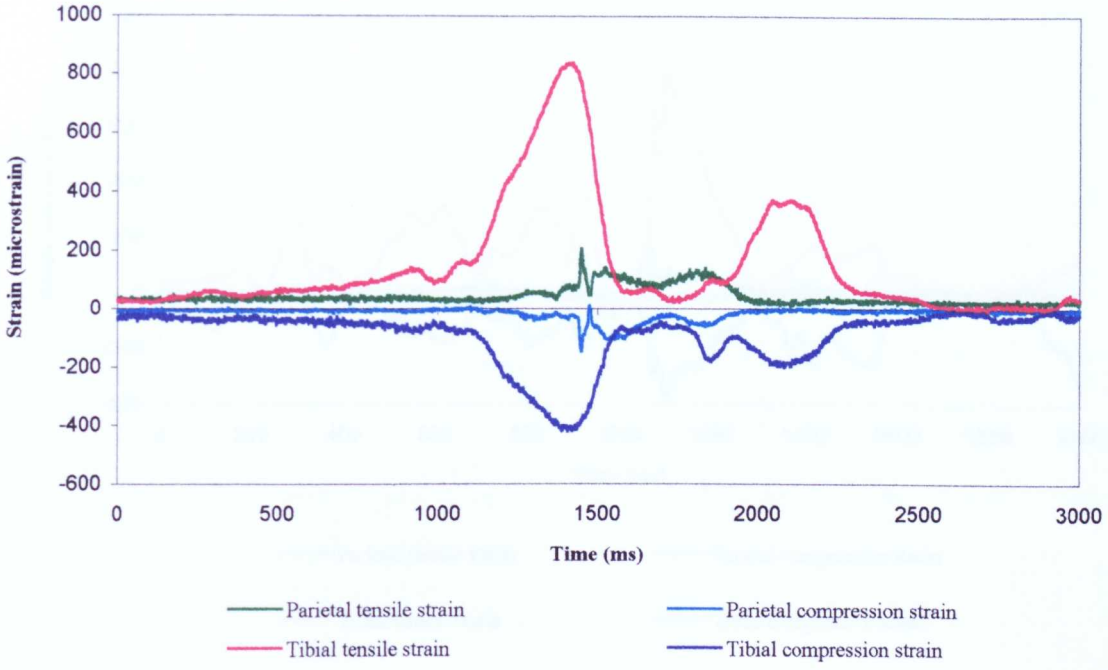

Figure 5.24
Parietal and tibial principal strains
recorded while heading a 4.5 kg medicine ball

(impact occurred just before 1500 ms)

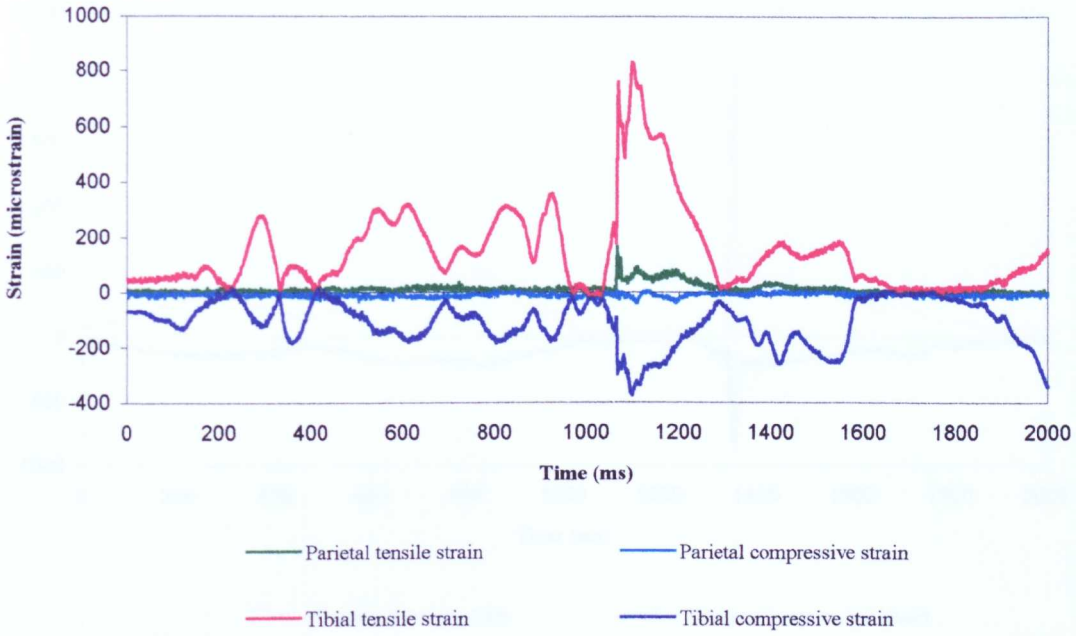

Figure 5.25
Parietal and tibial principal strains
recorded while climbing on to a chair
45 cm high, jumping and landing

(airborne at 1000 ms)

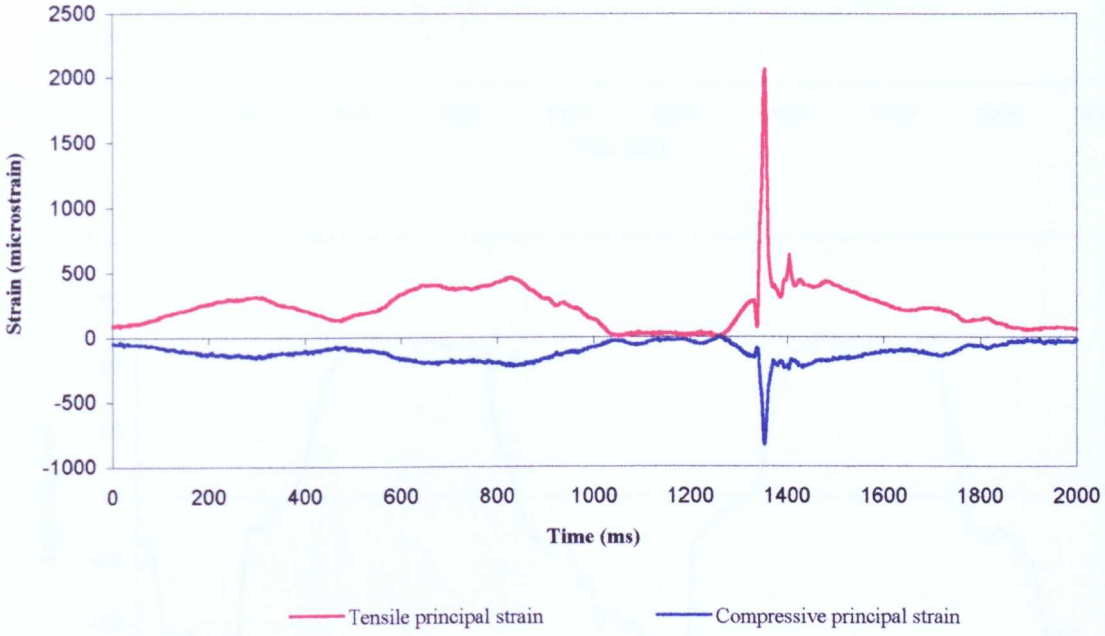

Figure 5.26
Tibial principal strains recorded while jumping and landing from a height of 1.3 m

(landing occurred just before 1400 ms)

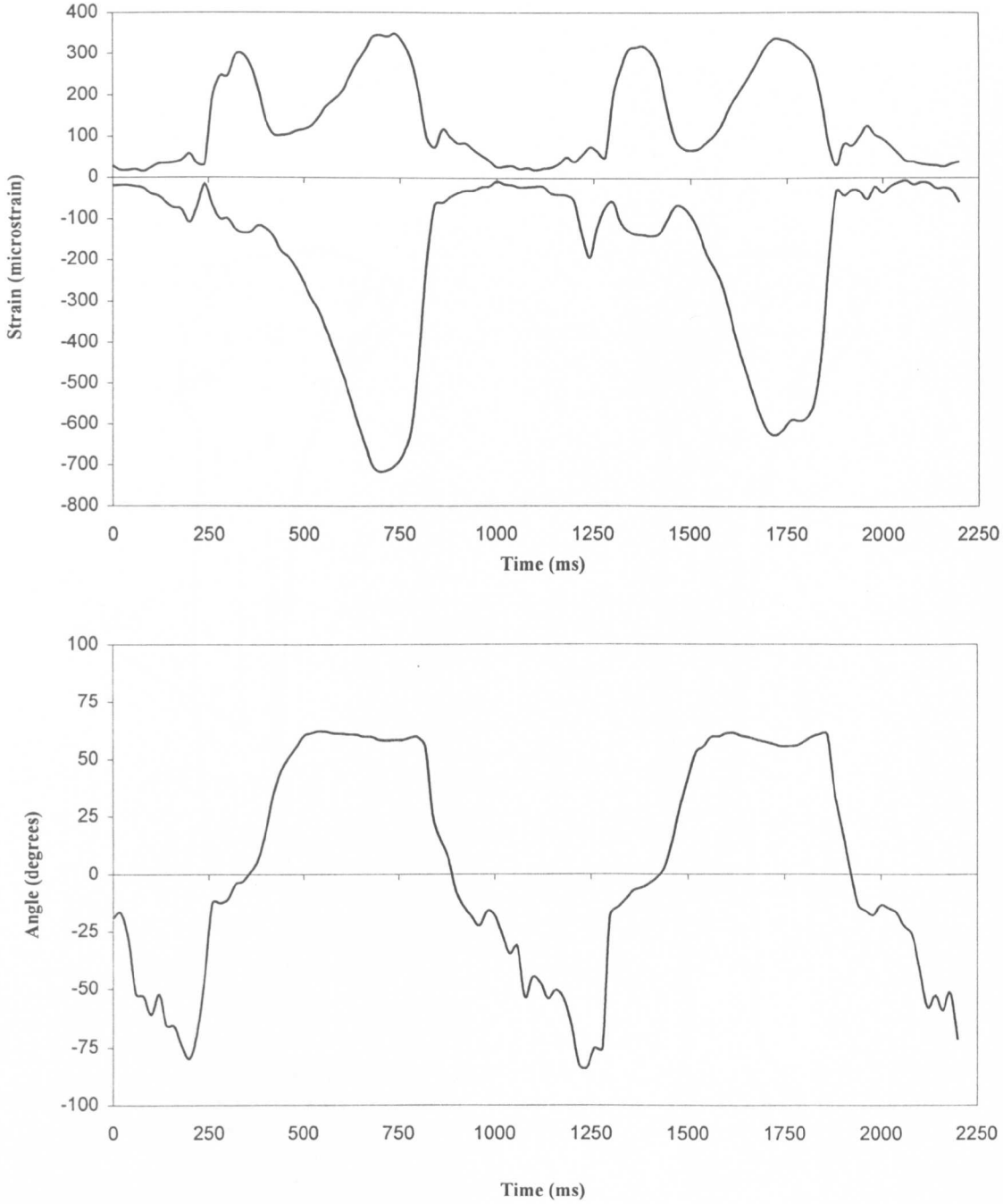

Figure 5.27
Tibial principal strains recorded from two strides with the angle of the principal tensile strain relative to the long axis of the bone
(A positive angle denotes a counter-clockwise direction)

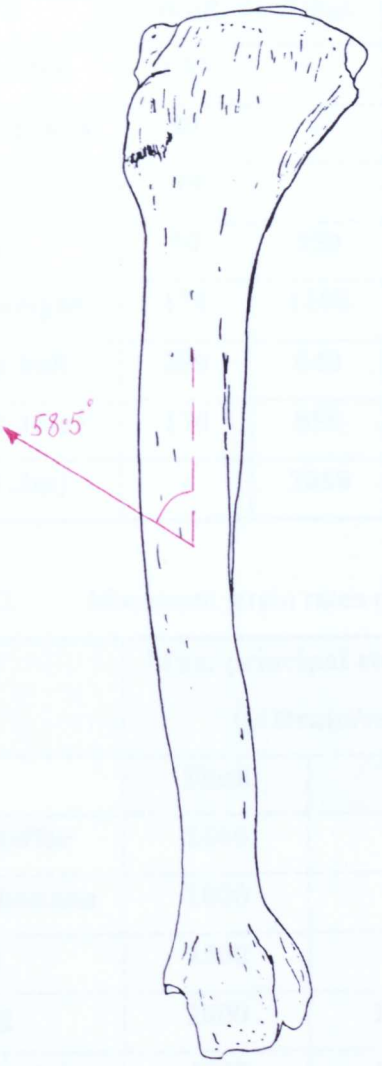

Fig. 5.28a

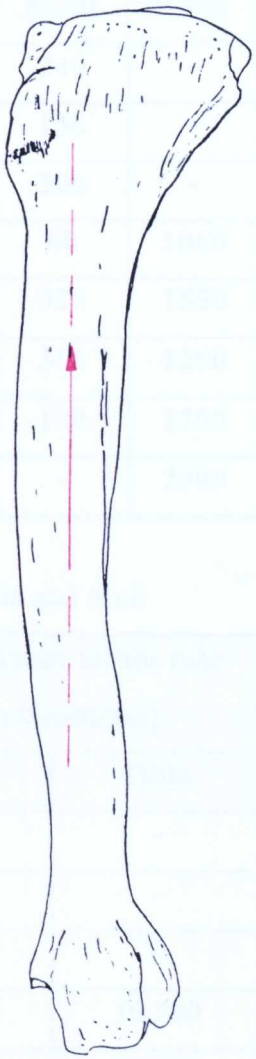

Fig. 5.28b

long axis of the tibial diaphysis

Figure 5.28

5.28a shows the angle of the principal tensile strain in the tibia during the stance phase
5.28b shows the angle of the principal tensile strain in the tibia during landing from 1.3 m

(Viewing the anterio-medial surface of the right tibia)

Table 5.1 Maximum strain magnitudes recorded from the tibia and skull

Activity	Maximum PS Tensile e1 (μ strain)		Minimum PS Compression e2 (μ strain)		Shear strain (e1-e2) (μ strain)	
	Skull	Tibia	Skull	Tibia	Skull	Tibia
Eating toffee	130	-	-110	-	240	-
Eating banana	80	-	-70	-	150	-
Smiling	100	-	-90	-	200	-
Walking	50	350	-30	-720	60	1060
Squat+weight	170	1100	-160	-470	320	1550
Heading ball	200	840	-150	-420	350	1250
Jump (0.45m)	170	850	-40	-400	190	1200
Jump (1.3m)	-	2060	-	-840	-	2900

Table 5.2 Maximum strain rates recorded from the tibia and skull

Activity	Max. principal strain rate (μ strain/sec)		Max. shear strain rate (μ strain/sec)	
	Skull	Tibia	Skull	Tibia
Eating toffee	2600	-	5300	-
Eating banana	1000	-	1300	-
Smiling	1500	-	2700	-
Walking	1600	11,800	2100	10,500
Squat+weight	5000	17,700	5700	24,300
Heading ball	30,100	15,100	47,800	24,000
Jump (0.45m)	44,000	180,800	51,600	244,200
Jump (1.3m)	-	245,300	-	336,700

Summary tables

Table 5.3 Summary of strain magnitude results

Maximum strain magnitudes	Tension (e1) (μ strain)	Compression (e2) (μ strain)	Shear (e1-e2) (μ strain)
Skull	**200**	**-160**	**350***
Tibia	**2060**	**-840**	**2900**

* Maximum tension, compression and shear strain values did not necessarily occur during the same activity, therefore, the shear value does not correspond with the values for e1 & e2.

Table 5.4 Summary of strain rate results

Maximum strain rates	Principal strain rates (μ strain/sec)	Shear strain rates (μ strain/sec)
Skull	**44,000**	**51,600**
Tibia	**245,300**	**336,700**

The maximum dynamic shear, tensile and compressive principal strain magnitudes and rates recorded from the parietal bone were considerably lower than those recorded from the tibia. Parietal strain magnitudes and rates were 4-10 times lower than those from the tibia. The rates are presented as numeric magnitude, irrespective of sign. In the summary tables, the data are presented including the recordings made from the 1.3 m jump. During this activity only data from the tibial gauge was collected. Therefore, it is likely that the maximum principal and shear strain rates would have been greater in the parietal bone than those measured previously in the other exercises.

The recordings made while heading the medicine ball showed results which were different from the other activities. The maximum principal and shear strain rates were double those recorded from the tibia. This is not surprising considering the weight of the ball. Despite this the maximum principal and shear strain magnitudes did not exceed 200 μstrain. However, this activity could not be considered physiological, although it would represent a minor traumatic blow to the skull.

Chewing soft foods and facial expressions produced higher strain magnitudes than biting as hard as possible onto a bite force transducer. Transient spikes were experienced in the skull as a result of jumping and were associated with transient spikes in the tibia. Not surprisingly, transients were also seen when the medicine ball was headed.

5.6 Discussion

In 1975 Lanyon *et al* made the first *in vivo* recordings of human bone strains during physiological activity (Lanyon *et al* 1975). Recently a similar experiment was repeated by Burr *et al* (1996). In both experiments, rosette strain gauges were bonded to the tibia only. The aim of Lanyon *et al* was to compare human strain data with that recorded previously from animals, so that the physiological relevance of similar animal studies could be established. Burr *et al* hypothesised that strains in excess of 3000 μstrain could be produced on the tibial midshaft during vigorous activities. The reason they investigated tibial strains was due to the high incidence of tibial fatigue fractures suffered by army recruits during basic training. This experiment is the first in which simultaneous recordings have been made from the skull and tibia and to my knowledge is the first in which any human skull strains have been measured *in vivo*. The aim of this experiment was to compare physiological strain magnitudes and strain rates recorded from the two sites within the same individual, during a range of sedentary and vigorous physiological activities.

The strain pattern recorded in the tibia when the subject was walking showed similar tensile and compressive principal strain magnitudes to those measured previously in the human tibia (Lanyon *et al* 1975). In addition, the angle of principal strains in the tibia correlated very well with those measured previously in the human tibia (Lanyon *et al* 1975). At the walk and during fairly sedentary activities, the greatest principal strain was compressive (720 microstrain) and the angle of principal tension was directed at 58.5 degrees to

the long axis of the bone (figure 5.28a). This implies that the distal end of the tibia is subjected to an internal torque (Lanyon and Bourn 1979). During more strenuous activities such as squatting with weights and jumping, the greatest principal strain was tensile and directed along the long axis of the bone (figure 5.28b). This might be expected when considering the natural curvature of the tibia which is bowed medially at the mid-diaphysis, however, it appears impossible to predict accurately from the external form of the bone how the bone is loaded *in vivo* (Lanyon and Bourn 1979). The similarities between our results and those of previous studies confirm that the techniques and equipment used were comparable.

During walking, the compressive principal strains of -720 μstrain were higher than those recorded by Lanyon *et al* (1975) and Burr *et al* (1996) who recorded -434 and -544 μstrain respectively. The maximum principal and shear strain rates (11,800 and 10,500 μstrain sec^{-1} respectively) were higher than those recorded by Lanyon *et al* (1975) whose maximum principal strain rate was 4000 μstrain sec^{-1} but very similar to those of Burr *et al* who recorded maximum principal and shear strain rates of 11,006 and 17,158 μstrain sec^{-1} respectively. Despite differences between the experiments, the values are still within the same order of magnitude. These differences could be attributable to differences in gauge positioning and natural biological variation.

The highest peak principal strain magnitude recorded was 2060 microstrain in tension and was recorded whilst landing from a height of 1.3 m. This produced a peak landing force of 13,250 N i.e. approximately 20 times greater than body weight. It was also during this activity that the highest principal strain rate was recorded (245,300 μstrain sec^{-1}) from the tibia. Unfortunately, the functioning gauge on the parietal bone had debonded by this stage in the experiment, therefore, no recordings from the head could be taken. However, jumping from such a height may not have represented a normal physiological activity, except possibly in army recruits!

Landing from a height of 0.45 m produced a landing force of approximately 4000 N, which was over five times body weight. This activity would be equivalent to jumping off a bus or jumping down the last few steps on a flight of stairs. Therefore it could be considered to be physiological. It was associated with maximum principal strain magnitudes of +840 and -420 μstrain in the tibia while those in the skull were +170 and -40 μstrain. These represent a difference in magnitude of between 5 to 10 fold. The maximum strain rate recorded from the tibia during this activity was 180,800 μstrain sec^{-1} while that recorded from the skull was 44,000 μstrain sec^{-1}. This was greater than that recorded while heading the medicine ball and represented the highest principal strain rate recorded in the skull. This was only a quarter of the maximum rate recorded in the tibia during the same activity.

The principal strain magnitudes measured in the parietal bone were very low i.e. 200 μstrain or less. Similar results were found in the para-sagittal suture region of the parietal bone in Macaca mulatta using single element strain gauges by Behrents *et al* (1978). It was an interesting finding that facial expressions produced strain magnitudes that were as high and often higher than those recorded whilst biting with maximum force against a solid bite-force transducer. Results of the parietal strain magnitude plotted against bite force (figures 5.11 - 5.19) showed that an increase in surface strain associated with biting was an inconsistent finding. Bite force and strain were recorded with the bite force transducer placed between the left cheek teeth, right cheek teeth and incisors. Three measurements were made for each site. Only one of the three recordings for each site demonstrated an increase in strain with biting. This suggests that biting does not load the parietal bone directly. The effects are likely to be as a result of grimacing because of the discomfort of biting onto the hard device. The maximum tensile and compressive principal strains recorded were 100 and -90 μstrain respectively and were associated with a bite force of 250 N. One recording made while biting on the right side produced forces of nearly 500 N, however, the strains generated were little more than electrical 'noise' i.e. unmeasurably small.

Strain rates in the skull were also much lower than those measured in the tibia. However, transient, high frequency peak strains did occur in the parietal bone and these were associated with transients that occurred in the tibia as a result of impact loading such as jumping, landing and heading the medicine ball. Heading the medicine ball did not represent a physiological activity. However, it would not be unreasonable to assume that this might be representative of an accidental blow the head. The forces of which, the cranium would be expected to withstand. Other than this activity, there are two explanations for the transients recorded from the calvaria: either they occurred as a direct result of muscle activity in the skull or there was transmission of an impact shock wave up the vertebral column. Similarly, maximum shear strain magnitudes and rates were much greater in the tibia compared with the calvaria.

The difference by a factor of 4-10 between the maximum strain magnitudes and rates recorded in the tibia and parietal bone, provides evidence to disprove the hypothesis that there are no differences in the strain magnitudes experienced by the parietal bone and the tibia. However, it has to be noted that a single rosette strain gauge can only be used to measure strain at the site directly under the gauge elements. In order to assess strain distributions across the bone, multiple gauges must be implanted over the bone surface (Rubin and Lanyon 1985). In this case, it was not practicable to implant three gauges around the tibial circumference under local anaesthesia because of the obstruction caused by musculature. To gain full exposure it would have been necessary to reflect the gastrocnemius and anterior tibialis muscles. In addition, there would have been an increased risk of complications associated with more extensive surgery.

The results of this experiment raise several questions about the biological control of bone mass. Do bone cells in the tibia have different thresholds for strain sensitivity compared with calvarial cells? Frost (1983) proposed a minimum effective strain threshold (800 - 2000 μstrain) for bone remodelling in lamellar bone. Turner *et al* (1994) demonstrated mechanical loading

thresholds for lamellar and woven bone formation in the tibia of nine month old rats and later described an increase in this threshold for 19 month old rats (Turner *et al* 1995). Similarly, Torrance *et al* (1994) reported a threshold of 1500 μstrain for medial periosteal bone formation at the mid-point of the ulna in 200-220 g rats. In the light of these reports, it is possible that the transduction mechanism which converts mechanical strain into a cellular response is more sensitive in calvarial bone compared with the tibia.

Recently, thin, unmineralised fibres have been described with attach the periosteum to the bone in rat parietal bone (Simmons *et al* 1993). The authors didn't say whether they examined other bones of the calvaria. They suggested that these fibres may be a way by which masticatory muscles may apply strain to the osteoblasts lining bones of the cranium. It may also explain why facial expression also produced strains as high as eating.

Is there a variation in genetic setpoint for bone mass in different bones which reflect the degree of mechanical usage and the roles of the individual bones?

Changes in bone mass are the net effect of all the different positive and negative osteotropic influences acting on the bone simultaneously. Comparing the tibia with the calvaria, it is possible that there are differences in the response of bone cells to individual or different combinations of osteotropic influences. It is possible that in the calvaria mechanical strain magnitude and strain rate are not as important in terms of their positive osteotropic effect compared with the tibia. After all, the calvaria needs to maintain its strength in order to protect the brain. However, it usually experiences very low mechanical strains. Therefore, adaptation to variations in this strain would not make sense because of the requirement for a large safety factor to withstand possible blows to the head. Indeed, if the tibia were subjected to the same mechanical environment as the calvaria, it would undergo disuse osteopenia. Skerry and Lanyon (1995) demonstrated profound disuse osteopenia in the calcanei of sheep that were immobilised by external fixators. The bone mineral

content fell by 22 % compared with controls. Interestingly, strain measurements recorded in the calcanei of controls showed that peak strain magnitudes were -1147 x 10^6. This value is similar to the that recorded from the human tibia during walking. In the immobilised calcanei, peak strain magnitudes were -71 x 10^6. This value was similar to that recorded in the human skull during walking. Two studies in humans also suggest that the skull may be resistant to disuse osteopenia. Leblanc *et al* (1990) demonstrated widespread bone loss in the entire skeleton except the skull following 17 weeks of bedrest. In fact, bone mass in the skull increased during this period. In another study, Garland *et al* (1992) showed bone loss in the entire skeleton except in the skull, following spinal cord injury. It is possible that in both studies, despite relatively severe disuse in the majority of the skeleton, the skull still would have been loaded through muscle action associated with talking, eating and facial expressions. This may well have represented normal activity, especially in the light of this experiment which has shown that apart from occasional physical blows to the head, facial expressions and eating appear to be responsible for the maximum strains experienced in the parietal bone.

One function of mechanical strain which has been considered recently is the role of strain frequency. McLeod and Rubin (1994) found that spectral analysis of avian tibial strain data showed that high magnitude strains occurred at low frequency (<10 Hz), however, the lower magnitude strains occurring at a frequency of 30-40 Hz represented a larger proportion of the spectral energy. They suggested that low magnitude strains at these frequencies may provide the primary osteogenic stimulus required to maintain bone mass, which is in contrast to the widely held belief that it is probably high strain magnitudes that provide this stimulus. However, earlier work by Rubin and McLeod (1990) investigating strain frequency is controversial. Turner *et al* (1995) claim that the conclusions drawn from that work were likely to be incorrect due to a systematic error in the experimental technique. Despite this, Rubin and McLeod (1994) have shown subsequently that bone ingrowth into implants can

be induced by low magnitude, frequency-specific strains. It was not possible to perform frequency analysis of the data obtained in this experiment because of lack of filtering and recording frequencies that were too low.

The non-functioning parietal gauge may have failed to work for several reasons: Firstly, the gain on the strain gauge amps may have been turned down accidentally after the initial set-up. Secondly, the rosette might not have been bonded firmly to the bone directly under gauge element b.

5.7 Conclusions

Since bone would be lost from the tibia if it was only exposed to the strains normal in the parietal bone it can be concluded that either:

1. Strains are not important in maintenance of bone mass in the parts of the skull.

or

2. Strain perception is enhanced in the skull compared with the tibia so that the low habitual strains provide a stimulus to maintain mass.

Chapter 6

General Discussion

The experiments described in this thesis have investigated various aspects of altered cellular activity associated with mechanically loading a modelling surface in a growing long bone, the interaction of oestrogen and parathyroid hormone, two systemic factors known to be important in the control of bone mass and regional differences in bone strain. All of these experiments were conducted *in vivo* in an attempt to understand their significance in living bone. However, mechanical load, oestrogen and parathyroid hormone do not represent all the factors which interact in bone's diverse environment. *In vivo* it is the balance between all the positive and negative osteotropic effects of the multitude of metabolic factors and the mechanical environment, which determines the final mass and architecture of a bone. The processes by which bone models and remodels to achieve its final form may vary in different regions of the skeleton.

Lieberman (1996) bonded rosette strain gauges to the tibiae and occipital bones of a group of exercised pigs. The maximum strain magnitudes recorded were 1800 μstrain in shear on the medial aspect of the proximal tibial and 170 μstrain in shear on the surface of the squamous part of the occipital bone. These magnitudes and regional differences were very similar to those in the human study described in this thesis. He described how the thickness of the cranial vault increased in the pigs, despite peak shear strain magnitudes that were so low. He proposed that the reason for this increase could be explained by systemic factors, for example growth hormone levels. Interestingly, Leblanc *et al* (1990) described an increase in skull bone mineral density in volunteers who underwent prolonged bed rest. They proposed that the bones of the skull may act as an *in vivo* 'sink' for increased levels of circulating calcium and phosphorus minerals, although it was possible that during bed rest the skull experienced strain levels above those experienced normally as a result of abnormal movements, increased amount of talking and eating. In contrast,

Karlsson (1996) described a lower BMD in the upper parts of the skull in athletes undertaking weight-lifting exercise. It is possible that large demands on the body for increased amounts of calcium for muscle activity and net bone formation in the exercising athletes may use the skull bones as a calcium 'sink'. However, if sufficient calcium was obtained through the diet, this would be unnecessary. In any event such a mechanism could prove catastrophic and appears to be an adaptive paradox. These discrepancies are difficult to explain without detailed analysis of all the experimental conditions but the findings may have been attributable to systemic factors. In any case, there was no assessment of changes in the material and structural properties of the skull bones. This would appear to be the important factor because of the protective role of the cranium. It is possible that under normal circumstances, the material and structural properties of the calvaria do not vary widely from a genetically determined (phylogenetic) range which provides an adequate 'safety factor' against impact fracture. Lieberman (1996), however, argued that cranial vault thickness was not very heritable and therefore, selection pressures in favour of thicker skulls were very weak. This was based on analysis of the fossilized remains of various primitive populations of the genus *Homo* which showed that variations in calvarial thickness may have been more dependent on levels of exercise and/or the duration of skeletal growth. Nonetheless, it is still possible that all forms of the genus *Homo* through time have possessed skulls with this phylogenetic 'safety factor', with selection favouring increased brain size with the ability to avoid dangerous situations and provide an indirect way of protection from injury.

The results of the human parietal strain gauge experiment in this thesis suggest that the entire parietal bone experiences low strain magnitudes and rates relative to a long bone but this, of course, assumes that the conditions are equal throughout the entire bone. However, results from other animal studies in which the parietal bone of several different species were investigated (Behrents *et al* 1978; Hillam *et al* 1994, Rawlinson *et al* 1995) support these findings. In contrast, it would be quite wrong to assume that all bones of the

skull were subjected to such a sedentary strain environment. Indeed, not all bones of the skull do demonstrate such low strain magnitudes during physiological activity (Hylander 1977; Hillam unpublished data). Principal strain magnitudes of nearly 500 μstrain were recorded on the surface of the sheep frontal bone during eating and vocalization (Hillam unpublished data). Behrents *et al* (1978) and recently, Jaslow and Biewener (1995) demonstrated in monkeys and the goat respectively that trans-suture strain magnitudes were high compared with the surrounding bone, suggesting that the sutures may function as shock-absorbers and act to partially mechanically isolate adjacent bones in the skull. In addition, Jaslow and Biewener (1995) recorded principal strain magnitudes in the goat parietal bone as high as - 850 μstrain, however, these were measured very close to the frontoparietal suture and during high impact loading of the horns *in vitro*. Direct comparisons should not be made between these data and strains measured in animals that are not in the Bovidae family. This is because sheep and goats have been shown to possess specially adapted skulls which can withstand forces associated with head-butting, that are at least 60 times greater than impact forces required to fracture the human skull (Jaslow and Biewener 1995). Other than members of the Bovidae family, few animals use their heads as a battering ram! Consequently they will not subject their skulls to high impact forces and it is highly unlikely that they will ever experience strain magnitudes within their parietal bones, as high as those measured in the goat skulls.

The findings of the three *in vivo* studies described in this thesis all warrant further investigation. This could be achieved with additional *in vivo* and complimentary *in vitro* experiments. The comments made by Lanyon *et al* (1977) when they stressed the importance of the physiological relevance of experiments applies to the design of both *in vivo* and *in vitro* experiments. Indeed, Nathan and Sporn (1991) described how many previous *in vitro* studies into the effects of cytokines had been conducted inappropriately, which had resulted in many contradictory results. They emphasized the need to assess the physiological relevance of a cytokine's action using tests in intact

organisms. This issue was reiterated by G.R. Mundy (Cells and Cytokines meeting, Davos, 1996) who described how research into bone physiology was becoming confused with "*in vitro* phenomenisation"! No experiment can ever reproduce the complex milieu to which bone is exposed *in vivo* so there has to an appreciation for the limitations of each study. Rawlinson *et al* (1995) demonstrated some profound differences in the response to loading *in vitro* comparing parietal bone with ulnar bone. However, calvarial bone has been used commonly for many years to research the effects of mechanical loading and effects of chemical factors on bone. The interpretations from these studies cannot necessarily be extrapolated to their possible effects on bone specimens originating from other skeletal regions. In 1995, Lean *et al* demonstrated IGF-I mRNA expression in rat caudal vertebrae following mechanical loading but not in control bones. In contrast, Mason *et al* (1996) demonstrated expression of IGF-I in loaded and control ulnae. It is possible that these differences represented site-specific regional differences in skeletal physiology, however, it is also feasible that the surgically invasive nature of the caudal vertebral loading model combined with load magnitudes which are likely to be pathological have confounded an understanding of the adaptive physiology.

The rat model of ulna loading is suitable for investigating cellular events associated with modelling and remodelling that occur in cortical bone. A high percentage of bones (75%) demonstrated reversal of resorption in response to mechanical loading and only a low percentage (12.5%) demonstrated lack of reversal or woven bone formation (12.5%). Although the model can't be used to investigate trabecular bone, it has been used recently (Mason *et al* 1995) to demonstrate expression of genes that regulate production of a glutamate aspartate transmitter molecules in control ulnae, whereas gene expression was down-regulated in the loaded bones. This molecule or one very similar is involved with post-synaptic reuptake of neurotransmitter in the brain. It has never been demonstrated previously in bone and may prove to be pivotal in the mechanotransduction mechanism in which osteocytes communicate via gap junctions. Further support for this possibility has been provided by the

identification and localisation of several different classes of glutamate receptors in bone cells (Skerry *et al* 1996).

The three areas of study covered in this thesis warrant further investigation but require the design of appropriate and physiologically relevant *in vivo* and *in vitro* experiments if they are to contribute to our understanding of bone physiology.

Proposals for further work

1. The results from chapter 2 demonstrated that non-invasive axial loading of the ulna in 90 g female Wistar rats could stimulate new bone formation on a surface previously resorbing through modelling activity. A logical extension of this work would be to subject the ulna to loading for a period, sufficient to produce reversal and consequently new bone formation, then stop loading and investigate the subsequent sequence of cellular events. This could prove a good model with which to study the processes leading to activation and osteoclastic resorption.

2. The results from chapters 3 and 4 showed that there was an interaction between oestrogen and parathyroid hormone at certain skeletal sites, affecting trabecular bone. This finding warrants further investigation. The adult ovariectomised rat would remain an appropriate model but future experiments would require larger numbers and it would be most appropriate to perform pure parathyroidectomies in preference to thyroparathyroidectomies when attempting to deprive the rats of their source of parathyroid hormone.

3. The failure to demonstrate any significant differences in calvarial porosity between any of the groups of rats in the experiment described in chapter 4 and profound differences in physiological strain magnitudes and strain rates between the sites measured on the human tibia and parietal bone in chapter 5, require further investigation to determine the mechanisms by which calvarial bone maintains its mass following declines in levels of circulating oestrogens and following surgical transplantation. In addition, the findings of these experiments suggest that the design of an appropriate non-invasive *in vivo* animal model of calvarial loading may be useful in determining the possible role of mechanical strain in calvarial bone physiology.

Appendix 1

Appendix to chapter 2

A.1.1 *In vivo* ulnar strain gauging

Five 290 g male Wistar rats were used. This weight of rat was chosen because they represented possibly the smallest size that could be successfully instrumented with strain gauges *in vivo* at that time. The ulna is a small bone and lighter rats may have presented difficulties in gauge placement. It is also very possible that the gauge may have produced reinforcement effects in very small bones (Little *et al* 1990). Bonded gauges could, theoretically, have acted as splints and the strains engendered may have been lower than in control bones.

Two rats were chosen for medial periosteal gauging, two for lateral strain gauging and one for both lateral and medial gauging.

Each rat was premedicated with pethidine at a dose rate of 20 mg/kg to act as an analgesic. From previous work, higher doses tended to greatly prolong recovery time following anaesthetic. The rats were anaesthetised with inhaled halothane Ph. Eur. (Fluothane, ICI Pharmaceuticals, Macclesfield, UK)) and maintained at a concentration of 1.5 % in oxygen. The hair was plucked from the antebrachium to provide a clear operating site. After making a skin incision, the lateral or medial aspect of the ulnar mid-diaphysis was exposed by blunt separation of the muscle groups. Good exposure was maintained by passing 3/0 silk suture (Ethicon Ltd., UK) through the muscle groups, which were then held apart under tension using artery forceps. The periosteum was carefully scraped away with a scalpel blade and the bone surface was degreased by swabbing the area with a cotton bud soaked in a 50:50 (by volume) mixture of diethyl-ether and acetone. A 120 Ω, single element strain gauge (type FLK-1-11, Tokyo Sokki Kenkyojo Co., Tokyo, Japan) prepared for *in vivo* use (appendix 3), was bonded to the bone surface. This was achieved by applying a small amount of commercial cyanoacrylate adhesive (Superglue, Loctite,

UK) to the back of the gauge. The gauge was then aligned with the long axis of the bone and placed in contact with the bone surface. Firm digital pressure was applied to the gauge for one minute to achieve a strong gauge-bone bond. The medial periosteal surface proved more difficult to gauge than the lateral surface due to differences in exposing the bone.

The lead wires were passed through a subcutaneous tunnel formed by passing the tips of a pair of fine artery forceps under the skin from the site of surgery, dorsally up the lateral aspect of the brachium to emerge finally between the scapulae. Before the surgical incision was closed, the lead wires were soldered to a connector which was then attached to a ribbon cable. This was connected to the strain gauge amplifiers (Bell and Howell, Basingstoke, UK) which had been given half an hour to warm up before the start of the surgery. The strain gauge was supplied with 2.35 volts, given a minute to stabilize then balanced. At this point no current flowed through the Wheatstone bridge circuit. Providing the gauge balanced, the incision was closed. If the gauge didn't balance, it was removed and replaced. The lead wires were sutured to the skin as they emerged from the incision between the shoulders. This was secured further with a drop of cyanoacrylate. This prevented any tugging of the lead wires resulting in detachment of the gauge from the bone surface. The output from the strain gauge amplifiers was 6.57 volts per 1000 μstrain.
Once surgery was completed the rats were removed from the anaesthetic. Recovery took between 10-20 minutes. Before starting to move about, the gauges were balanced so that zero represented a fully relaxed position, with minimal strain imposed on the bone surface directly under the gauge. Recordings were made during a range of activities including walking, grooming, landing from heights of between 18-30 cm and climbing up and down a 45° ramp. Data was collected by a personal computer fitted with a 12-bit capture card (RTI-815, Analog Devices, Norwood, MA, USA) using custom software ('Super', D. McNally, University of Bristol) which sampled at a frequency dependent on the sampling time. It sampled 512 data points

evenly divided over the recording period. This meant that sampling frequencies varied from approximately 50 - 250 Hz

A.1.2 *In vitro* load strain calibration of the ulnae

It was necessary to establish the axial load-strain calibration in the ulnae from 90 g rats. This would enable the calculation of the load required to produce -4000 μstrain on the medial periosteal surface, at the mid-diaphysis.

The left ulnae from three 90 g female Wistar rats were removed and minimally dissected to expose the medial periosteal surface at the mid-diaphysis. A 120 Ω, single-element strain gauge (type FLK-1-11, Tokyo Sokki Kenkyojo Co., Tokyo, Japan) was bonded to the bone surface in the same way as described in the *in vivo* experiment. The first preparation was placed in the cups of the loading jig after balancing the strain gauge. Static loads were applied by advancing the jig manually. Axial compressive force then strain amplifier output were recorded as voltages from digital volt meters. It was apparent that if the preparation was left for 30 seconds or more, the force and strain values fell off. As the load increased, this became less apparent. The result of this was that the load strain curve was not linear (figure A.1.1). 7 N produced between -3500 to -4500 μstrain on the medial periosteal mid diaphysis.

Another ulna prepared in the same way was dynamically loaded between 1 - 7 N at 1 Hz Ten seconds after the start of loading, the load and strain were recorded over a two second period using a computer and custom software at a sampling frequency of 250 Hz A plot of strain against load demonstrated that the relationship was linear (figure A.1.2). It was noted that a regression line did not pass through the origin. This could have been due to drift of the strain gauge amplifiers. If a new line was constructed which was parallel to the original trace and so that it passed through the origin, a force of 7 N produced a strain of -3700 μstrain.

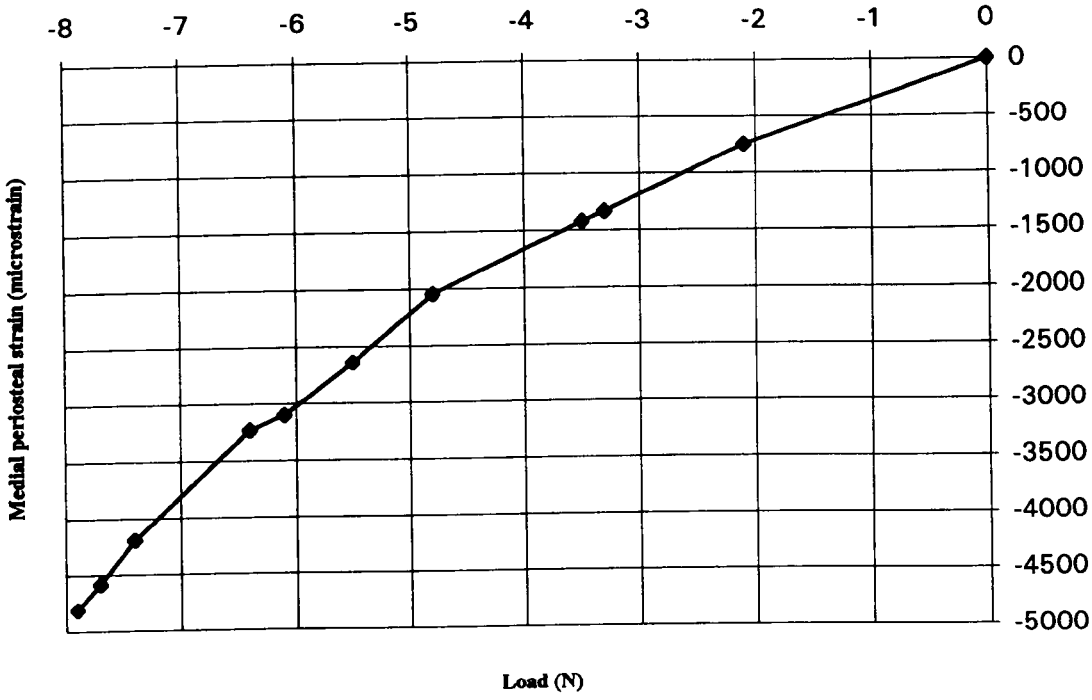

Figure A.1.1
Ulnar load strain calibration curve

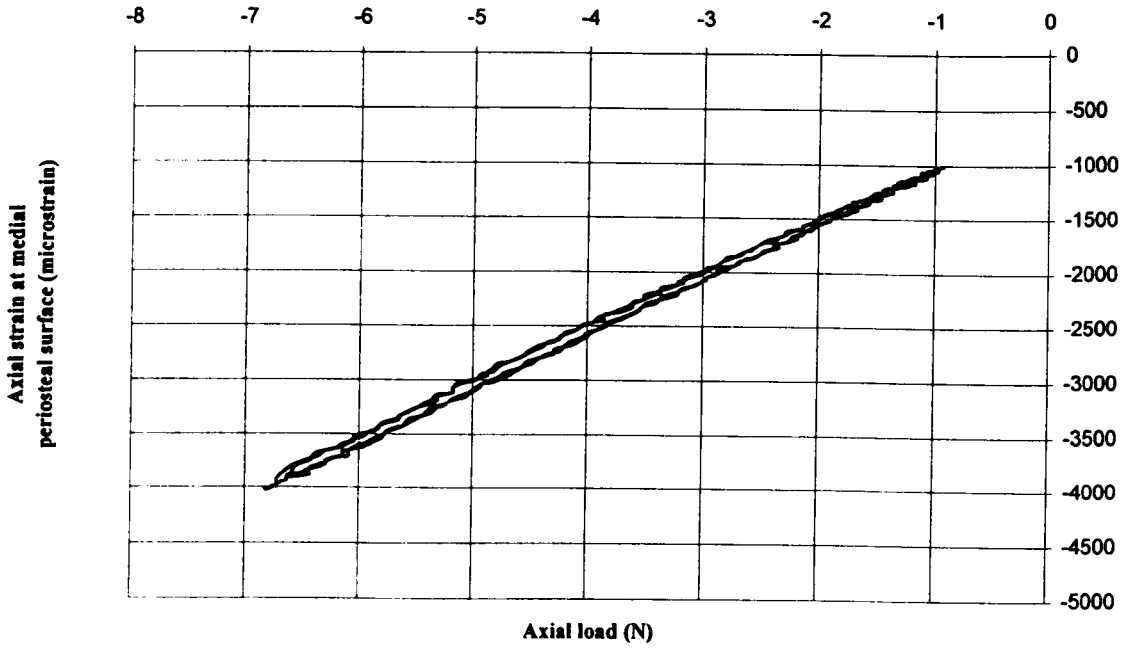

Figure A.1.2
Load strain calibration at 1 Hz

The procedure was repeated at a loading frequency of 10 Hz This time a plot of strain against load produced a trace which was not linear (figure A.1.3). The stress-strain relationship on loading was not the same as that on unloading. This pattern is called hysteresis. The area between the two curves represented the energy absorbed by the tissues during the loading cycle. It appeared to be much greater at 10 Hz than at 1 Hz It could be seen from the graph that apart from the two extremes of applied load, the strain engendered at the ulnar midshaft was greater upon loading than at unloading for a given load magnitude. A line drawn through the two end points did not pass through the origin. Again this may have been due to strain amplifier drift. If a new line parallel to this was constructed so that it passed through the origin, a load of 7 N produced a strain of -4250 μstrain. Mean (± SEM) peak strain rates for the loading part of each cycle were 116700 (800) μstrain/second whilst those for the unloading were 129700 (700) μstrain/second. Using an unpaired, two-tailed Student t-test, the differences between these strain rates were highly significant ($p < 0.0001$). Because the loading waveform was sinusoidal, it should be borne in mind that these peak strain rate magnitudes were only maintained for a very short period of the loading cycle near the points of the maximum and minimum loads (figure A.1.4).

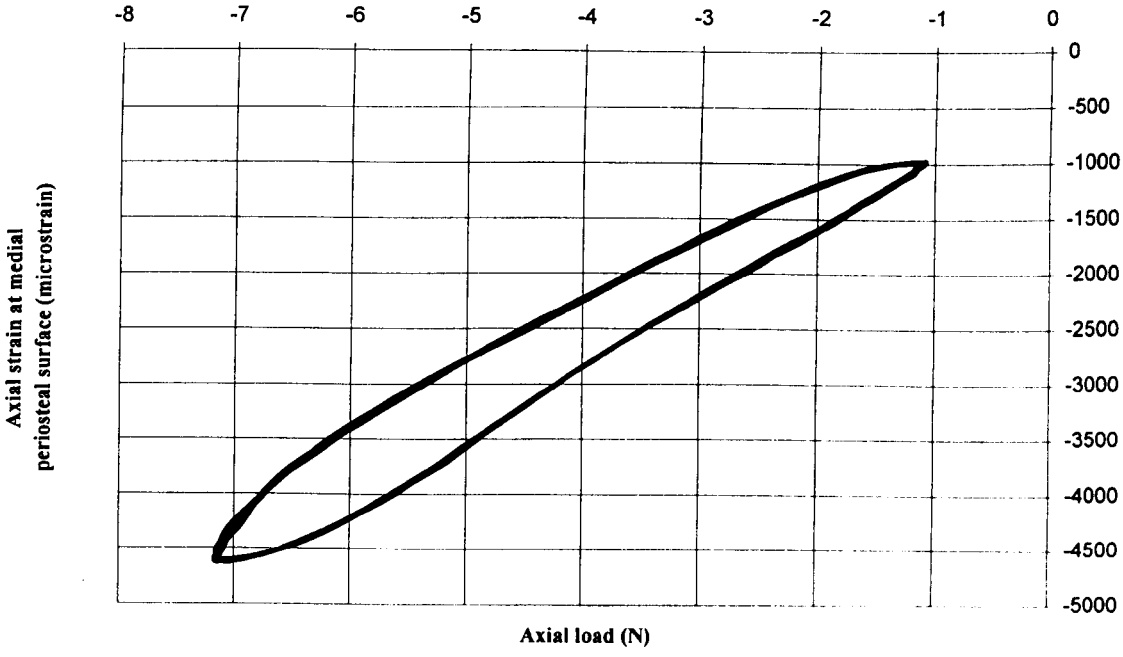

Figure A.1.3
Load strain calibration at 10 Hz

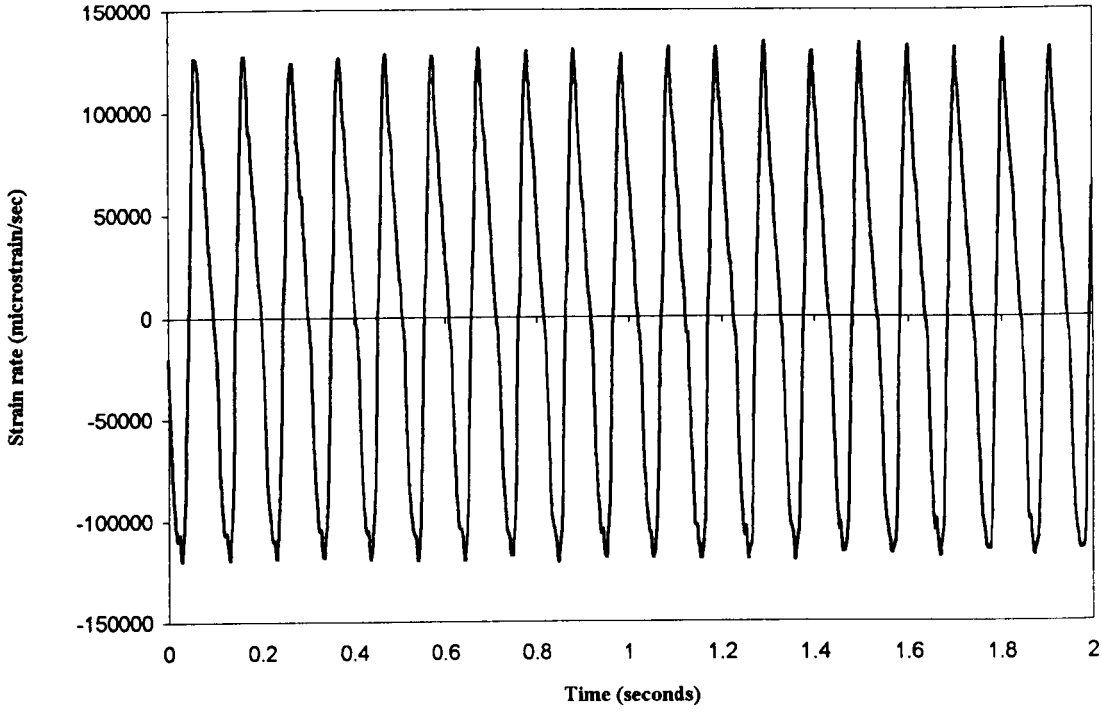

Figure A.1.4
Strain rates during axial loading at 10 Hz

A.1.3 Description of the ulnar mechanical loading apparatus

Figures A.1.5a & A.1.5b show the loading device and a rat during loading. Each anaesthetized rat was placed on its back and its flexed elbow and carpus were positioned in two nylon cups that were lined with rubber. One cup was connected directly to the 100 N strain gauge S-beam load cell (model TW750, Transducer World, Aylesbury, U.K.). This had the advantage that there were no frictional losses and therefore load was measured directly. This would have minimised systematic errors in loading at low load magnitudes. A strain gauge load cell was chosen in preference to a piezo electric load cell because the latter had been found previously to be very susceptible to temperature-dependent drift which arose from draughts etc. The load cell output was connected to a custom built amplifier which was calibrated to an output of 10 N per volt. Load was read from a cathode ray oscilloscope (Tektronix model 5111, Tektronix UK Ltd., Bucks, UK) The other nylon cup was milled out of a six cm long nylon rod which was connected to the ram of a custom-made servo-hydraulic actuator (Dartec, Stourbridge, UK). The rod passed through a nylon sleeve so that any bending was minimised during loading. This helped to maintain true axial loading of the rat antebrachium.

The movement of the servo-hydraulic actuator was controlled using the Dartec control panel. Frequency could be adjusted and the number of cycles could be preset by means of a manual counter. The actuator displacement amplitude and offset could be adjusted manually by means of two potentiometer dials. These controlled a linear voltage displacement transducer (LVDT) attached to the actuator. The loading was always performed using the Dartec in 'position control'. This meant that the actuator displacement characteristics were determined by the LVDT potentiometers. During loading, unless these were adjusted manually, the displacement would remain constant. However, it was necessary to control to a high degree of accuracy, the conditions of the applied axial load. Unfortunately the load conditions did not remain the same, despite constant displacement, due to laxity of the soft tissues. The ability to program precise loading-force parameters would have required a computer controlled 'load-control' facility. This was not available and was a disadvantage of this

apparatus. It meant that the displacement offset and amplitude had to be adjusted constantly by the operator during the entire duration of each loading session. This represented a significant source of potential operator error. For this reason, the same operator controlled the Dartec throughout the duration of each experiment.

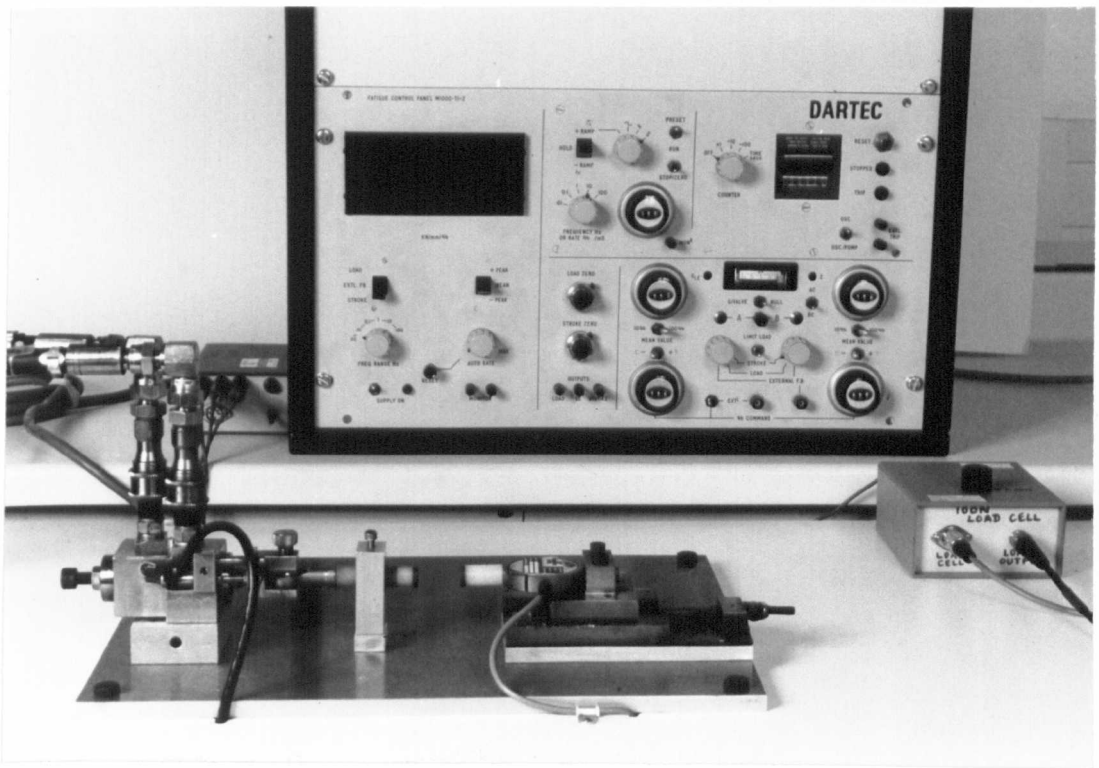

Figure A.1.5a
Photograph of the loading device and the Dartec control panel

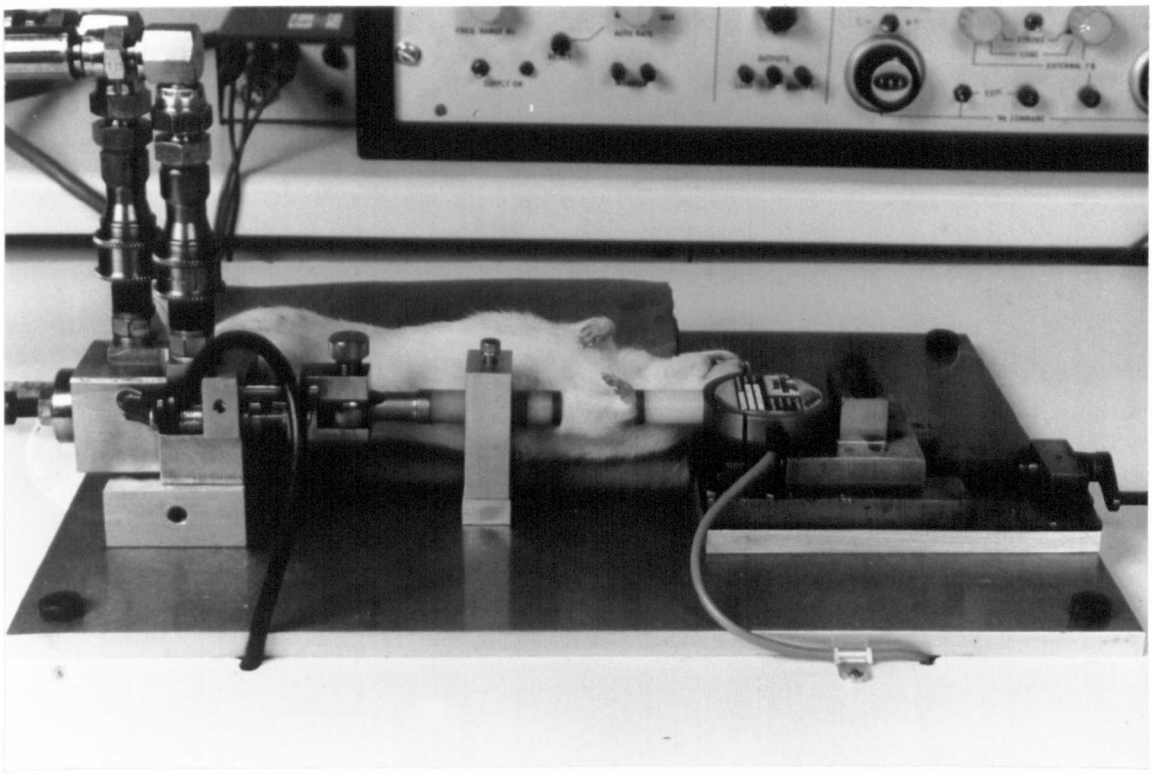

Figure A.1.5b
Photograph of the loading device during
a period of loading with a rat in position

A.1.4 Preparation of the methylmethacrylate (MMA) resin

1. Resin for infiltration

Methylmethacrylate (Sigma, USA) was washed three times in 5% NaOH solution for one hour on each occasion in a separating funnel. The NaOH was removed with three washes of distilled water. It was then dried by running the solution through $CaCl_2$ three times. To 90 mls of the washed methylmethacrylate was added 12 mls of dibutyl phthalate (Sigma, USA) and nine mls of polyethylene glycol (Sigma, USA). This solution was used for infiltrating the bones prior to polymerisation.

2. Resin for polymerisation

For the polymerisation process liquid resin was prepared as described above and to this solution was added 1.5 g of dried benzoyl peroxide (Sigma, USA), to act as a catalyst for the polymerisation process.

A.1.5 Infiltrating and embedding the ulnae in methylmethacrylate resin

The antebrachii were removed by disarticulation at the elbow joint. The muscles were carefully blunt dissected free from the bones taking great care to avoid damaging the periosteum. They were then placed in 70% ethanol. The bones were left in this for four days. Thereafter the bones were placed in ascending concentrations of ethanol every four days (80%, 90%, 100%) After being in 100% ethanol for a month the ethanol was replaced with fresh 100% ethanol in which they remained for a further month. After this time they were placed in methylmethacrylate prepared for infiltration. The laborious process of dehydration was essential because water could have adversely affected polymerisation of the methylmethacrylate resin, resulting in opaqueness and failure of the resin to harden fully.

The bones were placed in sealed glass tubes containing the liquid resin for two months to allow sufficient time for the infiltration process. During this time the

tubes were stored in the dark in a refrigerator (4°C) to prevent premature polymerisation.

After two months the bones were placed into resin for polymerisation. The bones and liquid resin were placed on a window sill at room temperature, but out of direct sunlight, for several days until the curing process was complete. A combination of ultraviolet light and heat promotes the curing process. Direct sunlight does speed up the process but can result in mass production of bubbles in the polymerised block. Also, if the resin cures too quickly the process can be so violent that small bones can fracture.

A.1.6 Chilling

The method of rapid freezing in n-hexane (Low in aromatic hydrocarbons, BDH, UK) chilled with industrial methylated spirit (IMS) and dry ice (figure A.1.6) has the advantage over liquid nitrogen in that there is no ice crystal formation within the tissues (Chayen *et al* 1973; Chayen and Bitensky 1991). When the tissue is placed in liquid nitrogen, a layer of insulating bubbles form around the specimen. This reduces the rate of freezing so that ice crystals form which damage the specimen because of disruption of lipid-protein complexes and cellular rupture.

A.1.7 Mounting of the antebrachium in preparation for cryosectioning

A block of aluminium 6 cm high x 6 cm x 3 cm was milled to form a well 1 cm deep x 3.5 cm x 1 cm. At room temperature, sufficient 10% PVA solution was placed into the well to fill it to a depth of approximately 5 mm. The aluminium block was then placed into a shallow chilling bath, made up of dry ice and IMS (figure A.1.7). As the PVA in the well began to solidify the antebrachium was placed into the well which was then filled to the top, so that the tissue was completely covered with PVA. It took another 30 seconds to one minute for the PVA to solidify, after which the block was placed on a hot plate. As the

well warmed up the PVA block containing the tissue could be removed. The block was then placed at a temperature below freezing so that the PVA did not thaw. The next step was to mount the blocks onto the brass microtome chucks. At room temperature, a little liquid PVA was placed onto the grooved surface of the chuck. The chuck was then placed in the shallow chilling bath until the PVA started to solidify. At this point, the block was placed distal end down into the PVA on the surface of the chuck, until the PVA started to set (figure A.1.8). Extra support was provided by pipetting additional PVA around the base of the block. Once completely solid, the block was ready for trimming. Prepared blocks were stored at -80° C until ready for cutting.

Sectioning from such blocks must be performed at temperatures below -30° C, otherwise friction generated during cutting can melt the tissue which then re-freezes and results in excessive tissue damage. Once the section has been cut, a glass slide at (room temperature) opposed to the knife causes the section to jump across onto the slide. During this process, it undergoes flash-drying. Chayen (1980) showed that such sections demonstrated the same sensitivity in bioassays as the original tissue.

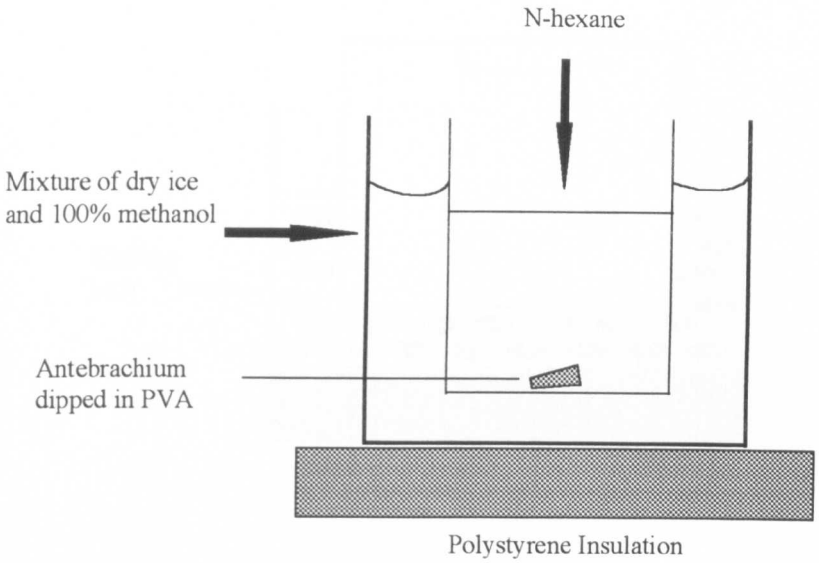

Figure A.1.6
Diagram illustrating the chilling bath for the preparation of the bones for cryostat sectioning.

The snap-frozen specimen was removed using forceps which had been kept cold in dry ice. This prevented the specimen from sticking to the forceps.

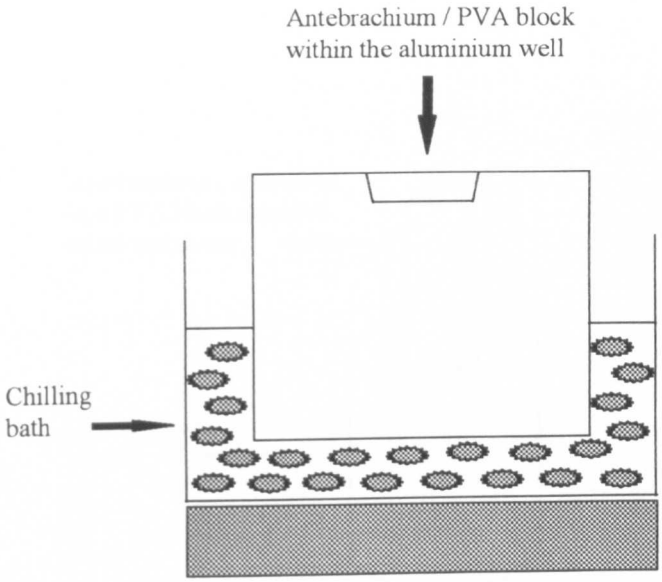

Figure A.1.7
Schematic of the aluminium block used to embed the antebrachii in 10 % PVA

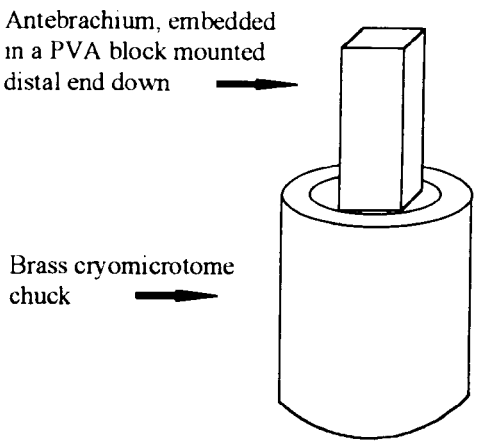

Figure A.1.8
Schematic of a PVA-embedded antebrachium mounted on a brass microtome chuck

A.1.8 Technique for demonstrating TRAP activity

A) First the TRAP stock solution was made up:

1. 100 mg of naphthol AS BI phosphate was dissolved in 1 ml on N,N dimethylformamide.
2. This was added to 199 ml of 0.25 M citrate acid buffer at pH 4.5.
3. 10 mM (0 4 g/200 mls) sodium tartrate was added.
4. The solution was stored at 4° C.

B) Reaction method:

1. The sections were incubated at 37° C for 10 minutes with the TRAP stock solution.
2. The sections were then rinsed in cold distilled water.
3. 1 mg/ml of fast Garnet GBC salt was added to 0.1M acetate buffer (pH 4.5, 4° C).
4. The solution was filtered through filter paper and kept at 4° C and the sections were incubated in this second solution at 4° C for 5 minutes.
5. The sections were then mounted in glycerol and were ready for examination.

A.1.9 Microdensitometry

Microdensitometry was the technique used to calculate the intensity of the TRAP reaction at the medial periosteal surface of the bone sections.

The integrating microdensitometer was designed to measure the optical intensity of colouration within the field of a section. Its advantage is that the instrument can be used on a conventional microscope and unlike conventional spectrophotometry, the colouration does not have to be homogeneous throughout the section.

The instrument works by optically masking off the area of interest within a section. A beam of light which produces a spot of light smaller than the resolving power of the microscope then scans this area of interest. Because

the spot is so small, the area scanned is effectively homogeneous and can subsequently be measured by a spectrophotometer, after amplification with a photomultiplier. The device automatically integrates the results of all the spot measurements and gives an overall reading for the masked area. To produce an absolute measure which is comparable between different machines, it is necessary to calculate the Mean Integrated Extinction (MIE) of the field. This is achieved by subtracting the extinction value obtained by scanning a blank field and then dividing this figure by the extinction value obtained by scanning a neutral density of 1. The final result is multiplied by 100 and expressed as MIE x 100.

A requirement for accurate comparisons between sections is that the value of extinction is dependent upon the section thickness. To ensure that the section thickness is consistent, a number of sequential sections can be analysed. If the variation is low, it suggests that variation in section thickness is low.

Appendix 2

Appendix to chapter 4

A.2.1 Fluorochrome labels

Chemical agents (fluorochromes) can be given which incorporate into newly mineralising bone fronts. When histological sections are examined under the appropriate wavelength of ultra violet light, the incorporated fluorochrome fluoresces. If two or more fluorochromes are administered at timed intervals, the distance between the two labels can be measured in a process called dynamic histomorphometry, to calculate the rate of new bone apposition. Inter-label distance, length of single and multiple labels, areas between labels etc. can all be used to calculate parameters of bone formation and resorption. When fluorochromes are used, the minimum dose required to produce a fine, well defined label should be administered. Also, the fluorochrome should not be toxic either systemically to the animal or to the bone cells.

Three fluorochromes were used in this experiment: calcein, xylenol orange and oxytetracycline.

Table A.2.1 Table giving details of the fluorochrome preparation & doses.

Fluorochrome	Preparation	Dose
Calcein	1 g calcein (Sigma, UK) + 2g $NaHCO_3$ dissolved in 100 ml sterile water. It is passed through a 0.22 micron filter and stored in the dark at 4°C.	1.5 ml/kg
Xylenol - orange	9 g of xylenol orange (Sigma) are dissolved in 80 ml of sterile water. The pH is adjusted to 7.2-7.4 with HCl. The total volume is then made up to 100 ml with sterile water. This is then passed through a 0.22 micron filter and stored in the dark at 4°C.	1.0 ml/kg
Oxytetracyline	Terramycin Q50 (Pfizer Ltd., UK), 50 mg/ml	0.4 ml/kg

A.2.2 Surgical techniques

Ovariectomy

The rats were blood sampled after anaesthesia with xylazine and ketamine. An area approximately 5 cm long x 4 cm wide centred on the spine and caudal to the thoraco-lumbar junction was clipped and prepared for aseptic surgery. Bilateral ovariectomy was performed through a single mid-line skin incision. The ovary on each side was exteriorised through a small opening formed in the lateral abdominal muscles on that side by blunt dissection. The ovarian pedicle was clamped with fine haemostats. A second pair of haemostats were used to clamp directly below the first pair and the ovary was removed by rotating the upper pair of clamps through 360 degrees. Haemostasis was achieved by the effect of tearing and crushing the blood vessels. The defect in the muscle was closed by a single interrupted suture of absorbable, synthetic 4/0 coated, braided polyglactin 910 (Vicryl, Ethicon). After closure of both muscle defects, the skin was closed using 3/0 monofilament nylon. Calcein was injected before recovery.

Thyroparathyroidectomy

This surgical technique is used widely and described by Waynforth and Flecknell (1992). The rats were anaesthetised with xylazine and ketamine and a blood sample obtained. The rats were placed on their backs and a support made out of a 5 ml syringe case was placed under the rats' neck to elevate the throat. Hair was clipped away from the throat and the area prepared for aseptic surgery. A midline incision 2 cm long was made from the sublingual region caudally towards the thoracic inlet. The sternocephalicus and under-lying sternohyoideus were divided along the midline by blunt dissection to expose the trachea and thyroid gland (figure A.2.1). The sternothyroideus was freed completely from the thyroid gland by blunt dissection. The thyroid gland was then picked up with very fine, plain-tipped ophthalmic forceps. Using a one inch 20 gauge hypodermic needle, the thyroid gland together with the parathyroid glands were dissected free of the trachea. The parathyroid glands could sometimes be seen as pale cream/grey structures in the cranial poles of

the thyroid glands (figures A.2.2 and A.2.3). Care had to be taken to avoid damaging or stretching the recurrent laryngeal nerves laterally, which were only just visible with the naked eye (Hirsch *et al* 1963). Sometimes, a dissecting microscope was required to visualise fully all the anatomic structures. The divided muscle groups were left to heal without stitching. The skin wound was then closed by suturing the skin with 4/0 silk. Upon recovery, the rats were observed closely for signs of stridor, indicative of recurrent laryngeal nerve injury or shaking and trembling, signs of hypocalcaemia, due to the parathyroidectomy.

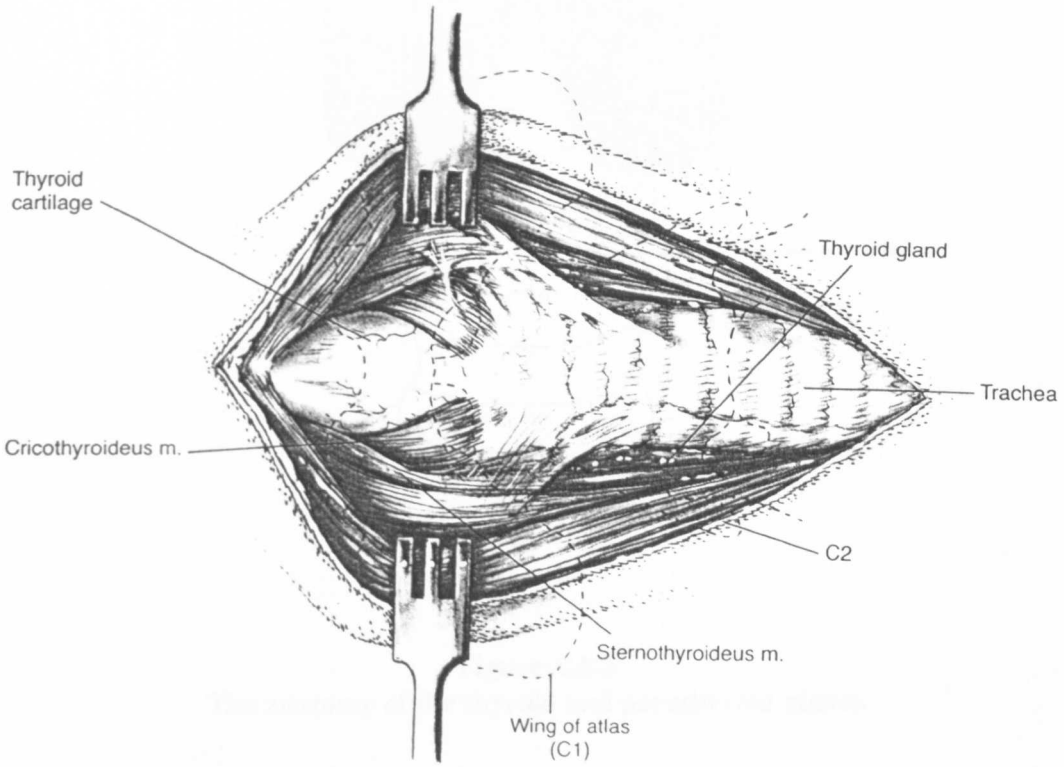

Figure A.2.1
Diagram showing the surgical anatomy
for the thyroparathyroidectomy procedure

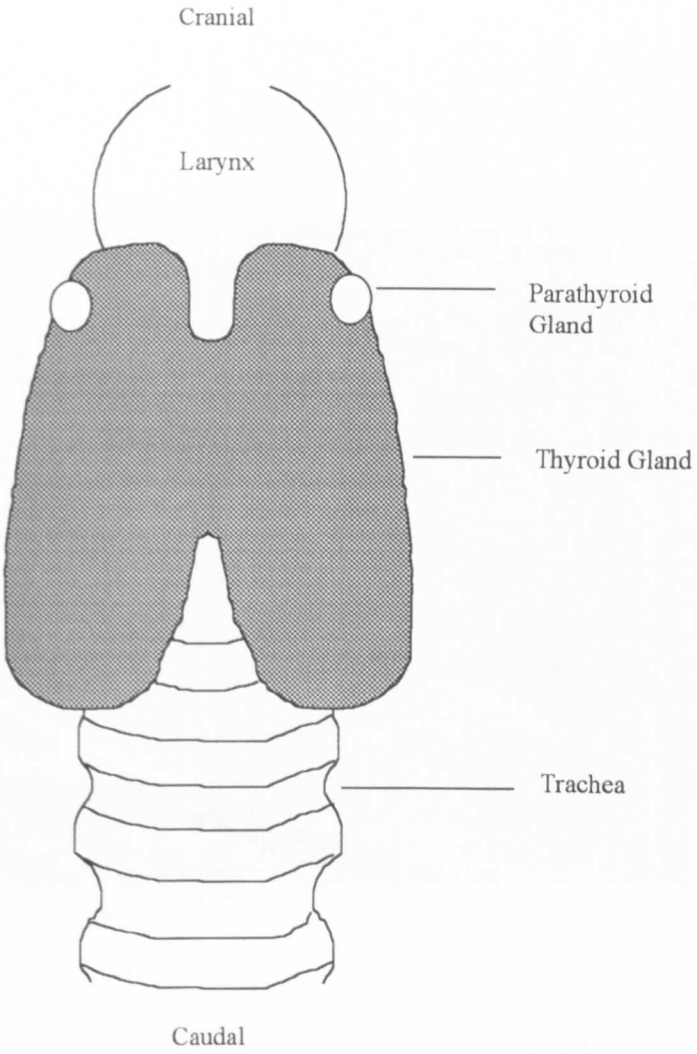

Figure A.2.2
The anatomy of the thyroid and parathyroid glands

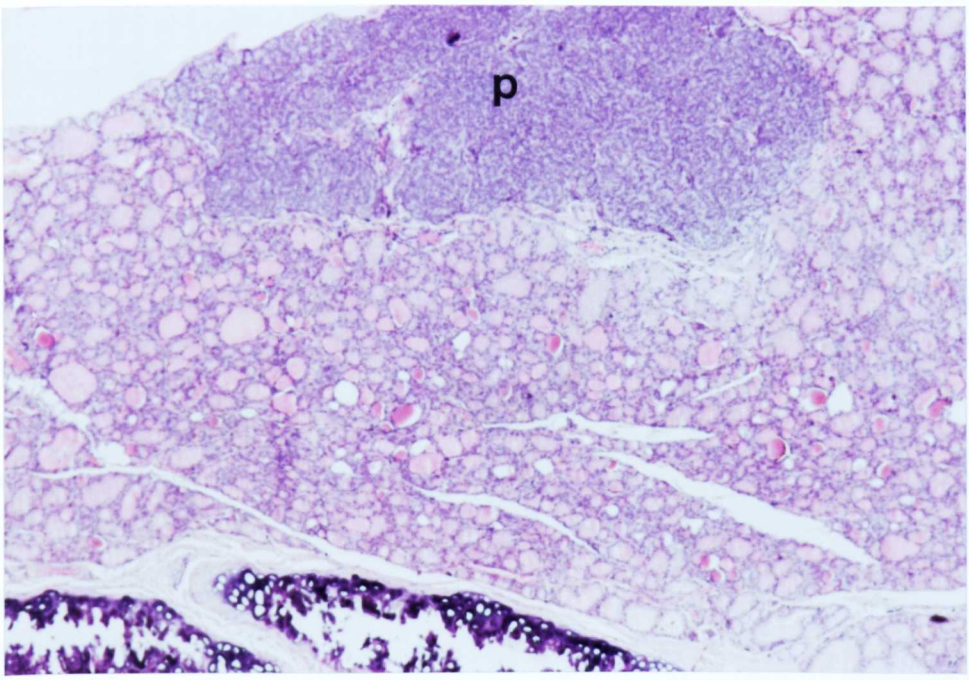

Figure A.2.3
Photograph of an H&E stained section of rat thyroid gland showing one of the parathyroid glands (P)

A.2.3 Mechanical tests of bones

Introduction

The comparison of ultimate strength between different whole bones is a useful way of assessing the effects of drugs and metabolic disturbances on the bone's material and structural properties. There are several basic configurations which can be used to perform the mechanical tests (figure A.2.4). In addition, there are other variables which can alter the results obtained for any given test configuration used. These are: specimen size, specimen orientation, history of hydration state, the current state of hydration, strain rate used during the testing procedure, previous loading history and temperature. Freezing may also be important particularly if the bone undergoes repeated freeze-thaw cycles. It is more likely to affect trabecular bone than cortical bone because ice crystals could disrupt the trabeculae. Rapid freezing may also adversely affect large bones because differential rates of freezing in various parts of the specimen may alter the bone architecture and affect the mechanical properties (Brinckmann *et al* 1988). Comparisons can only be made if the whole bones or bone samples are tested in the same configuration and all the variables are identical. A review article by Reilly and Burstein (1974) summarise the effects of these configurations and variables when making comparisons in the material properties of machined bone specimens. Burstein and Frankel (1971) and Currey (1970) consider mechanical testing of whole bones. Burstein and Frankel describe five criteria they consider when testing a whole bone:

1. Testing to produce failure similar to *in vivo* fractures.
2. Equal loading conditions are produced along the entire bone length so that the weakest part of the bone is identified.
3. The loading mode should not be too dependent on the bone geometry, in particular, bone length.
4. Testing should be controlled and reproducible and the conditions should be representative of normal trauma.
5. The testing method should be cheap and simple.

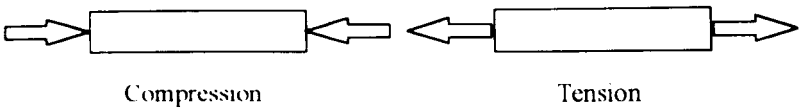

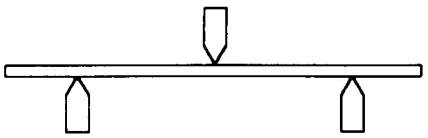

3 - point bending

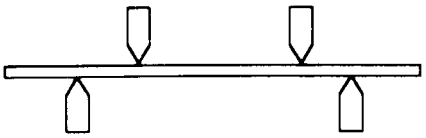

4 - point bending

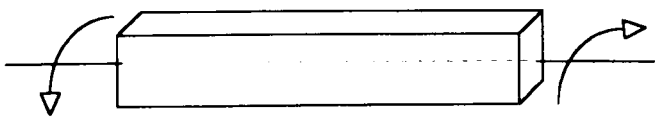

Torsional testing

Figure A.2.4
Configurations for mechanical strength testing of whole bones

Testing configurations for whole bones

I Axial Compression / Tension Tests

Applying true axial compression is difficult because it requires that all contact points between the bone mounts and test machine are completely and symmetrically in contact. In tension it is difficult to support equally the bone or bone specimen over its entire surface in the mounts. Neither are representative of failure in many bones, particularly long bones *in vivo.*

II Three-Point Tests

This is a way of mechanically assessing the material properties of a structure in bending. This means that the bone is tested in compression and tension. It is suited to long bones because of their shape. The apparatus is simple and cheap. Its disadvantages are that:

1. The maximum bending moment occurs at the single, central load point. Therefore, failure usually occurs at the level of contact with the point of the indenter, at the point of maximum tensile stress. In addition, the indenter may cause crushing and microcracks which provide a site for the initiation of failure. This means that unless the structure is highly uniform, the mechanical properties defined by this technique are highly site-specific and may not be representative of the bone as a whole. Therefore, consistent positioning is essential if comparisons are to be made.
2. Shape of the single contact point has a major bearing on the results because if sharp, it tends to deform the material at the point of contact and affect structural properties.

III Four-Point Tests

Advantages of four-point tests are that the bending moment produced is constant over the distance between the two inner contact points and therefore mechanical properties defined by this technique are less site-specific. However, it is less suited to smaller structures compared with three point testing.

IV Torsional Tests

Torsional tests load a bone in shear and are better suited to larger, non-uniform structures. Its advantage is that it produces a fairly constant shear stress over the entire cross-section of the structure and is better at testing the overall structural properties of a whole bone because it fulfills all five of the criteria (Burstein & Frankel 1971). The main disadvantages of this technique are that it requires the most complex apparatus. Bones that are small, highly non-uniform or vary greatly in length are not suitable.

Rat Vertebrae

It has been documented that changes in the lumbar vertebrae of rats can take up to nine months to become apparent (Wronski *et al* 1989). Assessment of the mechanical properties of rat vertebrae are difficult practically because of the size and shape of the bones. The vertebral bodies are small and are only symmetrical in the sagittal plane. In order to assess the bones as they would be loaded *in vivo* would require testing of intact motion-segments in compression. Their size makes this impracticable, so individual vertebral bodies must be tested in compression. Even then, this is made difficult by having end-plates which are neither parallel to one another and are not perpendicular to the long axis of the body. Salem *et al* (1989) described vertebral body mechanical compression tests where the end plates were trimmed down so that they were both parallel to each other and were also perpendicular to the long axis of the body. An advantage of this approach is that it facilitates reproducibility, however, it may not be representative of the bones' structural mechanical properties *in vivo*. In addition, trimming the end plates may actually fracture trabeculae within the medullary cavity and affect strength.

Advantages of the system of mechanical compression testing used in this experiment were:

1. The vertebral body was kept intact.
2. The enclosed apparatus prevented dehydration of the bones.

3. The end plates were fully supported by the dental plaster, which set quickly, was hard and very strong.
4. The curing process, although exothermic did not produce much heat. This was likely to be due to the small volume of plaster used and the heat sink properties of the brass cups. High temperatures could have affected the material properties of the bone because of dehydration.

Disadvantages were that the preparation of the bones and mounting were slow. Also, great care had to be taken to ensure that the mounting was as consistent as possible by ensuring:
1. That all air bubbles had been removed from the plaster before mounting. If not, high compressive loads could have resulted in collapse of regions of the supporting plaster. This was seen in several test bones which upon collapse of the plaster ended with the vertebral bodies rotating.
2. A consistent seating depth of the endplates.
3. That the body was as vertical as possible.

Consistency was ensured by practicing first with other bones. Any air bubbles were removed by firmly tapping the brass cases, filled with wet plaster, on a bench surface before starting to mount. The seating depth was kept to a minimum so that each bone was just supported in the plaster. Alignment was adjusted by eye. It was not difficult to keep the bones upright providing the plaster was made up to a thick consistency, which also reduced the time required for the plaster to set. Once set the bone could be sprayed with saline without affecting the properties of the plaster.

Rat Radii and Ulnae

The radii and ulnae were tested in a three-point bending system because they were too small to test reliably in either a four-point bending system or in torsion. It was easy to mark the mid-shaft of each bone with a pencil after measuring it then place it in the jig in the same orientation every time. The bones were placed such that the medial periosteal surface was in contact with

the middle indenter. The compression test bent the bone such that the bones' natural curvature was exacerbated. The reason for choosing this configuration was that the bone would be more likely to fail as a result of increasing, rather than reversing, its natural curvature *in vivo*.

A.2.4 Principles of Quantitative Computed Tomography

General introduction

Computed tomography (CT) is the process of production of cross-sectional images using x-rays images which are reconstructed using complex computer algorithms.

When x-rays pass through a tissue, the radiation undergoes absorption and scatter. Alternatively, the x-ray beam is described as being attenuated. The degree of attenuation is dependent on the atomic number of the tissue components and the tissue thickness. The higher the atomic number and the thicker the tissue, the greater the degree of attenuation. Air produces the lowest attenuation, followed by fat, then muscle and finally bone results in the highest attenuation. The thicker the bone and the higher its mineral content, the higher the attenuation. The degree of attenuation produced by a tissue is termed its linear attenuation coefficient.

A CT scanner incorporates an x-ray tube which rotates around the specimen. Instead of producing a latent image on radiographic film, the xrays having emerged from the specimen fall onto detectors. These may be xenon gas-filled detectors or scintillation crystals connected to photomultiplier tubes or photodiodes. The x-ray photons incident on the detectors result in an electrical signal whose magnitude is proportional to the energy of the x-ray beam.

The x-ray tube emits x-rays at a given start position then rotates a given angle then x-rays the specimen again. This process is repeated a number of times until a preset arc has been scanned. A computer stores all the data generated for each position scanned then performs algorithms to produce an image.

The image is made up of a matrix of small squares known as pixels. Each pixel is a two-dimensional representation of a block of the specimen. This block is called a tissue volume element or voxel. The dimensions of each voxel depend on the pixel size and the slice width of the scan. The smaller the pixels and the thinner the tissue slice scanned, the higher the resolution. A primary image is produced where each pixel is assigned a number (Hounsfield unit) which represents the linear attenuation coefficient of each voxel. To calculate the number, a scale is used This is known as the CT or Hounsfield scale. For example, the degree of attenuation produced by a voxel of pure cortical bone may be ascribed the number +1000 while that produced by air is ascribed a number of -1000. This scale includes every possible tissue type and therefore the 'window width' is wide The number given to any other pixel depends on the degree of attenuation produced by the tissue in its respective voxel. To increase sensitivity, the 'window width' can be reduced to only include linear attenuation coefficients of certain magnitudes ('window level').

The primary image is composed of a grid of numbers. For visual assessment, this would be difficult to interpret. Therefore, a grey scale is assigned to the CT scale. The grey scale ranges from black at one extreme to white at the other.

CT scanners used for whole body scans, where potentially any tissue type can be examined often require x-ray tubes which produce x-rays of dual energies. These are known as dual energy CT machines. This enables the machine to scan a wide range of tissues with very different linear attenuation coefficients. Each CT machine is calibrated with a standard calibration phantom.

The Stratec pQCT

This machine is designed for research. It utilises x-rays of a single energy. The reason for this is that the range of tissues likely to be scanned is very narrow, namely cortical and trabecular bone. Such machines produce higher precision (repeatability) than dual energy CT scanners.

Like all QCT scanners, it is not possible to scan specimens containing metal implants. Such implants cause 'streak artefacts'

The tibiae were placed in glass tubes filled with 70% ethanol. These were then held firmly in the machine's positioning device. After an initial scout view, three slices were scanned at seven, eight and nine mm from the proximal tibial condyles (tibial plateau). These positions had been determined following extensive characterization at Zeneca Pharmaceuticals (S. Breen, personal communication, 1995). They proved most sensitive at demonstrating changes in trabecular BMD.

The scans were performed at a resolution of 0.148 mm (voxel size: 0.148 x 0.148 x 1.000 mm^3). Trabecular bone mineral density (B.M.D.in mg cm^{-3}) was calculated using a COMAC European Forearm hydroxyapatite phantom to ensure correct calibration.

Analysis was performed with: 'Special Analysis Software version 5.1' (Stratec) using: contmode 2, peelmode 2 (threshold of 0.7), and cortmode 1. In the contmode 2 algorithm, low-attenuation (< 0.4) voxels outside the bone i.e. soft tissue were discarded. The remaining voxels (defined as 'Total') were then further segmented between 'cortical' (defined as: exceeding the threshold) and 'trabecular' (not exceeding the threshold).

Definition of the analysis terms

1. *Contmode*: This algorithm is used to 'remove' the soft tissues surrounding the bone. This algorithm automatically detects the outer bone edge and selectively eliminates all voxels with coefficients of attenuation below that of the cortical bone.

2. *Peelmode*: This algorithm uses an operator-defined threshold to remove the cortical shell, leaving only trabecular bone. A value of 0.7 had been chosen because this had proved the most accurate during evaluation trials at this site in

the tibia (S. Breen, Zeneca Pharmaceuticals, personal communication 1995). This meant that 70% of the outer area of the total bone area was peeled away.

3. *Cortmode*: This is the machine default setting for removing trabecular bone from the total bone. This just leaves the cortical envelope for analysis.

Partial volume effect

The computer algorithm assigns a value to each pixel after calculating the average coefficient of attenuation for its associated voxel. Problems arise when a voxel contains two tissue types with widely different coefficients of attenuation. The mean value can cause problems in defining the edge of the structure and is worse in the case of small structures with irregular outlines where the pixel dimensions cannot be reduced further in an attempt to increase the resolution. In these cases inaccuracies arise in the calculation of volume and BMD. It is a generally accepted problem in cortical bone parameters measured in rats (S. Breen, personal communication 1995; C. Jerome, Bowman Gray School of Medicine, North Carolina, personal communication 1996; G. Niemeyer, Stratec GmbH, Pforzheim, Germany, personal communication 1996). Partial volume artefacts can produce errors up to 20% of the true value for cortical bone parameters but are consistent for repeated measurements in longitudinal studies (J.A. Gasser, Sandoz Pharmaceuticals, Switzerland, personal communication 1996). The magnitude of the partial volume artefact is increased when small bones are scanned, especially where low resolution settings are used.

A.2.5 Histomorphometry of the calvarial bones

Bone removal and preparation

Immediately after killing the rats the calvariae were removed by cutting down the sagittal suture and laterally round the inter-parietal, parietal and caudal aspects of the frontal bones so that one complete half of calvaria, including one complete parietal bone, was excised. This was placed into 70% ethanol.

Every seven days the bones were placed into increasing concentrations of ethanol until they were in 100% ethanol. They were left in this for a week then the bones were placed into fresh 100% ethanol. After one further week, the bones were placed into methylmethacrylate solution for infiltration. The methylmethacrylate was prepared as described in appendix 1. After infiltrating for four weeks the calvaria were polymerised by placing them in glass vials suspended vertically using wooden cocktail sticks. Using a scalpel blade, the end of each cocktail stick was split so that the thin calvarial bone could be wedged into the split end. The bones were held as far away as possible from the sagittal suture (figure A.2.5).

Trimming the polymerised block ready for microtome sectioning

Once polymerised, the block of methylmethacrylate was removed by breaking the glass vial. The block was then trimmed down on a belt sanding machine so that the final block was approximately 1 cm x 1 cm x 2.5 cm in size. The face adjacent and perpendicular to the edge of the sagittal suture was trimmed so that the cut suture edge was covered by approximately 0.25 mm of methylmethacrylate. The block was then polished on a buffing wheel so that the bone could be visualised clearly when placed in the microtome to facilitate precise positioning.

Microtome sectioning the block

The block was placed in the clamps of the microtome (Reichert-Jung, model 2040, Germany) so that the bone was vertical and the flat plane of the plate of bone was perpendicular to the knife. The block was trimmed parallel to the sagittal plane of the calvaria in 2 micron sections starting at the sagittal suture and progressing laterally until the bone had been trimmed 2 mm from the sagittal suture (figures A.2.6 and A.2.7). At this point 5 micron sections were cut, stained with toluidine blue and mounted under cover slips. A distance of two mm was chosen after previously sectioning through calvaria, from and parallel to the sagittal suture to the mid-point of the parietal bone. From the suture to a distance 1.0 to 1.5 mm lateral to it, the bone on the endocranial surface was thicker than the bone at distances further from the sutures.

Generally, close to any of the sutures, the bone became increasingly porous (figure A.2.8). It was decided to sample at a site well away from the sagittal, coronal and lamboid sutures to ensure a representative assessment of the bone as a whole.

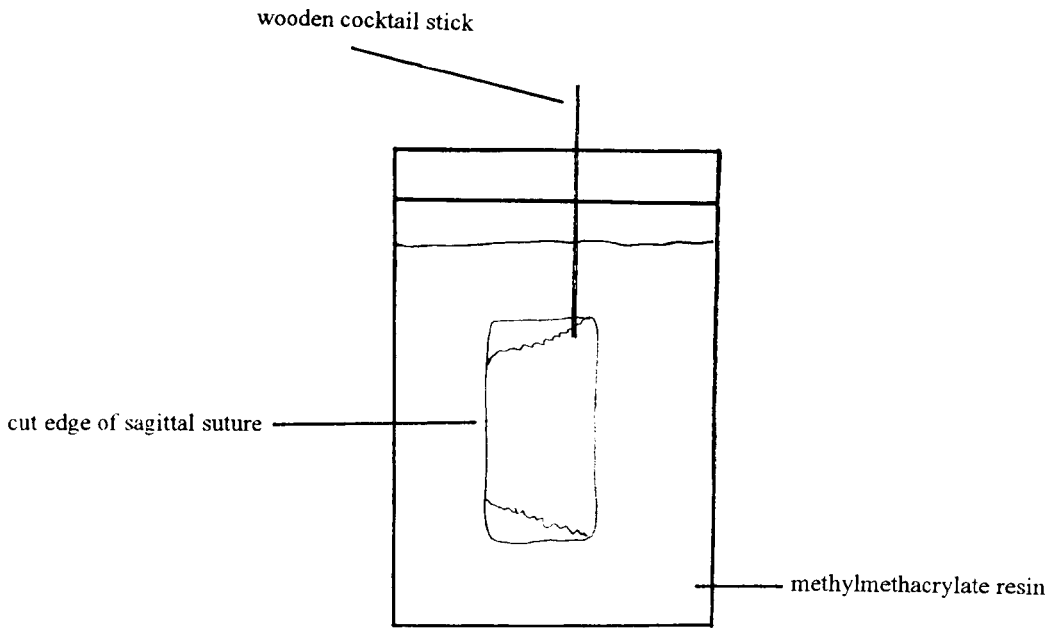

Figure A.2.5
Schematic showing how the calvariae were embedded in methylmethacrylate resin

2 mm

Figure A.2.6
Microradiograph of an adult rat calvaria.
The caudal part of the calvaria is at top of the photograph.

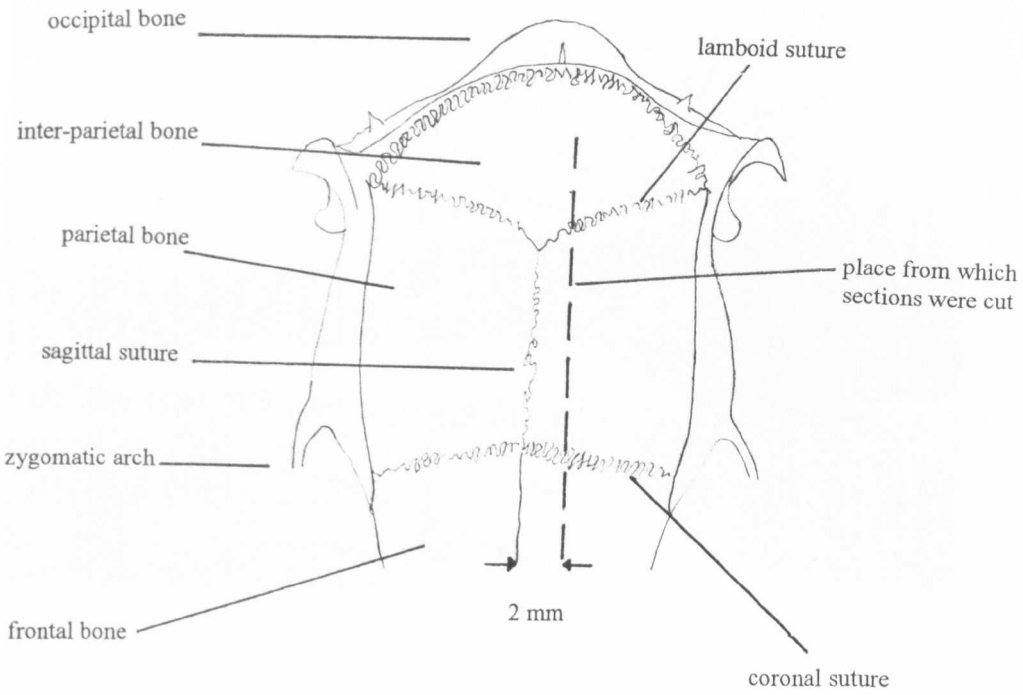

Figure A.2.7
Diagram showing the site from
which parietal bone sections were cut

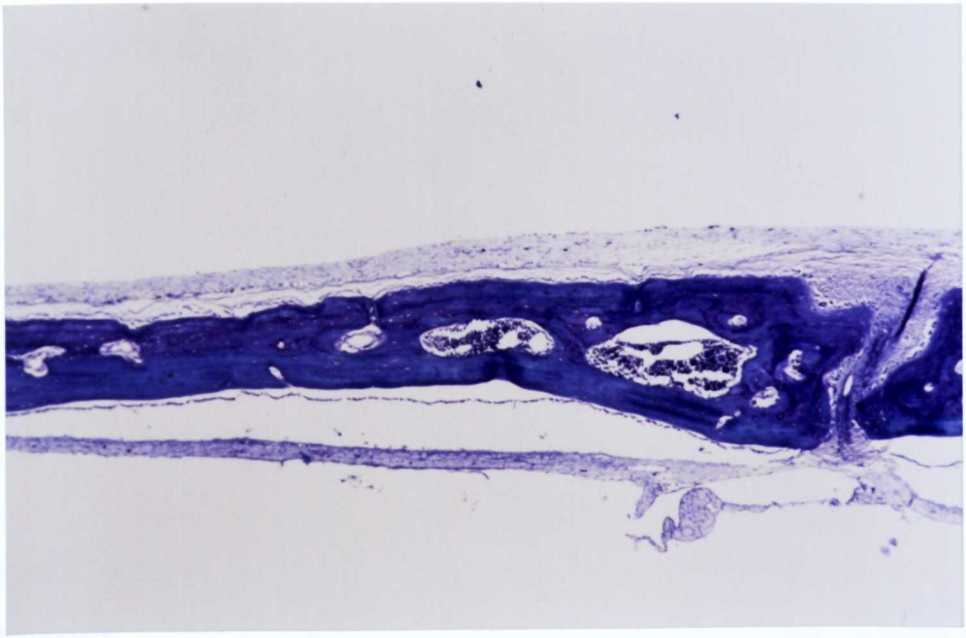

Figure A.2.8
Section of rat parietal bone cut perpendicular to the sagittal suture
to show how the porosity and thickness varies with distance from the suture,
which here, can be seen at the right hand side of the section.

Appendix 3

Appendix to chapter 5

A.3.1 Ethical committee approval

Before conducting this experiment, written approval had to obtained from Bristol Healthcare Trust Ethical Committee. Any human experiment or patient study requires such approval. If not obtained, it could jeopardise the chance of publishing the results in a scientific journal. The purpose of the ethical committee is to ensure that any experiment or study involving clinical patients or any human subjects has to be considered and approved before it can be conducted. This is to ensure that patient confidentiality is maintained, adequate safety precautions have been arranged and that all parties involved are informed and insured. Importantly, its purpose is also to ensure that there are logical grounds for performing the experiment. The forms are very long and in this case, it took approximately six months to obtain approval. This is partly because of the limited number of annual meetings held by the committee but also there were some major concerns about the safety of the procedure. Electrical safety and risk of osteomyelitis were the major concerns in this experiment.

A.3.2 Choice of strain gauges

Two different types of rosette gauges exist:

1. Stacked rosettes.
2. Planar rosettes.

Stacked rosettes (figure A.3.1) have all three gauge elements stacked on top of one another, whereas, the planar rosettes (figure A.3.2) have all three gauge elements situated in the same plane i.e. they are not stacked and are used to calculate principal strain information at a theoretical point. This being the point of convergence of the long axes of all three gauge elements. Both types of gauges have advantages and disadvantages:

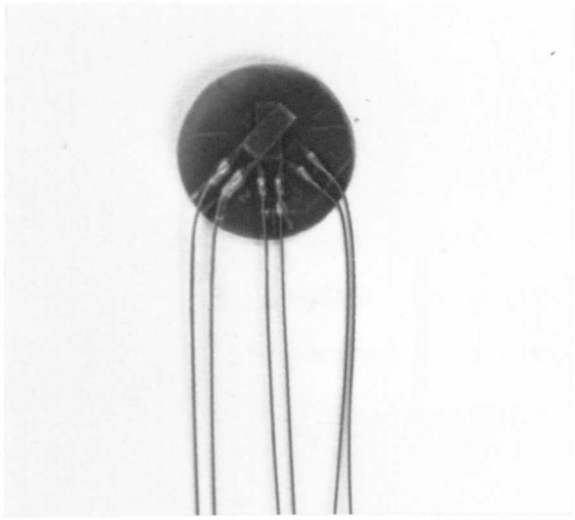

Figure A.3.1
Photograph of a stacked rosette strain gauge

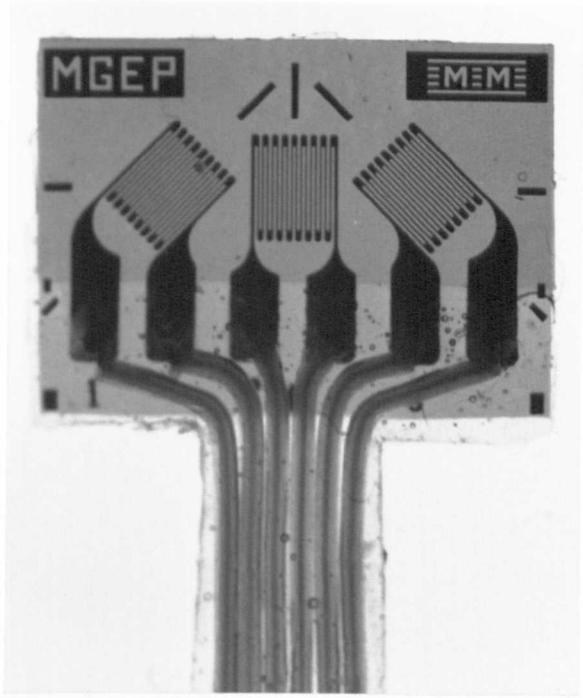

Figure A.3.2
Photograph of a planar rosette strain gauge

Stacked rosette

Advantages

a) Small surface area of the entire gauge, so it can be used on small bones.

b) Because all three gauge elements are stacked, they all measure strain at the same point on the substrate.

Disadvantages

a) Theoretically, the gauges are more susceptible to heating artefacts because of their apposition. This is a potentially more serious problem if high resistance (350 Ω) gauges and high excitation voltages are used. However, Biewener (1992) feels such heating effects *in vivo* are minimal.

b) Because the gauge elements are stacked, it is possible, theoretically, for shear through the depth of the stack to cause under-reading of strain by the uppermost gauge element.

c) The gauges tend to be less flexible than planar gauges and therefore may not conform very well to irregular surfaces.

Planar rosette

Advantages

a) These gauges are more flexible than stacked rosettes.

b) Less heating artefacts.

c) No shear effects because none of the gauge elements are stacked.

Disadvantages

a) The area of the gauge backing is relatively large, therefore, these are less suitable for small bones or small areas of bone.

b) All gauge elements are measuring strain at slightly different points on the bone surface. This may be significant if there is a steep strain gradient across the bone surface. Also, it is feasible that the gauge may be bonded only under one or two gauge elements. This would result in artefactual calculation of principal and consequently, shear strain magnitudes.

A.3.3 Preparation of the strain gauges

The strain gauges (Type EA-06-060RZ-120, Measurement Group, Basingstoke, UK) were soldered to fine (36 AGW) solid, insulated wires. Care had to be taken to prevent heat damage to the gauge. This was achieved by placing a small brass weight which acted as a heat-sink, onto the gauge element during soldering (figure A.3.3). The solder joints were coated using polyurethane (M-Coat A, Measurement Group, Basingstoke, Hants). The fine gauge wires were 6 cm long, i.e. just sufficiently long to emerge out of the skin and were soldered to a D connector (figure A.3.4). The purpose of minimising the length of these wires was because they were not shielded and could therefore pick up interference, which could have significantly altered the true strain signal. The gauges were wired up in a 3 wire, quarter bridge circuit (figure A.3.5). In a two wire quarter bridge circuit, the length of the lead wires connecting the strain gauges to the strain amplifier may introduce artefacts in the results because of the effects of lead and contact resistance (R_L and R_C respectively). It also reduces the system sensitivity. This can be overcome largely by the use of an additional lead in a circuit known as a 3 wire system and using as large a gauge resistance as possible (Pople 1979). There is only a small affect of R_{L3} and R_{C3} in the third lead. The connector could be separated into two parts which enabled convenient gauge sterilization by ethylene oxide.

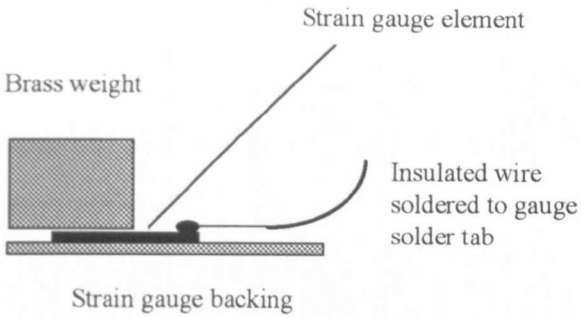

Figure A.3.3
Diagram to show the construction of the prepared strain gauge

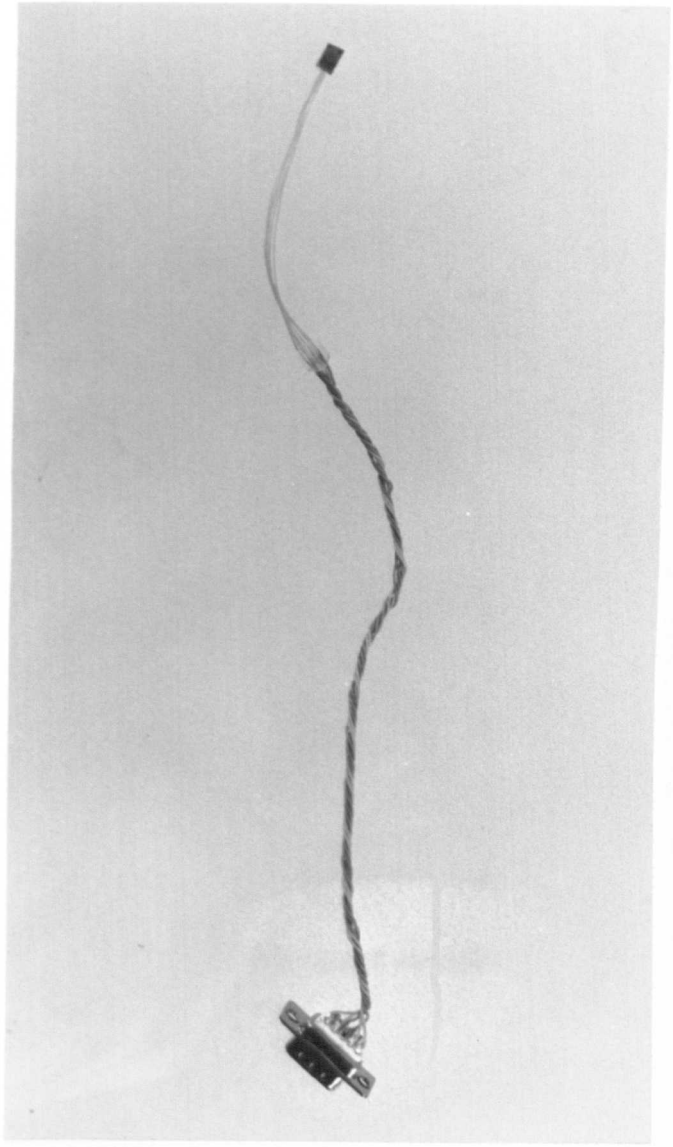

Figure A.3.4
Photograph of a planar strain gauge wired to a D-connector

Quarter bridge 2-wire system

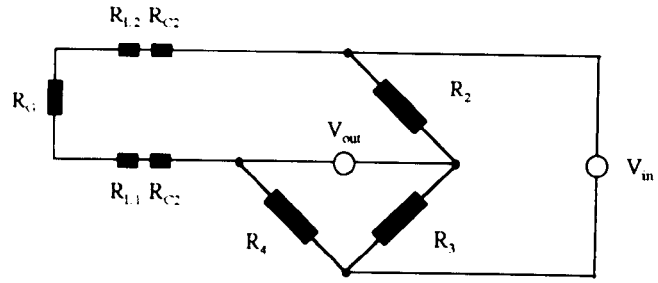

Quarter bridge 3-wire system

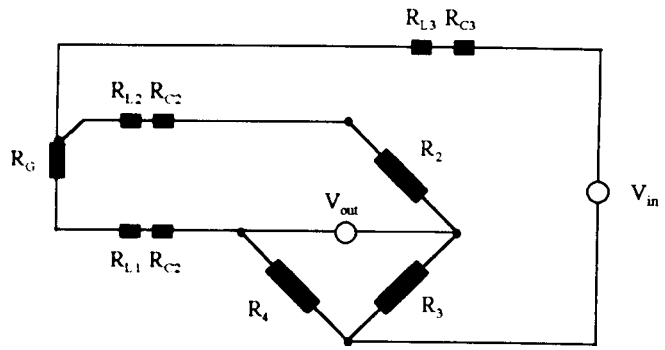

R_G is the strain gauge element
R_2, R_3 and R_4 are the internal resistors of the strain amplifier wheatstone bridge
R_L is the lead resistance
R_C is the contact resistance
V_{in} is the gauge excitation voltage
V_{out} is the voltage measured across the bridge

Figure A.3.5
Wiring diagram for the strain gauge circuit

A.3.4 Choice of adhesive

In engineering, cyanoacrylate monomer adhesives are used commonly for bonding strain gauges to the surface of their substrate. The monomer polymerizes in the presence of water and forms a strong bond between the gauge back and the substrate. In this experiment, an adhesive had to be chosen which was safe and would not biodegrade to release histotoxic compounds. In addition, the glue should have strong adhesive properties to faithfully transmit strain experienced at the surface of the substrate to the gauge grid, be easy to handle and polymerize rapidly.

Strain gauges have been applied to the bones of living animals for more than 50 years. Gurdjian and Lissner (1944) applied strain gauges to the parietal region of the skull in dogs using methyl methacryclate as an adhesive. However, it required two hours under a heat lamp to polymerise! It was only with the advent of cyanoacrylate 'superglues' that *in vivo* strain gauge studies of bones became a practical possibility. Cyanoacrylate monomers posses side chains. The length of these side chains determines the toxicity of the adhesive (Lanyon 1969; Hampel *et al* 1991). In the late 1950s methyl -2- cyanoacrylate was found to biodegrade to formaldehyde and methylacetate, which were histotoxic. It was found that monomers with longer side-chains were less toxic but possessed equal adhesive properties. Keller and Spengler (1982) suggest that isobutyl 2-cyanoacrylate may be better than ethyl-α-cyanoacrylate for prolonged use *in vivo* because the former degrades more slowly.

It was decided to use cyanoacrylate tissue adhesive (Histoacryl, B. Braun Melsungen AG, Melsungen, Germany) for bonding the gauges to the bone for several reasons. Firstly, the adhesive is licensed for human use and would therefore satisfy the ethical committee. Secondly, its successful use for bonding strain gauges *in vivo*, has been documented by Szivek *et al* (1992) in dogs and by Davies *et al* (1993) in horses.

A.3.5 Data capture

The signal from the strain gauges passed to the strain gauge amplifiers (model 2120A, Measurement Group, Basingstoke, UK) via five metres of shielded cable. Shielded BNC leads conducted the amplified signal to a custom built analogue to digital (A/D) box. From this box, the signal passed to a personal computer (Viglen 486DX, 33 MHz) and the data was collected using a 12-bit capture card (RTI-815, Analog Devices, Norwood, MA, USA) and custom software ('Sheepwalk', J. Leendertz, University of Bristol). Data was captured at either 50 Hz for low intensity activity or at 500 Hz for high intensity activity that involved impact loading.

All electrical equipment was electrically isolated from the mains electricity supply using an isolating transformer (type BBH TU250 safety transformer, BBH Coil & Transformer Manufacturing Company, Ltd., County Durham, UK).

A.3.6 Setting up the strain gauge amplifiers

Gauge excitation voltage was 1V and the amplifier output was calibrated using a dummy gauge to 1V/1000 μstrain.

A.3.7 Calibration of the gauges - simple cantilever beam calibration

A gauge, made up in an identical way to those used for *in vivo* implantation, was bonded onto a point along a uniform aluminium strip (figure A.3.6). Gauge placement was such that the central element was aligned exactly mid-width and so that its axis was parallel with the long axis of the strip. Cyanoacrylate (Superglue, Loctite, UK) was used to bond the gauge onto the strip after thorough cleaning and decreasing with an ether/chloroform mixture. The results obtained from theoretical calculation of the expected strain compared almost identically to the strain obtained from the middle gauge element/amplifier combination. This confirmed that the amplifier was correctly calibrated.

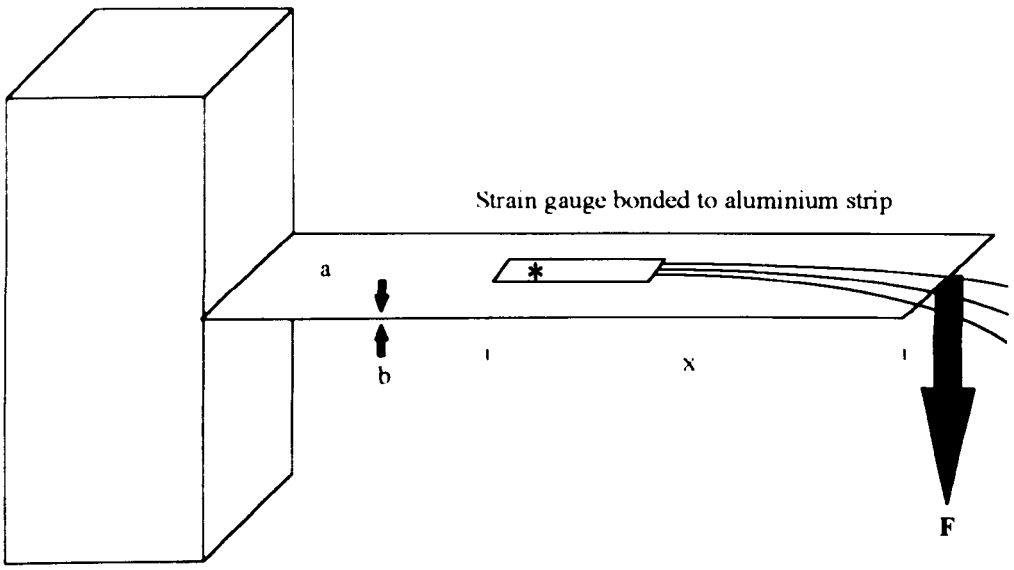

$$\textbf{Strain} = \frac{6Fx}{Eab^2}$$

Where
E = Young's Modulus of aluminium (Pa)
a = width of the aluminium strip (m)
b = thickness of the strip (m)
x = distance from the point of attachment of the gauge elements to the end of the strip (m)
* = strain gauge elements
F = applied load (N)

Figure A.3.6
Calibration of the strain gauge amplifiers

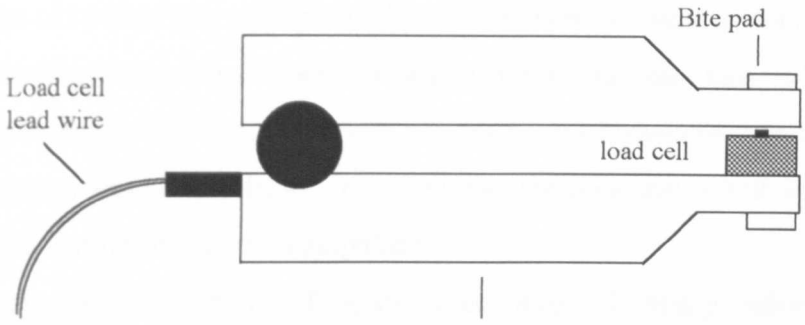

Biting onto the pastic bite pads compressed
the calibrated button load cell

Figure A.3.7
Schematic of the occlusal bite force device

A.3.8 Bite force measurements

Measurements of bite force were made by biting onto the plastic pads of a dental occlusal force meter (figure A.3.7). This was custom-made by the Regional Medical Physics Department, Sunderland District General Hospital, UK. The force generated between the pads compressed a small button load cell which was connected to an amplifier box. Its output was connected to the

computer which was used for the capture of the strain and force plate data. Calibration of the device was confirmed by hanging known masses from the plastic pads with the device held firmly in a clamp.

A.3.9 Suggestions for improving the strain measurement technique

1. Reducing the noise of the recording apparatus. The range of random noise was 8-10 μstrain. Lead wires were a possible source of this noise. However, the use of twisted pair wiring actually resulted in an increase in noise. Performing the experiment within a large Faraday cage may have helped to eliminate ambient noise but this was not practicable because a cage sufficiently big enough was not available. It is likely that the noise generated was an intrinsic feature of the strain amplifiers.

2. Increasing the sensitivity of the strain recording, allowing a higher resolution of strains. This would have been particularly beneficial with regard to the lower strains recorded in the skull. This could have been achieved by increasing the gain of the amplifiers, however, this may have amplified noise as well. In addition an improvement would have been possible by increasing the gauge excitation voltage and reducing the voltage range of the capture card. These adjustments in the system setup may have reduced the quantization of the low magnitude strain data recordings where A-D switch was evident at a resolution of 5 μstrain.

3. Recording at much greater frequencies. Generally, data should be sampled at a rate which is at least double the frequency expected (Niquist's formula). Often sampling rates of three to four times higher are used. A sampling frequency of 2 KHz may have been more appropriate in this experiment for the impact data. A useful guide for assessing the adequacy of sampling frequency is to ensure that there are at least three sampling points at the peaks of recorded data (J. Burn, University of Bristol personal communication). A single point means that higher values may have been missed. The use of inadequate sampling rates results in underestimates of both peak strain magnitudes and strain rates. This error is exaggerated for measurement of higher frequency data.

4. Incorporating a low pass filter before recording the data. This would have allowed frequency analysis of the strain data by fast fourier transformation. This would have been possible only if the sampling frequency was adequate.

5. Using a video camera to capture all details of the activities to enable a direct association to be made between a particular event and a specific strain recording.

6. The use of an increased number of gauges to allow a more thorough analysis of strain distribution.

7. Making recordings from more than one volunteer. Unfortunately, volunteers were not easy to find!

References

Aarden EM, Burger EH, Nijweide PJ. Function of osteocytes in bone. Journal of Cellular Biochemistry 1994;55(3):287-99.

Albright F, Bloomberg E, Smith PH. Postmenopausal osteoporosis. Trans Assoc Am Phys 1940;55:298-305.

Alini M, Kofsky Y, Wu W, Pidoux I, Poole AR. In serum-free culture thyroid hormones can induce full expression of chondrocyte hypertrophy leading to matrix calcification. J Bone Miner Res 1996;11(1):105-13.

Almaden Y, Canalejo A, Hernandez A, et al. Direct effect of phosphorus on PTH secretion from whole rat parathyroid glands in vitro. J Bone Miner Res 1996;11(7):970-6.

Au WYW. Calcitonin treatment of hypercalcemia due to parathyroid carcinoma: Synergistic effect of prednisolone on long term treatment of hypercalcemia. Arch Intern Med 1975;135:1594-1597.

Baggott DG, Lanyon LE. An independent 'post-mortem' calibration of electrical resistance strain gauges bonded to bone surfaces in vivo. J Biomech 1977;10:615-22.

Bargren JH, Bassett CAL, Gjelsvik A. Mechanical Properties Of Hydrated Cortical Bone. J Biomech 1974;7:239-45.

Baron R, Vignery A. Changes in the osteoclastic pools and the osteoclast nuclei balance after a single injection of salmon calcitonin in the adult rat. In: Meunier PJ, ed. Bone Histomorphometry. Paris: Armour Montagu, 1976:147.

Bassett CAL, Becker RO. Generation of Electric Potentials by Bone in Response to Mechanical Stress. Science 1962;137:1063-4.

Bassey EJ, Ramsdale SJ. Increase in femoral bone density in young women following high-impact exercise. Osteoporos Int 1994;4(2):72-5.

Becker KL, Monaghan KG, Silva OL. Immunocytochemical localization of calcitonin in Kulchitsky cells of human lung. Archives of Pathology and Laboratory Medicine 1980;104(4):196-8.

Becker RO. Electric Osteogenesis - Pro and Con. Calcified Tissue Research 1978;26:93-7.

Becker RO, Spadaro JA. Electrical stimulation of partial limb regeneration in mammals. Bull NY Acad Med 1972;48:627-41.

Behrents RG, Carlson DS, Abdelnour T. In Vivo Analysis of Bone Strain about the Sagittal Suture in Macaca mulatta during Masticatory Movements. J Dent Res 1978;57:904-8.

Bentolila V, Hillam RA, Skerry TM, Boyce TM, Fyhrie DP, Schaffler MB. Activation of Intracortical Remodeling in Adult Rat Long Bones by Fatigue Loading. (Orthop Trans. In press).

Berg BN, Harmison CR. Growth, disease and aging in the rat. J Gerontol 1957;12:370-7.

Biewener AA, ed. Biomechanics - Structures and Systems: A practical approach. 1st ed. v. 1. New York: Oxford University Press, 1992.

Biewener AA. Safety factors in bone strength. Calcif Tissue Int 1993;53(S1):S68-74.

Binstock ML, Mundy GR. Effect of calcitonin and glucocorticoids in combination in malignant hypercalcemia. Ann Med 1980;65:429-42.

Bouvier M, Hylander WL. In vivo bone strain on the dog tibia during locomotion. Acta Anat 1984;118(3):187-92.

Braidman IP, Davenport LK, Carter DH, Selby PL, Mawer EB, Freemont AJ. Preliminary in situ identification of estrogen target cells in bone. J Bone Miner Res 1995;10(1):74-80.

Brinckmann P, Biggemann M, Hilweg D. Fatigue fracture of human lumbar vertebrae. Clinical Biomechanics 1988 (Suppl. 1):S1-S23.

Broulik P, Kragstrup J, Mosekilde L, Melsen F. Osteon cross-sectional size in the iliac crest. Acta Pathol Microbiol Scand 1982;90:537-43.

Burkhart JM, Jowsey J. Parathyroid and Thyroid Hormones in the Development of Immobilization Osteoporosis. Endocrinology 1967;81:1053-62.

Burr DB. Remodeling and the repair of fatigue damage. Calcif Tissue Int 1993;53(S1):S75-81.

Burr DB, Milgrom C, Fyhrie D, et al. In vivo measurement of human tibial strains during vigorous activity. Bone 1996;18(5):405-10.

Burstein AH, Currey JD, Frankel VH, Reilly DT. The Ultimate Properties Of Bone Tissue: The Effects Of Yielding. J Biomech 1972;5:35-44.

Burstein AH, Frankel VH. A Standard Test For Laboratory Animal Bone. J Biomech 1971;4:155-8.

Burtis WJ, Wu T, Bunch C, et al. Identification of a novel 17,000-dalton parathyroid hormone-like adenylate cyclase-stimulating protein from a tumor associated with humoral hypercalcemia of malignancy. Journal of Biological Chemistry 1987;262(15):7151-6.

Calder A, Chilibeck P, Sale D, et al. Upper but not lower limb lateral asymmetry in lean mass and bone minerl density in young women. Med Sci Sports Exerc 1992;24:S45.

Carter D. Mechanical Loading History and Cortical Bone Remodeling. Calcif Tissue Int 1984;36:S19-24.

Casewell MW, Fennell RH. Supernumerary parathyroid structures in the neck and thymus of parathyroidectomised rats and their relationship to recovery from hypocalcaemia. Br J Exp Path 1970;51:197-202.

Casey ATH, Hayward RD, Harkness WF, Crockard HA. The use of autologous skull bone grafts for posterior fusion of the upper cervical spine in children. Spine 1995;20(20):2217-20.

Casez JP, Fischer S, Stussi E, et al. Bone Mass at Lumbar Spine and Tibia in Young Males - Impact of Physical Fitness, Exercise and Anthropometric Parameters: A Prospective Study in a Cohort of Military Recruits. Bone 1995;17(3):211-9.

Chambers TJ, Evans M, Gardner TN, TurnerSmith A, Chow JWM. Induction of bone formation in rat tail vertebrae by mechanical loading. Bone and Mineral 1993;20(2):167-78.

Cheng MZ, Zaman G, Rawlinson SCF, Suswillo RFL, Lanyon LE. Mechanical Loading and Sex Hormone Interactions in Organ Cultures of Rat Ulna. J Bone Miner Res 1996;11:502-11.

Cheng S, Toivanen JA, Suominen H, Toivanen JT, Timonen J. Estimation of Structural and Geometrical Properties of Cortical Bone by Computerised Tomography in 78 -Year-Old Women. J Bone Miner Res 1995;10, No. 1:139-48.

Chenu C, Pfeilschifter J, Mundy GR, Roodman GD. Transforming growth factor beta inhibits formation of osteoclast-like cells in long-term human marrow cultures. Proceedings of the National Academy of Sciences of the United States of America 1988;85(15):5683-7.

Chilibeck PD, Sale DG, Webber CE. Exercise and bone mineral density. Sports Med 1995;19(2):103-22.

Chow JWM, Jagger CJ, Chambers TJ. Characterization of osteogenic response to mechanical stimulation in cancellous bone of rat caudal vertebrae. American Journal of Physiology - Endocrinology and Metabolism 1993;265(2 28-2):E340-7.

Christiansen C, Riis BJ. The Silent Epidemic. Postmenopausal Osteoporosis. 1st ed. v. 1. Aalborg, Denmark: Handelstrykkeriet ApS, 1990. A Handbook for The Medical Profession.

Churches AE, Howlett CR, Waldron KJ, Ward GW. The Response of Living Bone to Time-Varying Loading: Method and Preliminary Results. J Biomech 1979;12:35-45.

Cochran GVB, Dell DG, Palmieri VR, Johnson MW, Otter MW, Kadaba MP. An improved design of electrodes for measurement of streaming potentials on wet bone in vitro and in vivo. J Biomech 1989;22:745-50.

Cole AA, Wezeman FH. Cytochemical localization of tartrate-resistant acid phosphatase alkaline phosphatase, and nonspecific esterase in perivascular cells of cartilage canals in the developing mouse epiphysis. Am J Anat 1987;180(3):237-42.

Currey JD. The Mechanical Adaptations Of Bones. 1st ed. v. 1. Guildford: Princeton University Press, 1984.

Currey JD. Changes In The Impact Energy Absorption Of Bone With Age. J Biomech 1979b;12:459-69.

Currey JD. Mechanical Properties of Bone Tissues With Greatly Differing Functions. J Biomech 1979a;12:313-9.

Currey JD. The mechanical properties of bone. Clin Orthop 1970;73:210-31.

Currey JD, Alexander RMcN. The thickness of the walls of tubular bones. J Zool, Lond 1985;206:453-68.

Danielsen CD, Mosekilde L, Svenstrup B. Cortical bone mass,composition,and mechanical properties in female rats in relation to age, long-term ovariectomy,and estrogen substitution. Calcified Tissue Research 1993;52:26-33.

Datta HK, Rathod H, McNeil CJ, Manning P, Turnbull Y. Parathyroid Hormone Directly Stimulates Superoxide Production by the Osteoclast. J Bone Miner Res 1995;10(Suppl. 1):S321.

Davies DT. Assessment of rodent thyroid endocrinology: Advantages and pit-falls. Comparative Haematology International 1993;3:142-52.

Davies HMS, McCarthy RN, Jeffcott LB. Surface strain on the dorsal metacarpus of thoroughbreds at different speeds and gaits. Acta Anat 1993;146(2-3):148-53.

Davies TS. Regional variation in the effects of ovariectomy on the skeleton. M.Sc. Thesis. University of Bristol, UK, 1995.

Deftos LJ. Calcitonin. In: Favus MJ, ed. Primer on the Metabolic Bone Diseases and Disorders of Mineral Metabolism. 2nd ed. New York: Raven Press, 1993:70-6.

Deftos LJ. Pituitary cells secrete calcitonin in the reverse hemolytic plaque assay. Biophys Research Commun 1987;146:1350-6.

Deftos LJ, Glowacki J. Mechanisms of Bone Metabolism. In: Kem DC, Frohlich E, eds. Pathophysiology. Philadelphia: JB Lippincott, 1984:445-68.

Dempster DW, Cosman F, Parisien M, Shen V, Lindsay R. Anabolic Actions of Parathyroid Hormone on Bone. Endocr Rev 1993;14, No 6:690-709.

Dempster WT, Liddicoat RT. Compact Bone As A Non-Isotropic Material. Am J Anat 1952;91, No. 3:331-62.

Dillaman RM, Roer RD, Gay DM. Fluid movement in bone: Theoretical and empirical. J Biomech 1991;24(S1):163-77.

Doty SB. Morphological evidence of gap junctions between bone cells. Calcified Tissue Research 1981;33:509-12.

Duncan CP, Shim S-S. The Autonomic Nerve Supply of Bone. J Bone Joint Surg (Br) 1977;59-B(3):323-30.

Eriksen EF, Mosekilde L, Melsen F. Kinetics of trabecular bone resorption and formation in hypothyroidism: Evidence for a positive balance per remodeling cycle. Bone 1986;7(2):101-8.

Eriksen EF, Colvard DS, Berg NJ. Evidence of estrogen receptors in normal human osteoblast-like cells. Science 1988;241:84-6.

Eriksson C. Electrical properties of bone. In: Bourne GH, ed. The Biochemistry and Physiology of Bone. 2nd ed. v. 4. New York: Academic Press, 1976.

Evans FG. Methods of Studying the Biomechanical Significance of Bone Form. Am J Phys Anthropol 1953;11:413-35.

Evely RS, Bonomo A, Schneider HG, Moseley JM, Gallagher JA, Martin TJ. Structural requirements for the action of PTHrP on bone resorption by isolated osteoclasts. J Bone Miner Res 1990;6:85-93.

Fawcett DW. The amedullary bones of the Floridan Manatee (Trichecus latirostris). Am J Anat 1942;71:271-309.

Fehling PC, Alekel L, Clasey J, Rector A, Stillman RJ. A Comparison of Bone Mineral Densities Among Female Athletes in Impact Loading and Active Loading Sports. Bone 1995;17:205-10.

Fell HB. Skeletal Development in Tissue Culture. In: Bourne GH, ed. The Biochemistry and Physiology of Bone. 1st ed. New York: Academic Press, 1956:401-41.

Fermor B, Skerry TM. PTH/PTHrP receptor expression on osteoblasts and osteocytes but not resorbing bone surfaces in growing rats. J Bone Miner Res 1995;10(12):1935-43.

Finkelman RD, Eason AL, Rakijian DR, Tutundzhyan Y, Hardesty RA. Elevated IGF-II and TGF-beta concentrations in human calvarial bone: Potential mechanism for increased graft survival and resistance to osteoporosis. Plast Reconstr Surg 1994;93(4):732-8.

Fischer JA, Born W. Calcitonin gene products: evolution, expression and biological targets. Bone and Mineral 1987;2(5):347-59.

Fox SW, Chambers TJ, Chow JWM. Nitric oxide is an early mediator of the induction of bone formation by mechanical stimulation. J Bone Miner Res 1995;10(Suppl. 1):S204.

Friedman J, Au WYW, Raisz LG. Responses of fetal rat bone to thyrocalctonin in tissue culture. Endocrinology 1968;82:149-56.

Frost HM. Bone "Mass" and The "Mechanostat": A Proposal. Anat Rec 1987;219:1-9.

Frost HM. The Regional Acceleratory Phenomenon: A Review. Henry Ford Hosp Med J 1983;31:3-9.

Frost HM. A determinant of bone architecture. The minimum effective strain. Clin Orthop 1983(175):286-92.

Frost HM. The Laws of Bone Structure. Springfield, Illinois: Charles C Thomas, 1964.

Frost HM. Bone modeling and skeletal modeling errors. Orthopaedic lectures ed. v. IV. Springfield, Illinois: Charles C Thomas, 1973.

Fujiyama K, Kirijama T, Ito M, Eijima E, Yokojama N, Nagataki S. Parathyroid Hormone has an Important Role in Postmenopausal High Turnover Bone Loss. J Bone Miner Res 1995;10, Supplement 1:S242.

Fukada E, Yasuda I. On the piezoelectric effect in bone. J Physiol Soc Japan 1957;12:1158.

Fukada E, Yasuda I. . J Appl Physiol 1964;3:117 (cited by Eriksson 1976).

Galileo. Mechanic, dialog 1 1638 (cited by S.P. Butler, PhD thesis, University of Bristol 1991).

Gallagher JC, Goldgar D, Moy A. Total Bone Calcium in Normal Women: Effect of Age and Menopause Status. J Bone Miner Res 1987;2:491-6.

Garcia-Ocana A, De Miguel F, Penaranda C, Albar JP, Sarasa JL, Esbrit P. Parathyroid hormone-related protein is an autocrine modulator of rabbit proximal tubule cell growth. J Bone Miner Res 1995;10(12):1875-84.

Garland DE, Stewart CA, Adkins RH, et al. Osteoporosis After Spinal Cord Injury. J Orthop Res 1992;10, No 3:371-8.

Gasser JA. Assessing bone quantity by pQCT. Bone 1995;17(4 S):145S-54S.

Goltzman D, Mitchell J. Interaction of calcitonin and calcitonin gene-related peptide at receptor sites in target tissues. Science 1985;227(4692):1343-5.

Goodship AE, Lanyon LE, McFie H. Functional Adaptation of Bone to Increased Stress. J Bone Joint Surg (Am) 1979;61(A):539-46.

Goulding A, Gold E. Estrogens and Progestogens Conserve Bone in Rats Deficient in Calcitonin and Parathyroid Hormone. Am J Physiol 1989;257:E903-8.

Grieg DM. Clinical observations on the surgical pathology of bone. Edinburgh: Oliver Boyde, 1931 (cited by S.P. Butler, PhD thesis, University of Bristol 1991).

Gros M. La disposition des nerfs des os. Bulletin de la Societe anatomique de Paris 1846;21:369-72 (cited by Duncan and Shim 1977).

Gross TS, McLeod KJ, Rubin CT. Characterizing bone strain distributions in vivo using three triple rosette strain gages. J Biomech 1992;25(9):1081-7.

Gunness-Hey M, Hock JM. Increased trabecular bone mass in rats treated with human synthetic parathyroid hormone. Metabolic Bone Disease and Related Research 1984;5(4):177-81.

Gurdjian ES, Lissner HR. Mechanism of head injury as studied by the cathode ray oscilloscope. J Neuroscience 1944;1:393-9.

Haapasalo H, Sievanen H, Kannus P, Heinonen A, Oja P, Vuori I. Dimensions and estimated mechanical characteristics of the humerus after long-term tennis loading. J Bone Miner Res 1996;11(6):864-72.

Hagaman JR, Ambrose WW, Hirsch PF, Kiebzak GM. Age-Related Changes in Rat Trabecular, Endosteal and Cortical Bone Demonstrated with Scanning Electron Microscopy. Cells and Materials 1991(Suppl. 1):37-46.

Hahn M, Vogel M, Amling M, Ritzel H, Delling G. Microcallus formations of the cancellous bone: A quantitative analysis of the human spine. J Bone Miner Res 1995;10(9):1410-6.

Hampel NL, Johnson RG, Pijanowski GJ. Effects of Isobutyl-2-cyanoacrylate on Skin Healing. Compendium on Continuing Education for the Practising Veterinarian (European Edition) 1991;13, No. 1:23-7.

Heaney RP. A unified concept of osteoporosis. Am J Med 1965;39:877-80.

Heaney RP, Becker RR, Saville PD. Menopausal changes in calcium balance performance. J Lab Clin Med 1978a;92:953-63.

Heaney RP, Becker RR, Saville PD. Menopausal changes in bone remodeling. J Lab Clin Med 1978b;92:964-70.

Heaney RP, Recker RR, Saville PD. Calcium balance and calcium requirements in middle-aged women. Am J Clin Nutr 1977;30:1603-11.

Hert J. Acceleration of the growth after decrease of load on epiphyseal plates by means of spring distractors. Folia Morph 1969;17:194-205.

Hert J, Liskova M, Landgrot B. Reaction of Bone to Mechanical Stimuli Part 1. Continuous and Intermittent Loading of The Tibia in The Rabbit. Folia Morph 1971(a);19:290-300.

Hert J, Liskova M, Landgrot B. Influence of the longterm continuous bending on bone. An experimental study on the tibia of the rabbit. Folia Morph 1969;17:389-99.

Hert J, Sklenska A, Liskova M. Reaction of Bone to Mechanical Stimuli Part 5. Effect of Intermittent Stress on The Rabbit Tibia After Resection of The Peripheral Nerves. Folia Morph 1971 (b);19:378-87.

Hietala EL. The effect of ovariectomy on peristeal bone formation and bone resorption in adult rats. Bone and Mineral 1993;20:57-65.

Hillam RA, Mosley J, Skerry TM. Regional Differences in Bone Strain. Bone and Mineral 1994;25(Suppl. 1):S32.

Hillam RA, Skerry TM. Inhibition of bone resorption and stimulation of formation by mechanical loading of the modeling rat ulna in vivo. J Bone Miner Res 1995;10(5):683-9.

Hillsley MV, Frangos JA. Osteoblast hydraulic conductivity is regulated by calcitonin and parathyroid hormone. J Bone Miner Res 1996;11(1):114-24.

Hirsch PF, Hagaman JR. Reduced bone mass in calcitonin-deficient rats whether lactating or not. J Bone Miner Res 1986;1, no. 2:199-206.

Horiuchi N, Caulfield MP, Fisher JE, et al. Similarity of synthetic peptide from human tumor to parathyroid hormone in vivo and in vitro. Science 1987;238(4833):1566-8.

Hume EL, Sutton DC, Perimutter MN, et al. Normalized bone mass and strength in exercising oophorectomized and sham operated rats. Orthop Trans 1989:289.

Humphry GM. A Treatise of the Human Skeleton. Cambridge 1858 (cited by Wolff 1892; Koch 1917).

Hylander WL. In vivo bone strain in the mandible of Galago crassicaudatus. Am J Phys Anthropol 1977;46(2):309-26.

Hylander WL. Stress and strain in the mandibular symphysis of primates: a test of competing hypotheses. Am J Phys Anthropol 1984;64(1):1-46.

Hylander WL, Picq PG, Johnson KR. Masticatory-stress hypotheses and the supraorbital region of primates. Am J Phys Anthropol 1991;86(1):1-36.

Hynes RO. Integrins: A family of cell-surface receptors. Cell 1987;48:549-54.

Ikegame M, Rakopoulos M, Zhou H, et al. Calcitonin receptor isoforms in mouse and rat osteoclasts. J Bone Miner Res 1995;10(1):59-65.

Ikegame M, Rakopoulos M, Martin TJ, Moseley JM, Findlay DM. Effects of continuous calcitonin treatment on osteoclast-like cell development and calcitonin receptor expression in mouse bone marrow cultures. J Bone Miner Res 1996;11(4):456-65.

Ikegami A, Inoue S, Hosoi T, et al. Cell cycle-dependent expression of estrogen receptor and effect of estrogen on proliferation of synchronized human osteoblast-like osteosarcoma cells. Endocrinology 1994;135(2):782-9.

Iwasaki K. Dynamic responses in adult and infant monkey craniums during occlusion and mastication. J Osaka Dent Univ 1989;23:77-97.

Jasani C, Nordin BEC, Smith DA, Swanson I. Spinal osteoporosis and the menopause. Proc R Soc Med 1965;58:441-4.

Jaslow CR, Biewener AA. Strain patterns in the horncores, cranial bones and sutures of goats (Capra hircus) during impact loading. J Zool, Lond 1995;235:193-210.

Jaworski ZFG, Uhthoff HK. Reversibility of Nontruamatic Disuse Osteoporosis During its Active Phase. Bone 1980;7:431-9.

Jee WSS, Mori S, Li XJ, Chan S. Prostaglandin E2 enhances cortical bone mass and activates intracortical bone remodeling in intact and ovariectomized female rats. Bone 1990;11(4):253-66.

Jee WSS, Ueno K, Deng YP, Woodbury DM. The effects of prostaglandin E2 in growing rats: Increased metaphyseal hard tissue and cortico-endosteal bone formation. Calcif Tissue Int 1985;37(2):148-57.

Jee WSS, Wronski TJ, Morey ER, Kimmel DB. Effects of Spaceflight on Trabecular Bone in Rats. Am J Physiol 1983;244:R310.

Jendrucko RJ, Hyman WA, Newell PH, Chakraborty BK. Theoretical Evidence For The Generation of High Pressure in Bone Cells. J Biomech 1976;9:87-91.

Jerome CP. Anabolic Effect of High Doses of Human Parathyroid Hormone (1-38) in Mature Intact Female Rats. J Bone Miner Res 1994;9(6):933-42.

Jones HH, Priest JD, Hayes WC, Tichenor CC, Nagel DA. Humeral Hypertrophy in Response to Exercise. J Bone Joint Surg (Br) 1977;59-A, No. 2:204-8.

Jones D, Fardell J. Hypochondriac laughs with Sheridan Poorly. Viz 1996;76:24.

Jowsey J, Raisz LG. Experimental Osteoporosis and Parathyroid Activity. Endocrinology 1968;82:384-96.

Justus R, Luft JH. A Mechanochemical Hypothesis for Bone Remodelling Induced by Mechanical Stress. Calcified Tissue Research 1970;5:222-35.

Kalu DN. The ovariectomised rat model of postmenopausal bone loss. Bone and Mineral 1991;15:175-92.

Karlsson MK, Johnell O, Obrant KJ. Bone mineral density in weight lifters. Calcif Tissue Int 1993;52(3):212-5.

Karlsson MK, Johnell O, Obrant KJ. Bone mineral density in professional ballet dancers. Bone and Mineral 1993;21(3):163-9.

Kawaguchi H, Pilbeam CC, Woodiel FN, Raisz LG. Comparison of the effects of 3,5,3'-triiodothyroacetic acid and triiodothyronine on bone resorption in cultured fetal rat long bones and neonatal mouse calvariae. J Bone Miner Res 1994;9(2):247-53.

Keller TS, Spengler DM. In Vivo strain gage implantation in rats. J Biomech 1982;15:911-7.

Kimmel DB. Quantitative Histologic Changes in the Proximal Tibial Growth Cartilage of Aged Female Rats. Cells and Materials 1991(Suppl. 1):11-8.

Kleerekoper M, Avioli LV. Evaluation and Treatment of Postmenopausal Osteoporosis. In: Favus MJ, ed. Primer on the Metabolic Bone Diseases and Disorders of Mineral Metabolism. 2nd ed. Philadelphia: Lippincott-Raven, 1993:223-8.

Klein DC, Raisz LG. Prostaglandins: Stimulation of bone resorption in tissue culture. Endocrinology 1970;86:1436-40.

Klein-Nulend J, Van der Plas A, Semeins CM, et al. Sensitivity of osteocytes to biomechanical stress in vitro. FASEB Journal 1995;9(5):441-5.

Koch JC. The Laws of Bone Architecture. Am J Anat 1917;21(2):177-298.

Kochersberger G, Buckley NJ, Leight GS, et al. What Is the Clinical Significance of Bone Loss in Primary Hyperparathyroidism? Arch Intern Med 1987;147:1951-3.

Koenig WJ, Donovan JM, Pensler JM. Cranial bone grafting in children. Plast Reconstr Surg 1995;95(1):1-4.

Kohrt WM, Snead DB, Slatopolsky E, Birge SJ. Additive Effects of Weight-Bearing Exercise and Estrogen on Bone Mineral Density in Older Women. J Bone Miner Res 1995;10(9):1303-11.

Komm BS, Terpening CM, Benz DJ, et al. Estrogen binding, receptor mRNA, and biologic response in osteoblast-like osteosarcoma cells. Science 1988;241(4861):81-4 .

Kronenberg HM, Bringhurst FR, Nussbaum S, et al. Parathyroid Hormone: Biosynthesis, Secretion, Chemistry and Action. In: Mundy GR, Martin TJ, eds. Physiology and Pharmacology of Bone. Berlin: Springer-Verlag, 1993:507-67.

Lanyon LE. The measurement of bone strain in vivo. Acta Orthop Belg 1976;42:98-108.

Lanyon LE. Experimental Support For The Trajectorial Theory of Bone Structure. J Bone Joint Surg (Br) 1974;56B:160-6.

Lanyon LE. Functional Strain as a Determinant of Bone Remodelling. Calcif Tissue Int 1984;36:S56-61.

Lanyon LE. In Vivo Bone Strain Recorded From Thoracic Vertebrae Of Sheep. J Biomech 1972;5:277-81.

Lanyon LE. Measurement of Natural Bone Strain in the Mammalian Vertebral Column. Ph.D. Thesis. University of Bristol, Bristol, UK, 1969.

Lanyon LE. Skeletal Responses to Physical Loading. In: Mundy GR, Martin TJ, eds. Physiology and Pharmacology of Bone. 1st ed. Heidelberg: Springer-Verlag, 1993:485-506.

Lanyon LE. The influence of function on the development of bone curvature. An experimental study on the rat tibia. J Zool, Lond 1980;192:457-66.

Lanyon LE, Bourn S. The Influence of Mechanical Function on The Development and Remodeling of the Tibia. J Bone Joint Surg (Am) 1979;61A(2):263-73.

Lanyon LE, Hampson WGJ, Goodship AE, Shah JS. Bone deformation recorded In Vivo from strain gauges attached to the human tibial shaft. Acta Orthop Scand 1975;46:256-68.

Lanyon LE, Hartman W. Strain Related Electrical Potentials Recorded in vitro and in vivo. Calcified Tissue Research 1977;22:315-27.

Lanyon LE, Magee PT, Baggott DG. The Relationship of Functional Stress and Strain to The Processes of Bone Remodelling. An Experimental Study on The Sheep Radius. J Biomech 1979;12:593-600.

Lanyon LE, O'Conner JA, Goodship AE. The Importance of Physiological Relevance in Biomechanical Experiments. J Biomech 1977;10:611.

Lanyon LE, Rubin C. Static Versus Dynamic Loads as an Influence on Bone Remodeling. J Biomech 1984;17:897-905.

Lanyon LE, Smith RN. Bone Strain In The Tibia During Normal Quadruped Locomotion. Acta Orthop Scand 1970;41:238-48.

Lanyon LE, Smith RN. Measurements of bone strain in the walking animal. Res Vet Sci 1969;10:93-4.

Lean JM, Jagger CJ, Chambers TJ, Chow JWM. Increased insulin-like growth factor I mRNA expression in rat osteocytes in response to mechanical stimulation. American Journal of Physiology - Endocrinology and Metabolism 1995;268:318-27.

Leblanc AD, Schneider VS, Evans HJ, Engelbretson DA, Krebs JM. Bone mineral loss and recovery after 17 weeks of bed rest. J Bone Miner Res 1990;5(8):843-50.

Li YP, Stashenko P. Characterisation of a TNF-responsive element which down-regulates the human osteocalcin gene. Molecular and Cellular Biology 1993;13:3714-21.

Lieberman DE. How and Why Humans Grow Thin Skulls: Experimental Evidence for Systemic Cortical Robusticity. Am J Phys Anthropol 1996;101:217-236.

Lin HY, Harris TL, Flannery MS, et al. Expression cloning of an adenylate cyclase-coupled calcitonin receptor. Science 1991;254:1022-4.

Lindsay R, Cosman F, Nieves J, Dempster DW, Shen V. A controlled clinical trial of the effects of 1-34 hPTH in estrogen treated osteoporotic women. J Bone Miner Res 1993;8(Suppl. 1):S130.

Lindsay R, Hart DM, Forrest G, Baird C. Prevention of spinal osteoporosis in oophorectomised women. Lancet 1980;11:1151-4.

Liskova M, Hert J. Reaction of bone to mechanical stimuli. Part 2: Periosteal and endosteal reaction of the tibial diaphysis in the rabbit to intermittent loading. Folia Morph 1971;19(3):301-17.

Lissner HR. The response of the human body to impact. In: Kenedi RM, ed. Biomechanics and Related Bio-Engineering Topics. :. 1964:135-40 (Proceedings of a symposium held in Glasgow, September 1964.).

Lissner HR, Roberts VL. Evaluation of skeletal impacts of human cadavers. In: Evans FG, ed. Studies on the Anatomy and Function of Bones and Joints. Berlin: Springer, 1966:113-20.

Little EG, Tocher D, O'Donnell P. Strain gauge reinforcement of plastics. Strain 1990;26:91-8.

Liu CC, Kalu DN. Human Parathyroid Hormone-(1-34) Prevents Bone Loss and Augments Bone Formation in Sexually Mature Ovariectomized Rats. J Bone Miner Res 1990;5:973-82.

Liu CC, Kalu DN, Salerno E, Echon R, Hollis BW, Ray M. Preexisting Bone Loss Associated with Ovariectomy in Rats Is Reversed by Parathyroid Hormone. J Bone Miner Res 1991;91:1071-80.

Lowe J, Bab I, Stein H, Sela J. Primary Calcification in Remodeling Haversian Systems Following Tibial Fracture in Rats. Clin Orthop 1983;176:291-7.

Lu KH, Hopper BR, Vargo TM, Yen SSC. Chronological changes in sex steroid, gonadotrophin and prolactin secretion in aging female rats displaying different reproductive states. Biol Reprod 1979;21:193-203.

Ma YF, Jee WSS, Ke HZ, et al. Human Parathyroid Hormone-(1-38) Restores Cancellous Bone to The Immobilized, Osteopenic Proximal Tibial Metaphysis in Rats. J Bone Miner Res 1995;10, No. 3:496-505.

Martin RB, Burr DB. Structure, Function & Adaptation of Compact Bone. 1st ed. New York: Raven Press, 1989.

Martin TJ. Properties of parathyroid hormone-related protein and its role in malignant hypercalcaemia. Quarterly Journal of Medicine 1990;76(280):771-86.

Mason DJ, Hillam RA, Skerry TM. Constitutive in vivo mRNA expression by osteocytes of beta-actin, osteocalcin, connexin-43, IGF-I, c-fos and c-jun, but not TNF-alpha nor tartrate-resistant acid phosphatase. J Bone Miner Res 1996;11(3):350-7.

Mason DJ, Stuekle S, Hillam RA, Suva LJ, Skerry TM. Novel Genes Regulated by Mechanical Loading of Bone in vivo Include a Glutamate/Aspartate (GLAST) protein. J Bone Miner Res 1995;10(Suppl. 1):S332.

Mason MW, Skedros JG, Bloebaum RD. Evidence of Strain-Related Cortical Adaptation in the Diaphysis of the Horse Radius. Bone 1995;17:229-37.

McLeod KJ, Rubin CT. Sensitivity of the Bone Remodeling Response to the Frequency of Applied Strain. Orthop Trans 1992;17:533.

McLeod K, Rubin C. The effect of low-frequency electrical fields on osteogenesis. J Bone Joint Surg (Am) 1992;74A:920-9.

McSheehy PMJ, Chambers TJ. Osteoblastic cells mediate osteoclastic responsiveness to parathyroid hormone. Endocrinology 1986;118(2):824-8.

Messerer O. Ueber Elasticitat und Festigkeit der menschlichen Knochen. Stuttgart 1880 (cited by Koch 1917).

Moonga BS, Towhidul Alam ASM, Bevis PJR, Avaldi F, Soncini R, Huang CLHZaidi M. Regulation of cytosolic free calcium in isolated rat osteoclasts by calcitonin. J Endocrinol 1992;132(2):241-9.

Mori S, Jee WS, Li XJ, Chan S, Kimmel DB. Effects of prostaglandin E2 on production of new cancellous bone in the axial skeleton of ovariectomized rats. Bone 1990;11(2):103-13.

Mosekilde L, Melsen F. Morphometric and dynamic studies of bone changes in hypothyroidism. Acta Pathol Microbiol Scand 1978;86:56-62.

Moseley JM, Kubota M, DiefenbachJagger H, et al. Parathyroid hormone-related protein purified from a human lung cancer cell line. Proceedings of the National Academy of Sciences of the United States of America 1987;84(14):5048-52.

Mosley J. The influence of mechanical load and oestrogen on the development of long bone architecture. Ph.D. Thesis. Royal Veterinary College, London, 1996.

Most W, Schot L, Ederveen A, Van Der WeePals L, Papapoulos S, Lowik C. In vitro and ex vivo evidence that estrogens suppress increased bone resorption induced by ovariectomy or PTH stimulation through an effect on osteoclastogenesis. J Bone Miner Res 1995;10(10):1523-30.

Mundy GR, Martin TJ. Physiology and Pharmacology of Bone. 1st ed. v. 1. Berlin,New York,Heidelberg.: Springer-Verlag, 1993.

Mundy GR, Roodman GD. . In: Peck WA, ed. Bone and Mineral Research. v. 5. Amsterdam: Elsevier, 1987:209.

Mundy GR, Shapiro JL, Bandelin JG, Canalis EM, Raisz LG. Direct stimulation of bone resorption by thyroid hormones. J Clin Invest 1976;58:529-34.

Nathan C, Sporn M. Cytokines in Context. J Cell Biol 1991;113:981-6.

Neidlinger-Wilke C, Stalla I, Claes L, et al. Human osteoblasts from younger normal and osteoporotic donors show differences in proliferation and TGFβ-release in response to cyclic strain. J Biomech 1995;28(12):1411-8.

Nicholson GC, Moseley JM, Sexton PM, Martin TJ. Chicken Osteoclasts Do Not Possess Calcitonin Receptors. J Bone Miner Res 1987;2(1):53-9.

Nijweide PJ, Burger EH, Feyen JHM. Cells of bone: Proliferation, differentiation and hormonal regulation. Physiol Rev 1986;66:855.

Notelovitz M, Martin D, Tesar R, et al. Estrogen therapy and variable-resistance weight training increase bone mineral in surgically menopausal women. J Bone Miner Res 1991;6(6):583-90.

Nowak RM. Walker's Mammals of the World. 5th ed. v. 2. Baltimore: John Hopkins University Press, 1991.

Nunamaker DM, Butterweck DM, Provost MT. Fatigue fractures in thoroughbred racehorses: Relationships with age, peak bone strain, and training. J Orthop Res 1990;8(4):604-11.

O'Connor JA, Lanyon LE, McFie H. The Influence of Strain Rate on Adaptive Bone Remodelling. J Biomech 1982;15:767.

Okimoto N, Nakamura T, Hori M, Okazaki Y, Aota S, Suzuki K. Protective Effects of Human Parathyroid Hormone(1-34) on Bone Mass and Strength in Ovariectomised Rats. J Bone Miner Res 1995;10, Supplement 1:S251.

Orimo H, Fujita T, Yoshikawa M. Increased Sensitivity of Bone to Parathyroid Hormone in Ovariectomized Rats. Endocrinology 1972;90:760-3.

Orloff JJ, Wu TL, Stewart AF. Parathyroid hormone-like proteins: biochemical responses and receptor interactions. Endocr Rev 1989;10:476-95.

Otter MW, Bronk JT, Wu DD, Bieber WA, Kelly PJ, Cochran GVB. Inflatable brace-related streaming potentials in living canine tibias. Clin Orthop 1996(324):283-91.

Otter MW, Palmieri VR, Cochran GVB. Transcortical streaming potentials are generated by circulatory pressure gradients in living canine tibia. J Orthop Res 1990;8(1):119-26.

Otter MW, Palmieri VR, Wu DD, Seiz KG, MacGinitie LA, Cochran GVB. A comparative analysis of streaming potentials in vivo and in vitro. J Orthop Res 1992;10(5):710-9.

Otter MW, Wu DD, Bieber WA, Cochran GVB. Intraarterial protamine sulfate reduces the magnitude of streaming potentials in living canine tibia. Calcif Tissue Int 1993;53(6):411-5.

Oursler MJ, Pyfferoen J, Osdoby P, Riggs BL, Spelsberg TC. Osteoclasts express mRNA for estrogen receptors. J Bone Miner Res 1990;5:517.

Oxlund H, Ejersted C, Andreassen TT, Torring O, Nilsson MHL. Parathyroid hormone (1-34) and (1-84) stimulate cortical bone formation both from periosteum and endosteum. Calcif Tissue Int 1993;53(6):394-9.

Parfitt AM, Mathews CHE, Rao D, Frame B, Kleerekoper M, Villanueva AR. Impaired osteoblast function in metabolic bone disease. In: DeLuca HF, Frost H, Jee W, Johnston C, Parfitt

AM, eds. Osteoporosis: Recent Advances in Pathogenesis and Treatment. Baltimore: University Park Press, 1981:321-30.

Parfitt AM, Mathews CHE, Villanueva AB, et al. Relationships between surface, volume, and thickness of iliac trabecular bone in aging and in osteoporosis. Implications for the microanatomic and cellular mechanisms of bone loss. J Clin Invest 1983;72(4):1396-409.

Parisien M, Cosman F, Mellish RWE, et al. Bone structure in postmenopausal hyperparathyroid, osteoporotic, and normal women. J Bone Miner Res 1995;10(9):1393-9.

Pead MJ, Lanyon LE. Adaptive remodelling in bone: torsion versus compression. Proc Orthop Trans 1990;15:104.

Pead MJ, Skerry TM, Lanyon LE. Direct Transformation from Quiescence to Bone Formation in the Adult Periosteum Following a Single Brief Period of Bone Loading. J Bone Miner Res 1988;3:647-56.

Pead MJ, Suswillo RFL, Skerry TM, Vedi S, Lanyon LE. Increased 3H-uridine levels in osteocytes following a single short period of dynamic bone loading in vivo. Calcif Tissue Int 1988;43:92-6.

Pensler JM, Radosevich JA, Higbee R, Langman CB. Osteoclasts isolated from membranous bone in children exhibit nuclear estrogen and progesterone receptors. J Bone Miner Res 1990;5(8):797-802.

Pfeilschifter J, Seyedin SM, Mundy GR. Transforming growth factor beta inhibits bone resorption in fetal rat long bone cultures. J Clin Invest 1988;82(2):680-5.

Phillips JH, Rahn BA. Fixation effects on membranous and endochondral onlay bone-graft resorption. Plast Reconstr Surg 1988;82(5):872-7.

Pilbeam CC, Raisz LG. In Vitro Inhibition of PTH-Stimulated Prostaglandin (PGE2) Production by 17b-estradiol (E2). J Bone Miner Res 1988;3:S219.

Pople J, ed. BSSM Strain Measurement Reference Book. Newcastle upon Tyne: BSSM, 1979.

Rauber. Elasticitat und Festigkeit der Knochen. Leipsig:, 1876 (cited by Koch 1917).

Rawlinson SCF, Mosley JR, Suswillo RFL, Pitsillides AA, Lanyon LE. Calvarial and Limb Bone Cells in Organ and Monolayer Culture Do Not Show the Same Early Responses to Dynamic Mechanical Strain. J Bone Miner Res 1995;10:1225-32.

Reeve J, Meunier PJ, Parsons JA, et al. Anabolic effect of human parathyroid hormone fragment on trabecular bone in involutional osteoporosis: A multicentre trial. BMJ 1980;280(6228):1340-4.

Reilly DT, Burstein AH. The Elastic And Ultimate Properties Of Compact Bone Tissue. J Biomech 1975;8:393-405.

Reilly DT, Burstein AH. The Mechanical Properties of Cortical Bone. J Bone Joint Surg (Br) 1974;56-A:1001-22.

Reilly DT, Burstein AH, Frankel VH. The Elastic Modulus For Bone. J Biomech 1974;7:271-5.

Ridgway SH, Harrison SR, eds. Handbook of Marine Mammals. v. 3. London: Academic Press, 1985.

Rodan GA. Mechanical loading, estrogen deficiency, and the coupling of bone formation to bone resorption. J Bone Miner Res 1991;6, No. 6:527-30.

Rodan GA, Martin TJ. Role of osteoblasts in hormonal control of bone resorption - a hypothesis. Calcif Tissue Int 1981;33:349-51.

Rosen HN, Sullivan EK, Middlebrooks VL, et al. Parenteral pamidronate prevents thyroid hormone-induced bone loss in rats. J Bone Miner Res 1993;8(10):1255-61.

Roux W. Der Kampf der Theile in Organismus. Biol Centralblatt 1881;1(8) (cited by Wolff 1892).

Rubin CT. Skeletal Strain and Functional Significance of Bone Architecture. Calcif Tissue Int 1984;36:S11-8.

Rubin CT, Bain SD, McLeod KJ. Suppression of the Osteogenic Response in the Aging Skeleton. Calcif Tissue Int 1992;50:306-13.

Rubin CT, Gross TS, McLeod KJ, Bain SD. Morphologic Stages in Lamellar Bone Formation Stimulated by a Potent Mechanical Stimulus. J Bone Miner Res 1995;10, No. 3:488-95.

Rubin CT, Lanyon LE. Regulation of bone formation by applied dynamic loads. J Bone Joint Surg (Br) 1984;66-A:397-402.

Rubin CT, Lanyon LE. Bone Remodelling in Response to Applied Dynamic Loads. Orthop Trans 1981;5:237-8.

Rubin CT, Lanyon LE. Regulation of Bone Mass by Mechanical Strain Magnitude. Calcif Tissue Int 1985;37:411-7.

Rubin CT, Lanyon LE. Limb mechanics as a function of speed & gait: a study of functional strains in the radius and tibia of horse and dog. J Exp Biol 1982;101:187-211.

Rubin CT, Lanyon LE. Dynamic Strain Similarity in Vertebrates; an Alternative to Allometric Limb Bone Scaling. J Theor Biol 1984;107:321-7.

Rubin CT, McLeod KJ. The Biophysical Control of Bone Morphology. In: Davidovitch Z, ed. The Biological Mechanisms of Tooth Eruption, Resorption and Replacement by Implants. Boston: Harvard, 1994:45-53.

Rubin CT, McLeod KJ. Promotion of bony ingrowth by frequency-specific, low-amplitude mechanical strain. Clin Orthop 1994(298):165-74 (Conference).

Rubin CT, McLeod KJ, Bain SD. Functional strains and cortical bone adaptation: Epigenetic assurance of skeletal integrity. J Biomech 1990;23, Suppl. 1:43-54.

Ruth EB. Bone studies II. An experimental study of the Haversian-type vascular channels. Am J Anat 1953;93:429-55.

Salem GJ, Zernicke RF, Vailas AC, Martinez DA. Biomechanical and biochemical changes in lumbar vertebrae of rapidly growing rats. Am J Physiol 1989;256:R259-63.

Saville PD. Changes in skeletal mass and fragility with castration in the rat: A model of osteoporosis. J Am Geriatr Soc 1969;17:155-66.

Schaffler MB, Choi K, Milgrom C. Aging and matrix microdamage accumulation in human compact bone. Bone 1995;17(6):521-5.

Schultz VL, Boass A, Garner SC, Toverud SU. Several anesthetics, but not diethyl ether, cause marked elevation of serum parathyroid hormone concentration in rats. J Bone Miner Res 1995;10(9):1298-302.

Sedlin ED. The ratio of cortical area to cross sectional area in the rib diaphysis. A quantitative index of osteoporosis. Clin Orthop 1964;36:161-8.

Seeman E, Wahner HW, Offord KP, Kumar R, Johnson WJ, Riggs BL. Differential effects of endocrine dysfunction on the axial and appendicular skeleton. J Clin Invest 1982;69:1302-9.

Sexton PM, Houssami S, Hilton JM, et al. Identification of brain isoforms of the rat calcitonin receptor. Mol Endocrinol 1993;7:815-21.

Simmons DJ, Menton DN, Miller S, Lozano R. Periosteal attachment fibers in the rat calvarium. Calcif Tissue Int 1993;53(6):424-7.

Simon MR. The effect of dynamic loading on the growth of epiphyseal cartilage in the rat. Acta Anat 1978;102:176-83.

Sims NA, Morris HA, Moore RJ, Durbridge TC. Parathyroidectomy Does Not Prevent Bone Loss in the Oophorectomized Rat. J Bone Miner Res 1994;9, No. 12:1859-63.

Skerry TM. Load related changes in bone cells and matrix. Ph.D. Thesis. Royal Veterinary College, London, UK, 1989.

Skerry TM, Bitensky L, Chayen J, Lanyon LE. Early Strain-Related Changes in Enzyme Activity in Osteocytes Following Bone Loading In Vivo. J Bone Miner Res 1989;4:783-8.

Skerry TM, Bitensky L, Chayen J, Lanyon LE. Loading-Related Reorientation of Bone Proteoglycan in Vivo. Strain Memory in Bone Tissue? J Orthop Res 1988;6:547-51.

Skerry TM, Lanyon LE. Interruption of Disuse by Short Duration Walking Exercise Does Not Prevent Bone Loss in the Sheep Calcaneus. Bone 1995;16:269-74.

Skerry TM, Suswillo R, El Haj AJ, Ali NN, Dodds RA, Lanyon LE. Load-Induced Proteoglycan Orientation in Bone Tissue In Vivo and In Vitro. Calcif Tissue Int 1990;46:318-26.

Skerry TM, Genever PG, Patton AJ, Grabowski PS, Stueckle S, Suva LJ. Glutamate Receptors in Bone Cells Suggest a Paracrine Role for Excitatory Amino Acids in Regulation of The Skeleton. J Bone Miner Res 1996;11(Suppl. 1):S141.

Slovik DM, Rosenthal DI, Doppelt SH, et al. Restoration of Spinal Bone in Osteoporotic Men by Treatment with Human Parathyroid Hormone (1-34) and 1,25 Dihydroxyvitamin D. J Bone Miner Res 1986;1:377-81.

Smith SD. Induction of partial limb regeneration in Rana pipiens by galvic stimulation. Anat Rec 1967;158:89.

Stewart AF. Humoral Hypercalcemia of Malignancy. In: Favus MJ, ed. Primer on the Metabolic Bone Diseases and Disorders of Mineral Metabolism. 2nd ed. New York: Raven Press, 1993:169-76.

Stewart AF, Wu T, Goumas D, Burtis WJ, Broadus AE. N-terminal amino acid sequence of two novel tumor-derived adenylate cyclase-stimulating proteins: Identification of parathyroid hormone-like and parathyroid hormone-unlike domains. Biochemical and Biophysical Research Communications 1987;146:672-8.

Suva LJ, Winslow GA, Wettenhall REH, et al. A parathyroid hormone-related protein implicated in malignant hypercalcemia: Cloning and expression. Science 1987;237(4817):893-6.

Szivek JA, Johnson EM, Magee FP. In Vivo Strain Analysis of the Greyhound Femoral Diaphysis. J Invest Surg 1992;5:91-108.

Tada K, Yamamuro T, Okumura H, Kasai R, Takahashi H. Restoration of Axial and Appendicular Bone Volumes by h-PTH(1-34) in Parathyroidectomized and Osteopenic Rats. Bone 1990;11:163-9.

Tashjian AH, Voelkel EF, Lazzaro M, et al. Alpha and beta transforming growth factors stimulate prostaglandin production and bone resorption in cultured mouse calvaria. Proceedings of the National Academy of Sciences of the United States of America 1985;82:4535-8.

Tessier P. Autogenous bone grafts taken from the calvarium for facial and cranial applications. Clin Plast Surg 1982;9(4):531-8.

Tong H, Lin H, Wang H, Sakai D, Minkin C. Osteoclasts Respond to Parathyroid Hormone and Express mRNA for its Receptor. J Bone Miner Res 1995;10(Suppl. 1):S322.

Torrance AG. The Effect of Controlled Mechanical Loading Upon The Development of Long Bone Architecture. Ph.D. Thesis. Royal Veterinary College, London, 1993.

Torrance AG, Mosley JR, Suswillo RFL, Lanyon LE. Non-invasive loading of the rat ulna in vivo induces a strain-related modeling response uncomplicated by trauma or periostal pressure. Calcif Tissue Int 1994;54(3):241-7.

Treharne RW. Review of Wolff's law and its proposed means of operation. Orthopaedic Review 1981;10(1):35-47.

Tsai Keh-S, Ebeling PR, Riggs BL. Bone Responsiveness to Parathyroid Hormone in Normal and Osteoporotic Postmenopausal Women. Journal of Clinical Endocrinology and Metabolism 1989;69:1024-7.

Turner CH, Akhter MP, Raab DM, Kimmel DB, Recker RR. A noninvasive, in vivo model for studying strain adaptive bone modeling. Bone 1991;12:73-9.

Turner CH, Forwood MR, Rho JY, Yoshikawa T. Mechanical loading thresholds for lamellar and woven bone formation. J Bone Miner Res 1994;9(1):87-97.

Turner CH, Takano Y, Owan I. Aging Changes Mechanical Loading Thresholds for Bone Formation in Rats. J Bone Miner Res 1995;10(10):1544-9.

Turner CH, Yoshikawa T, Forwood MR, Sun TC, Burr DB. High frequency components of bone strain in dogs measured during various activities. J Biomech 1995;28(1):39-44.

Uhthoff HK, Jaworski ZFG. Bone Loss In Response To Long-Term Immobilisation. J Bone Joint Surg (Br) 1978;60-B, No. 3:420-9.

Usdin TB, Gruber C, Bonner TI. Identification and functional expression of a receptor selectively recognizing parathyroid hormone, the PTH2 receptor. Journal of Biological Chemistry 1995;270(26):15455-8.

Variot G, Remy C. Sur les nerfs dc la moelle des os. Journal de l'Anatomie et de la Physiologie 1880;16:273-84 (cited by Duncan and Shim 1977).

Vaughan JM. The Physiology of Bone. 3rd ed. Oxford: Clarendon Press, 1981.

Von Meyer H. Die Architectur der Spongiosa. Reichert und Dubois-Reymond's Archiv. 1867. Page 615 (cited by Koch 1917).

Walsh CA, Birch MA, Fraser WD, et al. Expression and secretion of parathyroid hormone-related protein by human bone-derived cells in vitro: Effects of glucocorticoids. J Bone Miner Res 1995;10(1):17-25.

Wang N, Butler JP, Ingber DE. Mechanotransduction across the cell surface and through the cytoskeleton. Science 1993;260(5111):1124-7.

Wang N, Ingber DE. Control of cytoskeletal mechanics by extracellular matrix, cell shape, and mechanical tension. Biophysical Journal 1994;66(6):2181-9.

Ward FO. Outlines of Human Osteology. London:, 1838 (cited by Wolff 1892).

Waynforth HB, Flecknell PA. Experimental and surgical technique in the rat. 2nd ed. London: Academic Press, 1992.

Weinbaum S, Cowin SC, Zeng Y. A model for the excitation of osteocytes by mechanical loading-induced bone fluid shear stresses. J Biomech 1994;27(3):339-60.

Wessler S. What is a model? Animal models of thrombosis and hemorrhagic diseases. A workshop organised by the Institute of Laboratory Animal Resources Committee on Animal Models for Thrombosis and Hemorrhagic Diseases. March 12-13 1976. Washington DC, USA.

Wolff J. The Law of Bone Remodelling (Das Gesetz der Transformation der Knochen). Berlin: Springer-Verlag, 1892 (Translated from "Das Gesetz der Transformation der Knochen" Verlag, Berlin 1892 by P. Maquet and R. Furlong.).

Wronski TJ, Dann LM, Horner SL. Time course of vertebral osteopenia in ovariectomized rats. Bone 1989;10:295-301.

Wronski TJ, Dann LM, Scott KS, Cintron M. Long-Term Effects of Ovariectomy and Aging on the Rat Skeleton. Calcif Tissue Int 1989;45:360-6.

Wronski TJ, Yen C-F. The Ovariectomized Rat as an Animal Model for Postmenopausal Bone Loss. Cells and Materials 1991(The Aged Rat Model for Bone Biology Studies Suppl. 1):69-74.

Yeh C-K, Rodan GA. Tensile forces enhance prostaglandin E synthesis in osteoblastic cells grown on collagen ribbons. Calcif Tissue Int 1984;36:S67-71.

Zill SN, Seyfarth E-A. Exoskeletal Sensors for Walking. Scientific American 1996;275(2):70-4.

Zins JE, Whitaker LA. Membranous versus endochondral bone: Implications for craniofacial reconstruction. Plast Reconstr Surg 1983;72(6):778-84.

JOURNAL OF BONE AND MINERAL RESEARCH
Volume 10, Number 5, 1995
Blackwell Science, Inc.

Inhibition of Bone Resorption and Stimulation of Formation by Mechanical Loading of the Modeling Rat Ulna In Vivo

RICHARD A. HILLAM and TIMOTHY M. SKERRY

ABSTRACT

During normal growth of the rat ulna, bone is resorbed from the medial periosteal surface. This occurs as part of the modeling process by which the bone achieves its adult shape. By attaching strain gauges to the ulnae of rats in vivo, we measured the strains imposed on that surface of the bone during normal locomotion. We then applied mechanical loads to the ulnae of other rats in vivo for 6 consecutive days, inducing strains approximately double those we had measured. Fluorochromes were given on the 1st and 5th days. The histology of the medial ulnar periosteal surface was correlated with the amount of fluorochrome incorporation and tartrate resistant acid phosphatase (TRAP) activity in serial sections. In the nonloaded ulnae, the surfaces were lined with bone resorbing cells. Corresponding areas of the loaded bones were lined with osteoid and osteoblasts. There was insignificant label incorporation in the nonloaded bones but almost continuous label incorporation in the corresponding regions of the loaded bones, which was significantly different from the nonloaded bones. TRAP activity of the periosteal cells in the loaded bones was significantly less than in the nonloaded limbs. It is widely acknowledged that loading induces bone formation, and this implies that it also has the ability to inhibit resorption. However, to date there has been little direct evidence for the inhibition of resorption in vivo by mechanical loading. The changes we have observed are similar to the sequence of cellular events that occur during the reversal phase of bone remodeling, in which osteoclastic resorption ceases and osteoblasts are recruited and begin formation. This model may help increase understanding of that process.

INTRODUCTION

REGULATION of bone mass by mechanical loading is an important subject for study because of the prevalence of diseases such as postmenopausal osteoporosis and rheumatoid arthritis, in which functionally inappropriate bone loss occurs with consequent fracture and disability. Mechanical loading is an important determinant of bone mass and is currently one of the least well understood of the many osteotropic influences. Evidence exists to suggest that a sequence of changes occur in the matrix[1-3] and consequently in the cells of bone[4-6] after loading in vivo. This cascade of events has a positive effect on bone balance in the case of increased loading,[7] and a negative effect in disuse.[8] The mechanism by which bone mass changes with disuse or exercise is complex because the sum of all positive and negative osteotropic influences regulate the relative amounts of bone formation and resorption during the remodeling process. The effects of mechanical events on the skeleton therefore depend on their interactions with other local and systemic influences. For example, loading that stimulates bone formation on quiescent surfaces only modulates resorption in similar animals loaded while receiving calcium-deficient diets.[9] In a similar way, increased loading in ovariectomized animals or postmenopausal women may either be less effective in stimulating formation than in

Parts of this work have been presented at meetings of the Bone and Tooth Society, and the Fifth Workshop on Cells and Cytokines in Bone and Cartilage.

Department of Anatomy, University of Bristol, Bristol, United Kingdom.

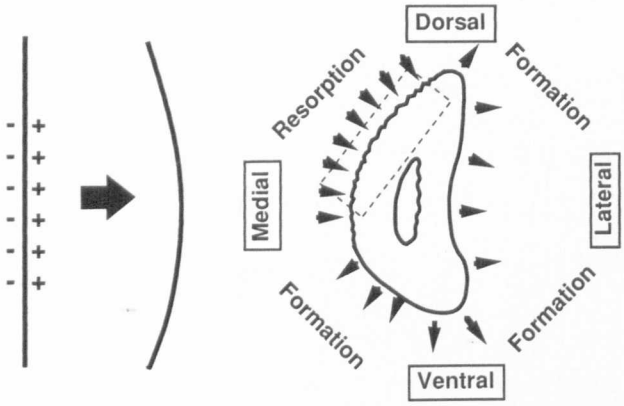

FIG. 1. During growth, the ulna develops the curved shape of the adult as a result of formation on the lateral surface and resorption from the medial periosteal surface (left). A schematic midshaft cross-section (right) shows formation on the ventral and lateral surfaces and resorption from the dorsomedial periosteal cortex. Approximately equal but opposite endosteal events maintain cortical thickness and the position of the medullary cavity of the bone. The dashed box indicates the region of the bone shown in the photomicrographs and represents the area in which the TRAP activity and the length of the labeled surface were measured.

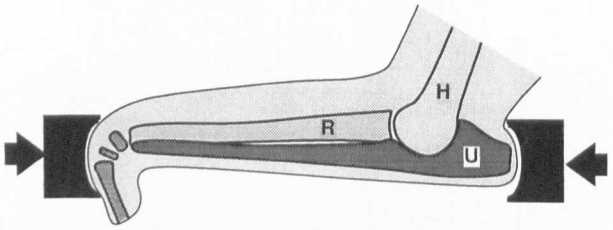

FIG. 2. The ulna is loaded by placing the elbow and flexed carpus between cups in a materials test machine, which applies axial compressive loads to the bone, bending the bone laterally. H = humerus, R = radius, U = ulna.

control groups or may only reduce bone resorption.[10–12] This suggests that the effect of loading is to inhibit bone resorption and stimulate formation, although the direct early consequences of loading on resorbing bone surfaces have not been studied previously.

Torrance et al.[13] developed a method of noninvasive mechanical loading of the rat ulna in vivo. We have used the same method to load the ulnae of younger rats in vivo and to study early effects of loading on cellular actions. In the animals we have used, there is marked bone resorption from the medial periosteum as a part of the normal modeling process by which the ulna develops its adult curved shape (Fig. 1).[14] The effect of the loading regime we applied was to transform the resorbing bone surface into one that formed bone. This change was induced as a result of elevated, but physiologically relevant strains in the bone, without significant trauma in the area of sampling.

During the change from bone resorption to bone formation over the 6-day period of the experiment, the medial ulnar periosteal surface experiences changes that are similar to the events in the reversal phase of the remodeling cycle.[15,16] Although that remodeling process in adults is different from the load-induced modulation of a modeling drift, which we describe, this model may shed light onto some of the cellular events of remodeling.

MATERIALS AND METHODS

In vivo strain measurement

In 5 female Wistar rats (body weight 200–250 g), we attached a single element strain gauge (Kenkyujo Co., Tokyo, Japan) to the midpoint of the medial surface of the left ulna of each animal, in line with the long axis of the bone. The lead wires from the gauges were passed subcutaneously (sc) to emerge between the shoulders. To measure strains, the leads from the gauge were connected to a strain gauge amplifier (Bell and Howell, Basingstoke, U.K.) whose output was fed into an A/D board (Amplicon, Brighton, U.K.) fitted to an Opus III PC/AT computer, sampling at a rate of 20 Hz. Custom software was used to capture and record bone strains. Zero strains were defined when the animals were lifted from the ground and did not struggle. Strains were recorded from the ulnae when the rats walked on a flat surface, climbed a 45° inclined plane, and when they jumped from a ledge 30 cm above a hard floor.

Load/strain calibration and loading

Both the forelimbs were removed from three Wistar rats (body weight 85–95 g). Using the same surgical approach as in the in vivo studies, so that there was minimal soft tissue disruption, single element strain gauges were attached to the midpoint of the bones, oriented as for the in vivo studies. The elbow and flexed carpus were placed between the padded cups of a materials test machine (Dartec, Stourbridge, U.K.) (Fig. 2) and compressed axially. Because of the natural curvature of the ulna, this loading caused the bone to bend in a similar direction as during physiological loading. The applied force was increased incrementally so that the relationship between applied load and bone strain could be determined.

Animals and loading

A group of 6 female Wistar rats (body weight 85–95 g) were anesthetized with a mixture of xylazine (Bayer U.K., Bury St. Edmunds, U.K.) (10 mg/kg) and ketamine (Parke-Davis, Pontypool, U.K.) (45 mg/kg) injected intraperitoneally (ip). The left elbow and flexed carpus were placed between the cups of the loading device and compressed cyclically at a frequency of 10 Hz and a peak force of 7 Newtons (N) for 4 minutes (Fig. 2). Immediately after the first period of loading, each rat was injected sc with calcein (Sigma, St. Louis, MO) (15 mg/kg), to mark sites of bone formation at the start of the experiment.

The 4-minute period of loading was repeated at 24-h intervals for a total of 6 days. On the 5th day of loading, a

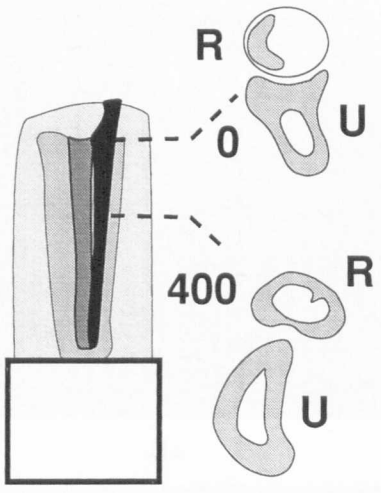

FIG. 3. The sample site at which sections are taken for analysis is located because of the fixed relationship of the radius and ulna. After chilling, the blocks are mounted perpendicularly on the microtome chuck, with the elbow uppermost, then trimmed until the first section is cut in which both the radius and ulna appear (0). At this level, the ulna (U) is predominantly cortical and trabecular bone, but the radial head (R) appears characteristically as a crescent of subchondral bone in an ellipse of hyaline cartilage. The block is then trimmed a further 4 mm (400 × 10 μm sections) to the sample site (400).

second calcein label was given. Six hours after the final period of loading, the animals were killed by cervical dislocation.

Tissue processing and sectioning

When the rats were killed, the entire antebrachii were dissected free from the skin and dipped for 20 s in a 10% solution of polyvinyl alcohol (PVA) (Sigma). The limbs were then chilled by plunging them into a bath of n-hexane (BDH Supplies, Poole, U.K.) cooled to −70°C with dry ice. The samples were then mounted perpendicularly on solid brass microtome chucks with more PVA so that the proximal (elbow) end was uppermost (Fig. 3). The blocks were trimmed using a heavy-duty cryomicrotome (Model OTF, Brights Instrument Co., Huntingdon, U.K.) fitted with a tungsten carbide edged blade, until both the radius and ulna were visible in sections, a common fixed anatomical landmark in all the samples. The blocks were then trimmed a further 4 mm from this point so that sections could be taken from relatively equivalent sites of each sample. Seven-micrometer undecalcified sections were collected onto slides coated with Vectabond (Vector Labs, Burlingame, CA) and stored at −35°C.

Histology and enzyme cytochemistry

Three sections from each block were mounted unstained in glycerol/PBS (Citifluor, Canterbury, U.K.) for UV microscopy. The length of labeled surface was measured over a 400 μm length of the ulnar medial periosteal surface from photographs of sections from control and loaded bones from each animal. The length of labeled surface was measured from the most medial point of the ulna in a dorsal direction (Fig. 1).

Serial sections were either stained for conventional histology in aqueous Wright's stain (Diffquick–Baxters, Reading, U.K.) or were reacted to demonstrate the activity of the enzyme tartrate-resistant acid phosphatase (TRAP) using a modification of the method of Webber et al.[17] by incubation first in naphthol AS BI phosphate solution at 37°C, followed by fast garnet GBC/sodium tartrate solution at 4°C.

Sections were photographed with a Leica DMRB microscope, and TRAP activity was measured in the cell layer immediately adjacent to the bone surface using a Vickers M85 microdensitometer (mask A2, spot size 1, wavelength 650 nm). Results of the microdensitometry were expressed as mean integrated extinction (MIE × 100), a standardized value comparable between different machines.[18] A paired Student's *t*-test was used to assess the significance of differences in the length of labeled surface and of the enzyme activity between the loaded and control limbs of each animal.

RESULTS

In vivo strain measurement and load/strain calibration

During walking on a flat surface, we measured strain magnitudes on the medial periosteal surface of the ulnae of each of the rats within one stride of greater than -850×10^{-6} (peak -1110×10^{-6}). When the rats climbed the inclined plane at 45° at walking pace, there was no increase in the strains we recorded; but when they jumped from a height of 30 cm, we measured strains over -1900×10^{-6} in all the rats (peak -2180×10^{-6}).

In the limbs loaded in vitro with attached strain gauges, we found that a peak-applied load of 7 N produced strain of -4000 to -4500×10^{-6} on the medial periosteal surface of the ulna.

Effects of loading in vivo

The medial ulnar periosteal surfaces of the right (non-loaded limbs) showed clear evidence of bone resorption. There was no continuous fluorochrome incorporation (Fig. 4A), and the scalloped edge of the bone matrix was lined with tightly adherent cells with no intervening osteoid (Fig. 5A). This layer of cells expressed high levels of TRAP activity (Fig. 6A). In contrast, in the equivalent regions of all of the left loaded limbs, there was almost continuous incorporation of the second fluorochrome label (Fig. 4B), which was significantly different from the control (non-loaded bones). In the controls, the mean length of labeled surface over the 400 μm length measured was 19.2 μm (±SEM 10 μm) compared with 340 μm (±SEM 31 μm) in the loaded bones ($p < 0.0005$; $n = 6$). The periosteal surface of the loaded bones was covered with osteoid and

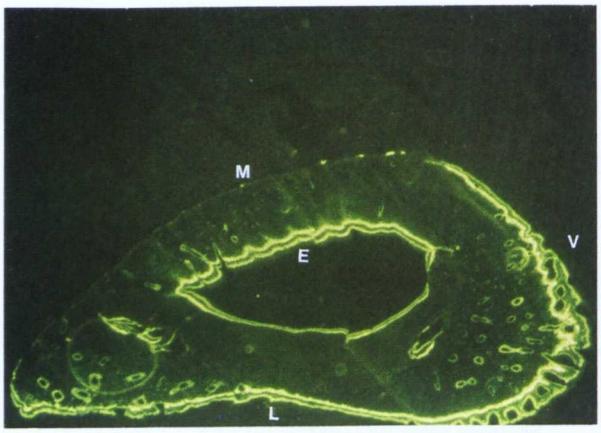

4A

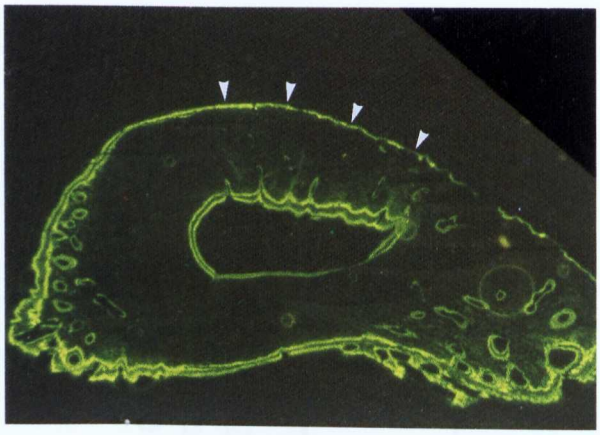

4B

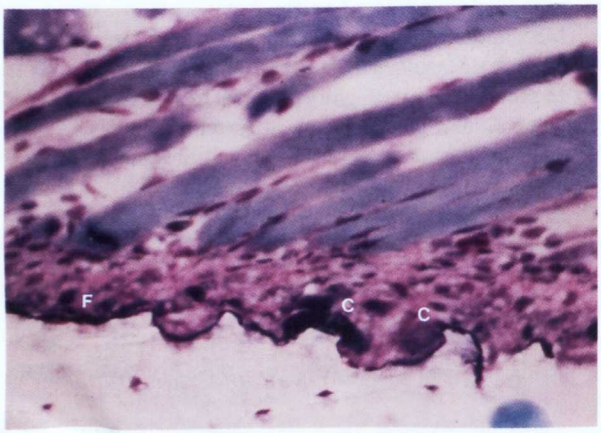

5A

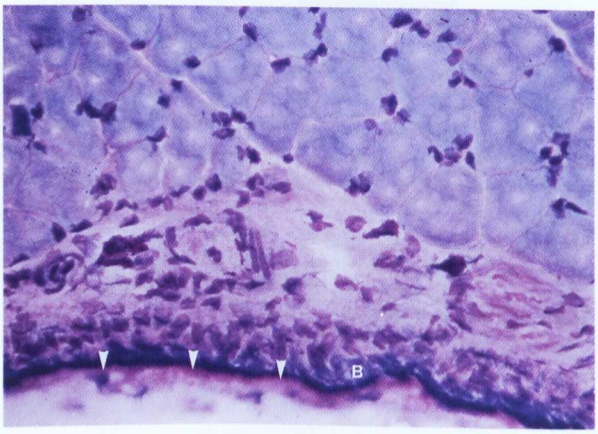

5B

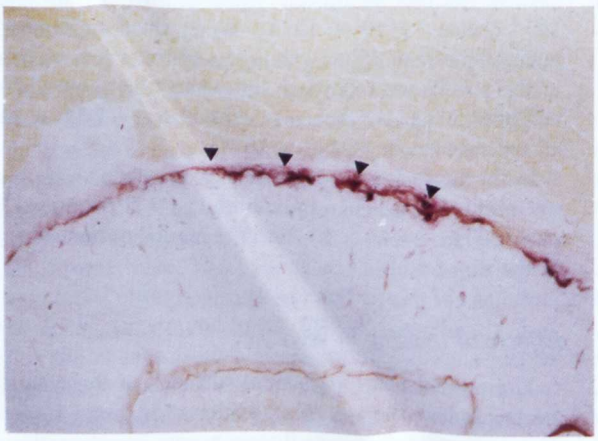

6A

6B

osteoblasts (Fig. 5B). TRAP activity in the loaded limbs was not evident (Fig. 6B). In the nonloaded bones, the TRAP activity (MIE $\times$ 100) was 22.3 ($\pm$SEM 4.5), compared with 4.8 ($\pm$SEM 0.8) in the loaded bones, a highly significant reduction of 80% ($n = 6$; $p < 0.0001$).

The loading procedure did not affect the normal use of the left foreleg by the rats. Immediately after the leg was removed from the loading device, the skin over the carpus and elbow was seen to be blanched as a result of the applied pressure. However, within approximately 30 s, there was reperfusion of the skin, and on recovery from the anesthesia, there was no lameness or favoring of the legs that had been loaded. When the animals were sacrificed and the skin removed, the elbow and carpal areas were examined carefully, but no signs of bruising, hemorrhage, or other gross pathology were visible.

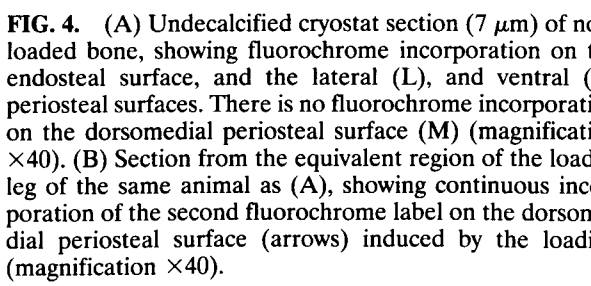

FIG. 4. (A) Undecalcified cryostat section (7 μm) of nonloaded bone, showing fluorochrome incorporation on the endosteal surface, and the lateral (L), and ventral (V) periosteal surfaces. There is no fluorochrome incorporation on the dorsomedial periosteal surface (M) (magnification ×40). (B) Section from the equivalent region of the loaded leg of the same animal as (A), showing continuous incorporation of the second fluorochrome label on the dorsomedial periosteal surface (arrows) induced by the loading (magnification ×40).

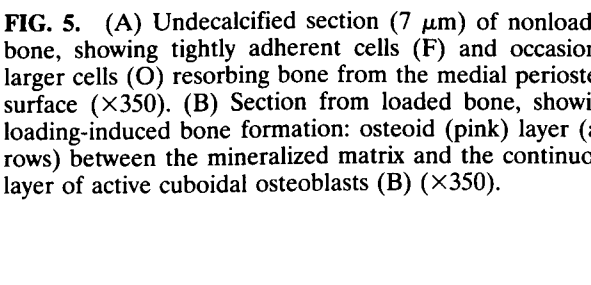

FIG. 5. (A) Undecalcified section (7 μm) of nonloaded bone, showing tightly adherent cells (F) and occasional larger cells (O) resorbing bone from the medial periosteal surface (×350). (B) Section from loaded bone, showing loading-induced bone formation: osteoid (pink) layer (arrows) between the mineralized matrix and the continuous layer of active cuboidal osteoblasts (B) (×350).

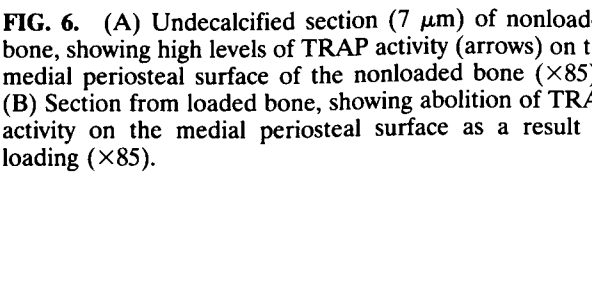

FIG. 6. (A) Undecalcified section (7 μm) of nonloaded bone, showing high levels of TRAP activity (arrows) on the medial periosteal surface of the nonloaded bone (×85). (B) Section from loaded bone, showing abolition of TRAP activity on the medial periosteal surface as a result of loading (×85).

DISCUSSION

These experiments demonstrate that six short daily periods of mechanical loading in vivo inhibit modeling-related bone resorption and stimulate formation in growing rats. Other models have been used to investigate ordered bone formation and resorption, utilizing, for example, responses of teeth to movement,[16,19] transplantation of bones,[20] or ablation of either bone marrow or trabeculae.[21,22] This model has the advantage that the changes are due to the application of mechanical forces which are measurable and are similar in magnitude, rate, and distribution to those experienced by the bone in vivo. The site of the changes we have recorded is one in which there is a modeling drift of bone as a part of normal growth. Periosteal bone resorption has been observed as a part of growth in many sites in growing animals.[23,24] The medial surface of the rat ulna is one site in which there is a particularly well-defined resorbing surface,[14] in a bone that can be loaded mechanically in vivo without gross trauma.[13]

The effect of mechanical loading on bone formation has been studied in a number of models in vivo,[25–28] but research is currently focusing on the rat. Different methods exist for studying the direct effects of loading on rat bone in vivo,[10,13,29,30] and this model shares with some of those the advantage that there is no surgical preparation associated with the loading technique. Direct trauma to bones (during surgery for example) provokes the regional acceleratory phenomenon (RAP), which can cause enhanced formation or resorption in the vicinity of the trauma.[31] We could observe no effect of the loading on subsequent use of the limbs by the rats, or any gross pathology at the sites of the application of force, so we feel that there is little if any significant trauma associated with the 7 N loads that we applied. The sections of bone used in this study were taken half way between the elbow and carpus, a site at least 7 mm away from either point of application of force, so there is certainly no direct periosteal pressure over the sample site.

In some of the loaded bones, it appeared that the surfaces that were already forming bone before the start of the experiment showed increased apposition rates in response to the loading. Although Torrance et al.[13] showed that this effect was significant in older rats loaded over a 19-day period, and formed part of the adaptive response to loading, we did not measure formation rates on existing forming surfaces in our experiments because the effect appeared not to be consistent in all the bones.

In experiments of this sort, it is important to distinguish between responses that are part of the adaptive response to applied loading with some physiological counterpart and those that are due to grossly hyperphysiological strains. We chose the magnitude of applied force in these experiments to cause double the highest strains we measured during moderate physical activity in vivo. Since the rats were naturally unwilling to indulge in extremely vigorous activity while instrumented with the gauges, we can only speculate that more extreme physiological activity would cause strains higher than the -2180×10^{-6} which was the highest that we recorded from the ulnae in vivo. The rats used for the in vivo strain gauge studies were larger than those that we loaded in vivo because we could not attach the gauges and leads to the ulnae of smaller animals without compromising their ability to use their legs relatively normally. In other species and sizes of animals, peak physiological strains in the long bones commonly exceed 3000×10^{-6} during high intensity activity.[32] It is likely therefore, that the loading regime in this experiment caused peak strains that were only ~30% higher than those experienced normally by the

animals in vivo. The orientation of the load-induced strains was close to those induced by physiological movements, since in both cases the medial ulnar surface was under compression. It is not certain that the whole bone was strained in a physiological orientation by applied loads, but the natural curvature of the ulna would be consistent with bending during use.

The frequency of 10 Hz was chosen because although it is also higher than that normally experienced in vivo during loading, there is evidence that frequencies of loading between 5 and 20 Hz are more potent osteogenic stimuli than lower frequencies.[33] This may simply be because high frequencies of loading are associated with higher strain rates than lower ones. It has been shown that high rate strains are more osteogenic than lower ones.[34]

The rapidity of the response is not surprising. We and others have shown similar or more rapid effects of brief periods of mechanical loading of bones in vivo.[4-6,30] The response we have seen in this experiment may be slower than in those experiments because the bone surfaces were quiescent, while these were actively resorbing. It is reasonable to suppose that it would be easier to convert a quiescent surface into a forming one than to inhibit resorption and stimulate formation.

In histological studies of this sort, it is critical that the sites at which the sections are cut are equivalent, because changes in the profile and cellular events may vary at different locations in the bones. The ulna is fairly consistent in this respect. Periosteal resorption on the medial ulnar surface is present for ~1.5 mm proximal to the site at which we take our sections and for over 3 mm distal to it. Since our methods allow relatively precise location of the site, and since we have compared the left-loaded leg with the non-loaded right leg in each animal, we are certain that the changes we have observed are due to the loading regime and not differences in the sample site.

Each of the three changes we have observed as a result of the 6 days of loading would be evidence for reversal of resorption. The loading-induced incorporation of fluorochrome on the surface, of which there is none in the non-loaded bones, provides evidence of formation of mineralized new bone. The change in histology is also clear. The loading induced a change from a surface with no osteoid and tightly adherent resorbing cells into one covered with osteoid and osteoblasts. TRAP activity is not a totally specific marker of osteoclastic activity, but in this site, in combination with the other changes, it provides convincing evidence of change from resorption to formation. It is not possible to identify all the resorbing cells positively as classical multinucleated osteoclasts because the undecalcified cryosectioning technique does not produce good enough sections. However, the technique does allow assessment of fluorochromes, histology, and enzyme activity in serial sections, which is not easy by other methods.

These experiments validate the rat ulna model as a method to study the cellular events during the inhibition of resorption and the initiation of formation by mechanical loading in vivo. The load-induced sequence of cellular events has some similarities with the reversal phase of bone remodeling, during which osteoclasts disappear and are replaced by osteoblasts that form new bone. The results we show represent extremes in that by the end of the loading period, there is complete inhibition of resorption and replacement of the pre-existing cell population with active osteoblasts. It will be interesting to observe changes at earlier times after the start of the loading. Future experiments should therefore allow determination of events that precede inhibition of osteoclasts in vivo and signals that cause their death or departure from the site of resorption. The process of initiation of bone formation by loading can also be studied in a detailed way. Further studies will identify early changes in gene or protein expression, which may uncover novel processes with the possibility of pharmacological targeting of such events as a means to manipulate pathological bone loss.

ACKNOWLEDGMENTS

We would like to thank Professor L. Lanyon and Mr. J. Mosley, for advice in setting up the loading device, and Mr. J. White and Mr. G. Gough for technical assistance. We are grateful to Dr. J. Beresford who allowed us to use the microdensitometer at the Bath Institute for Rheumatic Diseases. RAH is a BBSRC Veterinary Research Fellow, and TMS is funded by a Wellcome Trust Research Leave Fellowship.

REFERENCES

1. Skerry TM, Bitensky L, Chayen J, Lanyon LE 1988 Loading-related reorientation of bone proteoglycan in vivo. strain memory in bone tissue? J Orthop Res **6**:547–551.
2. Skerry TM, Suswillo RFL, El Haj AJ, Ali NN, Dodds RA, Lanyon LE 1990 Load-induced proteoglycan orientation in bone tissue in vivo and in vitro. Calcif Tiss Int **46**:318–326.
3. Weinbaum S, Cowin SC, Zeng Y 1994 A model for the excitation of osteocytes by mechanical loading-induced bone fluid shear stresses. J Biomech **27**:339–360.
4. Skerry TM, Bitensky L, Chayen J, Lanyon LE 1989 Early strain-related changes in enzyme activity in osteocytes following bone loading in vivo. J Bone Miner Res **4**:783–788.
5. Pead MJ, Suswillo RFL, Skerry TM, Vedi S, Lanyon LE 1988 Increased ^{3}H-uridine levels in osteocytes following a single short period of dynamic bone loading in vivo. Calcif Tissue Int **43**:92–96.
6. Pead MJ, Skerry TM, Lanyon LE 1988 Direct transformation from quiescence to bone formation in the adult periosteum following a single brief period of bone loading. J Bone Miner Res **3**:647–656.
7. Colletti LA, Edwards J, Gordon L, Shary J, Bell NH 1989 The effects of muscle-building exercise on bone mineral density of the radius, spine, and hip in young men. Calcif Tiss Int **45**:12–14.
8. Whedon GD 1984 Disuse osteoporosis: physiological aspects. Calcif Tiss Int **36**:S146–S150.
9. Lanyon LE, Rubin CT, Baust G 1986 Modulation of bone loss during calcium insufficiency by controlled dynamic loading. Calcif Tiss Int **38**:209–216.
10. Hagino H, Raab DM, Kimmel DB, Akhter MP, Recker RR 1993 Effect of ovariectomy on bone response to in vivo external loading. J Bone Miner Res **8**:347–357.

11. Lin BY, Jee WSS, Chen MM, Ma YF, Ke HZ, Li XJ 1994 Mechanical loading modifies ovariectomy-induced cancellous bone loss. Bone Miner **25**:199–210.
12. Smith EL, Gilligan C, McAdam M, Ensign CP, Smith PE 1989 Deterring bone loss by exercise intervention in premenopausal and postmenopausal women. Calcif Tiss Int **44**:312–321.
13. Torrance AG, Mosley JM, Suswillo RFL, Lanyon LE 1994 Noninvasive loading of the rat ulna in vivo induces a strain related modeling response uncomplicated by trauma of periosteal pressure. Calcif Tissue Int **54:3**:241–247.
14. Skerry TM, Gowen M, Dodds RA 1993 Formation and resorption in the modeling rat ulna. Bone **15**(4):454.
15. Tran Van P, Vignery A, Baron R 1982 An electron-microscopic study of the bone-remodeling sequence in the rat. Cell Tissue Res **225**:283–292.
16. Tran Van P, Vignery A, Baron R 1982 Cellular kinetics of the bone remodeling sequence in the rat. Anat Rec **202**:445–451.
17. Webber DM, Braidman IP, Robertson WR, Anderson DC 1988 A quantitative cytochemical assay for osteoclast acid phosphatase activity in foetal rat calvaria. Histochem J **20**:269–275.
18. Chayen J 1978 Microdensitometry. In: Slater TF (ed.) Biochemical Mechanisms of Liver Injury. Academic Press, London, pp. 251–291.
19. Roberts WE, Jee WSS 1974 Cell kinetics of orthodontically stimulated and non-stimulated periodontal ligament in the rat. Arch Oral Biol **19**:17–20.
20. Feik SA, Ellender G, Crowe DM, Rammanderson SM 1990 Periosteal response in translation induced bone remodelling. J Anat **171**:69–84.
21. Suva LJ, Seedor JG, Endo N, Quartuccio HA, Thompson DD, Bab I, Rodan GA 1993 Pattern of gene expression during bone formation following rat tibial marrow ablation. J Bone Miner Res **83**:379–388.
22. Aaron JE, Skerry TM 1994 Intramembranous trabecular generation in normal bone. Bone Miner **25**(3):211–230.
23. Frost HM 1982 Mechanical determinants of bone modeling. Metab Bone Dis Rel Res **4**:217–229.
24. Sorensen MS, Bretlau P, Jorgensen MB 1990 Bone modeling in the otic capsule of the rat. Acta Oto-Laryngol **110**:374–378.
25. Goodship AE, Lanyon LE, McFie H 1979 Functional adaptation of bone to increased stress. J Bone Joint Surg **61A**:53.
26. Churches AE, Howlett CR, Waldron KJ, Ward GW 1979 The response of living bone to controlled time varying loading method and primary results. J Biomech **12**:35–45.
27. Rubin CT, Lanyon LE 1984 Regulation of bone formation by applied dynamic loads. J Bone Joint Surg **66A**:397–402.
28. Skerry TM, Lanyon LE 1993 Immobilisation induced bone loss in the sheep is not modulated by calcitonin treatment. Bone **14**:511–516.
29. Chambers TJ, Evans M, Gardner TN, TurnerSmith A, Chow JWM 1993 Induction of bone formation in rat tail vertebrae by mechanical loading. Bone Miner **20**:167–178.
30. Dodds RA, Ali NN, Pead MJ, Lanyon LE 1993 Early loading-related changes in the activity of glucose 6-phosphate dehydrogenase and alkaline phosphatase in osteocytes and periosteal osteoblasts in rat fibulae in vivo. J Bone Miner Res **8**:261–267.
31. Frost HM 1983 The regional acceleratory phenomenon. A review. Henry Ford Hosp Med J **31**:3–9.
32. Rubin CT, Lanyon LE 1984 Dynamic strain similarity in vertebrates: an alternative to allometric limb bone scaling. J Theoret Biol **107**:321–327.
33. Rubin CT, McLeod KJ 1994 Promotion of bony ingrowth by frequency-specific, low-amplitude mechanical strain. Clin Orthop Rel Res **298**:165–174.
34. O'Connor J, Lanyon LE, McFie HF 1982 The influence of strain rate on adaptive bone remodelling. J Biomech **15**:767–781.

Address reprint requests to:
Dr. T. M. Skerry
Department of Anatomy
University of Bristol
Southwell Street
Bristol BS2 8EJ, U.K.

Received in original form June 1, 1994; in revised form January 6, 1995; accepted January 9, 1995.